

AMERICAN UNIVERSITY OF BEIRUT

INTER-ARCH ELASTICS AND CORRESPONDING STRESS
ON THE TEMPOROMANDIBULAR JOINT AND
MANDIBULAR TEETH
– A FINITE ELEMENT ANALYSIS STUDY –

by

JOE DAVID EL HELOU

A thesis
submitted in partial fulfillment of the requirements
for the degree of Master of Science in Orthodontics
to the Department of Orthodontics and Dentofacial Orthopedics
of the Faculty of Medicine
at the American University of Beirut

Beirut, Lebanon
July, 2017

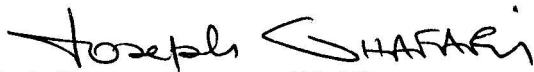
AMERICAN UNIVERSITY OF BEIRUT

INTER-ARCH ELASTICS AND CORRESPONDING
STRESS ON THE TEMPOROMANDIBULAR JOINT AND
MANDIBULAR TEETH
– A FINITE ELEMENT ANALYSIS STUDY –

by

JOE DAVID EL HELOU

Approved by:



Dr. Joseph G. Ghafari, Professor and Head
Orthodontics and Dentofacial Orthopedics

Advisor



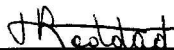
Dr. Samir A. Mustapha, Assistant Professor
Mechanical Engineering

Co-Advisor



Dr. Elie A. Shammass, Associate Professor
Mechanical Engineering

Member of Committee



Dr. Ramzi V. Haddad, Assistant Professor
Orthodontics and Dentofacial Orthopedics

Member of Committee

Date of thesis defense: July 19, 2017

AMERICAN UNIVERSITY OF BEIRUT

THESIS, DISSERTATION, PROJECT RELEASE FORM

Student Name:

EL HELOU JOE DAVID
Last First Middle

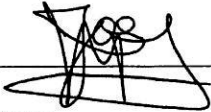
Master's Thesis Master's Project Doctoral Dissertation

I authorize the American University of Beirut to: (a) reproduce hard or electronic copies of my thesis, dissertation, or project; (b) include such copies in the archives and digital repositories of the University; and (c) make freely available such copies to third parties for research or educational purposes.

I authorize the American University of Beirut, to: (a) reproduce hard or electronic copies of it; (b) include such copies in the archives and digital repositories of the University; and (c) make freely available such copies to third parties for research or educational purposes

after:

One --- year from the date of submission of my thesis, dissertation, or project.
Two --- years from the date of submission of my thesis, dissertation, or project.
Three years from the date of submission of my thesis, dissertation, or project.


Signature

18-09-2017
Date

This form is signed when submitting the thesis, dissertation, or project to the University Libraries

ACKNOWLEDGMENTS

"Teamwork is the ability to work together toward a common vision. It is the ability to direct individual accomplishments toward organizational objectives. It is the fuel that allows common people to attain uncommon results."

Andrew Carnegie

To my late grandmother, Salwa, who has always believed in me,

Within this section, I dedicate the success of this thesis to every person who has contributed directly or indirectly in the making of this project.

To Dr. Ghafari, you have always pushed me further, much further than I thought I could. Thank you for your teachings, and transferring your knowledge over to me broadening the scope of my thinking in the various applications of science.

To Drs. Samir Mustapha, Elie Shammam and Georges Ayoub, thank you for facilitating, all the different engineering concepts, your continuous input in the process refined the numerous details in the project.

To Drs. Ramzi Haddad and Maria Saadeh, I sincerely thank you for being there along the path, escorting me through and beyond any difficulty. Dr. Saadeh, a special regards to you for the numerous hours spent on guiding and helping in my statistical analysis.

To Mr. Samah Al-Mohtar, collection of findings in this work was not possible without your dedication and contributions in the Abaqus program.

To my parents and family, I thank you for your wise counsel and sympathetic ear. You are always there for me. Words are never enough to express my gratitude. I hope to keep on pushing myself beyond what I can conceive. I love you and appreciate you, to the moon and back.

Finally, *to my warm circle of friends,* I thank you for bringing the encouragement, inciting me to keep on progressing. You have been behind the scenes, but you were the reason, my actions and my successes, came to light.

AN ABSTRACT OF THE THESIS OF

Joe David El Helou for

Master of Science

Major: Orthodontics

Title: Interarch Elastics and Corresponding Stress on the Temporomandibular Joint and on the Mandibular Teeth: A Finite Element Analysis Study

Introduction:

Orthodontic elastics are key auxiliaries used between the maxillary and mandibular arches for occlusal correction and interarch coordination during the treatment of malocclusions. Side effects have been described on neighboring teeth (e.g. altering the occlusal plane) and temporomandibular joints (TMJ; e.g. pain and discomfort). A comprehensive study of the simultaneous effects of interarch elastics on these components was warranted.

Aims:

1. Investigate the effects of orthodontic interarch elastics on the TMJ complex and the mandibular teeth under a new scheme of Finite Element Analysis (FEA) that would reflect human individual variation.
2. Compare the different stress generation and displacement potential among and between 3 types of interarch elastics: a- Class II elastics applied from maxillary canines to the mandibular 1st molars; b- Class II elastics applied from maxillary canines to the mandibular 2nd molars; and c- Class III elastics from the mandibular canine to the maxillary 1st molar on the TMJ and the mandibular arch.
3. Determine the associations among the responses of TMJ and teeth to the various elastics.

Methods:

A CBCT scan of an adult female was used to develop a 3D model of the maxilla and mandible (teeth, PDL, condyle, cortical and trabecular bone). The TMJ apparatus included the condylar head, articular disk and temporal fossa. Material properties were designated to each component based on corresponding determinations in earlier cadaver studies (Schwartz-Dabney and Dechow, 2003). The initial model was modified to reflect the variations in thickness and stiffness found in these studies. The obtained reproductions were then subjected to three types of interarch elastics: Class II from the mandibular 1st molars, Class II from the mandibular 2nd molars, and Class III from the mandibular canines. The applied force in each scenario was set at 1N. The resulting Von Mises stresses were recorded at different TMJ levels (condyle, disk, glenoid fossa) and at the mandibular 2nd molars, 1st molars, canines and central incisors on the left and right sides. Statistical methods included Shapiro-Wilk normality test, followed by t-test parametric variables, and Wilcoxon-Signed rank t-test for non-parametric variables. Freidman's ANOVA were used to compare the differences of stress and displacement between the investigated variations. Pearson correlations were employed to examine associations among variables.

Results:

Statistically significant higher stresses and dental displacement were recorded in the Class III group compared with the Class II elastics groups. Differences were also noted between the left and the right sides. On the right side, the stresses on the condyle tended to be reduced while the stresses on the teeth were elevated, opposite to the observed stresses on the left side. Stiffness produced significantly higher stresses as compared to thickness.

The correlations between stiffness and the various stresses at the level of the TMJ were high and statistically significant in both Class II groups, but not in the Class III group. Corresponding correlations at the dental level were high and significant in all groups, with a negative pattern for the mandibular posterior molar units, showing that stiffness modification was inversely related to stress on the teeth while positively correlated with the stress at the TMJ. Thickness modification was not correlated to stresses on TMJ and teeth in any of the elastics groups.

Stresses at the TMJ highly correlated ($p < 0.05$) with stresses on the teeth, as well as with initial tooth displacement in response to Class II elastics from the mandibular 1st molars, and Class III elastics.

Conclusions:

1. This study was novel in its investigation of inter-arch elastics on mandibular teeth, applied on the entire mandibular arch, incorporating human individual variation of material properties, and employing loading scenarios simulating the clinical settings of Class II and Class III malocclusions. This study also introduced a comparison between Class II elastics delivered from the mandibular 1st molars, 2nd molars, and Class III elastics from the mandibular canines.
2. A key determining factor in affecting initial stress and displacement was the original contact of teeth with the cortical bone. The response to force is shaped by the presence of the compact bone in the immediate vicinity of the teeth withstanding the orthodontic pressure.
3. Stiffness induced higher stresses and more variability on condylar and dental response. Under stiffness variation, Class III elastics demonstrated the highest stresses on the TMJ and mandibular teeth, while Class II elastics delivered from the mandibular 1st molars resulted in the weakest stresses on these components.
4. The anatomy and geometry of the mandible apparently play a primary role in defining condylar and dental response to the interarch elastics. More specifically the structural components include tooth dimension and orientation, alveolar width, tooth contact with the cortical bone, and the boundaries defining posterior and anterior position of the condyle.
5. Preliminary clinical implications would include the alignment of teeth within trabecular bone to facilitate their movement, or abutting them to the adjacent cortical bone to resist movement.
6. Future research should explore time-dependent analysis that would determine longer term displacement, individual variation from actual human material, as well as incorporating the response of bone and teeth in the maxillary arch in different variations of elastic configuration.

Table of Contents

ACKNOWLEDGEMENTS.....	v
ABSTRACT.....	vi
LIST OF ILLUSTRATIONS.....	xv
LIST OF TABLES.....	xxii
LIST OF ABBREVIATIONS.....	xxvi

1. INTRODUCTION.....	1
1.1. General introduction.....	1
1.2. Multifaceted contributions.....	2
2. BACKGROUND AND SIGNIFICANCE.....	3
2.1. Malocclusion.....	3
2.1.1. Classification of malocclusion.....	3
2.1.2. Etiology of malocclusion.....	5
2.1.3. General concepts.....	6
2.2. Treatment of Malocclusions.....	7
2.2.1. Orthopedic and orthodontic treatment.....	8
2.2.2. Appliance designs.....	9
2.3. Intermaxillary Orthodontic forces.....	11
2.3.1. Elastics in orthodontics.....	11
2.3.1.1. History and original industrial uses.....	11
2.3.1.2. Types and categories.....	13
2.3.2. Other appliances sagittal intermaxillary orthopedic effects.....	14
2.3.2.1. Chin cup.....	14
2.3.2.2. Facemask.....	14
2.3.2.3. Headgear.....	15
2.4. Elastics in Relation to Condyle.....	17

2.4.1.	Pressure by elastics transmitted to the condyle.....	17
2.4.2.	Elastics vs. other appliances in relation to the condyle.....	19
2.5.	Finite element analysis.....	24
2.5.1.	Applications in dentistry.....	26
2.5.2.	Application in Temporo-Mandibular Joint Studies.....	28
2.5.3.	Applications in Orthodontics.....	30
2.6.	Aims, objectives and hypothesis.....	34
2.6.1.	Aims.....	34
2.6.2.	Hypothesis and significance.....	35
3.	MATERIAL AND METHODS.....	36
3.1.	Material.....	36
3.1.1.	Anatomical record.....	36
3.1.2.	Patient variation and data collection process..	37
3.2.	Methods.....	43
3.2.1	Image importing and model recognition.....	44
3.2.1.1	Teeth mask.....	45
3.2.1.2	Bone mask.....	47
3.2.1.3	Periodontal ligament mask.....	49
3.2.1.4	Articular disk mask.....	51
3.2.1.5	Surface to surface interaction.....	51
3.2.2.	Incorporating patient variation into 3D model.....	53
3.2.2.1	Stiffness variation.....	54
3.2.2.2	Thickness variation.....	56
3.2.3.	Statistical consideration.....	57
3.2.4.	Implementation of thickness variations into the model.....	60
3.2.5.	Model processing.....	65
3.2.5.1.	Defining material properties.....	65
3.2.5.2.	Interaction properties.....	66

3.2.6. Loading scenario.....	67
3.2.6.1. Loading conditions.....	68
3.2.6.2. Boundary conditions.....	70
3.3. Data collection and export.....	71
3.3.1. Types of results.....	71
3.3.2. Data reporting.....	73
3.4. Statistical analysis.....	73
4. RESULTS.....	75
4.1. Comparisons between treatment groups.....	75
4.1.1. Comparisons of the TMJ complex.....	75
4.1.1.1. Comparisons under stiffness variation.....	75
4.1.1.2. Comparisons in the thickness variation.....	79
4.1.2. Comparisons of stresses at the periodontal ligament.....	80
4.1.2.1. Comparisons under stiffness variation.....	80
4.1.2.2. Comparisons under thickness variation.....	85
4.1.3. Comparisons of displacements at the dental Units.....	88
4.1.3.1. Comparisons of displacements by vector.....	88
4.1.3.2. Comparisons of displacements by magnitude.....	88
4.2. Comparisons within treatment groups.....	91
4.2.1. CI II/6s.....	91
4.2.1.1. Stiffness variation.....	91
4.2.1.1. A. TMJ.....	91
4.2.1.1. B. PDL.....	92
4.2.1.1. C. Dental displacement.....	92

4.2.1.2.	Thickness variation.....	93
4.2.1.2. A.	TMJ.....	93
4.2.1.2. B.	PDL.....	93
4.2.1.2. C.	Dental displacement.....	94
4.2.2.	CI II/7s.....	96
4.2.2.1.	Stiffness Variation.....	96
4.2.2.1. A.	TMJ.....	96
4.2.2.1. B.	PDL.....	97
4.2.2.1. C.	Dental displacement.....	97
4.2.2.2.	Thickness Variation.....	98
4.2.2.2. A.	TMJ.....	98
4.2.2.2. B.	PDL.....	99
4.2.2.2. C.	Dental displacement.....	99
4.2.3.	CI III.....	101
4.2.3.1.	Stiffness variation.....	101
4.2.3.1. A.	TMJ.....	101
4.2.3.1. B.	PDL.....	101
4.2.3.1. C.	Dental displacement.....	102
4.2.3.2.	Thickness Variation.....	103
4.2.3.2 A.	TMJ.....	103
4.2.3.2. B.	PDL.....	104
4.2.3.2. C.	Dental displacement.....	105
4.3.	Stiffness compared with thickness.....	105
4.3.1.	CI II/6s.....	105
4.3.1.1.	TMJ.....	105
4.3.1.2.	Dental components.....	106
4.3.1.3.	Dental displacement.....	107
4.3.2.	CI II/7s.....	108
4.3.2.1.	TMJ.....	108
4.3.2.2.	Dental components.....	108
4.3.2.3.	Dental displacement.....	109

4.3.3. Cl III's.....	110
4.3.3.1. TMJ.....	110
4.3.3.2. Dental components.....	111
4.3.3.3. Dental displacement.....	112
4.4. Correlations between stresses and variations in stiffness and thickness.....	112
4.4.1. Stiffness variations.....	112
4.4.1.1. Cl II/6s.....	112
4.6.1.1. A. TMJ.....	112
4.6.1.1. B. Dental Components.....	113
4.4.1.2. Cl II/7s.....	115
4.6.1.2. A. TMJ.....	115
4.6.1.2. B. Dental Components.....	116
4.4.1.3. Cl III.....	118
4.6.1.3. A. TMJ.....	118
4.6.1.3. B. Dental Components.....	118
4.4.2. Thickness variations.....	120
4.4.2.1. Cl II/6s.....	120
4.4.2.1. A. TMJ.....	120
4.4.2.1. B. Dental components.....	121
4.4.2.2. Cl II/7s.....	124
4.4.2.2. A. TMJ.....	124
4.4.2.2. B. Dental components.....	124
4.4.2.3. Cl III's.....	127
4.4.2.3. A. TMJ.....	127
4.4.2.3. B. Dental components.....	128
4.5. Correlations between model components.....	130
4.5.1. Cl II/6s.....	130
4.5.2. Cl II/7s.....	133
4.5.3. Cl III's.....	135

5. DISCUSSION.....	137
5.1. Strengths.....	137
5.1.1. Individual variation.....	138
5.1.2. Overcoming the difficulty of direct clinical investigation.....	139
5.1.3. Qualified research in the TMJ structure.....	140
5.1.4. Effect of bone characteristics on tooth movement.....	140
5.1.5. Model construction.....	141
5.2. Contributions of the study.....	143
5.2.1. Information at various levels of a multifaceted and multifactorial system.....	143
5.2.2. Comparison of treatment modalities.....	144
5.2.2.1. Stiffness variation.....	144
5.2.2.2. Thickness variation.....	146
5.2.3. Stiffness vs. thickness comparisons.....	147
5.2.4. Correlations.....	149
5.2.5. Applications of the different treatment modalities under stiffness and thickness variations.....	151
5.3. Comparison with other FEA studies evaluating condylar response to intermaxillary elastics.....	153
5.4. Clinical implications.....	154
5.4.1. From the comparisons between right and left findings.....	154
5.4.2. From the comparisons between stiffness and thickness.....	157
5.4.3. From the comparisons between the applied elastics.....	157
5.4.4. From the analysis of correlations of the various parts of the model.....	158
5.5. Limitations and research considerations.....	158
5.5.1. FE modeling.....	158
5.5.2. Data collection.....	159
5.5.3. Static versus dynamic loading.....	161
5.5.4. Considerations within model construction....	162
5.6. Future research.....	163

6. CONCLUSION	164
REFERENCES	168
Appendix.....	174

ILLUSTRATIONS

2.1. Ackerman-Proffit Classification system of malocclusions.....	4
2.2. The Ford Mandible picture from <i>AUB Museum Collection</i>	10
2.3. Evolution of fixed orthodontic appliances.....	10
2.4. Chin cup device with a chin strap and an occipital cover, to generate reverse pull to restrain mandibular growth.....	14
2.5. The orthodontic facemask.....	15
2.6. The highpull headgear.....	15
2.7. Bionator appliance versus the activator	16
2.8. The Frankel appliance.....	16
2.9. Twin block appliance.....	16
2.10. Virtual bridge under different physical experiments.....	24
2.11. Virtual car put into test simulating accident.....	24
2.12. Finite Element Analysis of the human knee.....	25
2.13. Finite Element Analysis of the dentulous human mandible.....	26
2.14. Finite Element Analysis of various types of implants.....	27
2.15. Finite Element Analysis of various types of implants. A. Full FE model of the mandible; B. In detail exploration of the TMJ.....	28
2.16. The standard healthy model is represented versus pathologic situations various degrees of anterior displacement.....	29
2.17. Stresses in the normal position of the disk versus a pathologic displacement of the disk.....	29
2.18. Von Mises' stress (A), 1 st principal stress (B), and 3 rd principal stress (C) in a coronal section of the alveolar bone.....	31
2.19. Mandibular molar protraction.....	31
2.20. Maxillary retraction of the canine after extraction of the 1 st premolars.	32
2.21. Mandibular protraction device.....	32

3.1.1.	Data collection samples from cadaver studies.....	38
3.1.2.	Bone cylinders represent a cortical plate specimen.....	39
3.2.1.	The approach for 3D patient-specific model reconstruction and FE simulation of tooth and PDL from in-vivo CBCT scans.....	43
3.2.2.	Initial capturing the CBCT image in DICOM format.....	44
3.2.3.	Initial capturing of the teeth mask with <i>Segmentation with Threshold</i> tool.....	45
3.2.4.	Initial modeling the CBCT image with <i>Segmentation with Threshold</i> tool followed by <i>3D editing</i> tool to delete undesirable elements.....	46
3.2.5.	<i>Paint tool</i> allow for manual selection of pixels per Greyscale reference of the DICOM image.....	46
3.2.6.	Separation of a single mask into multiple elements using <i>Split Merge tool</i> for a single object.....	47
3.2.7.	Two separation techniques to separate a single mask into multiple elements.....	48
3.2.8.	Mandibular bone mask captured and modeled in totality.....	48
3.2.9.	Modeling of the Periodontal ligament.....	50
3.2.10.	Modeling of the periodontal structures.....	50
3.2.11.	Surface selection for interproximal interaction.....	52
3.2.12.	Surface-to-surface interactions involve coupling of the selected sides to the respective mask.....	53
3.2.13.	Final version of initial model before applying patient-variations.....	54
3.2.14.	A. Elastic Moduli of the 62 different sites of both sides of the cortical plate of mandible B. Different zones sectioned of the mandible per the E ₃ map variation.....	55
3.2.15.	A. Cortical plate thickness B. Sectioning of the mandibular body...	57
3.2.16.	Sectioning of the mandibular bodies.....	59
3.2.17.	The initial state of the template model upon which the cadaver variations were input.....	62
3.2.18.	Sectioning of the mandibular bodies with tools like duplication of masks, merging and priority selection.....	62

3.2.19. Application of the individual variations in the various parts of the model.....	63
3.2.20. The different variations of models created per thickness of data extracted from the cadavers.....	64
3.2.21. Surface to surface interaction at different levels.....	67
3.2.22. Loading scenario 1: Configuration of Cl II elastics.....	69
3.2.23. Loading scenario 2: Configuration of Cl III elastics.....	69
3.2.24. Surface of application of the force of the elastics on the 1 st molars...	69
3.2.25. Surface of application of the force of the elastics on the 2 nd molars..	69
3.2.26. Surface of application of the force of the elastics on the mandibular canine.....	69
3.2.27. Application of boundary condition.....	71
3.2.28. Selection of element sets of the TMJ complex.	72
3.2.29. Selection of element sets at the level of the PDL.....	72
3.2.30. Selection of node sets at the level of the center of the crown.....	73
4.1.1. Stresses on mandibular body are represented in different treatment modalities under stiffness variations.....	77
4.1.2. Stresses on mandibular body and TMJ articular disk in the different treatment modalities under stiffness variations.....	78
4.1.3. Stresses on the temporal fossae in different treatment modalities under stiffness variations.....	79
4.1.4. Von Mises stresses at the PDL ligament and at the teeth within each modality of treatment.....	84
4.2.1. The pattern of distribution of the Von Mises stresses (MPa) in the stiffness category in Cl II/6's group.....	91
4.2.2. The pattern of distribution of the Von Mises stresses (MPa) in the thickness category in the Cl II/6's group.....	94
4.2.3. The pattern of distribution of the Von Mises stresses (MPa) in the stiffness category in the Cl II/7's group.....	96
4.2.4. The pattern of distribution of the Von Mises stresses (MPa) in the thickness category in the Cl II/7's group.....	99

4.2.5. The pattern of distribution of the Von Mises stresses (MPa) in the stiffness category in the C1 III's group.....	101
4.2.6. The pattern of distribution of the Von Mises stresses (MPa) in the thickness category in the C1 III's group.....	103
5.1. In display are the highest stresses in the stiffness variations group on the TMJ (comparison of both sides together).....	156
5.2. In display are the highest stresses in the thickness variations group on the TMJ (comparison of both sides together).....	156

TABLES

2.1. A report of the different findings of different authors investigating the mandibular advancement devices affecting the TMJ.....	23
3.1.1. Elastic and shear moduli for human dentate mandibles.....	42
3.2.1. Significance testing of the differences of thicknesses between the different region of both buccal and lingual sides.....	58
3.2.2. Different variations of thicknesses of the grouped regions retrieved from the different cadavers.....	60
3.2.3. Material properties of the different components of the models.....	65
3.2.4 Material properties for Light Lingual region.....	66
4.1.1. Freidman’s 2-way ANOVA of TMJ stresses under stiffness variation.....	76
4.1.2. Freidman’s 2-way ANOVA of TMJ stresses under thickness variation.....	80
4.1.3. Freidman’s 2-way ANOVA of stresses of dental units under stiffness variations (right side).....	82
4.1.4. Freidman’s 2-way ANOVA of stresses of dental units under stiffness variations (left side).....	83
4.1.5. Freidman’s 2-way ANOVA of stresses of dental units under thickness variations (right side).....	86
4.1.6. Freidman’s 2-way ANOVA of stresses of dental units under thickness variations (left side).....	87
4.1.7 Freidman’s 2-way ANOVA of displacement of dental units.....	89
4.1.8 Freidman’s 2-way ANOVA of displacement of dental units in magnitude (absolute value).....	90
4.2.1. Von Mises stresses on the TMJ complex under stiffness variations in Cl II/7s group.....	173
4.2.2. Right compared with left Von Mises stresses on TMJ components under stiffness variations in Cl II/6s group.....	91
4.2.3. Von Mises stresses on the PDL of dental units under stiffness variations in Cl II/7s group.....	174

4.2.4. Right compared with left / Von Mises stresses on PDL of dental components under stiffness variations in CI II/6s group....	92
4.2.5. Dental displacement of dental units under stiffness variations for models in the CI II/7s.....	175
4.2.6. Right compared with left/ dental displacement of dental components under stiffness variations in CI II/6s group.....	93
4.2.7. Von Mises stresses on the TMJ complex under thickness variations in CI II/7s group.....	175
4.2.8. Right compared with left Von Mises stresses on TMJ components under thickness variations in CI II/6s group.....	94
4.2.9. Von Mises stresses on the PDL of dental units under thickness variations in CI II/7s group.....	176
4.2.10. Right vs with left Von Mises stresses on dental components under thickness variations in CI II/6s group.....	95
4.2.11. Dental displacement of dental units under thickness variations in CI II/7s group.....	177
4.2.12. Right vs. left dental displacement of dental components under thickness variations in CI II/6s group.....	95
4.2.13. Von Mises stresses on the TMJ complex under stiffness variations in CI III group.....	177
4.2.14. Right compared with Left Von Mises stresses on TMJ components under stiffness variations in CI II/7s group.....	96
4.2.15. Von Mises stresses on the PDL of dental units under stiffness variations in CI III.....	178
4.2.16. Right vs left Von Mises stresses on the dental components under stiffness variations in CI II/7s group.....	97
4.2.17. Dental displacement of dental units under stiffness variations in the CI III group.....	179
4.2.18. Right compared with left / dental displacement of the dental components under stiffness variations in CI II/7s group.....	98
4.2.19. Von Mises stresses on the TMJ complex under thickness variations in the CI III's group.....	179
4.2.20 Right compared with Left Von Mises stresses (MPa) on TMJ components under thickness variations in CI II/7s group.....	99

4.2.21. Von Mises stresses on the PDL of dental units under thickness variations in the CI III's group.....	180
4.2.22. Von Mises Stresses of Right compared with left the dental components under thickness variations in the CI II/7s group.....	100
4.2.23. Dental displacement of dental units under thickness variations in CI III group.....	181
4.2.24. Right compared with left of Von Mises stresses on TMJ complex under thickness variations in CI II/7s group.....	100
4.2.25. Von Mises stresses on the TMJ complex under stiffness variations in CI II/6s group.....	182
4.2.26. Right compared with left Von Mises stresses on TMJ components under stiffness variations in CI III group.....	101
4.2.27. Von Mises stresses on PDL of dental units under stiffness variations in the CI II/6s group.....	183
4.2.28. Right compared with left of Von Mises stresses on dental components under stiffness variations in CI III group.....	102
4.2.29. Dental displacement (mm) of dental units under stiffness variations in CI II/6s group.....	184
4.2.30. Right (R) compared with left (L) Von Mises stresses on TMJ complex under stiffness variations in CI III group.....	102
4.2.31. Von Mises stresses at the TMJ complex under thickness variations in CI II/6s group.....	184
4.2.32. Right compared with left Von Mises stresses on TMJ components under thickness variations in CI III group.....	103
4.2.33. Von Mises stresses at the PDL of dental units under thickness variations in CI II/6s group.....	185
4.2.34. Right compared with left Von Mises stresses on dental components under thickness variations in CI III group.....	104
4.2.35. Dental displacement of dental units under thickness variations for models in the CI II/6s group.....	186
4.2.36. Right side compared with left Von Mises stresses (MPa) on dental units under thickness variations in CI III group.....	105
4.3.1. Von Mises Stresses of stiffness compared with thickness on TMJ components in the CI II/6s group.....	106

4.3.2. Von Mises stresses of stiffness versus thickness variations on PDL in CI II/6s group.....	107
4.3.3. Von Mises stresses comparing stiffness versus thickness variation on dental displacement in CI II/6s group.....	107
4.3.4. Von Mises stresses compared under stiffness versus thickness on TMJ components in CI II/7s group.....	108
4.3.5. Von Mises stresses compared under stiffness versus thickness on the PDL in CI II/7s group.....	109
4.3.6. Dental displacement under stiffness versus thickness in CI II/7s group.....	110
4.3.7. Von Mises stresses under stiffness versus thickness variations on TMJ components in CI III's group.....	110
4.3.8. Von Mises stresses compared under stiffness versus thickness on the PDL in CI III group.....	111
4.3.9. Dental displacement compared under stiffness versus thickness in the CI III group.....	112
4.4.1. Correlations between Von Mises stresses on TMJ and stiffness variations in CI II/6 group.....	113
4.4.2. Correlations between Von Mises stresses at the PDL and stiffness variations in CI II/6 group.....	114
4.4.3. Correlations between dental displacements and stiffness variations in CI II/6s group.....	115
4.4.4. Correlations between Dental displacements and stiffness variations in CI II/7s group.....	115
4.4.5. Correlations between dental displacements and stiffness variations in CI II/7s group.....	117
4.4.6. Correlations between Dental displacements and stiffness variations in CI II/7s group.....	118
4.4.7. Correlations between Von Mises TMJ stresses and stiffness variations in CI III groups.....	119
4.4.8. Correlations between Von Mises stresses at the PDL and stiffness variations in CI III group.....	119
4.4.9. Correlations between dental displacements and stiffness variations in CI III group.....	120

4.4.10. Correlations between Von Mises stresses on TMJ and thickness variations in CI II/6s group (right side).....	120
4.4.11. Correlations between Von Mises stresses on TMJ and thickness variations in CI II/6s group (left side).....	121
4.4.12. Correlations between Von Mises stresses at the PDL and thickness variations in CI II/6s group (right side).....	122
4.4.13. Correlations between Von Mises stresses at the PDL and thickness variations in CI II/6s group (left side).....	123
4.4.14. Correlations between dental displacements and thickness variations in CI II/6s group.....	123
4.4.15. Correlations between Von Mises stresses on TMJ and thickness variations in CI II/7s group (right side).....	124
4.4.16. Correlations between Von Mises stresses on TMJ and thickness variations in CI II/7s group (left side).....	124
4.4.17. Correlations between Von Mises stresses at the PDL and thickness variations in CI II/7s group (right side).....	125
4.4.18. Correlations between Von Mises stresses at the PDL and thickness variations in CI II/7s group (left side).....	126
4.4.19. Correlations between dental displacements on dental units and thickness variations in CI II/7s group.....	126
4.4.20. Correlations between Von Mises stresses on TMJ and thickness variations in CI III group (right side).....	127
4.4.21. Correlations between Von Mises stresses on TMJ and thickness variations in CI III's group (left side).....	127
4.4.22. Correlations between Von Mises stresses on PDL and thickness variations in CI III group (right side).....	128
4.4.23. Correlations between Von Mises stresses on PDL and thickness variations in CI III's group (left side).....	129
4.4.24. Correlations between dental displacements on dental units and thickness variations in CI III group.....	129
4.5.1. Correlations between Von Mises stress on PDL and dental displacement under thickness variations in CI II/6's group.....	131
4.5.2. Correlations between TMJ components and dental displacements under thickness variations in CI II/6's group.....	132

4.5.3.	Correlations between Von Mises stress on PDL and dental displacement under thickness variations in C1 II/7's group.....	133
4.5.4.	Correlations between TMJ components and dental displacements under thickness variations in the C1 II/7's group.....	134
4.5.5.	Correlations between Von Mises stresses on PDL and dental displacement under thickness variations in C1 III group.....	135
4.5.6.	Correlations between TMJ components and dental displacements under thickness variations in C1 III group.....	136

Abbreviations

FEM	Finite Element Method	FEA	Finite Element Analysis
FE	Finite Element	CBCT	Cone beam computed tomography
3D	Three Dimensional	TMJ	Temporo-Mandibular Joint
CT	Computed Tomography	TMD	Temporo-Mandibular Disorders
DICOM	Digital Imaging and Communications in Medicine	MAD	Mandibular Advancement Devices
PAR	Peer Assessment Ration	IOTN	Index Of Treatment Need
NaPog	Nasio-Pogonion Line	MPa	Megapascals
CI II/6s	Class II elastics delivered from mandibular first molars	CI II/7s	Class II elastics delivered from mandibular second molars
CI III	Class III elastics delivered from mandibular canines to maxillary first molars		

CHAPTER 1

INTRODUCTION

1.1. General introduction

There is no doubt about the increased importance of a physical appearance. Almost unmistakably out of all features in the human, the face is to some, one of the features that stand out the most. Unrivaled, facial esthetics, balance, and harmony, and/or their absence, have attracted attention from time immemorial, by artist and art viewer alike. For many, facial expressions can readily reflect various moods, emotions, and feelings, hence conveying unspoken messages. And out this whole complex, the mouth is an essential component for its anatomical–physiological–emotional role that participates in many functions (Kirishnan V., Davidovitch Z., 2012).

Malalignment of teeth, protrusion and crowding are factors among others that create dental disorders (malocclusions). These influences often compromise on oral esthetics in particular and facial esthetics as a whole. Attempts go back at least to 1000 b.c. with a numerous number of different civilizations (starting with the Greek and Etruscan) developing ways to correct such problems of teeth and their positions.

In other words, malocclusions are situations where individual teeth or entire dental arches are positioned in undesirable locations, either esthetically or functionally. The goal of orthodontics and dentofacial orthopedics is to correct or minimize deviations from accepted normal characteristics.

1.2. Multifaceted contributions

Contemporary approaches in modern science calls for a contribution in the different fields. The art of moving teeth in orthodontics involves several notions of engineering parameters e.g. center of resistance and degree of displacement.

Collaboration has also extended to other areas of engineering where recent advances in material science, metallurgy and biomedical engineering have introduced an increasing array of alloys, capable of generating a wide spectrum of mechanical forces (Kirishnan V., Davidovitch Z., 2012). A continuous interaction has produced major changes in the design of orthodontic brackets e.g. self-ligating brackets, and the composition of the metallic and nonmetallic wires that generate the proper orthodontic forces, while controlling factors such as friction and strain. This interaction is a fertile ground for many advances in the purpose of the development of new appliances engendering optimal tooth movement, biologically and mechanically, for each patient e.g. customized brackets.

In the present study, an example of such closely-related contribution is demonstrated where, through the different engineering programs, an exploration of a challenging region, temporo-mandibular joint, is made possible. Such investigation is performed in an active state, under a tension generated by inter-arch elastics, a tool that is often used in most orthodontic techniques in various treatments of malocclusions.

CHAPTER 2

BACKGROUND AND SIGNIFICANCE

2.1. Malocclusion

Orthodontics, the 1st specialty in Dentistry and the 2nd specialty in Medicine after Cardiology, started as early as the 18th century. Norman Kingsley was one of its early pioneers, also known as the founder or “father” of Orthodontics. With a rich background in sculpturing, he integrated his artwork in designing appliances to treat cleft lip and palate patients, and developed bite ramps or inclined planes of vulcanite to “jump the bite”, correct mandibular distoclusion and other jaw mal-alignments, later named malocclusions.

The term malocclusion is defined as “any deviation from the normal or ideal relationship of the upper and lower teeth, as they are brought into functional contact” (Wang et al., 2012). At the turn of the 19th century, Edward Hartley Angle, the “father of contemporary orthodontics”, categorized malocclusions in the sagittal direction into three classes: I, II, and III, and designed for each category of malocclusion a corresponding method to help correct the inter-arch discrepancy (Angle, 1899). At a later stage, classifications of malocclusions encompassed mal-relationships of the dental arches or jaws in any of the three planes of space, along with the alignment of individual (Ackerman and Proffit, 1969).

2.1.1. Classification of malocclusion

In a simple and basic description, Kingsley classified malocclusions as Clefts, Maxillary constrictions, and other malocclusions that he treated with removable

appliances. Angle's simple and practical classification is still adopted to date as the universal tool to generally categorize a patient's malocclusion. It revolves around the maxillary 1st permanent molar, which sits under the 'key-ridge'. Subsequently, the mandibular first molar's occlusion was graded in reference to its antagonist: Class II refers to distocclusion when the mandibular molar is posterior to the maxillary; Class III indicates mesiocclusion when the molar is anterior to its maxillary counterpart.

A more elaborate classification was later developed by Ackerman and Proffit (1969; Fig 2.1). Malocclusions are grouped in a diagram that displays irregularities in all 3 planes of space (sagittal, vertical and horizontal). The draw-back of this classification was that it is extensively elaborate and difficult to communicate.

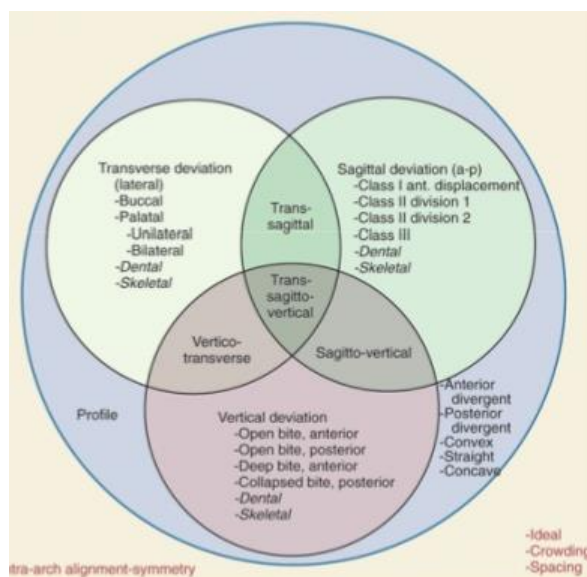


Fig. 2.1: Ackerman-Proffit Classification system of malocclusions (Ackerman and Proffit, 1969)

Other tools were later promoted to classify severity of malocclusions, including the Peer assessment ratio (PAR), the American Board of Orthodontics index (Nimeri et al.), and the Index of Orthodontic Treatment Need (IOTN). These indices evolved in

quantitative assessments of treatment severity and/or need, and cannot stand alone for diagnosis of malocclusions.

2.1.2. Etiology of malocclusion

Both, heredity and environment contribute to the development of malocclusion. A strong influence of heredity on facial features cannot be suppressed. A typical example is the Hapsburg family with their typical Class III strong mandibular prognathism perpetrated to present heirs. Two theories are advanced about the inherited or genetic characteristics: an inherited disproportion between the size of the teeth and the size of the jaws, which would produce crowding or spacing within the arch; and an inherited disproportion between the size or shape of the upper and lower jaws, which would cause improper occlusal relationships sagittally, transversally, or vertically (Proffit W. R, 2013).

Human evolution has been incriminated in the etiology of misalignment. Evolving from food hunters (ancient man) to restaurant eaters (modern alimentation life style), humans exerted less physical effort for food intake. Consequently, the oro-facial system required smaller jaw size and led to increased dental crowding. Because of a more rapid change of jaw-size in comparison to changes in tooth number and size, dental crowding becomes more prevalent more than the previous centuries (Kelly MA, Larsen CS, 1991).

Environmental factors also play a morphing role in the constitution of an individual. During the growth and development of the face, jaws, and teeth, environmental influences consist largely of pressures and forces related to physiologic activity (Proffit W. R, 2013).

The basic concept of environmental influences is summed up in the statement: 'form follows function', best captured through Melvin Moss's Functional Matrix theory (Moss and Salentijn, 1969), although injected with the influence of epigenetics. Moss described 'capsular matrices' such as the brain, the eyes or the oropharyngeal space, that dictate the position and the behavior of surrounding 'periosteal matrices', which include the soft tissues namely the muscles and the periosteum, and in turn shape the 'skeletal units'.

While this description remains a theory, many authors have advocated its validity. Harvold (1981) studied the occlusions of monkeys after having obstructed their nasal pathways and noted the constriction of their maxillary arch. Hence after violating the oropharyngeal 'capsular matrix', both the 'periosteal and skeletal matrices' reshaped the associated skeletal units.

2.1.3. General concepts

For over 100 years, orthodontic theory and practice have been based and debated on Angle's teleological belief that nature intends that all adults should have perfectly aligned dental arches with their full complement of teeth. With 16 teeth in each arch lined up in ideal articulation with their antagonists on the opposing arch, Angle maintained that the face should follow in perfect harmony and balance, and the oro-facial complex should function ideally. However, away from concepts of idealism, attempts to achieve perfection and completeness in occlusal and facial esthetics, have often called for un-natural solutions (extraction of teeth and/or orthognathic surgery) (Thomas M. Graber, 2000).

In precedent years, orthodontic limitations focused mainly on structural skeletal limitations to define therapeutic limitations. Currently, the soft tissues have been appropriately joined to define therapeutic modifiability. The boundaries of dental compensation include but are not limited to (Thomas M. Graber, 2000):

1. Pressures exerted on the teeth by the lips, cheeks, and tongue
2. Limitations of the periodontal attachment
3. Neuromuscular influences on mandibular position
4. The contours of the soft tissue facial mask
5. Lip-teeth relationships and anterior tooth display during facial animation

2.2. Treatment of malocclusions

The chief purpose of orthodontic treatment is to assist nature in the proper development of the orofacial system in growing children, and correct malocclusions in young and adult patients (Vinod Krishnan, 2012). Countless numbers of appliances were designed in multiple decades to correct dentally-related “orthodontic” and jaw-base orthopedic problems. In adolescence, preferably in the pre-pubertal period, a patient is a candidate to receive orthopedic appliances to correct jaw-related malocclusions (e.g. headgear or mandibular advancement devices in the treatment of Class II malocclusion). If treatment was not applicable during this period and the benefit of growth potential was missed, orthodontic treatment often aims at a so called “camouflage treatment” to compensate through dental inclinations for the underlying skeletal discrepancy, or a more comprehensive correction through orthognathic surgery to correct jaw-base positions for ideal esthetics and function commensurate with a correct inter-arch dental relationship.

The American Association of Orthodontics emphasizes that a child be checked by an orthodontist no later than the age of 7 for optimal results benefitting from growth modification orthopedic appliances (American Association of Orthodontists, 2013). The clinical relevance of this recommendation relates to capturing (and actually not missing) the opportunities to prevent or intercept interferences with normal growth, and escort a developing malocclusion with therapeutic modalities (such as functional jaw orthopedics) that may take advantage of growth events to better time and manage the intervention (Stahl et al., 2008).

2.2.1. Orthopedic and orthodontic treatment

The primary target of the orthodontic treatment is maintaining or bringing the lower third of the face in harmony with the other features of the face, subsequently hopefully with the body. Orthodontics affects the soft tissues indirectly by placing the underlying hard structures (teeth and bone) in their proper supportive positions. Dental tissues are to some extent dependent on the housing underlying bony elements, which should assume an optimal favorable position (orthopedics) to carry the teeth to their ideal position (orthodontics) and eventually support the soft tissues (facial esthetics). Thus, tooth movement alone, without the context of proper “orthopedic alignment” may fall short of enhancing or preserving facial esthetics.

Orthopedics applied at a young age consists of growth modification; in adulthood, it is orthognathic surgery. In growing children, the orthopedic appliances enhance differential growth between the jaws, through the cumulative effect of subtle to moderate changes of dental and skeletal components within each jaw (Efstratiadis et al, 2005). The process involves at the bony level Enlow’s V principle: as the bone is

deposited, the structure is carried away from the remaining neighboring tissues (Proffit W. R, 2013).

If growth modification is not performed in a timely manner before or around the growth spurt, and/or the objectives of growth modification were not fully met, orthognathic surgery aims at repositioning of the bony elements after a first phase of normalization of the compensatory dentoalveolar tooth inclinations, particularly the anterior teeth. In this first phase, the malocclusion is “decompensated” by repositioning the teeth upright over basal bone. During this process, the occlusal discrepancy worsens, a necessary step for optimal “rapprochement” of the bony parts during surgery. A postsurgical orthodontic phase procures final settling of the bite (Proffit W. R, 2013).

2.2.2. Appliance designs

Historical documentation of attempts to maintain and/or initiate tooth movement include the 5th century B.C “Ford Mandible’ whereby a Phoenician dentist connected with a gold wire the mandibular anterior teeth (*AUB Museum collection*; Fig 2.2). More recent advances in removable appliances were introduced by Norman Kingsley and later Angle, whose legacy of fixed appliances first included the E-ribbon arch, to eventually the edgewise bracket (1926), which persists to date without gross changes in main appearance (Green, 2014; Fig. 2.3).

Various appliances were developed for growth modification, targeting one or both jaws. In the treatment of a Class II malocclusion, a headgear worn against the maxillary molars would address maxillary prognathism, while a mandibular advancement device (MAD or functional appliance) would be used for mandibular retrognathism. Research has shown that each appliance also has an effect on the other jaw (Ghafari, 1998; Efstratiadis, 2005).

Originally designed by Kingsley (1866), the first reported use was performed after maxillary premolar extraction. A gold frame was made to fit around the upper anterior teeth and then attached via elastic ligatures to a leather headcap. Angle introduced the occipital anchorage to the headgear (1888). While gradually modified into the forms available today, the basic architecture is preserved (Proffit W. R, 2013).



The Ford Mandible

Fig 2.2: The Ford Mandible picture from AUB Museum Collection (aub.edu.lb)

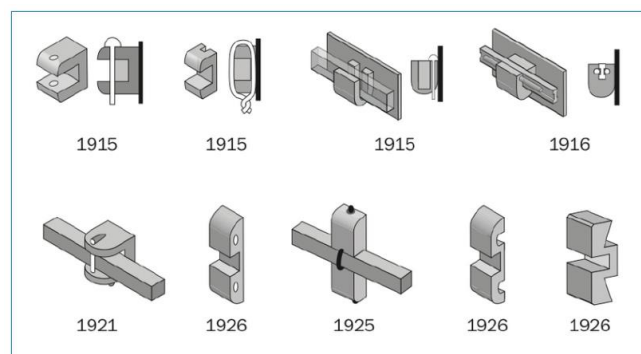


Fig 2.3: Evolution of fixed orthodontic appliances (Green, 2014)

Functional appliances (MADs) were introduced to promote growth at the mandibular condyle, primarily inducing changes in neuro-muscular anatomy and function that subsequently direct bone remodeling in a specific direction. Precursor of numerable appliances, the activator (Andresen,1902), and later all other appliances were

shown to produce differential growth between the jaws rather than additional mandibular growth beyond the growth potential. Most MAD's have the same principle mode of action, but many variations were brought into their designs, some with advantages more than others, such as a better control of mandibular incisor position, or a mechanism to widen the maxillary arch (e.g. buccal shield or coffin spring). Fixed variations included the Herbst appliance and the Jasper Jumper[®] particularly designed for non-compliant patients. In general, MADs remain bulky and annoying for long time wear.

2.3. Intermaxillary orthodontic forces

In any course of comprehensive orthodontic treatment, consideration of sagittal coordination is inevitable. Given that teeth are housed in an arch, the clinician must consider the tri-dimensional effect of forces applied antero-posteriorly, vertically, and transversally. For anteroposterior coordination of the teeth, numerous devices are available.

2.3.1. Elastics in orthodontics

2.3.1.1. History and original industrial uses

Elastics are materials or a property of a material that allows it to undergo stretching, conserving a certain amount of energy (kinetic energy) and allowing the material to preserve its tendency to revert to its previous shape after deformation. Almost universally used in any orthodontic treatment, elastics have become an integral part of any occlusal correction. Elastomers is the original general term that encompasses materials that deform to a certain degree and return to shape upon load removal.

Historically, ancient rubber was used by the Mayan people. Latex, a natural stretchy substance from which rubber is made, is extracted from large rubber trees (belonging to the spurge family Euphorbiaceae) in tropical areas. It was used to make rubber balls, hollow human figures, and as bindings to secure axe heads to their handles and other functions. After extraction, latex hardens into a springy mass when exposed to the air. The Mayan population learned to mix the rubber sap with the juice from morning glory vines so that it became more durable and elastic, without nonetheless having the material getting quite as brittle. Combining the juices, a black substance about the texture of a gum-type pencil eraser was formed.

Closer to the advent of vulcanization, rubber was first introduced in Europe (1736) where several rolled sheets of rubber were first brought into France. In 1791, inventor Samuel Peal English discovered a mean of waterproofing cloth by mixing rubber with turpentine (a technique better developed later with Macintosh). English inventor, Joseph Priestly, also realized it could be used to erase pencil marks on sheets of paper, one of its current uses today. Thomas Hancock, the English inventor and founder of the British rubber industry, invented the masticator, a machine that shredded rubber scraps, allowing rubber to be recycled after being formed into blocks or rolled into sheets. Hancock (1820) patented elastic fastenings for gloves, suspenders, shoes and stockings. In 1823, Charles Macintosh patented a method for making waterproof garments by using rubber dissolved in coal-tar naphtha for cementing two pieces of cloth together.

In the pre-vulcanization rubber age, the masticated rubber that Hancock invented was used for pneumatic cushions, mattresses, pillows and bellows, hose, tubing, solid tires, shoes, packing and springs. With the advent of vulcanization by Charles Goodyear

(1839), the use of natural rubber increased greatly, and the American Goodyear tire-manufacturing industry is credited with the modern form of rubber. Originally subject to the conditions of the weather (e.g. sticky rubber in hot weather, and brittle in cold weather), Goodyear's recipe of vulcanization (a mixture of rubber, lead and sulfur accidentally dropped onto a hot stove) resulted in a substance unaffected by weather, that could snap back from its stretched to its original form. Resistant to water and chemical interactions and non-conductive of electricity, the material was suited for a variety of other products.

2.3.1.2. Types and categories

The current use of elastics ranges from tooth separators, elastomeric ligatures to power chains. However, elastics in orthodontics were initially applied extra-orally, with the chin cup developed by John Hunter (c. 1802), but actually first used by Friedrich Christoph Kneisel (1836), the dentist to Prince Charles of Prussia, who fitted his mandibular prognathic patient with a chin strap (Wahl, 2005). Elastics were also the active component of the occipital anchorage device, currently known as headgear, first designed by J. S. Gunnell (1822), and survived to date barely changed in nearly two centuries (Wahl, 2005).

Calvin Case and later Henry A. Baker (1893) described the use of intra-oral elastics, originally in a Class II configuration (Asbell, 1990), at one time recognized as the Baker Anchorage (Wahl, 2005). Angle (1902) further contributed to engaging the technique in mainstream orthodontics. A former student of Angle, Charles H. Tweed (1932) described the use of interarch elastics to achieve retraction of teeth into extraction spaces.

Eventually, elastics were adapted to the various clinical needs to achieve proper occlusal relationships of teeth commonly used as interarch Class II, Class III, crossbite (criss cross) and vertical seating, in addition to their use as intra-arch elastics and as removable adjuncts with both fixed and removable appliances.

2.3.2. Appliances used for sagittal intermaxillary orthopedic effects

Many appliances, both extra-oral and intra-oral are sought to effect intermaxillary sagittal changes. The extra-oral group of devices includes:

2.3.2.1. Chin cup: Originally used by Friedrich Christoph Kneisel in 1836 to correct Class III jaw-relationship (Mandibular prognathism patients as shown in Fig 2.4).

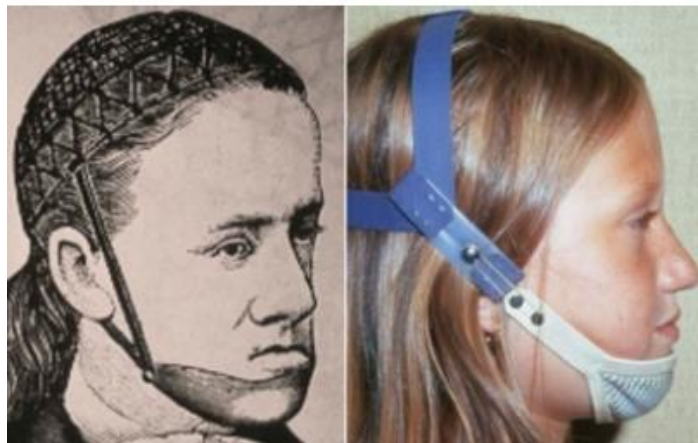


Fig 2.4: Chin cup device with a chin strap and an occipital cover to generate reverse pull to restrain mandibular growth (Proffit W. R, 2013)

2.3.2.2. Facemask: Another appliance used for Class III malocclusions, the facemask or reverse-pull headgear, originally developed by French orthodontist Jean Delaire (1971), targets the retrognathic maxilla (Fig. 2.5).

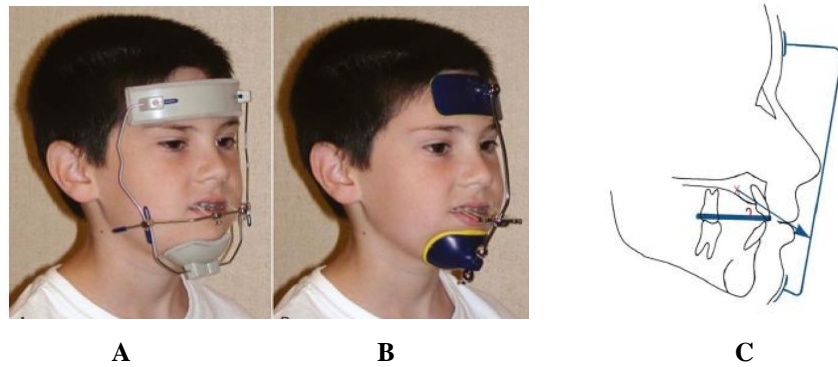


Fig 2.5:The orthodontic Facemask **A.** Delaire-type Facemask **B.** Rail-Style Facemask for more comfort **C.** Mechanism of action of facemask with the area of pull with respect to the center of resistance (Proffit W. R, 2013)

2.3.2.4. Headgear: Used in the treatment of Class II malocclusion where the maxilla is forward relative to the mandible, unlike intra-oral devices, the headgear affects principally the maxilla, with indirect effects on the mandible (Fig 2.6.).

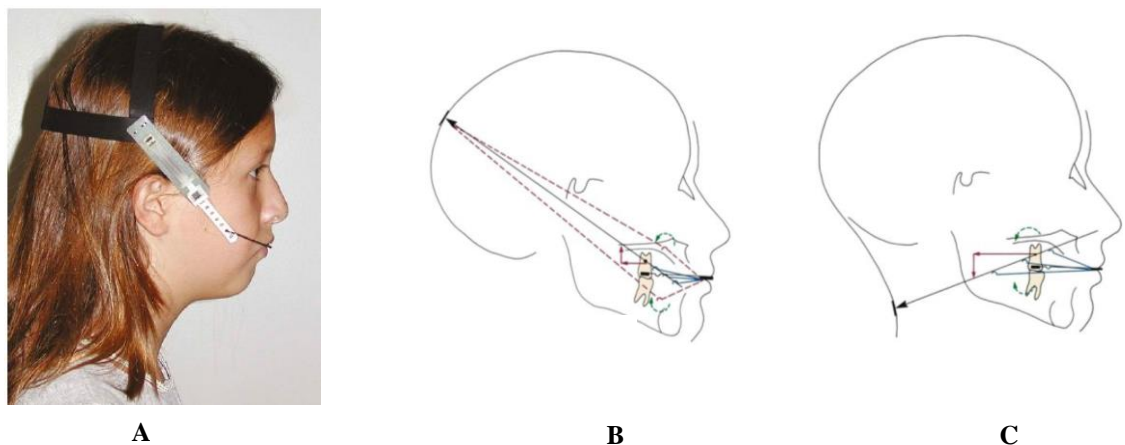


Fig. 2.6: The highpull headgear **A.** Clinical illustration of a highpull headgear. **B.** Mode of action of a high-pull headgear with respect to the center of resistance of maxillary molars **C.** Mode of action of a low-pull headgear with respect to the center of resistance of maxillary molars (Proffit W. R, 2013)

A number of intra-oral removable devices are available to produce sagittal effects. Mostly passive with no intrinsic force-generating capacity from springs or screws, these appliances rely on soft tissue stretch and muscular activity to produce treatment effects through mouth closure and muscular rest activity. The appliances include the activator,

Herbst, bionator (Fig 2.7.), Fränkel regulator (Fig 2.8.), and Twin Block (Fig 2.9.)
(Proffit W. R, 2013).

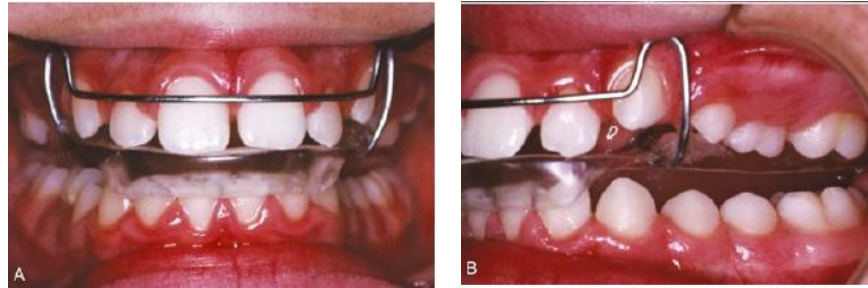


Fig 2.7: Bionator appliance differs from the activator with less bulk of acrylic.. (Proffit W. R, 2013)

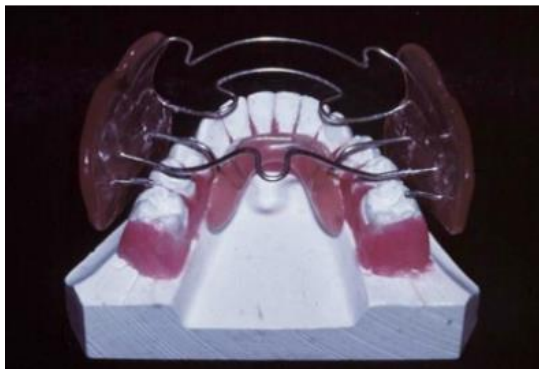


Fig 2.8: In principle a tissue-borne device, rather than a tooth borne device, the Frankel regulator (in each of its four types) stretches the buccal tissues to allow for a “new equilibrium” of the oral complex and better tooth alignment. The lingual shield enables the protrusive mandibular position in CI II patients. (Proffit W. R, 2013)

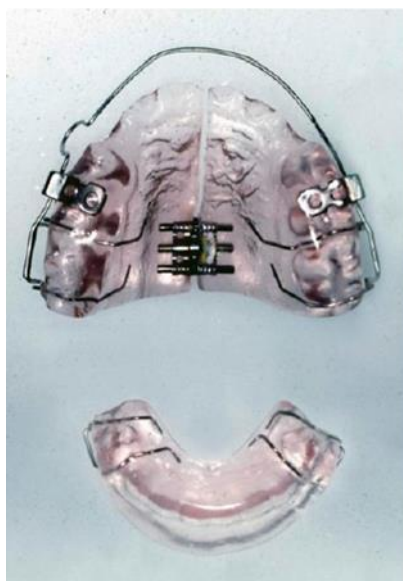


Fig 2.9: The Twin block is comprised of two elements, with a ramp that forces the patient to bite in a forward position. In the illustration, an expansion screw has been added to allow for maxillary expansion. Also, headgear tubes on the sides allow the use of a headgear for further maxillary restraint. (Proffit W. R, 2013)

2.4. Elastics in relation to condyle

The mandible is the only osseous structure in the human body that articulates with the rest of the neighboring bones with 2 joints that work simultaneously, in the same or opposite direction sagittally and with variable intensity, to allow different movements of the mandibular jaw (Meyer, 1990, Beek et al., 2000). Due to its complex action, it is imperative to preserve this articulation healthy to insure proper function (Zhang, 2009). The articulating surface, located between the condyle and the temporomandibular fossa, is submitted to various stresses from bruxism, mastication, parafunctional activities and malocclusion (Beek et al., 2000, McNamara et al., 1995, Beek, 2001).

2.4.1. Pressure by elastics transmitted to the condyle

In the 1970s and 1980s orthodontic therapy was frequently recommended to prevent or cure temporomandibular dysfunction (TMD), but no strong evidence exists that poor occlusion is the primary etiologic agent in TMD (Thomas M. Graber, 2000). While many studies show a correlation between malocclusion and arousal of temporomandibular disorders, others report weak correlation (McNamara et al, 1995). Occurrence of TMJ dysfunctions during orthodontic treatment were not reported to be related to treatment (McNamara et al, 1995). The etiology seems to be an independent variable that appears increasingly with age. Likewise, reports indicate that orthodontic treatment is neutral in regards to TMD worsening or improving (Luther, 1998). In addition, as more adults seek orthodontic care to improve quality of life (Oliveira et al., 2013), the risk of TMD appearing during orthodontic treatment may actually be related to older age rather than orthodontic treatment.

As described in the Bolton growth studies, adolescents keep experiencing sagittal maxillo-mandibular growth changes until the ages of 14-16 in girls and the early 20's in boys (Op Heij et al., 2003). Therefore, skeletal discrepancies in late adulthood are likely corrected with dental compensation with little or no effect of mandibular growth (Kinzinger et al., 2009). With a decreased ability of the condyle to remodel, orthodontic compensation may contribute to the development of TMD. Some authors relied on this argument to incriminate orthodontic treatment in the development of TMD. Contradicting earlier studies, O'Reilly et al (1993) reported that even with younger patients, 40% of the population with a mean age of 15.3 years treated with fixed appliance, and whose treatment included tooth extraction and Class II elastics, showed mild TMJ pain.

CI II and CI III configurations exhibit the most horizontal line of action of force. With much controversies in the literature, reports show to some extent remodeling of the condylar head following interarch elastics. De Clerck (2012) showed that all patients in the study group had posterior displacement of the mandible as a result of CI III elastics applied on bone anchored devices, with remodeling of the glenoid fossa at the anterior eminence (mean, 1.38 ± 1.03 mm) and bone resorption at the posterior wall (mean, -1.34 ± 0.6 mm).

In a study involving the use of CI II elastics, some patients experienced TMJ pain of moderate intensity after use of only 1 month (A. Ortega, 2016). The finding was not statistically significant, but worthy of attention; elastics are usually applied over a period of 4-6 months, hence if moderate pain was reported on the 1st month, it may be indicative of significant amounts of pressure exerted on the TMJ. On the other hand, many reports including a systematic review (Luther et al., 2010) concluded that

orthodontic treatment does not have a direct link to causing, worsening or curing TMJ dysfunction (McNamara et al., 1995).

In a different perspective, CI II elastics applied from the mandibular 1st molars may behave differently compared to CI II elastics applied from the mandibular 2nd molars. However, to date, the literature lacks such comparison.

2.4.2. Elastics vs. other appliances in relation to the condyle

No conclusive pattern of response of the TMJ to elastics, nor to other extra-oral or intra-oral appliances. In a systematic review, chin cup therapy did not represent a risk of developing TMD; no difference was detected in the number of symptoms in the control or the treated group (Zurfluh et al., 2015). The same systematic review included a report of high incidence of TMD in 6- to 10-year old children treated by chin-cup therapy with symptoms occurring in the first 6 months of wear.

The authors of the systematic review accounted for an adaptive response of the TMJ apparatus with the chin cup, mostly due to the growth potential and including alteration in mandibular shape and a decrease in the condylar head angle (angle between the condyle and collum). Further craniofacial adaptations such as posterior displacement of the glenoid fossa or alteration of disc position remain subject to controversy. Yet, the data suggest that chin-cup use does not decrease the overall mandibular growth; rather it contributes to changing of the direction of growth, eventually modifying the form of the mandible and affecting the facial profile (Zurfluh et al., 2015). The authors concluded that chin cup therapy was neither a risk factor nor may prevent TMD.

In a systematic review (Luther et al., 2010) of all appliance types with a potential to displace teeth (excluding occlusal splints), the authors concluded that TMJ response was rather vague with an insufficient research data on which to base clinical

practice regarding active orthodontic intervention and TMD. Accordingly, a seemingly random development or alleviation of TMD signs and symptoms would exist during active orthodontic treatment.

Changes following fixed mandibular advancement devices were addressed in a systematic review discussing changes in joint morphology in treated class II patients. The authors concluded that current findings were not sufficient to develop trends of appearance of TMJ symptoms (Al-Saleh et al., 2015). Although several articles used adequate imaging devices to explore the joint area, (e.g. magnetic resonance imaging for soft tissues and computed tomography (CT) or cone-beam CT images for hard tissue changes), the results were not conclusive. All reported articles in the review showed a high risk of bias due to deficient systematic methodology: inadequate consideration of confounding variables, blinding of image assessment, selection or absence of control group and outcome measurement. Reported changes in osseous remodeling, condylar and disc position were contradictory (Al-Saleh et al., 2015).

In a more recent systematic review investigating the effect of mandibular advancement devices on the TMJ complex (Ivorra-Carbonell et al., 2016) the condyle was found to be in a more advanced position after treatment with functional appliances. The appliances included the Herbst, Twin Block, Bionator, Activator, Fränkel, and Van Beek. The advanced condylar position produced a reported remodeling of the condyle and morphological adaptation of the glenoid fossa. No significant adverse effects were found on the TMJ in healthy patients. However, the appliances could improve joints that initially presented forward dislocation of the disk.

Concerning disk shape, some authors observed that at the end of treatment the number of biconcave discs on MRI had increased significantly in the patients treated

with the Fränkel regulator. The finding suggests that the use of this appliance at the beginning of the growth acceleration could help avoid future intra-TMJ problems (Franco et al., 2002).

As for changes in condyle shape and position, the authors of a case-control study (LeCornu et al., 2013) observed forward adaptive displacement of the condyles followed by remodeling of the glenoid fossa, after treatment with the Herbst appliance relative to a control group treated with fixed devices and class II elastics. Other authors (Chintakanon et al., 2000, Chavan et al., 2014), found similar results in the application of the Twin Block appliance and the Bionator. When investigating differences between hyper and hypodivergent patients, Pancherz and Michailidou (2004) observed that changes in condyle growth were greater in men than in women and that treatment with the Herbst appliance temporarily stimulated condyle growth. A year later, the authors followed 118 patients classified according to their growth pattern and concluded that condylar growth took place and was more posterior in hyperdivergent than in hypodivergent subjects.

Condylar remodeling reported with mandibular advancement devices included increased bone apposition on condylar heads, as determined by pre- and post-treatment scintigraphic studies, and compared to the control group (Guner et al., 2003). New bone formation in the mandibular condyles was concomitant with cephalometric significant increases in the NaPog ($P < 0.001$) and SNB ($P < 0.05$) angles. However, long-term effects and clinical significance of the statistically significant changes are not addressed (Guner et al., 2003).

While this area remains subject to controversy (Table 2.1.) mandibular advancement orthopedic therapy apparently does not produce TMJ disorders in the

healthy individual. Consequent to treatment with functional appliances, the condyle was found to be in a more advanced position, but remodeling around this position seems related to timing and length of treatment, as well as growth potential. Advancement appliances could improve joints that initially presented forward dislocation of the disk (Ivorra-Carbonell et al., 2016). However, alleviation of TMJ symptoms is random and in rare cases (Fricton et al., 2010).

The response of the condyle to interarch elastics and functional appliances is at best variable and subject to the influence of different individual factors. A complete assessment would ideally relate biologic response to quantitative stresses generated at the condyle by the applied forces. Such invasive assessment is not feasible in-vivo, whereby the justification for recreating the system experimentally under conditions that mimic the clinical settings.

Table 2.1. A report of the different findings of different authors investigating the mandibular advancement devices affecting the TMJ (Ivorra-Carbonell et al., 2016).

TMJ	Author/year	Q
After treatment with the Twin Block, the condyle occupied a more anterior position. There was no evidence that the Twin Block had a positive or negative effect on disk position, or that the disk was recaptured after the treatment.	Chintakanon <i>et al.</i> 2000 (19)	M
The functional appliances did not cause temporomandibular disorder. The condyles were displaced forwards. Although changes in disk position took place, the differences were not statistically significant.	Arat <i>et al.</i> 2001 (25)	M
No significant changes were found following treatment (Bionator). The TMJ and condyle-disk relationship retained their normal physiological status after treatment.	Watted <i>et al.</i> 2001 (27)	M
Favourable changes in the TMJ were observed in the sagittal plane, but were faster and better oriented for correcting the sagittal problem in the Herbst group than in the Activator group.	Baltromejus <i>et al.</i> 2002 (5)	M
There was no change in the position of the disk, but its shape improved (nearer to its normal biconcave form). The Fränkel appliance can help to avoid future TMJ problems.	Franco <i>et al.</i> 2002 (17)	M
Condylar growth was observed after using the functional appliance.	Güner <i>et al.</i> 2003 (2)	M
Changes in the angle and height of the articular eminence were observed, but were not statistically significant.	Katsavrias <i>et al.</i> 2003 (6)	M
The amount and direction of growth in parts of the TMJ such as the glenoid fossa and condyles were favourably affected, temporarily, in an anterior direction (Herbst).	Pancherz <i>et al.</i> 2003 (21)	M
The changes in the condyle and glenoid fossa were minor and not clinically relevant. The nature of the remodelling of condyle and fossa was not established.	Popovich <i>et al.</i> 2003 (18)	H
Antero-inferior displacement of the glenoid fossa and postero-superior condylar growth were observed. The latter was greater in hyperdivergent patients (Herbst).	Pancherz <i>et al.</i> 2004 (22)	M
No adverse effects were encountered in patients with no pre-existing disorder, and in patients with disorders the disk position improved.	Kinzinger <i>et al.</i> 2006 (28)	M
No change in the condyle-fossa relationship were observed following treatment, and the TMJ remained in a healthy state.	Kinzinger <i>et al.</i> 2006 (7)	M
The treatment has no adverse effects on patients without pre-existing disorders, and in patients with partial or total disk displacement prior to treatment, an improvement in disk position may take place.	Kinzinger <i>et al.</i> 2006 (8)	M
The Van Beek activator contributes to changes in the direction of condylar, maxillary and chin growth.	Ruf <i>et al.</i> 2007 (26)	M
Significant improvements in joints that presented forward disk dislocation.	Kinzinger <i>et al.</i> 2007 (20)	M
The condyle was shifted in a postero-superior direction in the group treated with the Herbst appliance. There were no adverse changes.	Serbesis-Tsarudis <i>et al.</i> 2008 (4)	H
The changes that took place returned to their initial state when the treatment ended, although the condyle and glenoid fossa were remodelled in a more forward position.	Wadhawan <i>et al.</i> 2008 (15)	M
In patients without a pre-existing disorder, no adverse changes took place. There were no changes in disk position or shape following treatment. However, adverse effects in disk shape (from biconcave to not biconcave) were observed in some patients.	Aidar <i>et al.</i> 2010 (1)	M
More anterior condyle position with adaptation of the glenoid fossa morphology and restricted maxillary growth (Herbst).	Le Cornu <i>et al.</i> 2013 (3)	M
The condyles moved forward during the treatment and returned to their initial position when it ended, although somewhat anterior to their pre-treatment location, while the disks presented a more posterior repositioning.	Chavan <i>et al.</i> 2014 (16)	M
Increased condyle volume, mandibular length and inter-condyle distance were observed, but no adverse effects.	Yildirim <i>et al.</i> 2014 (23)	M

Q = quality, M = medium, H = high.

2.5. Finite element analysis

Finite element modeling is a computerized analytical method that aims to construct a virtual (digital/numerical) model with a finite number of elements. The main objective is to test different experiments by imitating real-time occurrences that are otherwise unethical/not possible to test on the actual physical structure. Examples include the construction of a virtual building and simulating the impact of an earthquake. Accordingly, weak corners could be visualized that may allow the structure to collapse under the respective accident. Engineers could simulate loads and analyze stress lines and pressure points to enhance bridge and buildings' ability to sustain the vibrations and constructions. The different combination of metals used in the construction may be implemented to allow for a certain degree of bending to prevent collapse (see Fig 2.10).

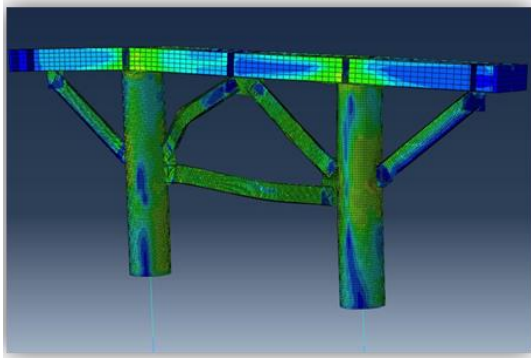


Fig. 2.10: Virtual bridge constructed and put under different physical experiments

Image source: <https://goo.gl/ygKvCw>

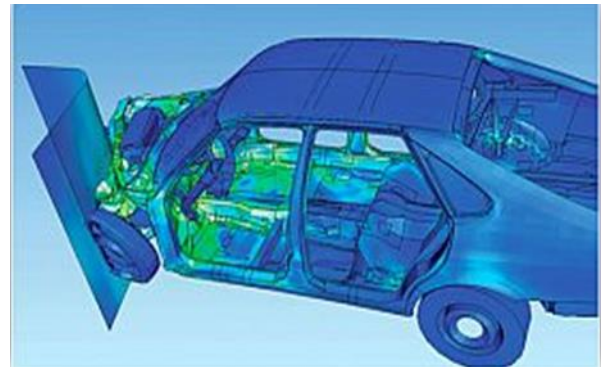


Fig. 2.11: Virtual car put into test simulating accident

Image source: <https://goo.gl/D67d7K>

Other examples include assessment of driver-related safety in car manufacturing. Virtual cars are modeled numerically on-screen and tested in simulating a real-time accident to examine a car's durability and weak points (Fig 2.11.). Adequate information is input in the system, e.g. the car is made of 40% of steel and 20%

aluminum, with each component fed with the most realistic values of stiffness (steel has a stiffness of 9×10^9 Pascal). All information is gathered and computed in the different software databases taking into consideration the different load applications generate the results that include among others deformation, stress, strain, displacement, effective strain

In the medical field, FEA was used to simulate virtual patients on whom experiments cannot be conducted in-vivo. To best simulate the anatomy, the models are often created based on patient X-rays, which are imported into a modeling software that builds models based on DICOM images (Simpleware®). At a later stage, the model is processed and exported into another stress-solver software (Abaqus®) in which the clinically-similar, real-time loads are applied and later analyzed (Fig 2.12.).

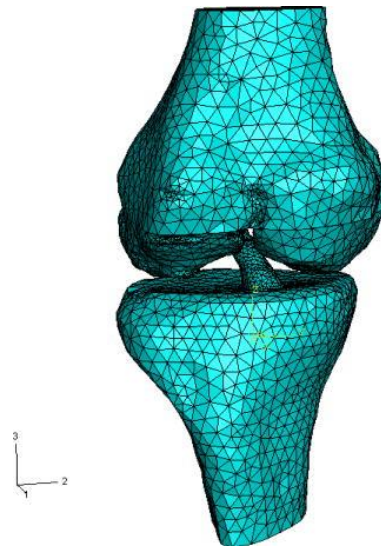


Fig. 2.12: Finite Element Analysis of the human knee. This study was done to investigate the relationship between overall nodal forces and the displacement of the ACL under anterior loads of the tibia (Xie et al., 2009).

2.5.1. Applications in dentistry

In the field of dentistry, FEA has been applied in all dental specialties, including surgical restoration plates (Narra et al., 2014), evaluation of stresses distribution between submerged and non-submerged implants (Dos Santos et al., 2011), and evaluation of retention strength of prosthetic cavity shapes (Asmussen, Peutzfeldt, 2008). Even in geriatric dentistry, FEA was used in studying the patterns of mandibular fractures in edentulous patients (Santos et al., 2015), whereby the authors subjected the mandible to different kind of loads (trauma), from symphyseal, para-symphyseal, and mandibular body regions (Fig. 2.13).

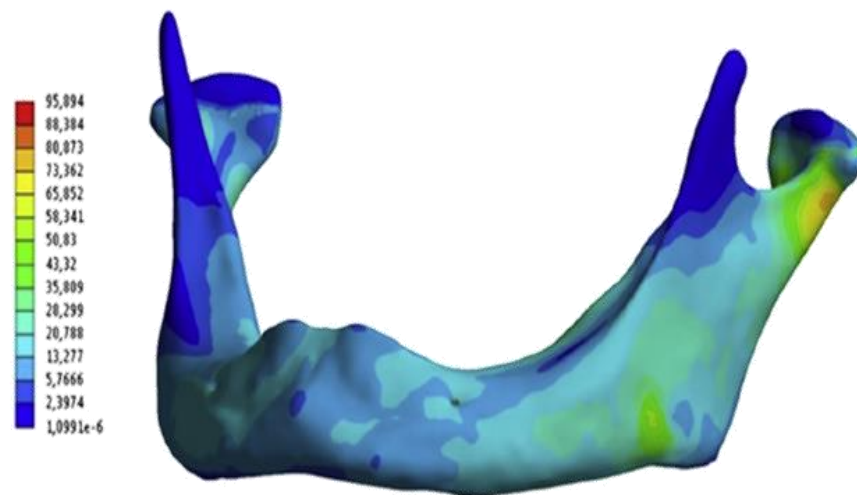


Fig. 2.13: Finite Element Analysis of the dentulous human mandible. Three different loading scenarios are applied onto the mandible to observe its resistance to fracture. In this example, the mandible is subjected to a lateral load (Santos et al., 2015).

In restorative dentistry, FEA has contributed in solving questions related to occlusal loading. Ichim et al. (2007a) investigated the relations of cavity shape, depth and occlusal forces with durability of glass ionomer restoration. They concluded that depth and shape have no significant effect on restoration and emphasized the re-adjustment of the interocclusal contacts for better retention of restoration. In another

FEA article, the same authors, using nonlinear technique for crack propagation, aimed to demonstrate the mechanical failure of biomaterials in clinical loading conditions. In further studies on elastic modulus of materials, the authors stated that more flexible materials with elastic modulus of 1 GPa should be used for cervical restorations to obtain the better results (Ichim et al., 2007b).

FE analysis included implant studies, one of which is representative, reporting on a comparison of different commercial brands. The authors investigated different propagation of stress lines and pressure points into the neighboring trabecular bone around the implants (Fig. 2.14). Different dental implant designs were modeled under similar loading scenarios (Gupta et al., 2009). As a result, the Straumann bone-levelled implant showed the least amount of stresses at the color of the implant. On the hand, the Straumann tissue-levelled implant showed the highest stresses at its collar.

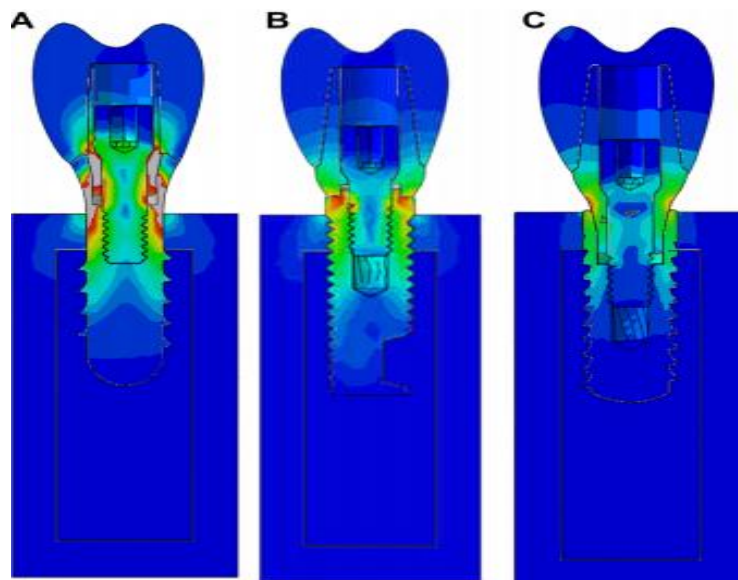


Fig. 2.14: Finite Element Analysis of various types of implants. **A.** Straumann tissue-levelled implant; **B.** NobelBiocare MK III tissue-levelled implant; **C.** Straumann bone-levelled implant. Same loading scenarios angulated at 30° are applied onto the different implant types (Gupta et al., 2009).

2.5.2. Applications in temporomandibular joint studies

Explorations of the TMJ complex articulation have been less elaborate than other FE dental models because it is more difficult to morph and simulate. Of the available studies is an examination of the human mastication cycle through FEA (Commisso et al., 2015). One of the highlights of this report was the ability to model and account for the mastication muscles and ligaments (Fig. 2.15). The authors examined the contribution of muscles during this cycle, and the stress generated on the

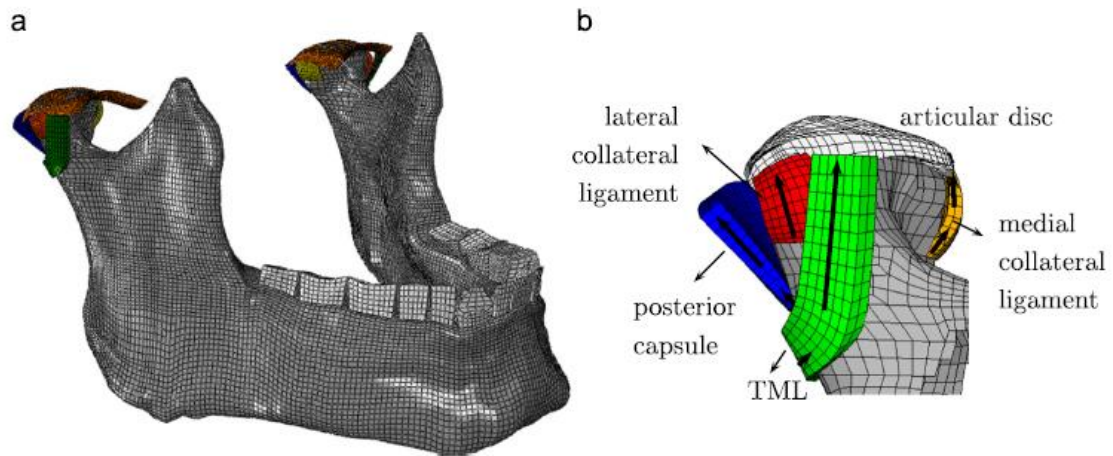


Fig. 2.15: Finite Element Analysis of various types of implants. **A.** Full FE model of the mandible; **B.** In detail exploration of the TMJ (Commisso et al., 2015)

mandibular body during function.

Not only has the mastication cycle been studied in FE analysis, but also, the effect of premature contacts during maximum intercuspation (Kayumi et al., 2015). The influence of occlusal forces (the contractile force of masticatory muscles) exerted during occlusal adjustment was simulated by applying three kinds of maximum biting forces (40 N, 200 N, and 400 N). The studied parameters were stress distribution of the forces among teeth, dental implants, and temporomandibular joint in intercuspation clenching.

Other studies aiming to explore the TMJ function investigated the stress distribution in the joint during anterior disk displacement upon maximum clenching (Tanaka et al., 2000). The standard model used was from a healthy young cadaver; two other models were designed to simulate various degrees of anterior disk displacements (Fig. 2.16).

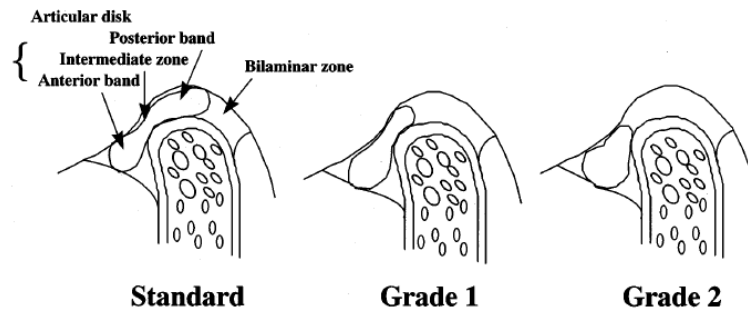


Fig 2.16: The standard model is represented using the healthy cadaver as well as two other simulated models with various degrees of anterior displacement (Tanaka et al., 2000).

Significantly higher stresses were reported in the situation where the disk was displaced anteriorly (Fig 2.17).

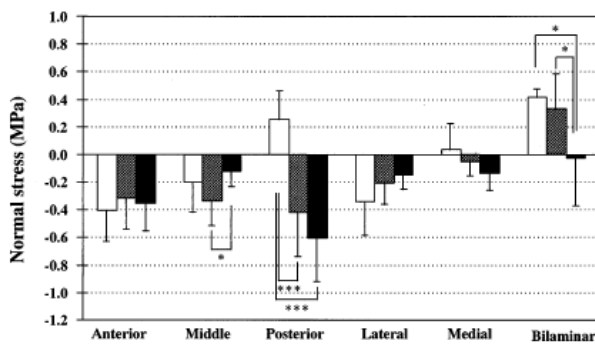


Fig 2.17: In the standard model, stresses are more anterior compared to the models where the disk is displaced anteriorly. In the latter, the stresses occur differently from the normal situation (Tanaka et al., 2000).

Different removable dental prosthesis designs and stress distribution patterns were studied in FE analysis (El-Zawahry et al., 2015). To explore the TMJ function in patients wearing acrylic splints, the authors used a CT scan of an edentulous patient upon which an acrylic splint was constructed. They concluded that a stiffer acrylic splint

may be required to better distribute the stresses along the alveolar border of the mandible to reduce stress levels on the articular disk.

2.5.3. Applications in Orthodontics

Among all disciplines in dentistry, orthodontics is amenable to exploration with FE modeling because of its reliance on engineering mechanical principles, whereby force systems are established relative to centers of resistance, engendering bodily movements, pure rotations, and moments of forces. Tooth movements and applications of orthopedic appliances are primary examples.

The behavior of the PDL along with other element of the human maxilla were subjected to different testing scenarios (Cattaneo, 2005). The conclusion was that the loading of the periodontium by orthodontic forces cannot be explained in simple terms of compression and tension along the loading direction but rather the effect is more complex and propagates in different directions (Fig. 2.18).

FEA was most explored in tooth movement studies because of detailed and accurate representation of the force systems with corresponding different reactions. Most experiments involved a limited number of teeth to predict a pattern of stresses respective to each movement (Rudolph et al., 2001, Nihara et al., 2015) (Fig. 2.19).

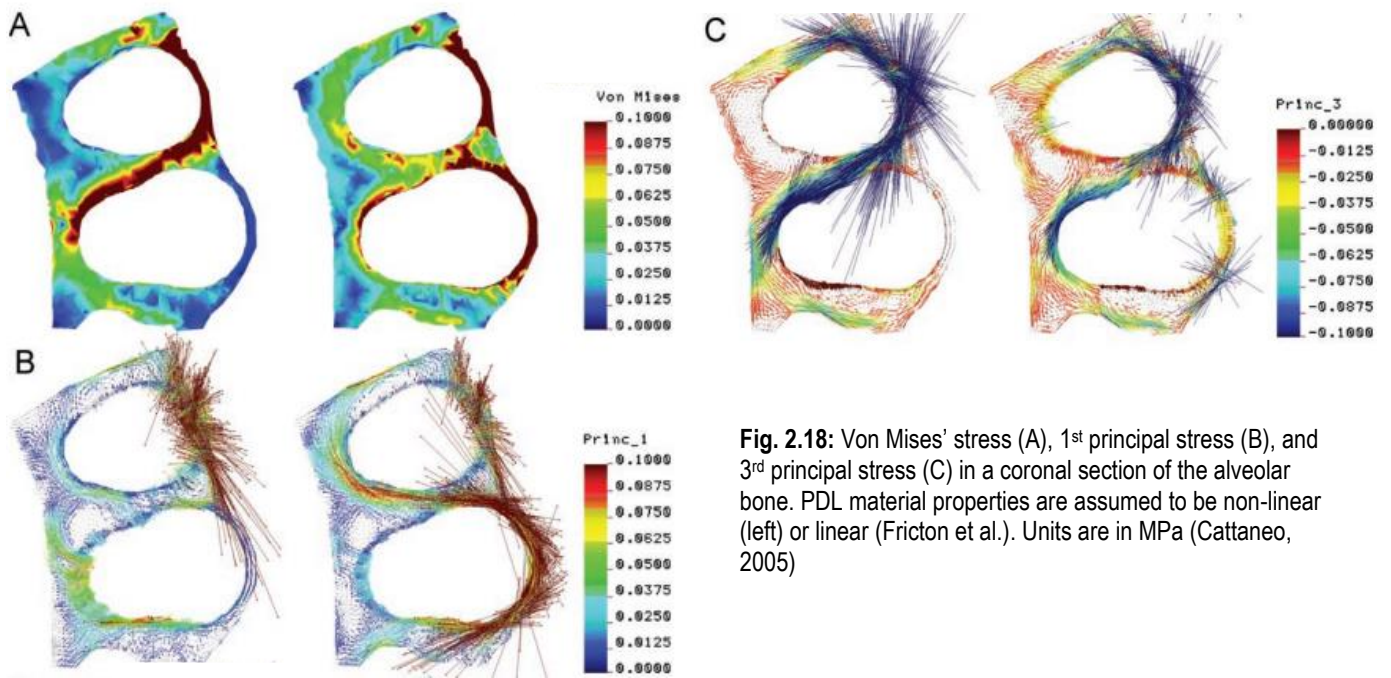


Fig. 2.18: Von Mises' stress (A), 1st principal stress (B), and 3rd principal stress (C) in a coronal section of the alveolar bone. PDL material properties are assumed to be non-linear (left) or linear (Fricton et al.). Units are in MPa (Cattaneo, 2005)

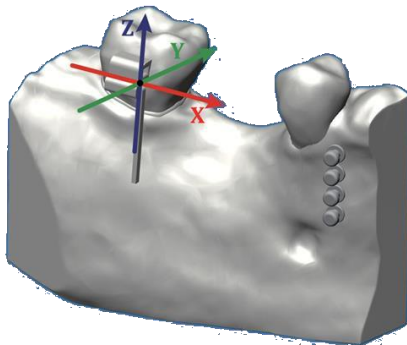


Fig. 2.19: Mandibular molar protraction. The force is directed differently at 4 levels. The simulated miniscrews mesial to the premolar serve as anchorage to specify the direction of the pull. (Nihara et al., 2015)

Other studies have focused on the effects caused on a group of teeth by specific appliances, such as the headgear distalizing the maxillary teeth (Maruo et al., 2016) and the distalisation of maxillary teeth against miniscrews with corticotomy assisted movements (Yang et al., 2015) (Fig. 2.20).

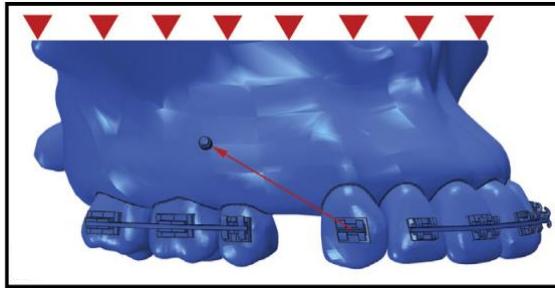


Fig. 2.20: Maxillary retraction of the canine after extraction of the 1st premolars. Long arrow shows the direction of the pull against the miniscrew. Top multiple arrows show the boundary conditions of the maxillary model. (Yang et al., 2015)

Few studies evaluate the condyle as an entity throughout the different orthodontic force scenarios. Mostly, during therapies like mandibular advancement devices and orthodontic elastics, the condyle is sought to be at risk of sustaining levels of stresses. In a study on the effect of mandibular protraction devices on the TMJ complex (Gupta et al., 2009), the condyle was shown to experience high levels of stress indicating possibilities of resorptive phenomena (Fig 2.21). Another protraction scenario was simulated with a Herbst appliance (Hu et al., 2001), but the article lacked concrete findings related to stress distribution around the condyle, in addition difficult reporting in Chinese language.

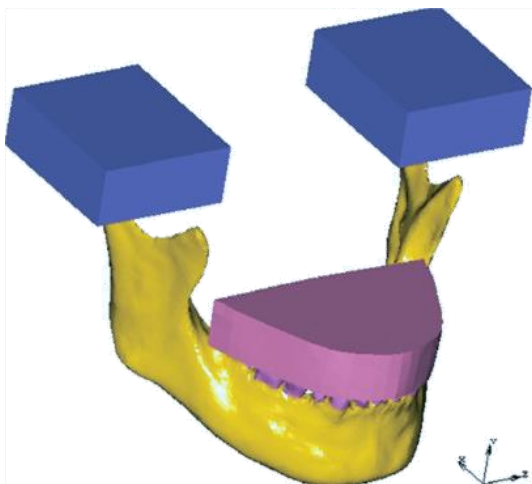


Fig. 2.21: Mandibular protraction device: the Class II activator is simulated and modeled on the mandibular teeth giving a mesial direction of movement. Boundary conditions are applied on the TMJ to simulate the fixed position of the cranial base. (Gupta et al., 2009)

A more recent article analyzing mandibular protraction (Shrivastava et al., 2015), investigated through FEA the stress patterns in the TMJ during mandibular protraction applied with different horizontal advancements and keeping the vertical height constant in a construction. The anterior part of the condyle and the glenoid fossa experienced compressive stresses, whereas tensile stresses in the posterosuperior aspect of the condylar head and on the posterior aspect of the glenoid fossa shifted more posteriorly with increased bite advancements. The magnitude of stress increased with sagittal bite advancements.

Specific scenarios, like juvenile arthritis, were also evaluated through FEA (González, 2015). The authors examined condylar and mandibular growth in juvenile arthritis patients treated with a distraction splint assessed on 3D images. The simulation showed a greater physical degeneration on the affected side.

Stress distribution in the TMJ during chin cup therapy was investigated in a three-dimensional FE model of the mandible. Tensile stresses were induced in the anterior region of the articular disk, irrespective of force direction, although the remaining areas experienced compressive stresses. The authors adjusted the angulations of the forces to examine the different responses on the TMJ complex. When the directional angle was around -50° , the variation in stresses in the TMJ was greatest. As the angle was changed to 30° or 40° , the stresses approached a certain level of compressive stress, which indicated the optimal direction of chin cup force in relation to biomechanically balanced stress distribution for the TMJ components (Tanne et al., 1996, Tanne et al., 1993).

The TMJ was also explored in scenarios of mandibular distraction of the ramus, (Katada et al., 2009). Stress generation from unilateral horizontal lengthening of the

mandibular body and vertical lengthening of the mandibular ramus were studied. Under both loading conditions, stress distribution around the TMJ was greater on the loading side compared to the non-loading side. However, compared to horizontal lengthening, stress was greatest on the affected side during mandibular vertical ramus lengthening (Katada et al., 2009).

2.6. Aims, objectives and hypothesis

2.6.1. Aims

In the past three decades, finite element analysis has emerged as a numerical computer-generated tool that allows the study of clinical scenarios not amenable to direct and precise assessment (Cattaneo, 2005). FEA has proven to be helpful in health care research. Although several studies include numerical experiments on the TMJ, none, in the English literature have addressed the effect of stresses generated by interarch elastics on the condyle and the teeth. Accordingly, the aim of this thesis project was to investigate the effects of orthodontic interarch elastics on the TMJ complex and the mandibular teeth.

Secondary objectives were to:

- Investigate differences of stress generation with the CI II elastics delivered from the mandibular 2nd molars compared to CI II elastics from the mandibular 1st molars.
- Compare the effects generated by CI II versus CI III elastics on the TMJ complex and the mandibular teeth
- Evaluate the amount of Von Mises stresses dissipated on the condyle versus the mandibular teeth

- Analyze dental displacements in response to the applied interarch elastics
- Quantify the variation of stresses and displacements under variations of stiffness and thickness of mandibular cortical parts
- Attempt the identification of patterns of response with potential negative effect on the TMJ discomfort following application elastics

2.6.2. Hypothesis and significance

Our main hypothesis was that CI II and CI III elastics create different effects on the TMJ complex. Under different engineering parameters, variations of stiffness and thickness (volume), differences in the stress responses are expected. Also, elastic configurations with the most sagittal direction of force may be associated the most with condylar interference.

The main contribution is quantifying in an objective method the amount of stress generated on both the teeth and the TMJ in the different facial configurations of mandibular cortical bone. This objective will be tested with the fabrication of a 3D virtual model to test clinical applications, forces and stresses that cannot be tested on an actual patient in a clinical setting. To date, such variation has not been incorporated into finite element analysis studies and should shed light on the simultaneous effects of the elastics on dentition and TMJ. This knowledge should indicate patterns of response that are more advantageous and physiologic in orthodontic treatment, and further reveal future tracks of meaningful research. In this context, specific clinically relevant findings would be to determine which elastics would generate the least amount of pressure on the condyles and respond better to occlusal clinical needs.

CHAPTER 3

MATERIAL AND METHODS

3.1 Material

3.1.1. Anatomical record

Pretreatment cranial CBCT scan, in DICOM format, of an adult patient seeking orthodontic care at the Division of Orthodontics and Dentofacial Orthopedics at the American University of Beirut Medical Center was used for 3D model generation.

The following criteria were basis for selection:

- Young adult with a healthy dentition (DMFT score = 0).
- Relatively well-aligned arches with parallel roots.
- Normal divergence pattern ($25^{\circ} < PP/MP < 29^{\circ}$).
- Full permanent dentition (at least 2nd molar to 2nd molar in both arches).
- At least one side in a CI I (left side) while the other was in CI II occlusion (where elastics can be applied)
- Maxillary and mandibular midlines are off (allowing for use of parallel elastics e.g. CI III and CI II on each side)

Characteristics for exclusion were:

- Craniofacial anomalies (e.g. condylar hyperplasia, hemifacial macrosomia...).
- Previously undergone orthodontic treatment.
- Crowded teeth.
- Missing or extracted teeth.
- Medical conditions involving structures of the oro-facial complex (e.g. cleft lip/palate).

- Limited field-of-view CBCT image, with a resolution that doesn't allow to distinguish the different structures (e.g. cortical bone, trabecular bone...).

Although both diagnostic x-rays, CT or CBCT scan offer valuable exploration possibilities of the bony and dental structures, CT scan have higher resolution with greater possibility of varying the contrast to better visualize bone density. In the current study, a high resolution CBCT with small voxel size was used, providing better quality than the conventional CBCT, with better ability to systematically differentiate bony structures, cortical and trabecular bones through the different cross-sections. The used CBCT also had a small cross-section (voxel size 0.3 x 0.3 x 0.3mm) with high contrast, allowing for better anatomical reproduction during the 3D model re-construction. The patient name was blinded and the DICOM image was imported for image processing.

3.1.2. Patient variation and data collection process

Variations of individual data were collected from a 10 cadavers study by Schwartz-Dabney, Dechow on the “variations in cortical material properties throughout the human dentate mandible” (2002), which was supported by The National Institutes of Health (NIH), National Institute of Dental and Craniofacial Research (NIDCR); Grant sponsor: VA Dental Research Fellowship; Grant sponsor: NIH; Grant numbers: DE05691, DE07256.

Measurements such as site-specific thickness and stiffness of cortical bony sections were imported to the finite element modeling softwares for study.

The main objective of the study by Schwartz-Dabney, Dechow was to investigate the individual physical characteristics of the cortical bone of the dentate mandible. The null hypothesis was that there was no statistically significant difference

between the various mandibular regions (and corresponding specimens). Their rationale was that these different areas undergo variant tension and compression conditions; accordingly, they would exhibit different physical properties to resist such conditions.

Buccal and lingual specimens were removed from 62 different areas of the mandibular cortical sections (Fig 3.1.1). The sample consisted of 10 Caucasian cadavers of both genders (7 males and 3 females), aged 48-81 years. The cadavers were selected from donations to the willed body program at the University of Texas Southwestern Medical School, based on the following criteria.

- Posterior vertical molar support bilaterally.
- Minimum of 12 mandibular teeth (allowing for missing third molars and two other teeth, either two non-adjacent teeth).
- No documented history of bone disease.
- Availability of basic demographic and medical data.

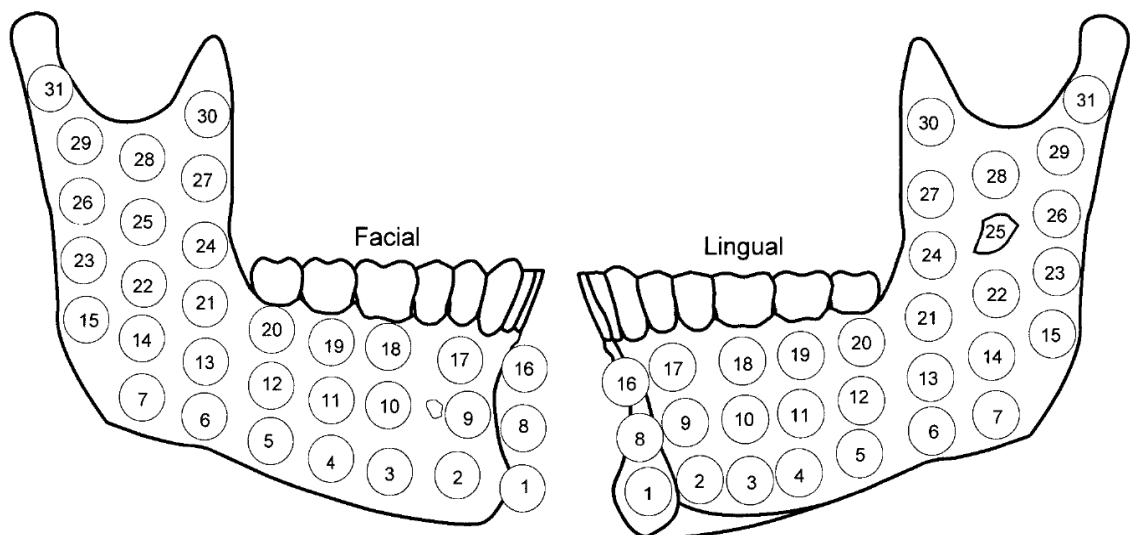


Fig 3.1.1 Thirty-one samples were taken from both the facial and lingual cortices of the human mandible. Samples from sites 1, 8, and 16 were taken from sympheseal midline (*Schwartz-Dabney & Dechow, 2003*).

The heads were embalmed and frozen. The freezing process has minimal effects on the elastic properties of bone compared to the larger effects of embalming (Schwartz-Dabney & Dechow, 2003). Bone cylinders were harvested from the left mandibular cortex, and the cancellous bone on the inner surface of the cortical specimens was removed.

The samples were stored in a solution that maintains the elastic properties of cortical bone over time, consisting of equal parts ethanol (95%) and isotonic saline (Ashman, Cowin, Van Buskirk, & Rice, 1984; Schwartz-Dabney & Dechow, 2003).

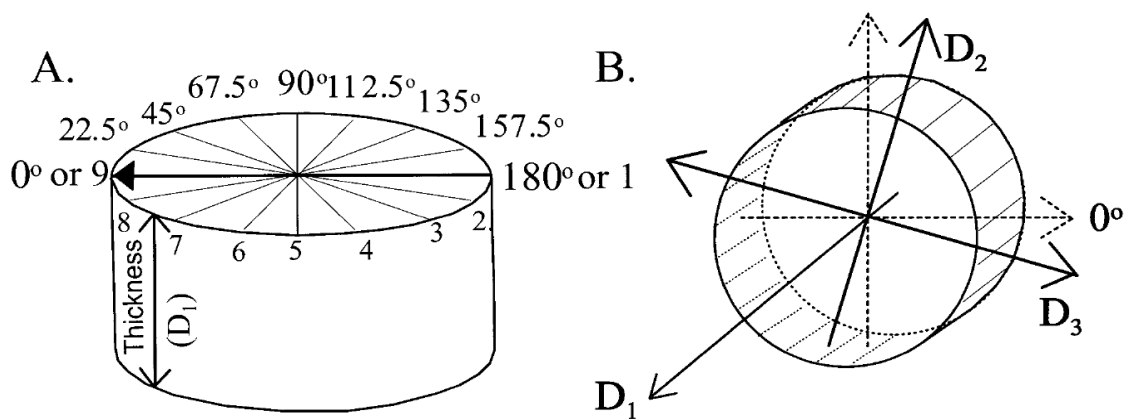


Fig 3.1.2 Bone cylinders represent a cortical plate specimen. Cortical thickness was identified as D1. **A.** Arrow parallels occlusal plane. Measurements were taken at angular rotations of 22.5° to determine orientation of principal axes. **B.** D3: axis of maximum stiffness; D1: axis of minimum stiffness (Schwartz-Dabney & Dechow, 2003).

The thickness of each bone specimen was measured with a Max-Cal digital caliper. Cortical thickness was defined as the thickness from periosteum to the cortical-trabecular interface. Densities were calculated using Archimedes' buoyancy principle (Ashman et al., 1984) from weight measurements made with a Mettler PM460 analytical balance and densitometry kit.

Ultrasonic velocities were measured with a pulse transmission technique (Ashman et al., 1984; Ashman & Van Buskirk, 1987; Dechow, Nail, Schwartz-Dabney, & Ashman, 1993). Ultrasonic waves were generated with a Hewlett-Packard pulse generator and two sets of mounted piezoelectric transducers (2.25 MHz longitudinal, Panametrics V323-SU, and 5.0 MHz shear, Panametrics V156-RM). Both longitudinal and transverse ultrasonic waves were passed through various axes, including the principal axes (D2 and D3) and the cortical thickness (D1) of each specimen (Fig. 3.1.2).

The direction of each axis was defined as follows:

- The axis of maximum stiffness (**D3**) corresponded with the direction of peak ultrasonic velocity and was parallel to the long axis of the specimen.
- The axis of minimum stiffness (**D2**) was perpendicular to the axis of maximum stress within the specimen of cortical plate.
- The cortical thickness axis (**D1**) was perpendicular to the planes of both D3 and D2, and cut through the thickness of the specimen.

Time delays were measured using an oscilloscope (Tektronix TDS 420) to make a phase comparison of the signal before and after its transmission through a specimen. Ultrasonic velocities were calculated by dividing the specimen thickness or diameter by the apparent time delay minus the system time delay.

The elastic properties were calculated from ultrasonic velocities, using a program written in Mathcad. The equations for these calculations were based on mathematical relationships derived from the principles of linear elastic wave theory and Hooke's law (Ashman et al., 1984). Ultrasonic velocities and densities were used to calculate 6 _ 6 matrices, or "C" matrices, including 8 unique elastic coefficients (c_{11} ,

c_{22} , c_{33} , c_{44} , c_{55} , c_{66} , c_{12} , and c_{23}) and then technical constants (elastic and shear moduli, and Poisson's ratios). In essence, Young's modulus or the elastic modulus (E) measures axial stiffness or the amount of deformation (strain) of a specimen, under an applied load (stress). Subscripts, as in E_1 , E_2 , or E_3 , indicate the appropriate axis for each elastic modulus illustrated (Table 3.1.1).

Poisson's ratio (ν_{ij}) is a measure of stiffness of a structure perpendicular to that of the applied load. It is a ratio of the strain in the secondary direction (response direction) divided by strain in the primary direction (applied load direction). The first subscript indicates the axis of the applied load and the second subscript indicates the response direction as in ν_{12} , ν_{13} , ν_{21} , ν_{23} , ν_{31} , and ν_{32} .

As defined by Schwartz-Dabney, Dechow (2002), shear modulus (G) (Table 3.1.1) measures stiffness in shear or angular deformation relative to applied shearing loads in a plane between two axes indicated by the subscripts (G_{12} , G_{31} , or G_{32}).

TABLE 4. Elastic and shear moduli (in GPa) for human dentate mandibles¹

St	Sd	Area	E ₁		E ₂		E ₃		G ₁₂		G ₃₁		G ₂₃	
			Mean	SD	Mean	SD	Mean	SD	Mean	SD	Mean	SD	Mean	SD
1	F	Sym	12.1	2.0	14.8	1.3	22.0	4.2	4.4	0.9	4.7	0.5	6.3	0.8
2	F	Sym	11.8	1.4	15.9	1.9	21.4	4.2	4.7	0.6	5.2	0.7	7.2	0.7
3	F	Infbor	12.3	1.7	16.6	2.3	23.0	3.1	4.9	0.9	5.5	0.8	7.7	0.8
4	F	Infbor	13.0	1.8	17.9	1.7	25.0	4.3	5.0	0.5	5.6	0.7	7.8	0.9
5	F	Infbor	12.1	1.2	18.4	2.3	21.8	3.8	4.9	0.3	5.6	0.6	7.6	0.8
6	F	Angle	11.2	0.9	17.3	1.5	19.1	3.3	4.8	0.4	5.2	0.4	7.6	0.3
7	F	Angle	11.5	1.1	18.8	2.9	21.1	5.5	4.6	0.4	5.0	0.2	6.9	0.7
8	F	Sym	11.0	1.2	15.8	2.8	19.5	4.6	4.3	0.5	4.8	0.6	6.4	0.8
9	F	Sym	11.5	1.2	14.6	1.5	19.8	4.0	4.6	0.4	5.2	0.6	7.2	0.9
10	F	Midbod	11.9	2.2	18.0	2.9	20.3	5.7	4.8	0.5	5.4	0.9	7.4	1.3
11	F	Midbod	13.0	1.3	17.6	3.0	22.5	5.6	5.1	0.5	5.8	0.5	7.6	0.6
12	F	Midbod	13.7	1.4	19.2	1.3	24.2	4.5	5.3	0.7	5.8	0.7	7.9	0.5
13	F	Midram	13.6	1.6	19.3	1.5	25.5	4.5	5.0	0.3	5.9	0.5	7.8	0.6
14	F	Angle	14.0	1.7	19.8	2.3	28.5	5.5	5.2	0.8	5.8	0.7	7.9	0.3
15	F	Posbor	13.2	1.0	17.0	1.6	25.1	3.1	4.8	0.5	5.5	0.7	7.4	0.7
16	F	Sym	11.2	1.1	14.8	2.6	18.3	4.3	4.5	0.7	4.7	0.6	5.7	0.7
17	F	Sym	11.5	1.6	16.4	2.1	19.0	4.5	4.9	0.9	5.3	0.8	6.6	0.7
18	F	Alv	13.0	1.9	18.7	1.8	22.2	4.1	5.2	0.6	5.4	0.5	7.5	0.7
19	F	Alv	13.8	2.8	17.6	2.7	23.8	6.8	5.3	0.7	5.8	0.7	7.6	0.6
20	F	Alv	14.1	2.1	18.4	2.1	26.2	6.9	5.4	0.7	5.9	0.8	7.9	1.0
21	F	Midram	14.3	1.8	20.5	2.4	27.8	4.8	5.1	0.6	5.8	0.5	8.2	0.6
22	F	Midram	12.9	1.9	18.6	1.6	23.5	4.7	5.3	0.8	5.7	0.9	7.8	0.8
23	F	Posbor	14.0	2.0	18.8	1.8	27.3	6.5	5.4	0.7	5.6	0.4	7.8	0.7
24	F	Midram	12.9	1.0	19.3	1.4	22.7	4.6	4.9	0.6	5.4	0.7	7.7	0.5
25	F	Midram	12.9	1.7	19.9	1.1	23.8	5.1	5.2	0.5	5.6	0.5	7.6	0.7
26	F	Posbor	13.7	1.9	18.6	1.7	25.9	7.2	5.2	0.4	5.5	0.5	7.6	0.7
27	F	Cor	13.9	1.8	20.2	2.2	27.3	5.2	5.2	0.6	5.7	0.4	7.8	0.7
28	F	Midram	11.5	1.8	19.3	2.6	19.6	3.4	5.0	0.5	5.5	0.7	7.7	0.7
29	F	Cond	13.3	1.7	17.7	1.3	26.6	5.5	4.9	0.6	5.5	0.3	7.7	0.5
30	F	Cor	14.1	2.1	18.9	1.8	29.8	6.4	5.2	0.4	5.8	0.7	7.5	0.7
31	F	Cond	13.1	1.7	18.3	1.5	25.3	4.1	5.2	0.6	5.6	0.7	7.2	0.4
1	L	Sym	12.2	2.3	16.6	2.1	18.5	4.7	5.2	0.6	5.9	0.8	7.1	1.0
2	L	Sym	13.0	2.3	16.9	1.4	21.1	5.5	5.2	0.7	6.0	0.7	7.6	0.8
3	L	Infbor	12.9	2.1	17.0	3.4	22.0	6.6	5.1	0.6	5.7	0.4	7.6	0.9
4	L	Infbor	12.3	2.0	17.7	2.3	21.0	3.2	5.0	0.7	5.5	0.8	7.5	0.8
5	L	Infbor	12.5	1.7	18.8	1.3	20.7	3.1	5.0	0.6	5.4	0.6	7.8	0.6
6	L	Angle	12.7	1.8	20.2	2.6	22.9	4.1	5.0	0.6	5.5	0.6	8.0	0.7
7	L	Angle	12.6	1.1	18.6	2.5	22.3	4.5	5.1	0.5	5.4	0.6	7.5	0.8
8	L	Sym	13.1	1.7	17.5	1.5	22.0	5.2	5.0	0.5	5.7	0.5	7.2	0.8
9	L	Sym	13.2	1.4	17.9	1.5	22.8	6.2	5.3	0.4	5.7	0.4	7.6	0.7
10	L	Midbod	12.1	1.3	19.2	2.2	20.1	3.7	4.9	0.3	5.5	0.5	7.6	0.8
11	L	Midbod	11.7	1.6	18.1	2.4	17.9	2.6	5.0	0.5	5.4	0.6	7.0	0.8
12	L	Midbod	11.6	1.9	18.0	3.2	19.0	3.7	5.1	0.7	5.0	0.6	7.1	0.8
13	L	Midram	12.4	1.3	19.6	1.6	20.0	2.5	5.1	0.6	5.1	0.7	7.4	0.6
14	L	Angle	13.2	2.4	21.1	2.1	26.4	6.3	5.0	0.5	5.8	1.1	8.1	0.4
15	L	Posbor	12.1	1.3	17.3	2.6	26.7	5.3	4.5	0.5	5.2	0.5	6.7	0.6
16	L	Sym	12.1	1.5	17.7	1.8	19.5	3.7	4.9	0.6	5.1	0.6	6.5	0.4
17	L	Sym	12.4	1.6	17.3	2.5	22.0	6.0	4.9	0.6	5.5	0.7	7.5	0.6
18	L	Alv	13.4	1.2	16.3	2.0	21.4	3.0	5.2	0.7	5.5	0.4	6.9	0.5
19	L	Alv	12.6	1.9	16.2	2.6	20.2	5.0	5.2	0.6	5.3	0.5	6.8	0.6
20	L	Alv	12.6	2.1	17.2	1.9	19.8	4.3	5.1	0.7	5.5	0.6	6.8	0.6
21	L	Midram	12.5	1.6	19.0	2.2	22.4	3.0	5.0	0.6	5.6	0.6	7.5	0.7
22	L	Midram	12.4	1.9	19.1	3.4	21.8	5.5	5.3	1.0	5.4	0.7	7.3	0.8
23	L	Posbor	12.9	1.8	18.2	2.3	25.9	4.7	4.9	0.5	5.2	0.6	6.9	0.7
24	L	Midram	12.8	2.0	18.2	2.8	24.1	5.5	5.0	0.8	5.3	0.6	7.3	0.7
25	L	Midram	12.1	2.1	17.7	2.5	23.7	6.7	4.8	0.4	5.2	0.6	6.9	1.0
26	L	Posbor	12.5	1.4	16.5	2.9	23.2	4.3	4.7	0.7	5.0	1.0	6.8	0.8
27	L	Cor	12.6	1.5	18.4	1.7	24.8	5.2	5.0	0.2	5.1	0.7	7.4	0.5
28	L	Midram	13.4	1.4	16.1	2.4	23.1	3.0	5.0	0.4	5.5	0.7	7.0	1.1
29	L	Cond	13.1	1.1	18.1	1.9	26.5	4.1	5.0	0.5	5.3	0.5	7.5	0.7
30	L	Cor	13.9	2.7	16.1	0.8	26.2	9.4	5.4	0.6	5.7	1.0	6.8	1.3
31	L	Cond	12.2	1.5	17.4	2.0	21.7	4.9	5.1	0.8	5.4	0.7	7.1	0.5

1 St, site; Sd, side; F, facial; L, lingual; Sym, symphysis; Infbor, inferior border; Midbody, midbody; Alv, alveolar process; Cor, coronoid

process; Cond, condylar process; Midram, middle of ramus; Posbor, posterior border.

* No significant orientation within a site.

3.2. Methods

The raw CBCT DICOM image of the selected patient was converted into a 3D model that could ultimately be processed by the engineering software. The steps followed from X-ray acquisition to stress evaluation are illustrated Fig 3.2.1. The process essentially consists of two parts. Part 1 includes the Model Generation using the ScanIP® 7.0 program (Simpleware Ltd., Exter UK), where a numerical model is modeled using a CBCT image. Part 2 consists of importing the fabricated model into the stress solver program Abaqus Simulia®. At this stage, the model is configured and the loading scenarios are applied, whereby the model is observed and data is collected about the behavior of the model under the tested settings.

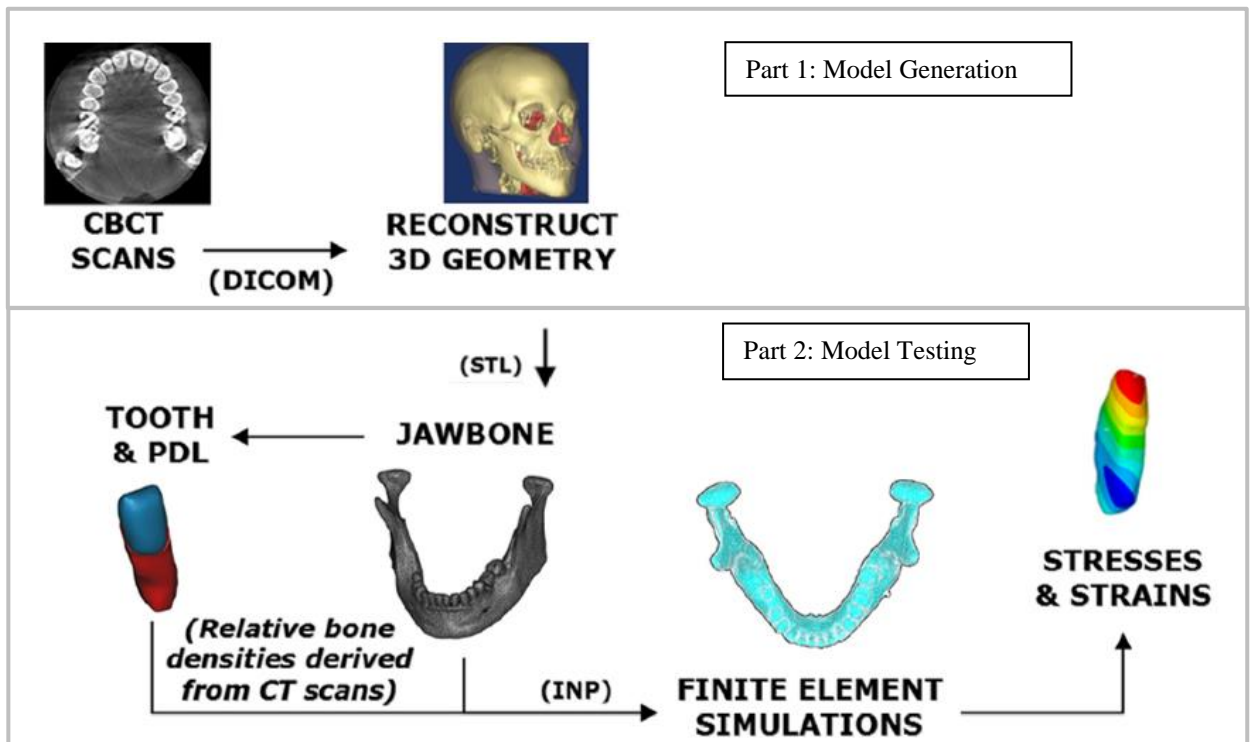


Fig. 3.2.1 The approach for 3D patient-specific model reconstruction and FE simulation of tooth and PDL from in-vivo CBCT scans. (Adapted from Ammar et al 2011)

3.2.1. Image importing and model recognition

The initial step of image importing and processing was conducted with the digital reconstruction software ScanIP™ 7.0 (Simpleware Ltd., Exter UK). The CBCT image was cropped and saved in the 3D modeling program. Areas of interest (ROI) were set and non-significant areas deleted (Fig. 3.2.2).

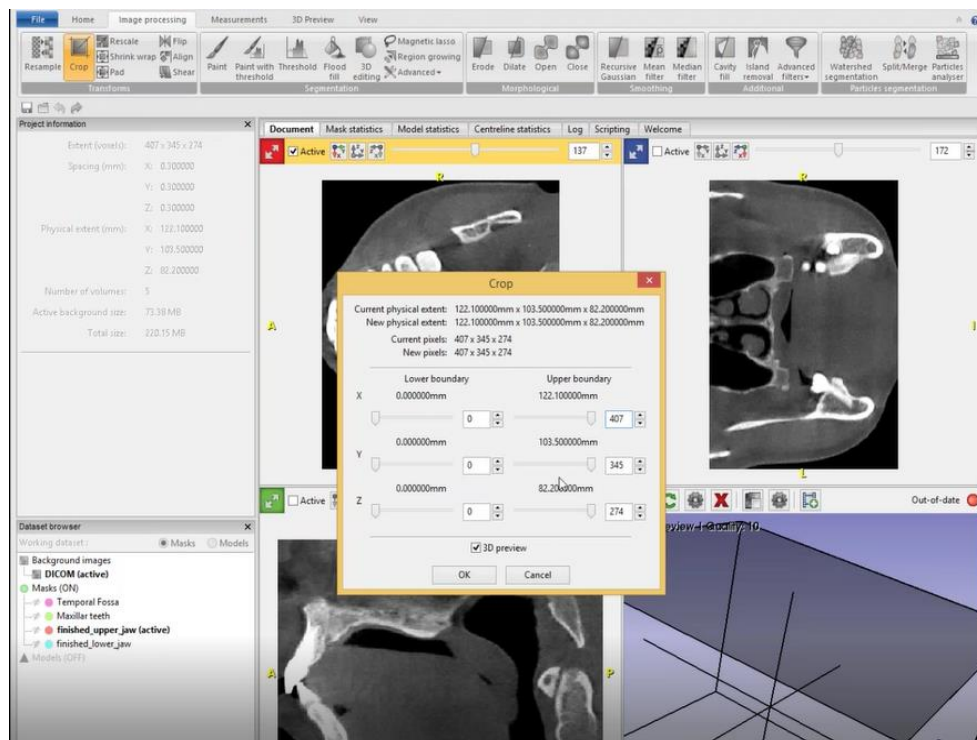


Fig 3.2.2 Initial capturing the CBCT image in DICOM format. Region of Interest (ROI) is selected and the other boundaries of the X-ray are deleted. Cropping defines the ROI to transformed into a 3D model

Every element/member of the model was designed by creating its specific mask. Initial capturing of the volumes of the elements was achieved with automated tools (e.g. *Segmentation with Threshold* tool) that allow for better capturing of element volumes of selected ROI's (Fig. 3.2.3).

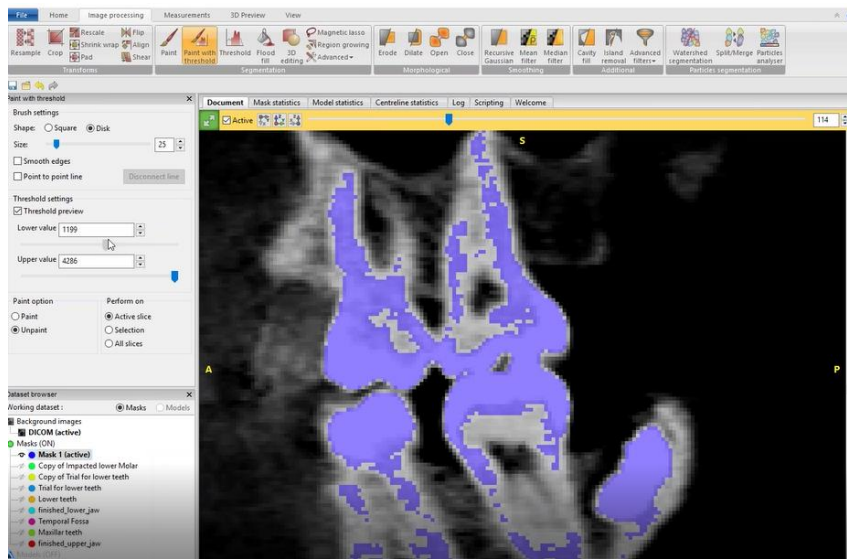


Fig 3.2.3: Initial capturing of the teeth mask with the *Segmentation with Threshold* tool.

Consequently, the modeled/illustrated regions were edited manually either with 3D editing tool (Fig 3.2.4), a pixel manual selection and de-selection tool (Fig 3.2.5), or a combination of both. this process provided a maximum coverage of all ROI's, starting with a general encompassing of all voxels and then manually removing undesirable ones.

3.2.1.1. Teeth mask:

Representing the ‘primary mask’, the teeth were modeled first. Also, by priority, the dental mask should be deducted from other masks during the modeling process (as detailed in the next sections). Given that the teeth had similar attenuation properties of the X-ray, they were all identifiable with the *Segmentation with Threshold*, initially capturing the combination of all the sets of teeth, later to be individually processed and edited (Figs. 3.2.3-5).

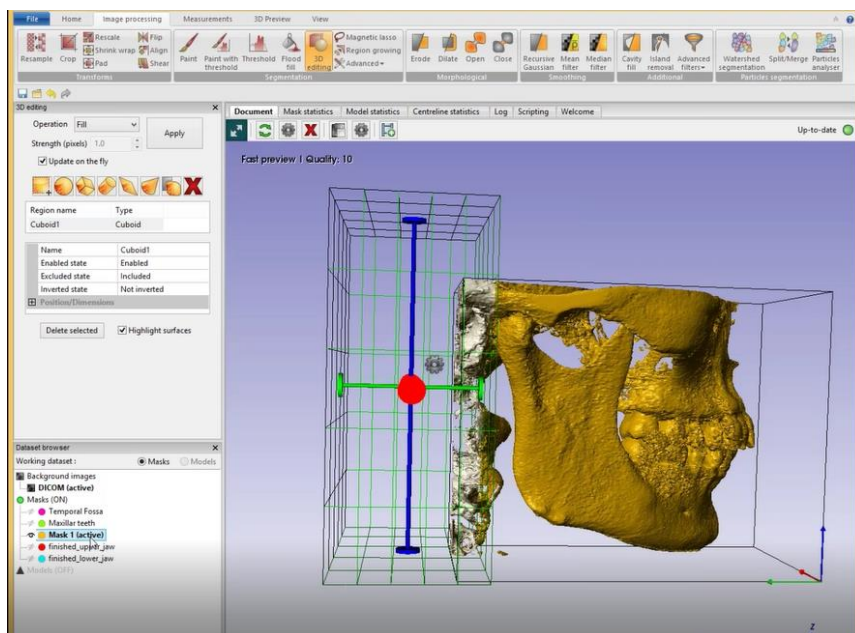


Fig 3.2.4: Initial modeling the CBCT image with *Segmentation with Threshold* tool. Editing is done with *3D editing* tool to delete undesirable elements.

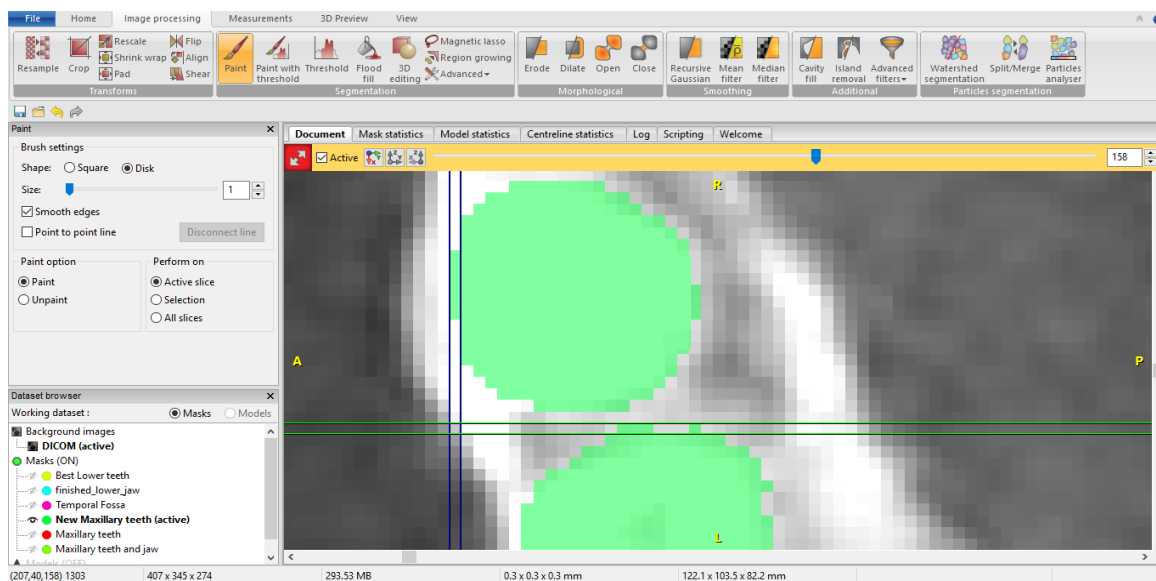


Fig 3.2.5: *Paint* tool allows for manual selection of pixels per Greyscale reference of the DICOM image.

More editing options included the *Open/Close* tool, to separate or close two adjacent masks closely located (Fig. 3.2.6) into distinguishable elements (Fig 3.2.7).

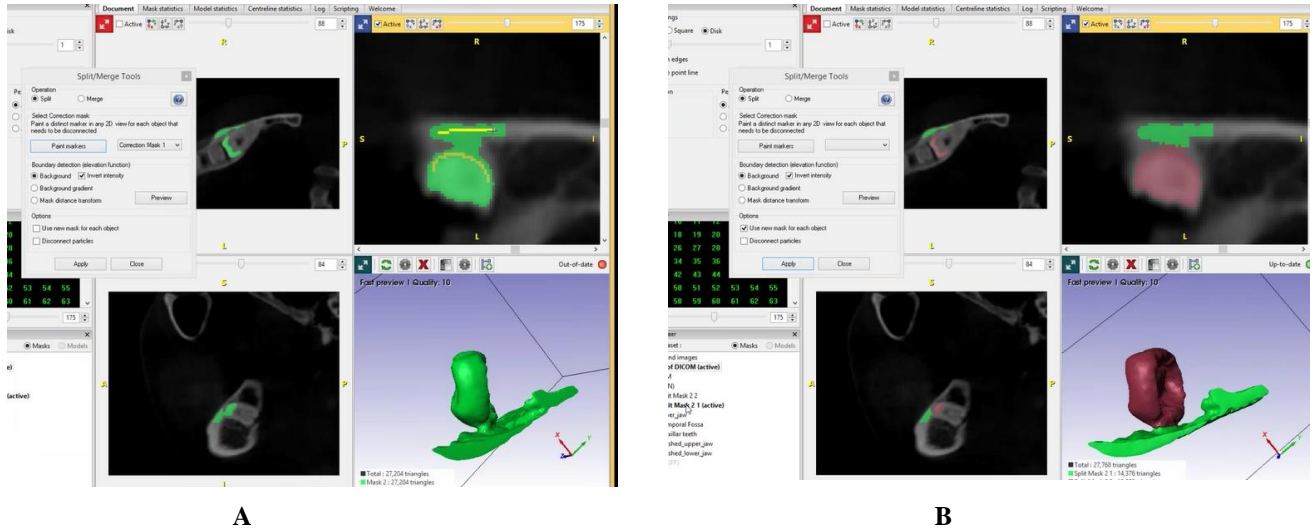


Fig 3.2.6: Separation of a single mask into multiple elements using *Split Merge* tool for a single object. **A.** Before separation of the body in contact, delineation lines are drawn to allow creation to two different bodies. **B.** After application of the command *Split Merge*, the old mask is dis-integrated into two new masks.

3.2.1.2. Bone mask

Once the teeth mask is fully selected, the bone mask was identified as any hard tissue structure that the *Segmentation with Threshold* tool can detect (Fig 3.2.4) initially representing everything the model can capture from the jaw region at the exception of the teeth.

Such a priority ordering of one mask with respect to the other can be assigned by placing the mask with a higher priority at the top of the mask list. The bone mask was modeled in totality, however the teeth mask remained a priority for total incorporation (Fig 3.2.8).

Alternatively, another technique can be used to achieve the same objective, applying a *Boolean Operation* to subtract the teeth mask from the bone mask.

The bone mask was divided into two segments: the cortical bone mask and the trabecular mask. The cortical bone was easier to detect with the *Segmentation with Threshold* tool. Then, it was subtracted from the total bone mask (Fig. 3.2.8). The remainder of the bone mask was the trabecular bone mask.

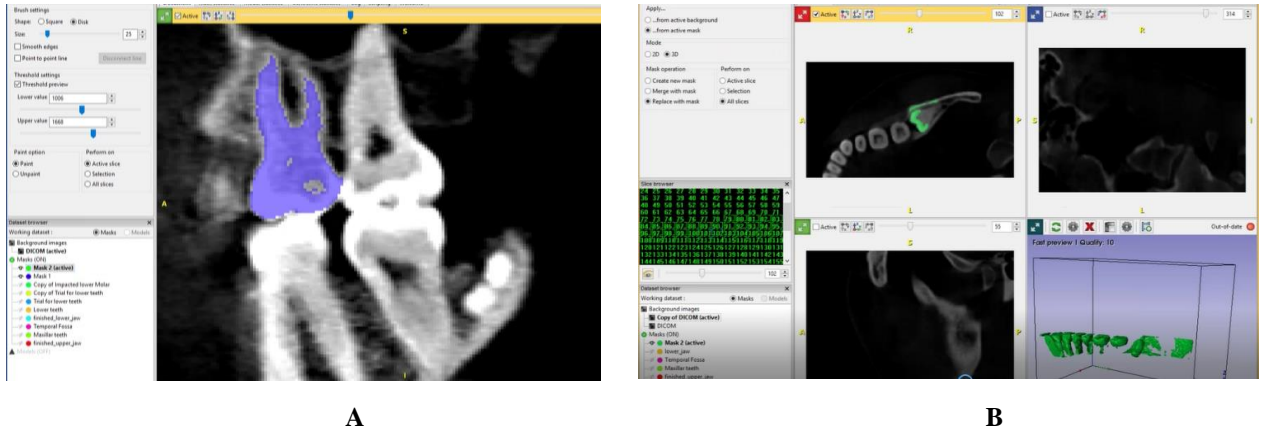


Fig 3.2.7: Two separation techniques to separate a single mask into multiple elements. **A.** *Split Merge* tool to separate teeth in contact **B.** *Flood Fill* tool to eliminate non-relevant disconnected pixels

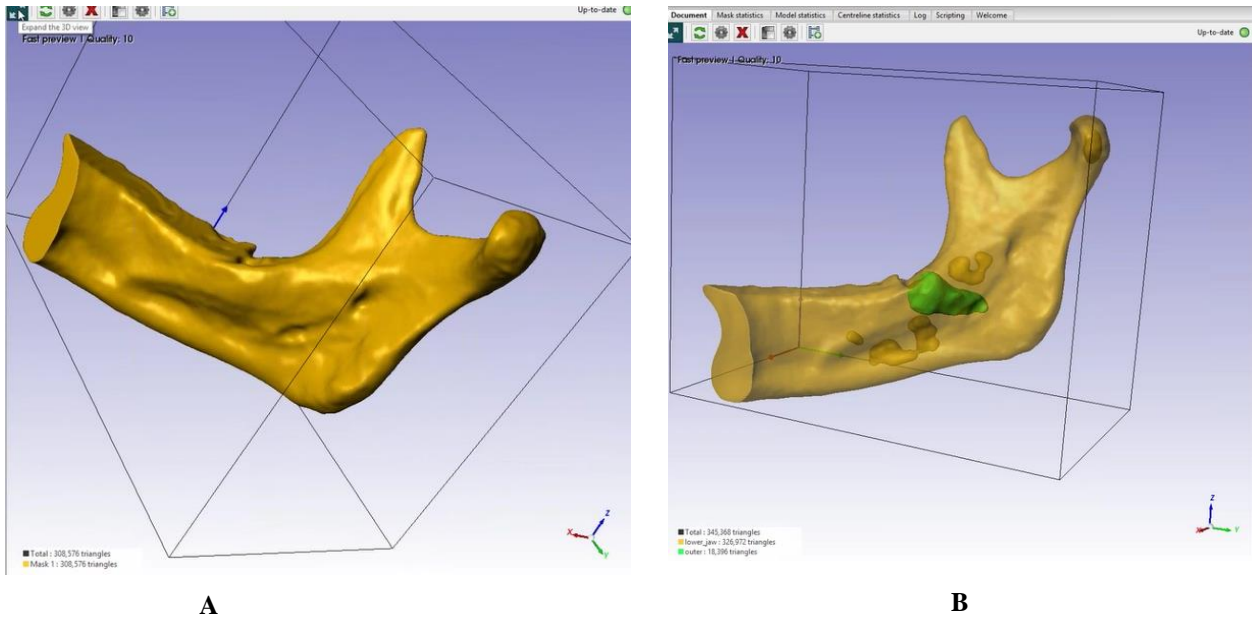


Fig 3.2.8: Mandibular bone mask captured and modeled in totality. **A.** Before the teeth mask is made a priority. **B.** After the teeth mask is set as a priority. In this example, the teeth mask 'Outer' is set higher than the 'Lower_jaw' mask. This operation allows the third molar to appear at an advantage with respect to the bone mask.

For the remaining hard tissue elements of the model including the Temporal bone and the Maxillary bone, selection and modeling were performed with the *Segmentation with Threshold* tool because they were not subdivided into smaller sections (i.e. there was no interest in dividing the maxillary bone into trabecular and cortical bones because the study scope was only the mandibular bone).

3.2.1.3. Periodontal Ligament Mask:

As a soft tissue, the periodontal ligament, is not distinguishable on X-rays. Therefore, it was constructed with an assumed thickness of 0.3 mm (Bowers, 1963). Until this step, the teeth were in contact with the bone mask. To provide the PDL thickness, the teeth were dilated with the *Dilate* tool, because the PDL mask was created without modifying the volume of the teeth mask, but rather the volume of the bone mask. The construction of a PDL membrane only in contact with the cementum of teeth and the opposing alveolar bone required the following steps (Figs 3.2.9, 3.2.10):

- Duplication of the teeth mask
- Dilation of the teeth masks in all directions using the *Dilate* tool
- Intersection of the dilated mask with the bone mask

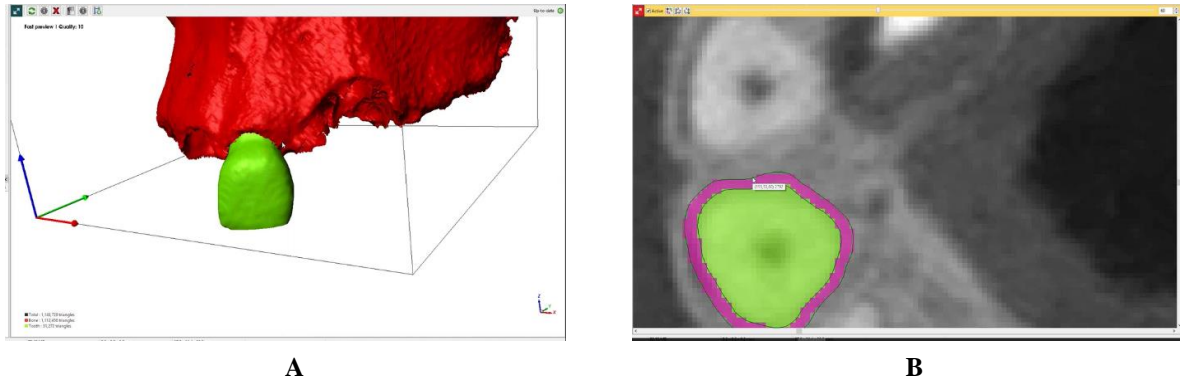


Fig 3.2.9: Modeling of the periodontal ligament. **A.** Initial situation where the tooth mask – central incisor – is in direct contact with the bone mask in red. **B.** Periodontal ligament in purple, after the tooth mask was dilated, and then subtracted from the bone mask. Later the PDL ligament was intersected with the bone mask: to be in contact only with the bone-tooth interface.

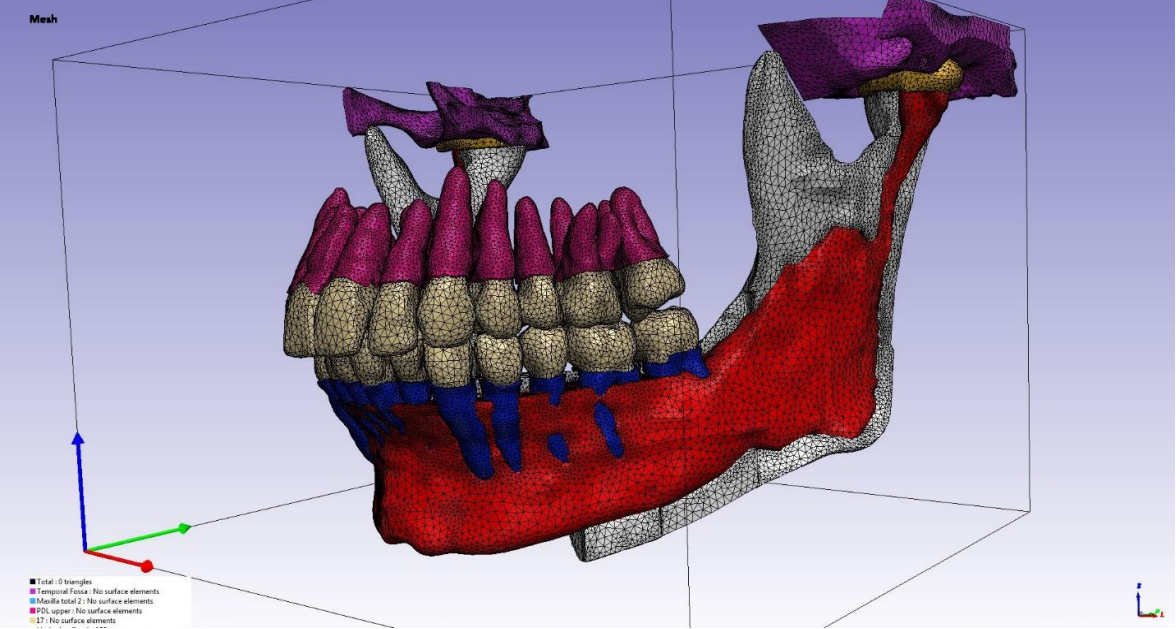


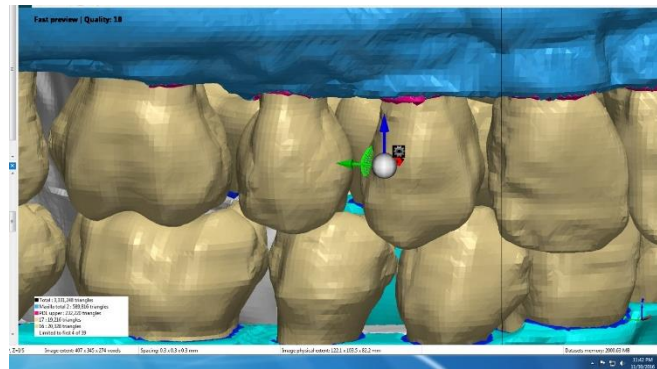
Fig 3.2.10: Modeling of the periodontal ligament around the teeth (ivory white); PDL visible independently for the maxillary teeth in pink (the maxillary bone mask has been removed for better visualization). The periodontal ligament of the mandibular teeth in blue is reproduced to cover the height the cementum at the tooth to bone interface. In red, the trabecular bone is shown after removing the buccal plate of the mandibular cortical section. In yellow, the articular disks of both sides. The caption above is taken at the final stage of Meshing where the model is finally transformed into a Finite Element Model (+FE Module) ready to be imported into the stress solver program *Abaqus*.

3.2.1.4. Articular disk mask

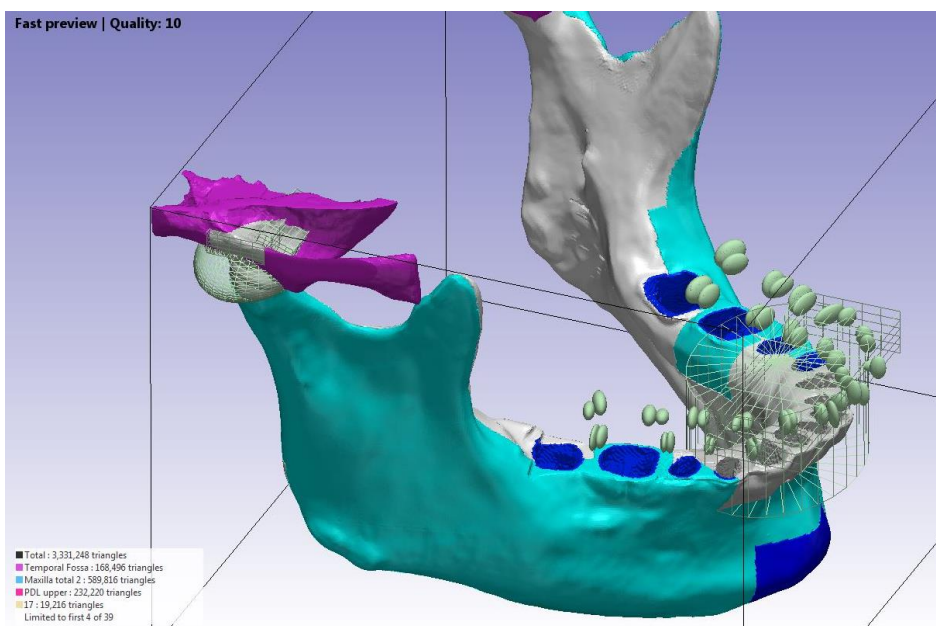
Although the articular disk is a soft tissue, it is detectable on the CBCT. Hence, modeling the disk required adjusting the *Segmentation with Threshold* tool to lower threshold values where it is easier to detect soft tissues. After extensive capture of the disk, the protocols employed for the bone mask were used to subtract the undesired masks and obtain an anatomic form of the articular disk. Consequently, the manual *Paint* brush tool was used for final editing to fill in missing elements (Fig. 3.2.10).

3.2.1.5. Surface to surface interactions

Since the teeth masks have been separated into different singular entities, to behave more independently, it was imperative to define surface-to-surface interactions that will be later used in Abaqus program (Fig. 3.2.11-12). In anticipation of this step, surfaces were defined in Simpleware Scan IP program, to later be matched together with interaction properties, enabling them to interact within specific definitions.



A



B

Fig. 3.2.11. A. Surface selection of the interproximal sides to interact with each other. The elliptical shapes (green) serve as tools to select the surfaces. **B.** Full demonstration of the surface selection areas between all mandibular teeth (teeth are hidden in this schematic). To select an interproximal area, two elliptical shapes are created, one to select each proximal side. The anterior gridded box serves to select areas of interaction between maxillary and mandibular teeth should flaring and anterior guidance be modeled at a later stage.

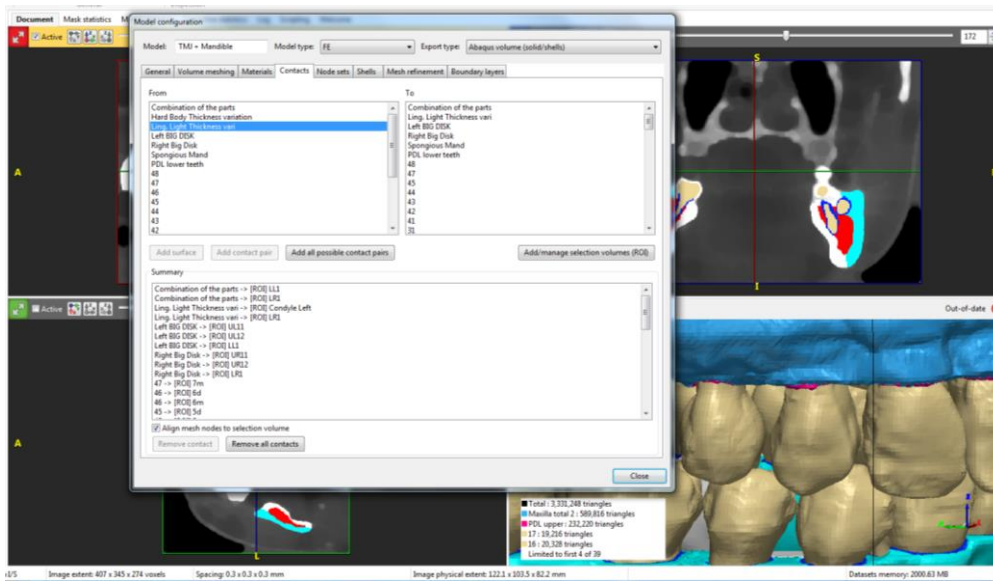


Fig. 3.2.12. Surface-to-surface interactions involve coupling of the selected sides to the respective mask. For example, the defined contour (in Scan IP) of the mesial side of tooth #47 is assigned to the mask of this tooth. This coupling allows its identical recognition in the Abaqus program.

3.2.2. Incorporating patient variations into the 3D model

Once all components of the CBCT image have been transformed into a 3D model (Fig 3.2.13), the initial template model was ready to receive the different patient variation configurations – for both stiffness and thickness variations – from the cadaver studies (Schwartz-Dabney & Dechow, 2003). Changes were applied in the 3D modeling software ScanIP™ 7.0 via drawing and modeling tools. Among these tools, *3D editing tool* was used to edit the geometry of the mask, and *Flood Fill tool* to isolate the regions to be processed. The mask of each region is later duplicated and merged with the masks of other regions (3.2.17). A separate mask was created for each grouped region to which a specific property was assigned in the solver stress-solver software Abaqus-Simulia v6.13 (*Dassault Systèmes, Tokyo Japan*).

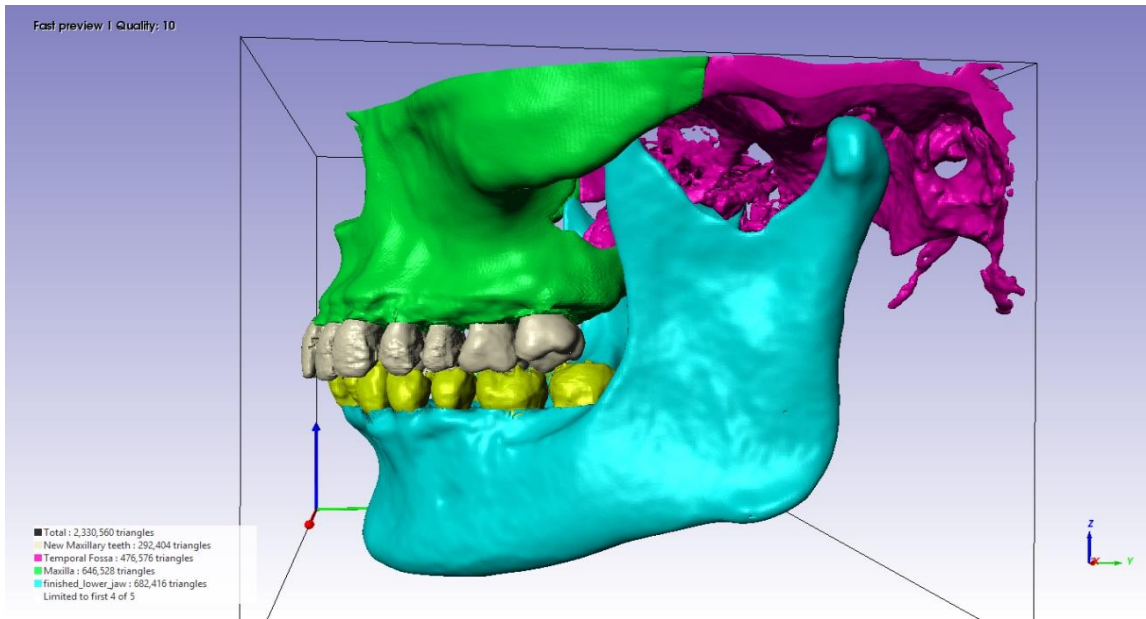
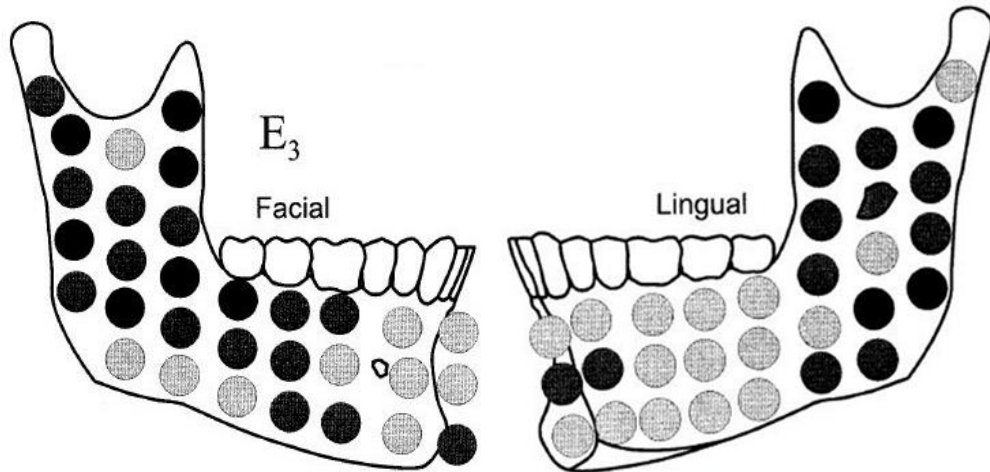


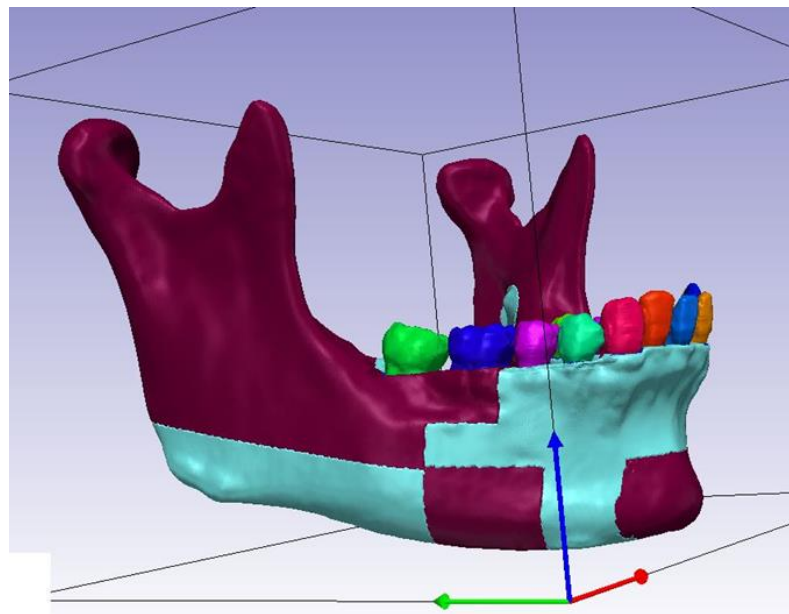
Fig. 3.2.13. Final version of initial model before incorporating patient-variations.

3.2.2.1. Stiffness Variation

In the cadaver studies, 62 different zones were harvested and investigated for stiffness variations in each of the 10 frozen mandibles. The initial modeled parts according to stiffness variation are shown in Fig. 3.2.14. Because of the similarity in physical/mechanical behavior between the neighboring zones without statistical difference between them, these areas were re-grouped and combined into one mask in the initial model. The light blue section represents the areas with light stiffness; the burgundy section represents areas with higher stiffness values (Fig. 3.2.14). These zones were grouped together because of their similar physical behavior following the trend of the E_3 stiffness variation map (Figs 3.2.14 - A).



A



B

Fig 3.2.14. A. Elastic Moduli of the 62 different sites of both sides of the cortical plate of mandible. B. Different zones of the mandible sectioned per the E_3 map variation.

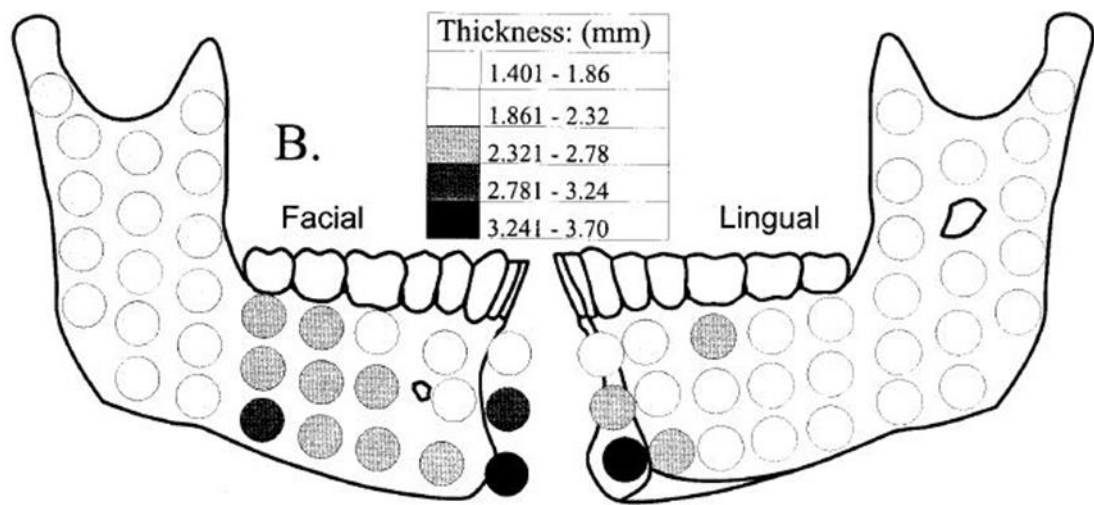
Specifically, the regions that were grouped together were:

- Buccal Side: - Blue portion includes zones: 2, 5-10, 16, 17, 28
 - Burgundy portion includes zones: 1, 3, 4, 11-15, 18-27, 29, 30, 31
- Lingual Side: - Blue portion includes zones: 1-5, 10-13, 16-22
 - Burgundy portion includes zones: 6-9, 14, 15, 21, 23-31

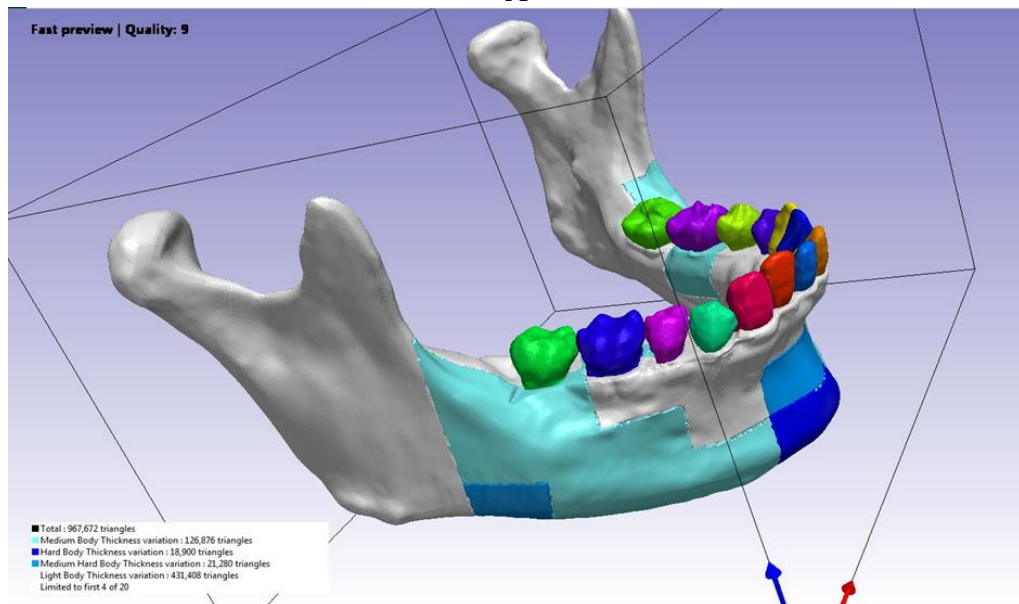
3.2.2.2. Thickness Variation

The same 62 sites were also measured to analyze cortical thickness in all the 10 mandibles (Fig 3.2.15 - A). The different sectioning of the model in Scan IP according to thickness map was as follows (Fig 3.2.15 - B)

- Buccal Side:
- Light thickness portion includes zones 6, 7, 9, 13-18, 21-31
 - Light-Medium thickness portion includes zones 2-4, 10-12, 19, 20
 - Hard-Medium thickness portion includes zones 5, 8
 - Hard thickness portion includes zone 1
- Lingual Side:
- Light thickness portion includes zones 3-7, 9-17, 19-31
 - Light-Medium thickness portion includes zones 2, 8, 18
 - Hard thickness portion includes zone 1.



A



B

Figs 3.2.15. A. Cortical plate thickness (mm) – distribution of the different zones. The cortex is thickest at the inferior symphysis and thinnest throughout the lingual ramus. B. Sectioning of the mandibular body: **white pearl**: thinnest region from the thickness map; **light blue**: light-medium thickness region; **dark Navy Blue**: hardest-medium region of thickness; **dark Navy Blue**: thickest region.

3.2.3. Statistical consideration

After configuring the thickness model, statistical tests were applied to investigate differences between the grouped areas (Table 3.2.1). The parts that differed significantly from the others were the Light Lingual and the Hard body regions; the rest

of the parts were grouped together into one region (Fig. 3.2.16). Significant differences were found only for the Light Body between the lingual side (identified by white pearl color) and buccal sides, and the Hard Body lingual (in dark navy-blue color), which differed from all other regions, which were accordingly considered as one group (identified by a light blue color; Fig. 3.2.15.).

The thickness variation scheme was used to carry both stiffness and thickness experimentations because the results extracted from stiffness variation models were similar in pattern, although with different values. While the results between the different virtual models under different thickness conditions of the cortical bone demonstrated unpredictable patterns of stresses, it was nevertheless used for better statistical comparisons and correlations of findings (Fig 3.2.16).

Table 3.2.1. Comparison of thickness regions (p values) defined on the buccal and lingual sides of the mandible

Computation Table	Light Body Buccal	Light Body Lingual	Medium Body Buccal	Medium Body Lingual	Medium Hard Body Buccal	Hard Body Buccal	Hard Body Lingual
Light Body Buccal	N/A	0.0008	0.008	0.006	0.001	0.011	0.001
Light Body Lingual		N/A	0.239	0.372	0.977	0.317	0.011
Medium Body Buccal			N/A	0.788	0.239	0.124	0.002
Medium Body Lingual				N/A	0.377	0.157	0.003
Medium Hard Body Buccal					N/A	0.308	0.010
Hard Body Buccal						N/A	0.410
Hard Body Lingual							N/A

Variables listed in the vertical columns are compared with those on the horizontal rows.

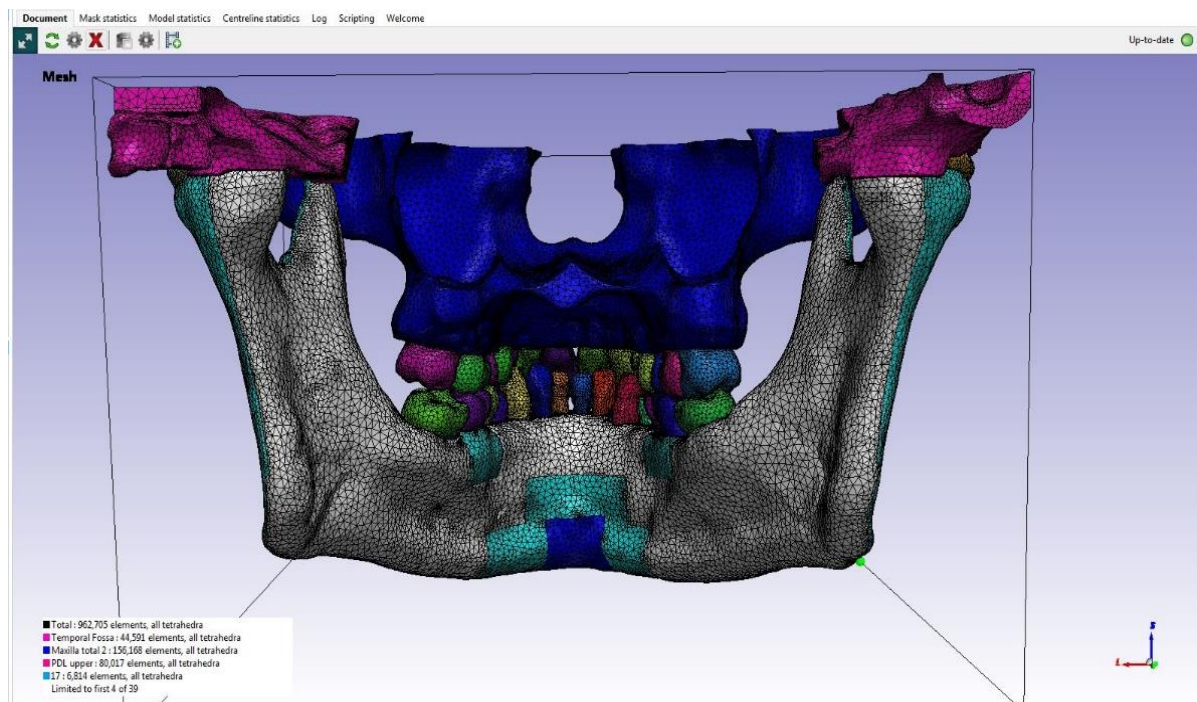
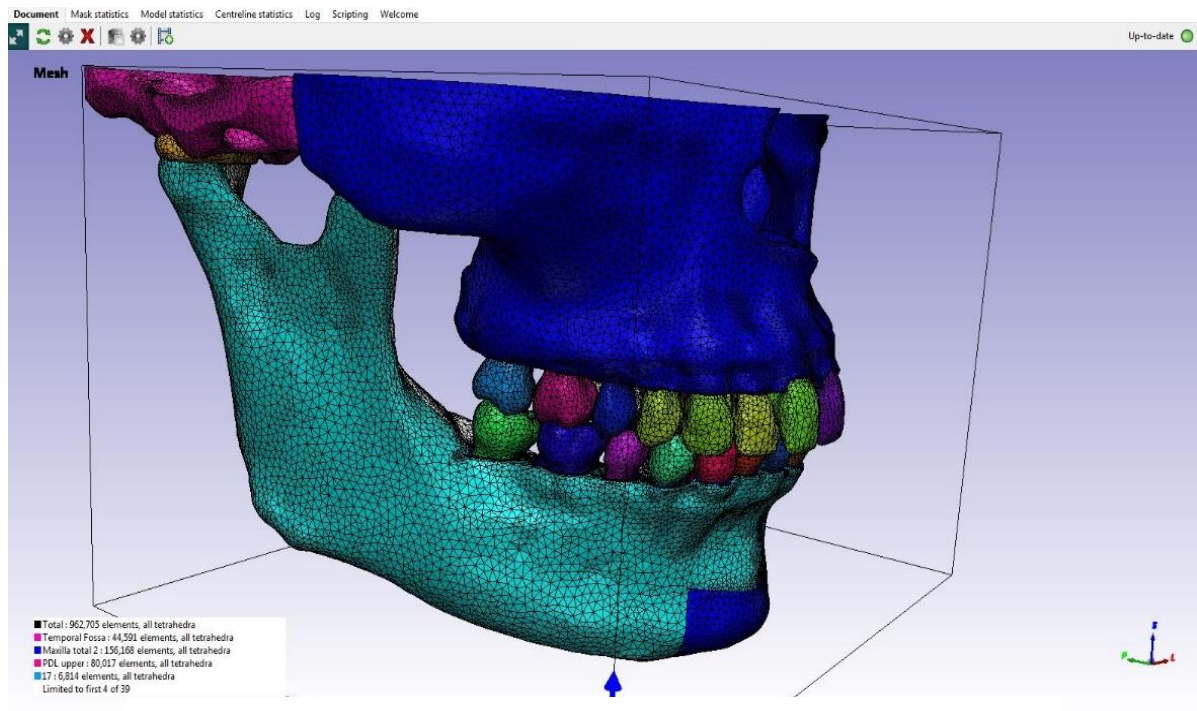


Fig 3.2.16. Sectioning of the mandibular body. **A.** Buccal side with two distinct regions corresponding to different thickness variations: moderate thickness (light blue region- grey in thickness map, Fig 3.2.14); harder thickness (dark blue region- black in thickness map, Fig 3.2.14). **B.** Lingual side with three distinct regions accounting for the different thickness variations. White pearl region corresponds to light thickness (white in thickness map, Fig 3.2.14).

3.2.4. Implementation of Thickness Variations into the model

Once the regions have been defined, the variations of thickness drawn from the respective cadavers were imported in the different sections (Table 3.2.2). The three different regions (**Light Lingual**, **Light buccal** and **Dark Buccal + Lingual** region at the chin level) on the original model, representing the different cortical plate, buccally or lingually, were modified to create the different thicknesses.

Table 3.2.2. Different variations of thicknesses of the grouped regions retrieved from the different cadavers.

Pat.	Light B.	Var.	In voxel	Med B.	Var.	In voxel	High B.	Var.	In voxel
1	2.875	0.054	0.18	2.596	0.0807	0.2689	3.64	0.1385	0.4616
2	2.291	-0.5293	-1.764	2.454	-0.061	-0.2017	3.195	-0.307	-1.0217
3	3.769	0.9482	3.161	2.468	-0.047	-0.1583	4.72	1.2185	4.0616
4	3.423	0.6021	2.008	2.335	-0.18	-0.5991	1.855	-1.647	-5.4883
5	2.291	-0.5293	-1.764	2.812	0.2971	0.9904	4.01	0.5085	1.6955
6	2.384	-0.4364	-1.454	2.369	-0.146	-0.4868	2.89	-0.612	-2.0383
7	2.481	-0.3395	-1.131	2.177	-0.338	-1.1281	2.58	-0.922	-3.0717
8	2.921	0.099	0.337	3.107	0.5922	1.9741	4.8	1.2985	4.3283
9	2.695	-0.1253	-0.417	2.608	0.0934	0.3114	3.755	0.2535	0.8454
10	3.081	0.259	0.8633	2.228	-0.287	-0.9556	3.57	0.0685	0.2283

Each region was compared to the baseline normal reference; differences with the baseline was calculated in pixels, then added or subtracted from the original reference model.

For computations of variations, every cadaver region data was compared to the baseline reference value. The difference between both values was transformed into voxel units. The baseline used as a reference originates from two sources:

- a. a calculated source, which was the average of all 10 cadavers of the regions under study.
- b. an anatomical variation, which was averaged from a number of randomized sections on CBCT of the region in question.

Both the recorded (from X-ray) and calculated (from cadaver) reference values were averaged to come up with a single value that represents the reference value for a single region. The values were averaged together to reduce the error between the CBCT values of a true patient with the values extracted from the cadavers. To introduce the variation into the model, the cadaver data were each individually compared to the reference value, and the difference was divided by three because each voxel size was: $0.3 \times 0.3 \times 0.3 \text{ mm}^3$. The value was rounded up to define the (non-decimal) number of voxels that were needed to be removed or added. Fig 2.3.17. illustrates this procedure through a sagittal cut of the chin area showing the initial position in the reference model. The thickening or thinning of each of the parts is performed by creating another mask in the Scan IP software®. The newly created mask will be of a certain thickness and added to the side that needs to be thickened (Fig. 3.2.18). This action is performed with *Boolean operation*.

Thinning or thickening of the cortical is countered with thickening or thinning of the trabecular bone, respectively. The changes affect the inner interface without changing the thickness away from the teeth; the outer border of the regions of interest does not change in shape, while the inner contour does. This process is shown in Fig 3.2.19 whereby the thickness is altered corresponding to the individual cadaver values. Following this critical procedure (Fig. 3.2.20), all virtual models are meshed and a Finite Element model is created for each “subject.” At this point, all sets of 10 thickness models and 1 initial template model to test stiffness variation are ready to be imported into the solver stress-solver software Abaqus-Simulia v6.13 (Dassault Systèmes, Tokyo Japan).

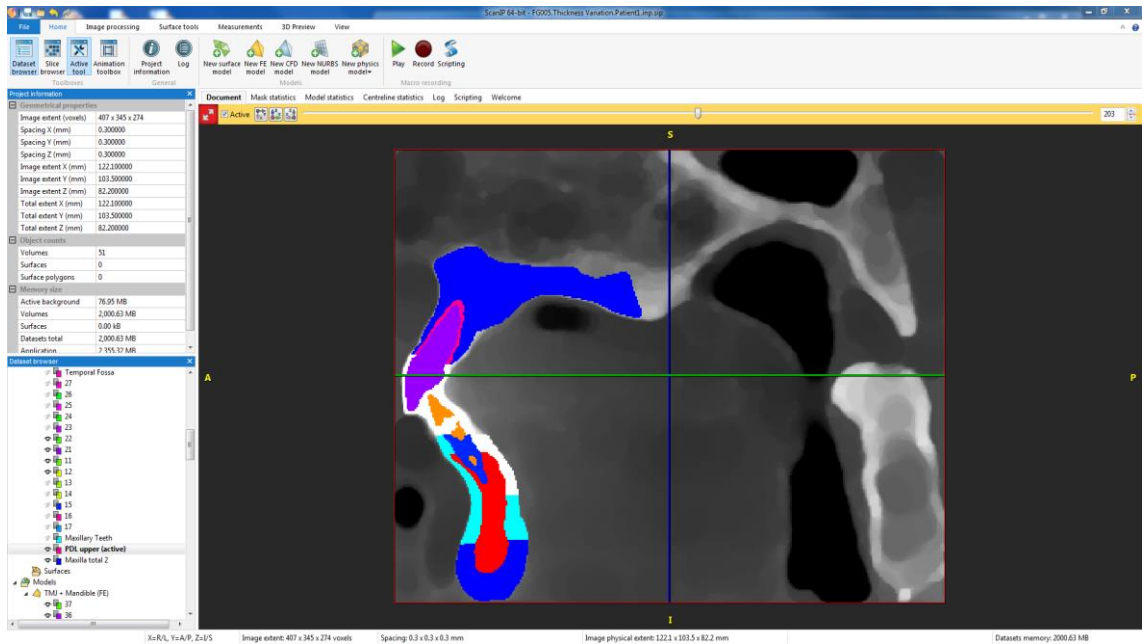


Fig 3.2.17. The initial state of the template model upon which the cadaver variations were input. The symphyseal area is shown including the trabecular bone (red), the mask (light blue) of the different sectioned areas (Table 3.2.1), the hard body mask (dark navy-blue) and the mask of the light lingual region (white).

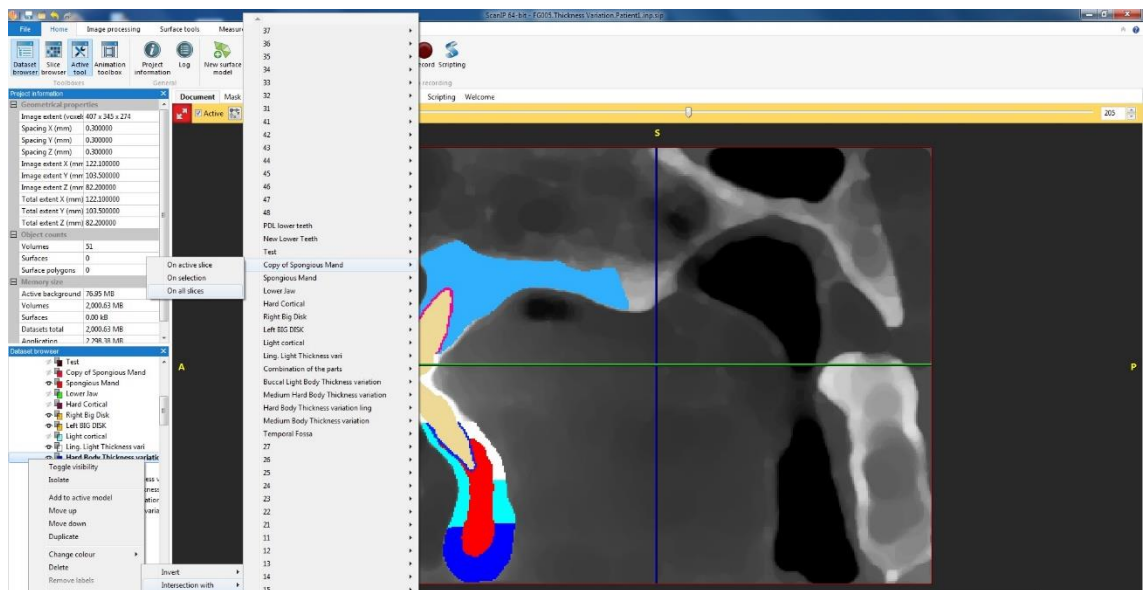
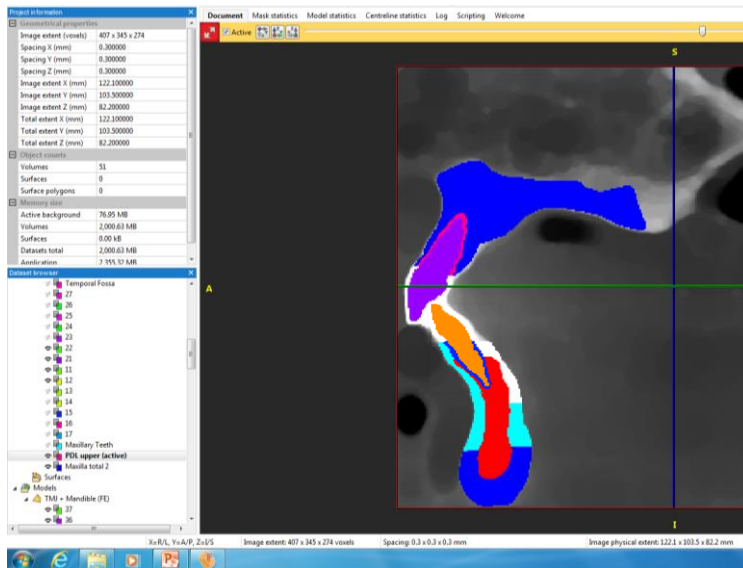
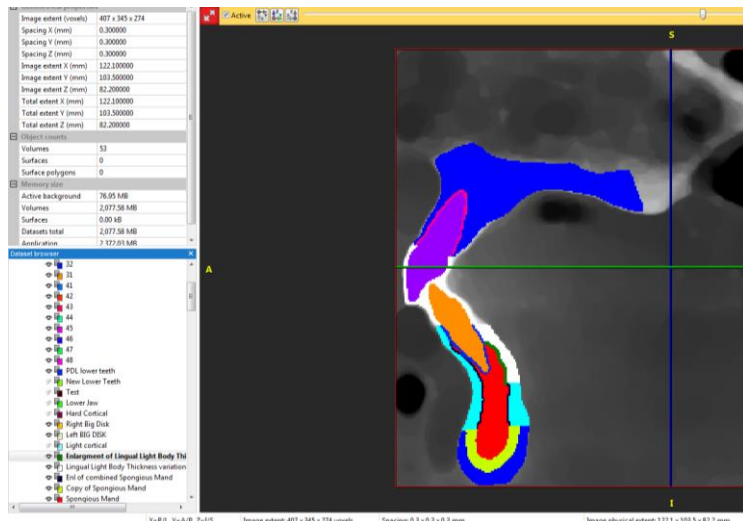


Fig 3.2.18. Sectioning of the mandibular bodies was accomplished with tools like *duplication of masks*, *merging* and *priority selection*. In this section, the outcome of this procedure is shown for the chin region,



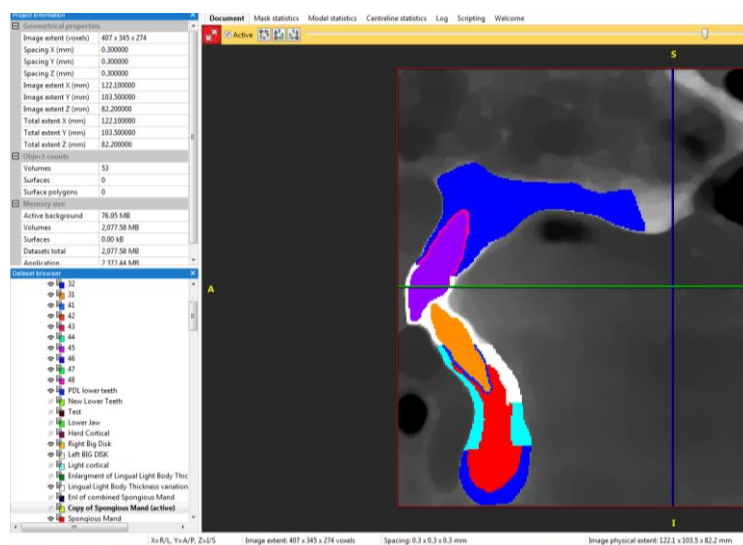
A

Fig 3.2.19. A. The initial state of the template model. In this section, cortical and trabecular bone thicknesses of the anatomical components are at their baseline thickness.



B

Fig 3.2.19. B. creation of a new mask for cadaver # 4. A thinning of 5 voxels of the Hard Body Cortical (dark navy blue), a thickening of one voxel on the Lingual White body (white colored), and a thinning of 1 pixel of the Combination Body (light Blue) were performed.



C

Fig 3.2.19. C. After the new masks (yellow) were created with thickness change applied in all directions with the *Dilate tool*, the masks (yellow in Fig. 3.3.21B) were merged with the original existing mask (red) using the *Boolean operator* to obtain the individualized thickness in the pertinent region (in this instance the symphysis). In this model, since the Hard Body needed to be thinned, the yellow newly created mask was merged with the trabecular bone. The thickness alteration modifies the inner geometry of the model closer to the teeth without affecting the outer appearance.

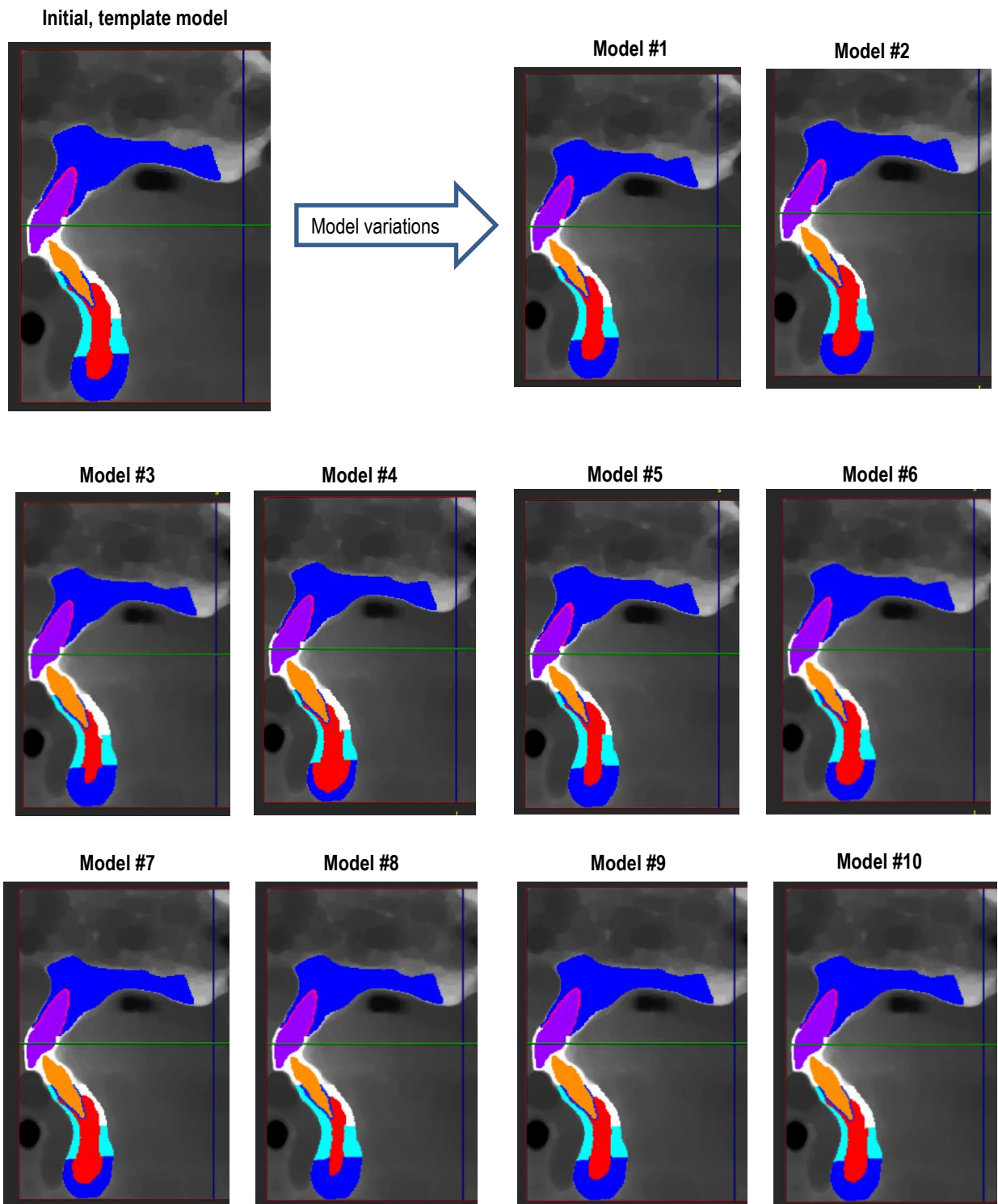


Fig 3.2.20. Variations of thickness in all cadaver specimens

3.2.5. Model processing

At this stage, the meshed models were in FE (Finite Element) format (Fig. 3.2.16) ready to be imported into the stress solver software for load application and stress testing.

3.2.5.1. Defining material properties

Every section of the model is defined by specific material properties of stiffness that defines its behavior under any loading condition. In fact, the virtual cadavers were approximated as much as possible to real-life values to mimic clinical biological responses (Middleton, Jones, & Wilson, 1996; Strait et al., 2005).

Material properties (Young's Modulus of Elasticity and Poisson's ratios) of trabecular bone, teeth, articular disk and PDL ligament were defined from available data in the literature (Table 3.2.3). Many authors studied material properties of the mandible and the TMJ complex, whereby the values used in the present study (Table 3.2.3) are drawn from their common rationale and usage (Carter & Spengler, 1978; Chen, Akyuz, Xu, & Pidaparti, 1998; Gupta, Kohli, Hazarey, Kharbanda, & Gunjal, 2009; Kayumi, Takayama, Yokoyama, & Ueda, 2015; Tanaka et al., 2004; Tanaka et al., 2000; Tanaka et al., 2001; Tanne, Tanaka, & Sakuda, 1996). All materials used in this study are assumed to be homogenous, isotropic, and linearly elastic (Tanne, Lu, Tanaka, & Sakuda, 1993; Tanne et al., 1996).

Table 3.2.3. Material properties of the different components of the models

Material	Elastic Modulus (in MPa)	Poisson's Ratio
Cortical Bone	13700	0.3
Trabecular Bone	7900	0.3
Articular Disc	44.1	0.45
Teeth	20000	0.3
PDL	0.68	0.45

Cortical bone stiffness was modified according to values extracted from cadaver study (Schwartz-Dabney & Dechow, 2003), but the stiffness of the cortical bone remained stable through the thickness group. Due to region groupings, it was not possible to account for all the engineering parameters (e.g. orthotropic material properties) when assigning them to the different parts. For example, only the E_3 Young's modulus of elasticity was studied (Table 3.2.4) because of the variation of the orientation of the principal axis of the members grouped.

Table 3.2.4 Material properties for Light Lingual region.
Highlighted in blue in the E_3 modulus of elasticity. p12-p13-p21-p31: Poisson's ratio; G12-G31-G23; Shear stiffness

Light Lingual Region	E1	E2	E3	G12	G31	G23	p12	p13	p21	p31
Pat. 1	12.181	18.394	19.254	5.065	5.54	7.16	0.13	0.38	0.19	0.58
Pat. 2	13.283	17.126	19.944	5.311	5.45	7.12	0.19	0.38	0.24	0.55
Pat. 3	11.280	16.498	18.643	4.68	4.66	6.93	0.15	0.34	0.21	0.55
Pat. 4	12.060	17.174	21.688	5.066	5.52	7.28	0.13	0.3	0.18	0.54
Pat. 5	11.93	17.039	18.226	4.971	5.58	7.09	0.13	0.4	0.19	0.6
Pat. 6	13.118	17.511	22.448	5.268	5.92	7.49	0.18	0.31	0.23	0.53
Pat. 7	12.423	17.585	21.542	5.045	5.17	7.35	0.16	0.34	0.22	0.56
Pat. 8	12.731	18.399	20.37	5.188	5.82	7.45	0.16	0.36	0.21	0.56
Pat. 9	11.898	17.241	19.429	4.915	5.4	6.79	0.14	0.36	0.19	0.59
Pat. 10	13.252	20.125	21.644	5.189	5.54	7.74	0.17	0.34	0.25	0.55

3.2.5.2. Interaction properties

Given that the teeth should behave as in the clinical setting (one-point contact per tooth), an interaction modality was needed to accurately represent load transmission. Such interaction configuration increases the contact area between the teeth. Therefore, instead of the force being transmitted through one point, interproximal surfaces between the teeth are minimally deformed to 'bend' to allow for surface-to-surface transmission of the load. To mark surface-to-surface interaction (explained in section: 3.2.1 section E.), the interproximal sides facing each other were coupled to model interproximal behaviors (Fig 3.2.21).

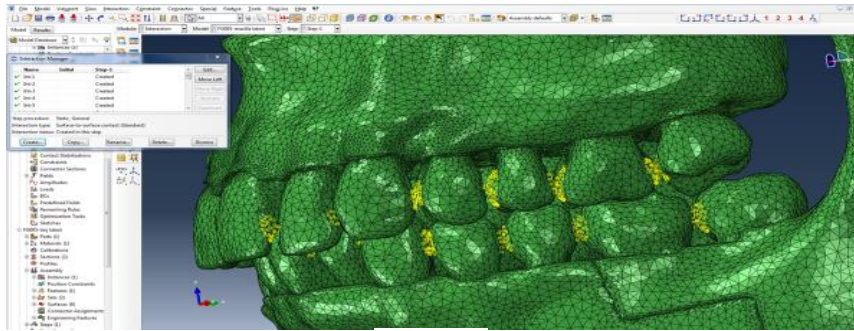


Fig 3.2.21. A. Surface to surface interaction applied at interdental level.

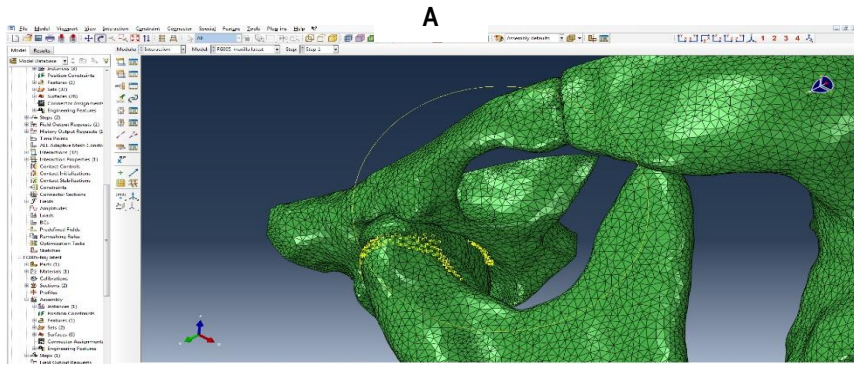


Fig 3.2.21. B. Surface to surface interaction applied at a condylar level, defined between the condyle, disk and the temporal bone to mimic incidents of friction.

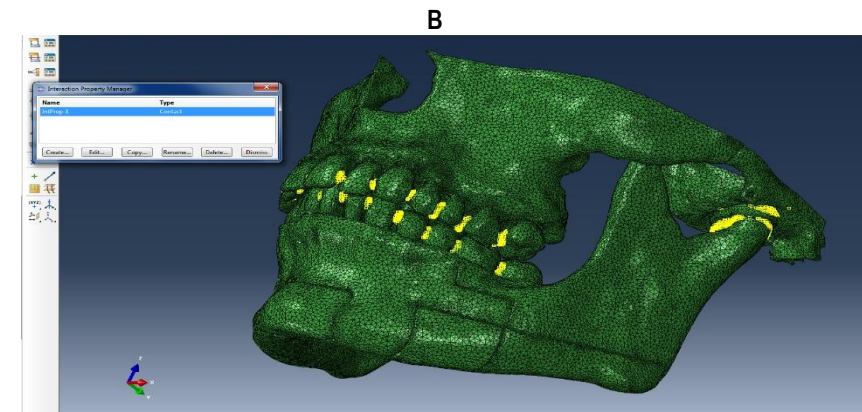


Fig 3.2.21. C. Full model representation showing all interactions defined in the model.

3.2.6. Loading scenario

At this stage, the models were prepared to be submitted to forces (loads) mimicking the effects of the elastics. The models were also put under restraining limitations to hold the models in various directions of space (boundary conditions).

The basic arrangements set to be tested were the CI II and the CI III elastic configurations (Fig. 3.2.22-3). Within the CI II model, 2 variations were tested related to hooking the elastics on the mandibular 1st molars and 2nd molars.

3.2.6.2. Loading conditions

To define a specific load, it was preferable to apply the load on a group of nodes on the crown, rather than a solitary node to better mimic the bracket interface in a clinical setting. To prevent load application on a point node, a set comprising a minimum of 8 nodes was defined. In the Cl II groups where the load was applied from the 1st or 2nd molars, the sets were defined in the middle of the crown mesio-distally and almost 3 mm away from the crown levels on the buccal side (Figs. 3.2.24, 3.2.25), representing the ideal bracket position. In the Cl III group, loading was performed on sets defined in the middle of the crown of the canines, on the buccal side, mirroring the normal position where a bracket is bonded in ideal position (Fig. 3.2.26).

Upon application of the load, a local datum axis system was defined. This orientation system allows the accurate definition of load direction in space (Fig.3.2.24). The datum axis system was constructed using 3 points: origin of the axis, located at the center of the crown; a second landmark, located at the center of the canine to which the elastic is applied; the third landmark is in a position perpendicular to the x-axis (Fig 3.2.23). The load applied had a magnitude of 1.5 Newtons (= 153 grams), and was equally divided on all the nodes of the defined set.



Fig. 3.2.22 Loading scenario 1: Configuration of CI II elastics
<https://goo.gl/KI08jv>



Fig. 3.2.23. Loading scenario 2: Configuration of CI III elastics
<https://goo.gl/KI08jv>

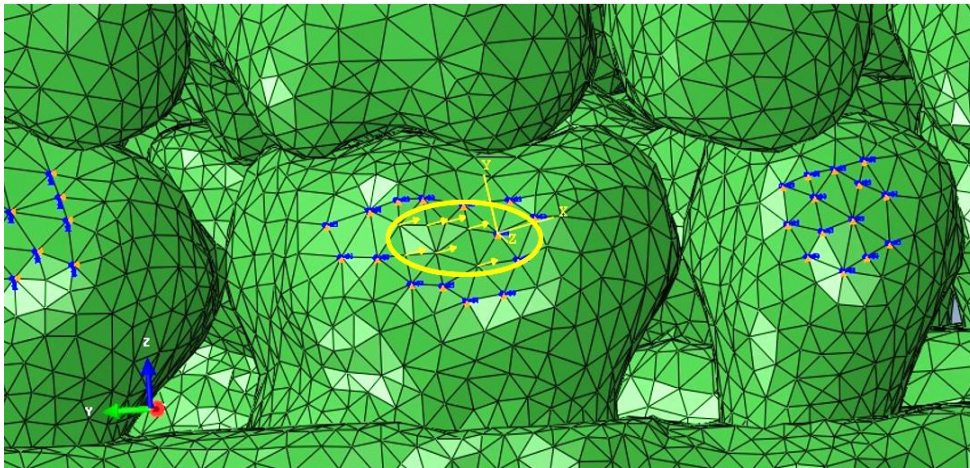


Fig 3.2.24. The yellow circle encapsulates arrows at the level of the 1st molars. The local axis system or datum defines the direction of the CI II elastic applied at the crown. The force, represented by the yellow arrows follow the x-axis of the local datum system defined.

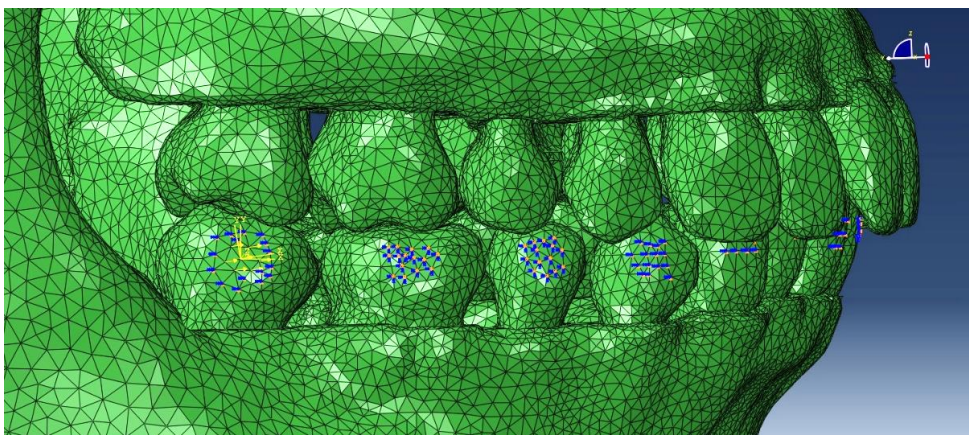


Fig 3.2.25. The load is represented by yellow arrows at the level of the 2nd molars. The local datum axis system defines the direction of the CI II elastic applied at the crown following the x-axis.

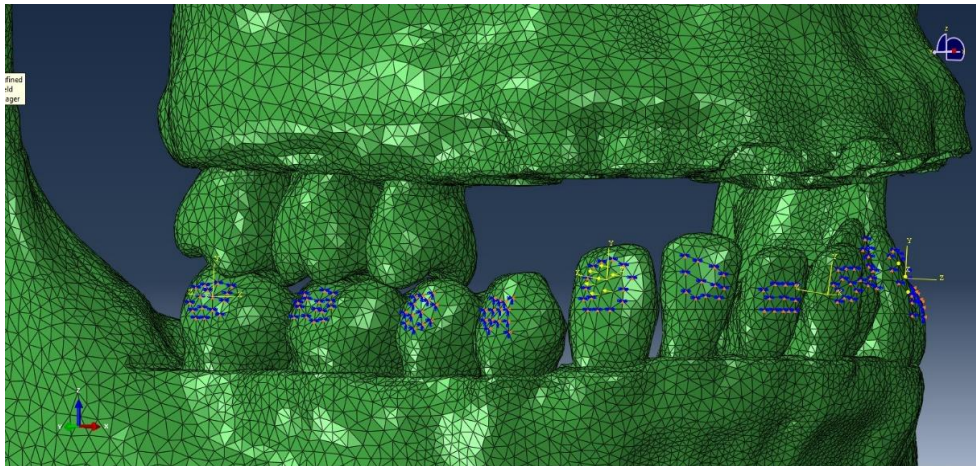


Fig 3.2.26. The load is represented by yellow arrows at the level of the canines. The local datum axis system was defined by the direction of the CI III elastic applied at the crown of the canine following the x-axis towards the maxillary 1st molars.

3.2.6.2. Boundary conditions

Boundary condition is the property given to a model to limit its unrestricted movement in the planes of space. This property allows a better replication of a clinical scenario, whereby the maxilla is fixed to the rest of the cranium and the mandible is kept mobile. Another boundary condition was set for the teeth, which were made to follow a specific path, replicating their motion on a stiff ‘heavy’ archwire fully occupying the bracket slot. The same boundary conditions were applied within all three loading scenario groups. For instance, the maxilla was selected to ‘*Encaster*’ and hence restricted in all planes of space where both the rotational and the displacement degrees of freedom are constraint: $U_1 = U_2 = U_3 = UR_1 = UR_2 = UR_3 = 0$ (Fig 3.2.27). Another type of boundary condition was applied on all the teeth (Fig 3.2.24-6). Highlighted in blue markings on the crowns of the teeth, are defined sets that are restricted to certain degrees of freedom; *XASYMM* where: $U_2 = U_3 = UR_1 = 0$. Such a constraint was applied to block the teeth from translating vertically, and bucco-lingually.

However, the teeth are allowed to rotate, tip but not to change their torque control. In conclusion, the teeth are allowed to displace in translation only in the x-axis, allowing a antero-posterior movement of the teeth.

3.3. Data collection and export

3.3.1. Types of results

FEA is an engineering tool that measures physical and mechanical parameters that include stresses, strains, energy storage, vibration and displacements. In the present study, we report on Von Mises stresses in the condylar region at three levels: condyle, articular disk, temporal bone (Fig 3.2.28), and in the PDL of all the mandibular teeth on their mesial and distal aspects, each divided into three levels: coronal, middle, and apical (Fig. 3.2.29). Also, displacements of all the mandibular teeth were evaluated at the crown level. For this purpose, sets were created at the occlusal level of the teeth, each set comprising no less than 7 nodes (Fig. 3.2.30).

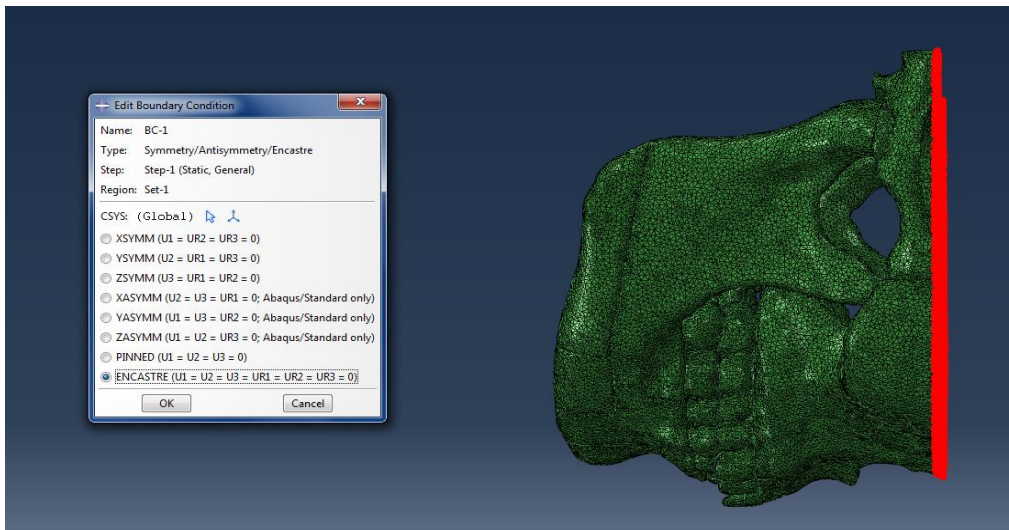


Fig 3.2.27. Boundary condition, shown in red, serves to fix the upper maxillary border as a fixed body. Such a property allows the maxilla to behave as if it was confined to rest of the cranium.

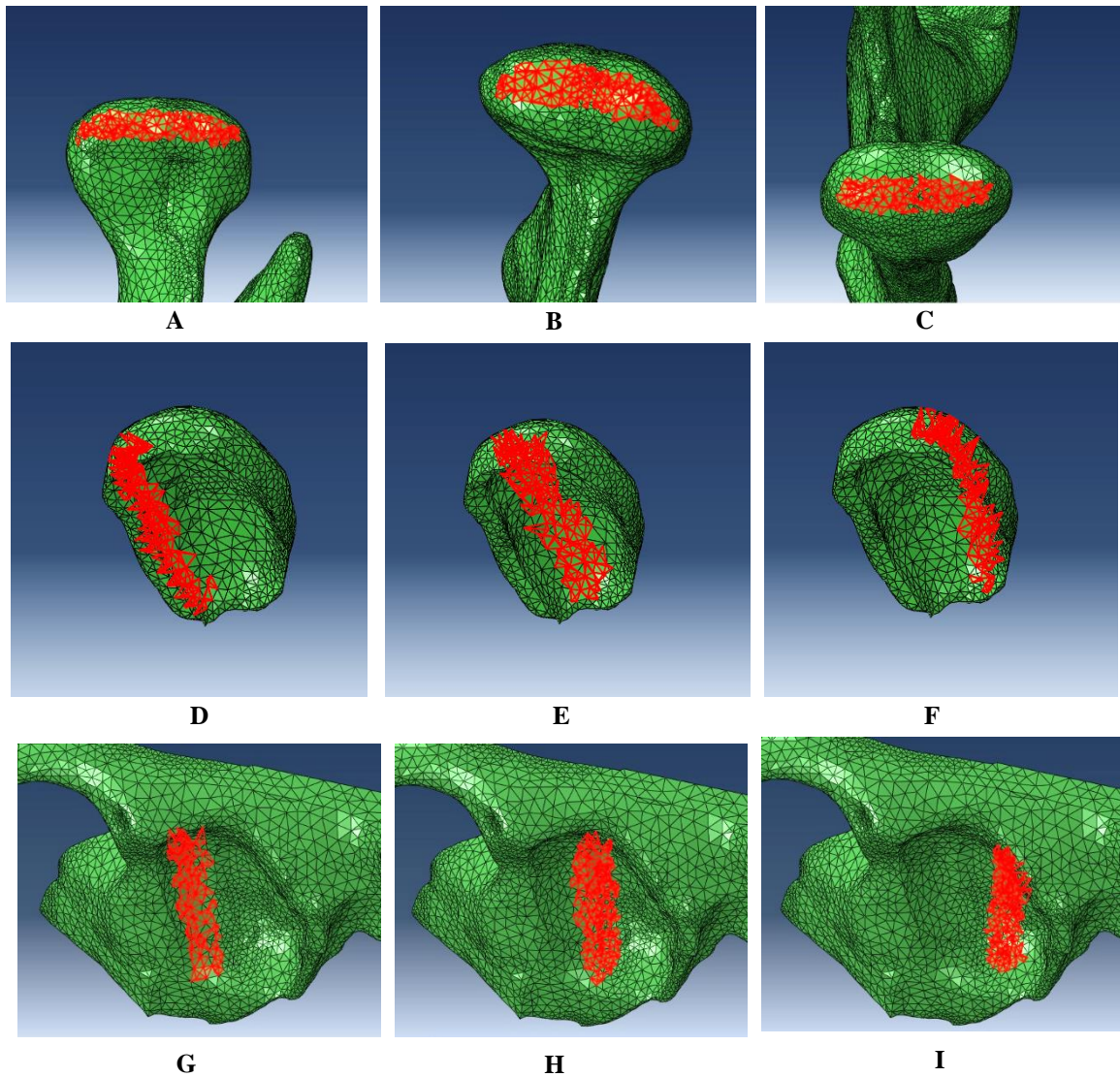


Fig 3.2.28. Selection of element sets of the TMJ complex. **A.** Anterior area of the condyle **B.** Middle area of the condyle **C.** Posterior area of the condyle **D.** Anterior area of the disk **E.** Middle area of the disk **F.** Posterior area of the disk **G.** Anterior area of the temporal bone **H.** Middle area of the temporal bone **I.** Posterior area of the temporal bone

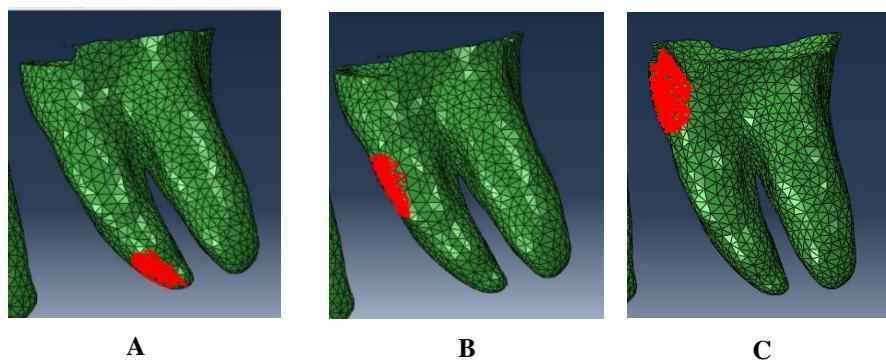


Fig 3.2.29. Selection of element sets at the level of the PDL. **A.** Apical section of the mesial side. **B.** Middle section of the mesial side. **C.** Coronal section of the mesial side.

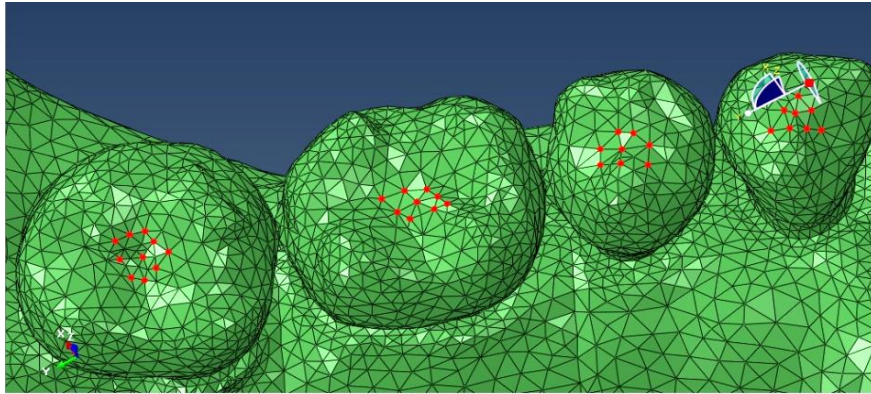


Fig 3.2.30. Selection of node sets to account for displacements at the level of the center of the crown.

3.3.2. Data reporting

When the model configuration was complete, a *Job* was created, and the model *Submitted* for analysis to solve for the required data under the applied loading conditions. The first representation of results came out in colored schematic diagrams that could be animated to simulate initial displacement and appearance of stresses. This representation gives a panoramic view. Data export was performed for full tabulation in excel to run the adequate statistical analysis. Data export entails that element and node sets must be reported as DAT. Files where the data can be organized in excel. Von Mises element stresses and nodal displacement during export were named according to the area they represent, to allow for better tabulation of results.

3.4. Statistical Analysis

Descriptive statistics were generated for all measurements in all subsamples of both stiffness and thickness variations, right and left sides, and the three treatment modality groups.

Normality was tested using the Shapiro-Wilk test. The variables in CI II/6s and CI II/7s were normally distributed; hence parametric tests were applicable. In the CI III

group, the distribution of the variables was not normal, thus non-parametric tests were applied.

Two-tailed paired t-tests (or Wilcoxon signed rank test) were performed to compare stresses at the different surfaces and crown displacement between right and left, and under variations of stiffness and thickness. The difference in the studied variables between the three groups (Cl II/6s, Cl II/7s and Cl III) was evaluated using the Friedman's Analysis of Variance, followed by a pairwise comparison with a Bonferroni correction.

All variables were correlated using the Pearson product correlation coefficient when the data was normally distributed or the Spearman correlation coefficient when the normality assumption was not met.

The level of significance was set at 0.05. All statistical computations were performed using the Statistical Package for Social Sciences (SPSS[®], version 20.0, IBM[®]).

CHAPTER 4

RESULTS

A large amount of data has been computed. To sustain the flow of the narrative, the descriptive data for each component are presented in tables in corresponding appendices. The mean of those data and accompanying statistics are displayed within the Results chapter.

4.1. Comparisons between treatment groups

The CI III group findings were not normally distributed per Shapiro-Wilk Normality tests. Hence, when combining the data, the comparisons were performed in a non-parametric ANOVA, the Freidman's analysis.

4.1.1. Comparisons of the TMJ complex

4.1.1.1. Comparisons under stiffness variation

All comparisons showed a significant difference at all levels of the TMJ on both sides, between the stress levels of CI II elastics delivered from the mandibular 1st molars (CI II/6s) compared with CI III elastics delivered on the lower canines ($p = 0.001$) (Table 4.1.1). A difference was observed between the elastics delivered on the mandibular 1st molars compared to those delivered on the mandibular 2nd molars. Although this difference was not significant ($p = 0.076$), the elastics delivered from the mandibular 2nd molar (CI II/7s) exhibited a greater stress effect on the condyle. Comparisons between the CI III elastics and the CI II/7s showed no significant difference ($p=0.35$).

Visual stress comparisons showed the effects of the pull of the elastics in the different modalities of treatment. On the condylar area, the CI II/6s model (Fig 4.1.1, A) revealed almost similar stress when compared with the CII/7s model (Fig 4.1.1, B). However, the greatest difference was noted between both CI II models and the CI III model in which the stresses were different on the neck of the condyle (Fig 4.1.1, C).

Table 4.1.1. Freidman’s 2-way ANOVA of TMJ complex under stiffness variation

		Right Side							
Region	Area	1	2	3	Freidman Analysis				
		CI II/6s	CI II/7s	CI III	Test Statistic	p	1 vs. 2	1 vs. 3	2 vs. 3
Cond	Anterior	0.1372	0.1477	0.1712	14600	0.001	0.076	0.0001	0.3530
	Middle	0.0811	0.0876	0.1033	14600	0.001	0.076	0.0001	0.3530
	posterior	0.0992	0.1060	0.1249	14600	0.001	0.076	0.0001	0.3530
Disk	Anterior	0.0292	0.0315	0.0362	14600	0.001	0.076	0.0001	0.3530
	Middle	0.0203	0.0226	0.0258	14600	0.001	0.076	0.0001	0.3530
	posterior	0.0324	0.0351	0.0408	14600	0.001	0.076	0.0001	0.3530
Temp	Anterior	0.1216	0.1302	0.1532	14600	0.001	0.076	0.0001	0.3530
	Middle	0.0978	0.1090	0.1268	14600	0.001	0.076	0.0001	0.3530
	posterior	0.0510	0.0537	0.0631	14600	0.001	0.076	0.0001	0.3530

		Left Side							
Region	Area	1	2	3	Freidman Analysis				
		CI II/6s	CI II/7s	CI III	Test Statistic	p	1 vs. 2	1 vs. 3	2 vs. 3
Cond	Anterior	0.1434	0.1568	0.2026	14600	0.001	0.076	0.0001	0.3530
	Middle	0.0924	0.0981	0.1307	14600	0.001	0.076	0.0001	0.3530
	posterior	0.1031	0.1089	0.1457	14600	0.001	0.076	0.0001	0.3530
Disk	Anterior	0.0335	0.0358	0.0473	14600	0.001	0.076	0.0001	0.3530
	Middle	0.0369	0.0378	0.0517	14600	0.001	0.076	0.0001	0.3530
	posterior	0.0216	0.0221	0.0303	14600	0.001	0.076	0.0001	0.3530
Temp	Anterior	0.0824	0.1096	0.1212	14600	0.001	0.076	0.0001	0.3530
	Middle	0.0836	0.1046	0.1200	14600	0.001	0.076	0.0001	0.3530
	posterior	0.0470	0.0688	0.0699	14600	0.001	0.076	0.0001	0.3530

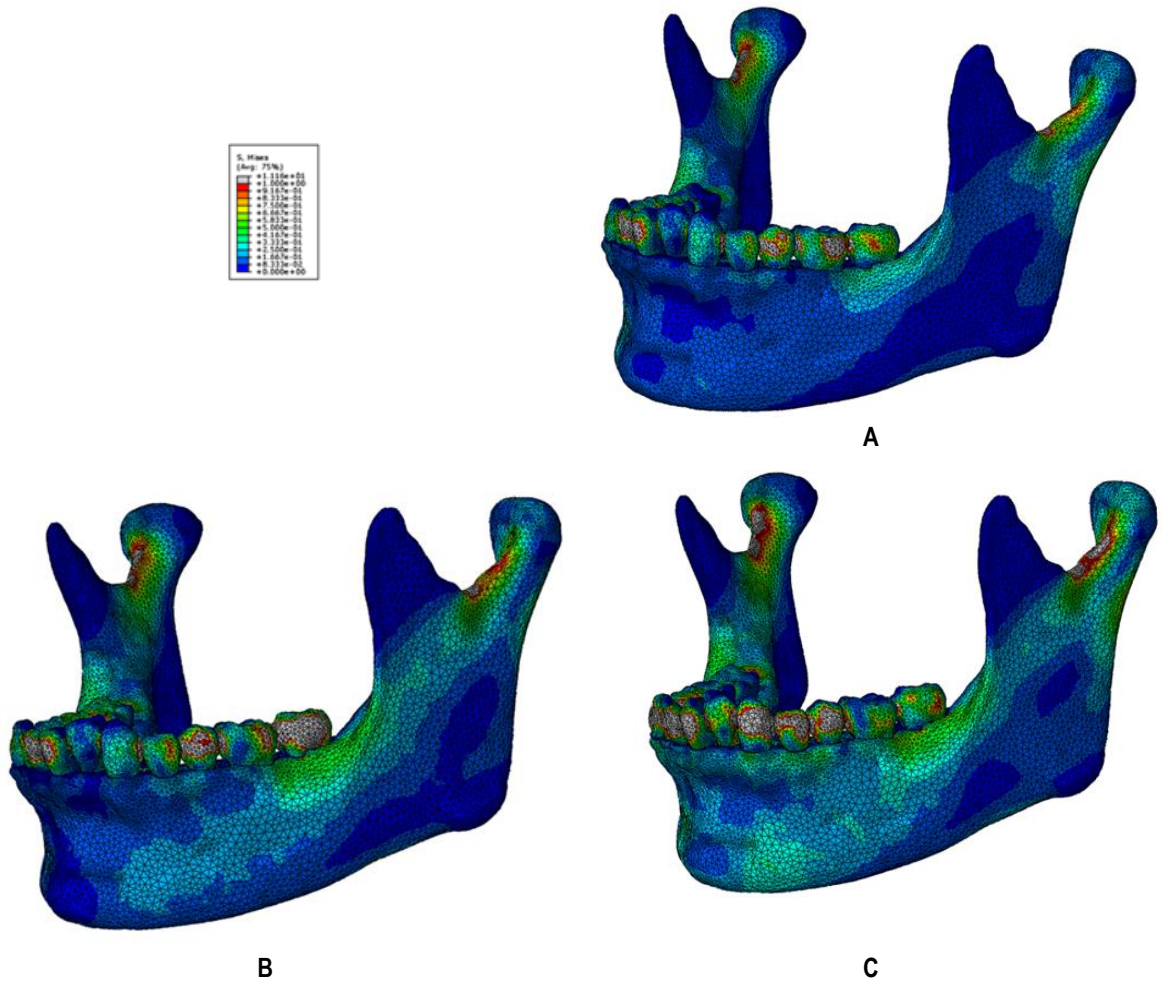
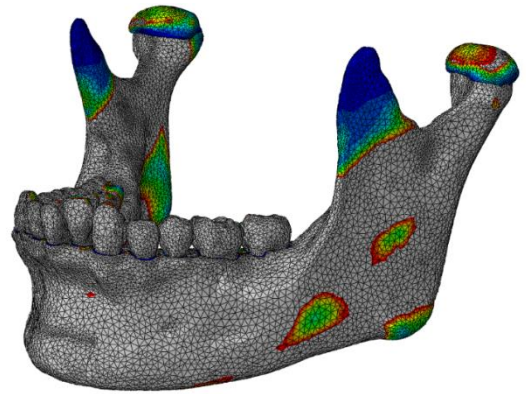
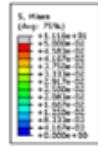


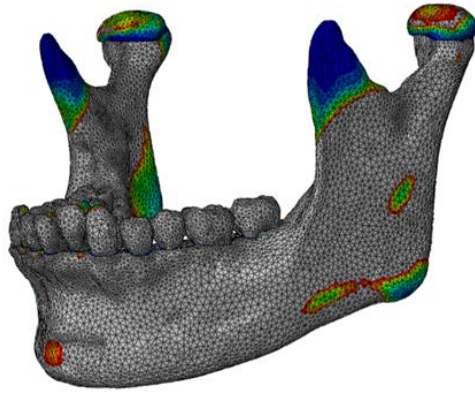
Fig 4.1.1. Stresses on mandibular body are represented in different treatment modalities under stiffness variations. A. CI II/6s variation, B. CI II/7s variation, C. CI III's variation

At the level of the articular disk, the highest stress (grey color) was noted in the CI III group (Fig 4.1.2, C), followed by the CI II/7s group (Fig 4.1.2, B) then in the CI II/6s (Fig 4.1.2, A). In the CI III group, the highest stress was at the middle level of the articular parts compared with the other groups where the stress was more diffused.

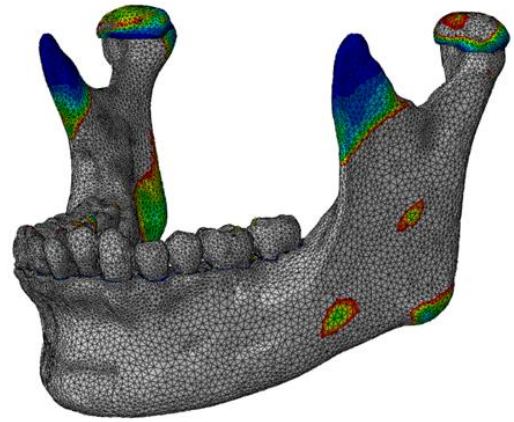
At the level of the temporal bone, the lowest Von Mises stresses were found in the CI II/6s group (Fig. 4.1.3, A). Although differences existed between right and left sides, both exhibited lower stress values compared with other modalities of elastics. Both CI II/7s (Fig 4.1.3, B) and CI III (Fig. 4.1.3, C) shared nearly similar patterns with similar degrees of Von Mises stress.



A



B



C

Fig 4.1.2. Stresses on mandibular body and TMJ articular disk in the different treatment modalities under stiffness variations. A. CI II/6s variation, B. CI II/7s variation, C. CI III's variation

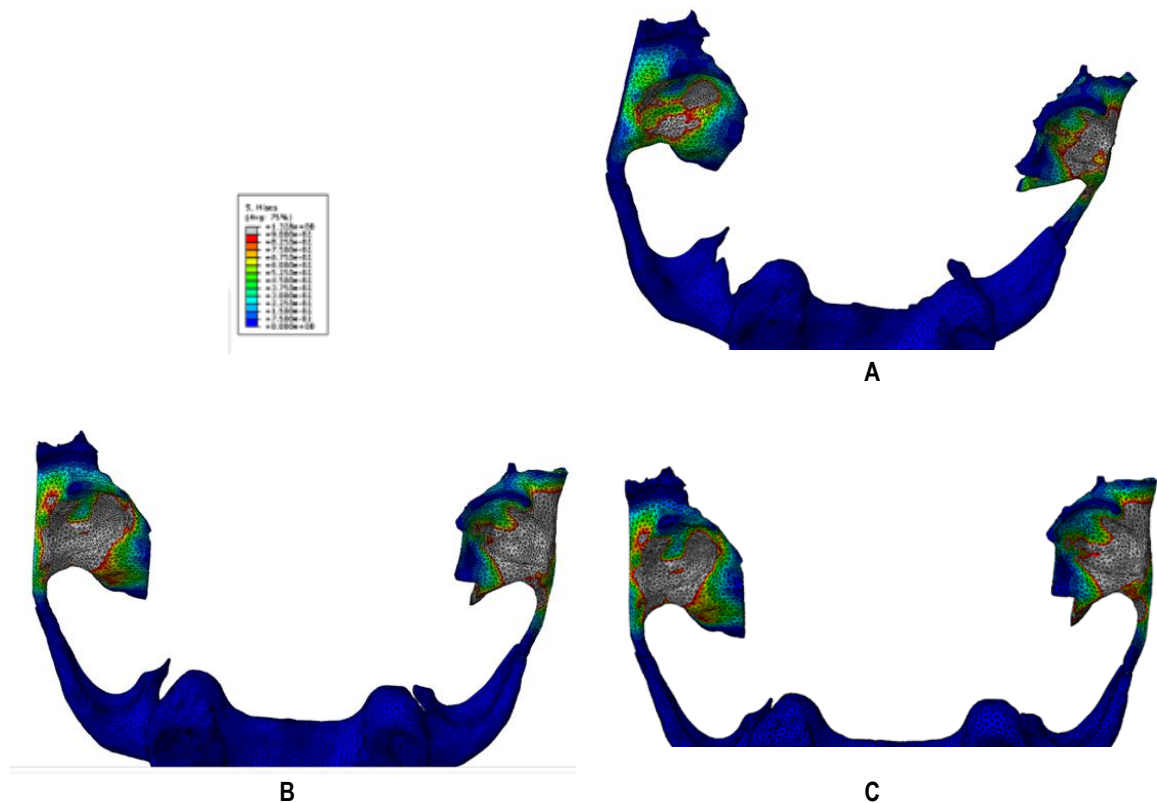


Fig 4.1.3. Stresses on the temporal fossae in different treatment modalities under stiffness variations. A. CI II/6s variation B. CI II/7s variation C. CI III's variation

4.1.1.2. Comparisons in the thickness variation

Less statistically significant findings were prevalent in the comparisons under thickness variation group (Table 4.1.2). Statistically significant comparisons indicated a higher stress at the level of the CI III elastics compared to the CI II elastics delivered from the mandibular 1st molars. The latter generated less stress on the TMJ complex compared with those delivered from the mandibular 2nd molars. While this finding was not significant under the stiffness variation group, it was prevalent across all areas of comparisons.

Table 4.1.2. Freidman's 2-way ANOVA of stress (MPa) of TMJ complex thickness variation

Right Side

Region	Area	1	2	3	Freidman Analysis				
		CI II/6s	CI II/7s	CI III	Test Statistic	p	1 vs. 2	1 vs. 3	2 vs. 3
Cond	Anterior	0.1116	0.1010	0.0960	5000	0.082	0.353	0.353	0.353
	Middle	0.0846	0.0724	0.0705	5600	0.061	0.353	0.353	0.353
	posterior	0.0972	0.0903	0.0878	5000	0.082	0.353	0.353	0.353
Disk	Anterior	0.0245	0.0227	0.0207	6200	0.045	1	0.0420	0.353
	Middle	0.0219	0.0180	0.0164	6200	0.045	1	0.0420	0.353
	posterior	0.0494	0.0378	0.0349	9800	0.007	0.353	0.0050	0.353
Temp	Anterior	0.1275	0.1127	0.1098	6200	0.045	0.353	0.042	1
	Middle	0.0878	0.0831	0.0818	5000	0.082	0.353	0.353	0.353
	posterior	0.0979	0.0773	0.0751	6200	0.045	0.353	0.042	1

Left Side

Region	Area	1	2	3	Freidman Analysis				
		CI II/6s	CI II/7s	CI III	Test Statistic	p	1 vs. 2	1 vs. 3	2 vs. 3
Cond	Anterior	0.1568	0.1406	0.1401	2600	0.273	0.353	0.353	0.353
	Middle	0.0994	0.0848	0.0851	6200	0.045	0.353	0.0420	1.0000
	posterior	0.1154	0.1070	0.1078	5000	0.82	0.353	0.353	0.353
Disk	Anterior	0.0363	0.0322	0.0313	3800	0.15	0.353	0.353	0.353
	Middle	0.0349	0.0321	0.0320	2600	0.273	0.353	0.353	0.353
	posterior	0.0325	0.0241	0.0233	5600	0.061	0.353	0.353	0.353
Temp	Anterior	0.1121	0.0978	0.0907	6200	0.045	1	0.0420	0.3530
	Middle	0.1330	0.1188	0.1083	2600	0.273	0.353	0.353	0.353
	posterior	0.0846	0.0778	0.0652	5000	0.082	0.353	0.353	0.353

4.1.2. Comparisons of stresses at the periodontal ligament

4.1.2.1. Comparisons under stiffness variation

Highly statistically significant differences were observed at various levels of the PDL areas on both sides ($p < 0.05$). The greatest differences were noted between CI II/6s and the CI III mainly at the level of the canines and incisors (Tables 4.1.3, 4.1.4).

Differences between the CI II/6s and CI III's were at the level of the 2nd molars. CI III

was the elastic configuration with the most generating stress potential, (except on the lower 2nd molar with CI II/7s where the mandibular 2nd molars were the anchor teeth).

This group had the second highest stress generation except on the 1st molars where the CI II/6 group exhibited higher stress on the anchoring first molars. (Tables 4.1.3. 4.1.4)

The stress related diagrams on the PDL and on the crowns of the teeth was demonstrated on the teeth supporting the pressure of the elastics (Fig 4.1.4, B, D, F). A normal (crown-to-crown) transmission of stress was shown across the crowns of the teeth.

In CI II/6s, the 1st molars that supported the elastics, exhibited the highest stress (gray color) (Fig 4.1.4, B). The lowest stresses are observed at the level of the PDL compared with other modalities of treatment (Fig 4.1.4, A).

In the CI II/7s, the PDL at the distal side of the 2nd molar showed the highest stress compared with the other elastics (Fig 4.1.4, C). At the level of the teeth, the greatest dental stress was seen on the 2nd molar with also a high transmission of stress to the adjacent 1st molar and premolars (Fig 4.1.4, D).

In the CI III group, a higher level of stress than the other modalities was demonstrable at the level of the crowns of the incisors.

Table 4.1.3. Freidman's 2-way ANOVA of stress (MPa) of dental units under stiffness variations (right side)

Region	Area	1	2	3	Freidman Analysis				
		CI II/6s	CI II/7s	CI III	Test Statistic	p	1 vs. 2	1 vs. 3	2 vs. 3
47 D	Coronal	0.0035	0.00637	0.00300	20000	0.0001	0.076	0.076	0.0001
	Middle	0.0026	0.00593	0.00279	20000	0.0001	0.0001	0.076	0.076
	Apical	0.0021	0.00536	0.00281	20000	0.0001	0.0001	0.076	0.076
47 M	Coronal	0.0029	0.00378	0.00356	20000	0.0001	0.0001	0.076	0.076
	Middle	0.0028	0.00409	0.00339	20000	0.0001	0.0001	0.076	0.076
	Apical	0.0023	0.00395	0.00317	20000	0.0001	0.0001	0.076	0.076
46 D	Coronal	0.0031	0.00326	0.00366	20000	0.0001	0.076	0.0001	0.076
	Middle	0.0030	0.00280	0.00338	20000	0.0001	0.076	0.076	0.0001
	Apical	0.0027	0.00276	0.00340	20000	0.0001	0.076	0.0001	0.076
46 M	Coronal	0.0047	0.00456	0.00564	20000	0.0001	0.076	0.076	0.0001
	Middle	0.0050	0.00460	0.00584	20000	0.0001	0.076	0.076	0.0001
	Apical	0.0044	0.00420	0.00530	20000	0.0001	0.076	0.076	0.0001
43 D	Coronal	0.0037	0.00381	0.00493	20000	0.0001	0.076	0.0001	0.076
	Middle	0.0034	0.00361	0.00466	20000	0.0001	0.076	0.0001	0.076
	Apical	0.0035	0.00384	0.00528	20000	0.0001	0.076	0.0001	0.076
43 M	Coronal	0.0038	0.00409	0.00527	20000	0.0001	0.076	0.0001	0.076
	Middle	0.0038	0.00399	0.00508	20000	0.0001	0.076	0.0001	0.076
	Apical	0.0037	0.00400	0.00551	20000	0.0001	0.076	0.0001	0.076
41 D	Coronal	0.0025	0.00300	0.00439	20000	0.0001	0.076	0.0001	0.076
	Middle	0.0021	0.00243	0.00355	20000	0.0001	0.076	0.0001	0.076
	Apical	0.0019	0.00212	0.00297	20000	0.0001	0.076	0.0001	0.076
41 M	Coronal	0.0019	0.00241	0.00292	20000	0.0001	0.076	0.0001	0.076
	Middle	0.0019	0.00233	0.00205	20000	0.0001	0.0001	0.076	0.076
	Apical	0.0020	0.00247	0.00210	20000	0.0001	0.0001	0.076	0.076

Table 4.1.4. Freidman's 2-way ANOVA of stress (MPa) of dental units under stiffness variations (left side)

Region	Area	1	2	3	Freidman Analysis				
		CI II/6s	CI II/7s	CI III	Test Statistic	p	1 vs. 2	1 vs. 3	2 vs. 3
37 D	Coronal	0.0020	0.00840	0.00287	20000	0.0001	0.0001	0.076	0.076
	Middle	0.0013	0.00755	0.00196	20000	0.0001	0.0001	0.076	0.076
	Apical	0.0009	0.00639	0.00138	20000	0.0001	0.0001	0.076	0.076
37 M	Coronal	0.0023	0.00198	0.00348	20000	0.0001	0.076	0.076	0.001
	Middle	0.0020	0.00176	0.00303	20000	0.0001	0.076	0.076	0.001
	Apical	0.0011	0.00200	0.00172	20000	0.0001	0.001	0.076	0.076
36 D	Coronal	0.0022	0.00262	0.00337	20000	0.0001	0.076	0.0001	0.076
	Middle	0.0016	0.00194	0.00241	20000	0.0001	0.076	0.0001	0.076
	Apical	0.0014	0.00171	0.00195	20000	0.0001	0.076	0.0001	0.076
36 M	Coronal	0.0038	0.00514	0.00513	16800	0.0001	0.0001	0.022	0.076
	Middle	0.0033	0.00500	0.00467	20000	0.0001	0.0001	0.076	0.076
	Apical	0.0025	0.00417	0.00372	20000	0.0001	0.0001	0.076	0.076
33 D	Coronal	0.0023	0.00310	0.00324	20000	0.0001	0.076	0.0001	0.076
	Middle	0.0018	0.00252	0.00171	20000	0.0001	0.076	0.076	0.0001
	Apical	0.0014	0.00223	0.00167	20000	0.0001	0.0001	0.076	0.076
33 M	Coronal	0.0024	0.00328	0.00327	20000	0.0001	0.0001	0.076	0.076
	Middle	0.0020	0.00284	0.00225	20000	0.0001	0.0001	0.076	0.076
	Apical	0.0017	0.00254	0.00210	20000	0.0001	0.0001	0.076	0.076
31 D	Coronal	0.0020	0.00247	0.00345	20000	0.0001	0.076	0.0001	0.076
	Middle	0.0019	0.00223	0.00299	20000	0.0001	0.076	0.0001	0.076
	Apical	0.0018	0.00210	0.00275	20000	0.0001	0.076	0.0001	0.076
31 M	Coronal	0.0025	0.00303	0.00446	20000	0.0001	0.076	0.0001	0.076
	Middle	0.0021	0.00242	0.00349	20000	0.0001	0.076	0.0001	0.076
	Apical	0.0019	0.00217	0.00311	20000	0.0001	0.076	0.0001	0.076

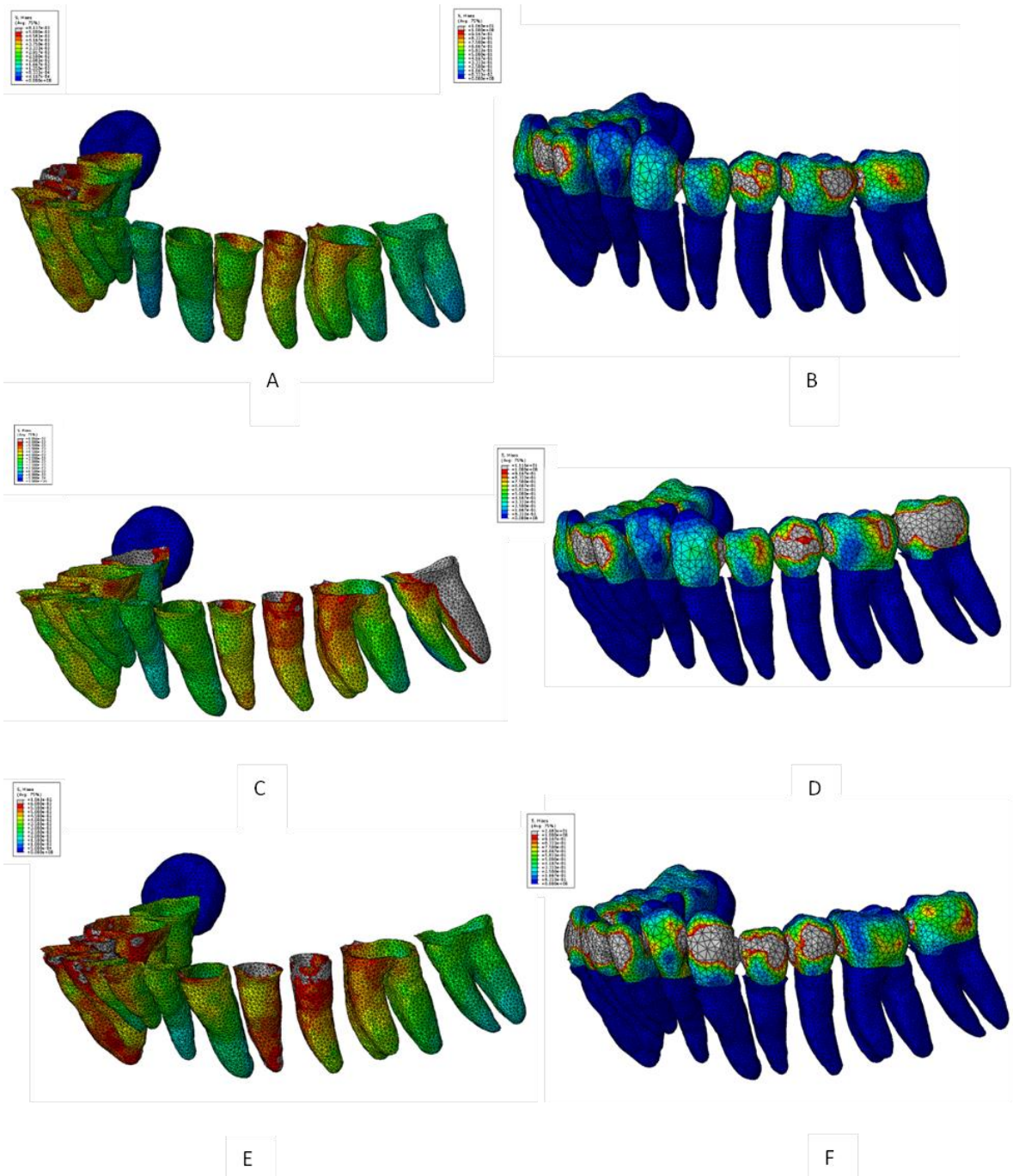


Fig 4.1.4. Von Mises stresses at the PDL ligament and at the teeth within each modality of treatment. A. C1 II/6s B. C1 II/7s C. C1 III

4.1.2.2. Comparisons under thickness variation

A low pattern of statistically significant differences was observed under thickness variations mainly at the level of the mandibular 2nd molar between the different modalities of treatment (Tables 4.1.5, 4.1.6). On the right side, most significant comparisons were present at the level of the 2nd molars between both types of the CI II elastics and between the CI II/7s and the CI III groups. Other significant findings were prevalent between the CI III and the CI II/6s groups.

On the left side, a more prevalent pattern of statistical difference existed between the different regions of the dental units. The most significant differences were between the CI III and the CI II/6s groups, whereby the CI III elastic configuration produced a greater stress on the dental units.

Table 4.1.5. Freidman's 2-way ANOVA of stress (MPa) in dental units under thickness variations (right side)

Region	Area	1	2	3	Freidman Analysis				
		CI II/6s	CI II/7s	CI III	Test Statistic	p	1 vs. 2	1 vs. 3	2 vs. 3
47 D	Coronal	0.0057	0.00972	0.0044	16800	0.0001	0.022	0.539	0.0001
	Middle	0.0054	0.00917	0.0042	16800	0.0001	0.022	0.539	0.0001
	Apical	0.0032	0.00702	0.0029	12600	0.002	0.022	1.000	0.002
47 M	Coronal	0.0039	0.00456	0.0037	5600	0.061	0.353	0.353	0.353
	Middle	0.0038	0.00478	0.0040	1800	0.407	0.353	0.353	0.353
	Apical	0.0050	0.00671	0.0046	9800	0.007	0.011	1.000	0.042
46 D	Coronal	0.0034	0.00370	0.0031	6200	0.045	1.0000	0.0420	0.3530
	Middle	0.0026	0.00310	0.0025	3800	0.15	0.353	0.353	0.353
	Apical	0.0025	0.00323	0.0026	3200	0.202	0.539	0.539	0.539
46 M	Coronal	0.0046	0.00467	0.0041	3800	0.15	0.539	0.539	0.539
	Middle	0.0048	0.00478	0.0042	3800	0.15	0.353	0.353	0.353
	Apical	0.0045	0.00454	0.0040	2600	0.273	0.353	0.539	0.353
43 D	Coronal	0.0046	0.00394	0.0037	5000	0.082	0.539	0.539	0.353
	Middle	0.0043	0.00357	0.0035	4200	0.122	0.539	0.353	0.539
	Apical	0.0044	0.00341	0.0039	5000	0.082	0.353	0.353	0.539
43 M	Coronal	0.0047	0.00389	0.0037	5000	0.082	0.539	0.353	0.353
	Middle	0.0047	0.00392	0.0036	4200	0.122	0.539	0.539	0.539
	Apical	0.0045	0.00360	0.0039	4200	0.122	0.353	0.539	0.539
41 D	Coronal	0.0030	0.00224	0.0027	5600	0.061	0.539	0.353	0.353
	Middle	0.0025	0.00175	0.0021	1400	0.497	0.539	0.353	0.353
	Apical	0.0022	0.00152	0.0017	600	0.741	0.539	0.353	0.539
41 M	Coronal	0.0035	0.00248	0.0029	7400	0.025	0.0760	1.0000	0.0420
	Middle	0.0030	0.00208	0.0022	1400	0.497	0.539	0.353	0.353
	Apical	0.0026	0.00161	0.00161	1556	0.459	0.539	0.353	0.353

Table 4.1.6. Freidman's 2-way ANOVA of stress (MPa) of dental units under thickness variations (Left side)

Region	Area	1	2	3	Freidman Analysis				
		CI II/6s	CI II/7s	CI III	Test Statistic	p	1 vs. 2	1 vs. 3	2 vs. 3
37 D	Coronal	0.0036	0.00805	0.0021	14600	0.001	0.076	0.353	0.0001
	Middle	0.0027	0.00816	0.0016	14600	0.001	0.076	0.353	0.0001
	Apical	0.0030	0.00737	0.0014	16200	0.0001	0.133	0.133	0.0001
37 M	Coronal	0.0045	0.00346	0.0022	11400	0.003	0.539	0.002	0.133
	Middle	0.0036	0.00325	0.0020	9800	0.007	1.000	0.011	0.042
	Apical	0.0101	0.00395	0.0077	9800	0.007	1.000	0.042	0.011
36 D	Coronal	0.0046	0.00334	0.0022	11400	0.003	0.539	0.002	0.133
	Middle	0.0041	0.00253	0.0018	8600	0.014	0.791	0.011	0.221
	Apical	0.0040	0.00215	0.0016	11400	0.003	0.133	0.002	0.539
36 M	Coronal	0.0042	0.00386	0.0031	8600	0.014	0.791	0.011	0.221
	Middle	0.0041	0.00341	0.0029	7200	0.027	0.539	0.022	0.539
	Apical	0.0036	0.00274	0.0023	6200	0.045	0.353	0.042	1.000
33 D	Coronal	0.0041	0.00330	0.0030	7200	0.027	0.539	0.022	0.539
	Middle	0.0037	0.00296	0.002	8600	0.014	0.791	0.011	0.221
	Apical	0.0037	0.00269	0.0023	9800	0.007	0.353	0.005	0.353
33 M	Coronal	0.0044	0.00339	0.0032	7200	0.027	0.539	0.022	0.539
	Middle	0.0041	0.00325	0.0027	8600	0.014	0.791	0.011	0.221
	Apical	0.0039	0.00297	0.0024	6200	0.045	1.000	0.042	0.353
31 D	Coronal	0.0033	0.00231	0.0027	7400	0.025	0.042	1.000	0.076
	Middle	0.0029	0.00194	0.0023	5600	0.061	0.221	1.000	0.076
	Apical	0.0028	0.00177	0.0021	7400	0.025	0.042	1.000	0.076
31 M	Coronal	0.0038	0.00265	0.0033	9600	0.008	0.022	1.000	0.022
	Middle	0.0029	0.00200	0.0025	3800	0.15	0.042	1.000	0.076
	Apical	0.0027	0.00169	0.0021	5600	0.061	0.221	1.000	0.076

4.1.3. Comparisons of displacements at the dental units

4.1.3.1. Comparisons of displacements by vector

A high pattern of significance existed between the comparisons under thickness and stiffness variations. In the stiffness variation, a highly significant difference was present between the CI III and the CI II/7s groups (Table 4.1.7).

Although not statistically significant, the displacement from CI III was in opposite direction than that of the CI II/6s, which was in line with the CI II/7s ($p=0.076$). The CI III elastic was the most affective in producing dental displacement. However, when comparing CI II groups, the CI II/7s produced a greater mesialising effect on the lower dentition.

A greater pattern of significance was observed under thickness variation. The highest significant difference in displacement was between the CI II/6s compared with the CI III elastics. A weaker significance was noted between CI II/7s and the CI III elastics. The CI III group demonstrated the highest degree of displacement followed by CI II/7s, then the group where the CI II/6s.

4.1.3.2. Comparisons of displacements by magnitude

Upon comparing the magnitude of the produced displacements, negating the direction of movement produced by the dental units, a similar pattern of significance was observed.

Under stiffness variation, the highest significant difference was between the displacements produced by the CI III and the CI II/7s elastics (Table 4.1.8).

Under thickness variation, only the displacements of the posterior teeth were significantly different between the CI III and the CI II/6s elastics groups.

Hence on average, the CI III elastics produced the greatest displacements followed by the CI II/7s and last, the CI II/6s configurations.

Table 4.1.7. Freidman's 2-way ANOVA of displacement of dental units (mm)

Variation: Stiffness		1	2	3	Freidman Analysis			
Measure	CI II/6s	CI II/7s	CI III	Test Statistic	p	1 vs. 2	1 vs. 3	2 vs. 3
Disp 47	-0.0101	-0.01009	0.01155	15200	0.001	1.000	0.001	0.005
Disp 46	-0.00867	-0.00885	0.01075	20000	0.0001	0.076	0.076	0.001
Disp 43	-0.00837	-0.01056	0.01511	20000	0.0001	0.076	0.076	0.001
Disp 41	-0.00992	-0.01231	0.01768	20000	0.0001	0.076	0.076	0.001
Disp 37	-0.01134	-0.01183	0.01274	20000	0.0001	0.076	0.076	0.001
Disp 36	-0.01127	-0.00995	0.01226	20000	0.0001	0.076	0.076	0.001
Disp 33	-0.00878	-0.01156	0.01593	20000	0.0001	0.076	0.076	0.001
Disp 31	-0.00783	-0.01178	0.01667	20000	0.0001	0.076	0.076	0.001

Variation: Thickness		1	2	3	Freidman Analysis			
Measure	CI II/6s	CI II/7s	CI III	Test Statistic	p	1 vs. 2	1 vs. 3	2 vs. 3
Disp 47	-0.02838	-0.01547	0.01301	15800	0.0001	1.000	0.0001	0.011
Disp 46	-0.02752	-0.01352	0.01248	18200	0.0001	0.221	0.0001	0.042
Disp 43	-0.02698	-0.01427	0.01507	16800	0.0001	0.539	0.001	0.022
Disp 41	-0.02841	-0.01612	0.01721	16800	0.0001	0.539	0.001	0.022
Disp 37	-0.03042	-0.01407	0.01275	16800	0.0001	0.539	0.001	0.022
Disp 36	-0.03092	-0.01239	0.01234	16800	0.0001	0.539	0.001	0.022
Disp 33	-0.03115	-0.01401	0.01443	16800	0.0001	0.539	0.001	0.022
Disp 31	-0.02812	-0.01595	0.01691	16800	0.0001	0.539	0.001	0.022

**Table 4.1.8. Freidman's 2-way ANOVA of displacement (mm)
of dental units in magnitude(Absolute value)**

Variation: Stiffness		1	2	3	Freidman Analysis			
Measure	CI II/6s	CI II/7s	CI III	Test Statistic	p	1 vs. 2	1 vs. 3	2 vs. 3
Disp 47	0.0101	0.01009	0.01155	15200	0.00100	1.000	0.001	0.005
Disp 46	0.00867	0.00885	0.01075	20000	0.00010	0.076	0.001	0.076
Disp 43	0.00837	0.01056	0.01511	20000	0.00010	0.076	0.001	0.076
Disp 41	0.00992	0.01231	0.01768	20000	0.00010	0.076	0.001	0.076
Disp 37	0.01134	0.01183	0.01274	20000	0.00010	0.076	0.001	0.076
Disp 36	0.01127	0.00995	0.01226	20000	0.00010	0.076	0.001	0.076
Disp 33	0.00878	0.01156	0.015.3	20000	0.00010	0.076	0.001	0.076
Disp 31	0.00783	0.01178	0.01667	20000	0.00010	0.076	0.001	0.076

Variation: Thickness		1	2	3	Freidman Analysis			
Measure	CI II/6s	CI II/7s	CI III	Test Statistic	p	1 vs. 2	1 vs. 3	2 vs. 3
Disp 47	0.02838	0.01547	0.01301	6200	0.045	1.000	0.042	0.353
Disp 46	0.02752	0.01352	0.01248	8600	0.014	0.221	0.011	0.791
Disp 43	0.02698	0.01427	0.01507	3800	0.15	0.221	0.221	0.791
Disp 41	0.02841	0.01612	0.01721	5600	0.061	0.791	0.221	0.791
Disp 37	0.03042	0.01407	0.01275	7200	0.027	0.539	0.022	0.539
Disp 36	0.03092	0.01239	0.01234	6200	0.045	0.353	0.042	1.000
Disp 33	0.03115	0.01401	0.01443	5600	0.061	0.539	0.791	0.221
Disp 31	0.02812	0.01595	0.01691	5600	0.061	0.539	0.791	0.221

4.2. Comparisons within treatment groups

4.2.1. CI II/6s

4.2.1.1. Stiffness Variation

4.2.1.1. A. TMJ

In the Class II/6s group, Von Mises stresses at the level of the disk were lower than those at the condyle and temporal bone (Appendix 1, Table 4.2.1). The stress differences between right and left sides were statistically significantly different at all TMJ levels tested in the stiffness variation (Table 4.2.2).

Table 4.2.2. Right compared with Left Von Mises stresses (MPa) on TMJ components under stiffness variations in CI II/6s group

Region	Area	Mean		p
		R	L	
Cond	Anterior	0.1373	0.1434	0.00001
	Middle	0.0812	0.0925	0.00001
	Posterior	0.0993	0.1032	0.00001
Disk	Anterior	0.0293	0.0336	0.00001
	Middle	0.0204	0.0374	0.00001
	Posterior	0.0324	0.0216	0.00001
Temp	Anterior	0.1216	0.0825	0.00001
	Middle	0.0978	0.0837	0.00001
	Posterior	0.0512	0.0471	0.00001

Cond: Condyle; **Temp:** Temporal Bone
D: Distal; **M:** Mesial

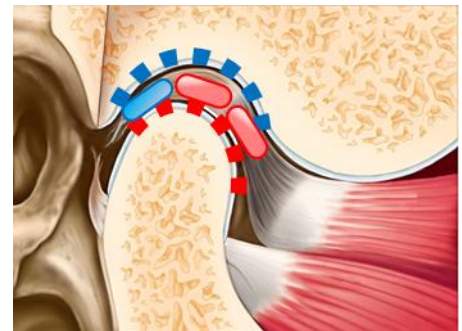


Fig. 4.2.1. The pattern of distribution of the Von Mises stresses (MPa) in the stiffness category is illustrated comparing right (blue) and left (red) sides. Stresses were higher at the anterior and middle levels of the disk and all parts of the condyle (anterior, middle, posterior) on the left side. On the right side, higher stresses were found on the posterior disk and all parts of the temporal bone. Modified from image by www.thenextdds.com

The left side of the joint demonstrated higher stress at all condylar areas (anterior, middle, posterior) and in the middle part of the disk. The regions of the posterior disk and all the temporal bone parts showed higher stresses on the right side (Fig 4.2.1.). On average, the left side exhibited the highest stress levels compared to the right side.

4.2.1.1. B. PDL

The differences between right and left sides for all regions were statistically significant. Higher stresses on the PDL were probed on the right side, except for the central incisor on the left sides in 4 out of the 6 mesial and distal regions (Appendix 1 Table 4.2.3, Table 4.2.4).

Table 4.2.4. Right compared with left / Von Mises stresses (MPa) on periodontal ligament of dental components under stiffness variations in CI II/6s group

Region	Area	Mean		p
		R	L	
47 D vs 37 D	Coronal	0.0035	0.0020	0.0001
	Middle	0.0026	0.0013	0.0001
	Apical	0.0021	0.0009	0.0001
47 M vs 37 M	Coronal	0.0029	0.0023	0.0001
	Middle	0.0028	0.0020	0.0001
	Apical	0.0023	0.0011	0.0001
46 D vs 36 D	Coronal	0.0031	0.0022	0.0001
	Middle	0.0030	0.0016	0.0001
	Apical	0.0027	0.0014	0.0001
46 M vs 36 M	Coronal	0.0047	0.0038	0.0001
	Middle	0.0050	0.0033	0.0001
	Apical	0.0044	0.0025	0.0001
43 D vs 33 D	Coronal	0.0037	0.0023	0.0001
	Middle	0.0034	0.0018	0.0001
	Apical	0.0035	0.0014	0.0001
43 M vs 33 M	Coronal	0.0038	0.0024	0.0001
	Middle	0.0038	0.0020	0.0001
	Apical	0.0037	0.0017	0.0001
41 D vs 31 D	Coronal	0.0025	0.0020	0.0001
	Middle	0.0021	0.0019	0.0001
	Apical	0.0019	0.0018	0.0001
41 M vs 31 M	Coronal	0.0019	0.0025	0.0001
	Middle	0.0019	0.0021	0.0001
	Apical	0.0020	0.0019	0.0001

D: Distal; **M:** Mesial

4.2.1.1. C. Dental displacement

A lower degree of displacement was noted at the crowns of the mandibular teeth on the right side compared to the left side (Appendix 1 Table 4.2.5). The displacement differences between right and left sides were statistically significantly different at all crown levels except at the central incisor (Table 4.2.6).

Table 4.2.6. Right compared with left/ dental displacement (mm) of dental components under stiffness variations in C1 II/6s group

		Mean		p
		R	L	
Stiffness	47 vs 37	-0.0101	-0.01134	0.0001
	46 vs 36	-0.00867	-0.01127	0.0001
	43 vs 33	-0.00837	-0.00878	0.0001
	41 vs 31	-0.00992	-0.00783	0.0001

R: Right; **L:** Left

Values have a negative sign indicating mesial direction of displacement.

4.2.1.2. Thickness Variation

4.2.1.2. A. TMJ

Higher levels of Von Mises stresses were gauged on the left joint (Appendix 1, Table 4.2.7). The differences between variables were statistically significant except for the posterior section of the temporal bone (Table 4.2.8).

The left side of the TMJ demonstrated higher stress levels from anterior to posterior condyle, middle disk and middle temporal bone areas. The regions of the posterior disk and anterior temporal bone showed higher stresses on the right side (Fig 4.2.2).

4.2.1.2. B. PDL

At the level of the PDL, higher mean Von Mises stresses were observed on the left side. Remarkably, higher standard deviations were also noted (Appendix 1, Table 4.2.9).

Statistically significant stresses were observed between right and left sides at the distal side of the mandibular 1st molar and of the central incisor (Table 4.2.10).

Table 4.2.8. Right compared with Left Von Mises stresses (MPa) on TMJ components under thickness variations in CI II/6s group

Region	Area	Mean		p
		R	L	
Cond	Anterior	0.111	0.156	0.0001
	Middle	0.084	0.099	0.004
	Posterior	0.097	0.115	0.021
Disk	Anterior	0.024	0.036	0.001
	Middle	0.021	0.034	0.003
	Posterior	0.049	0.032	0.003
Temp	Anterior	0.127	0.112	0.014
	Middle	0.087	0.133	0.002
	Posterior	0.097	0.084	0.363

Cond: Condyle; **Temp:** Temporal Bone
D: Distal; **M:** Mesial

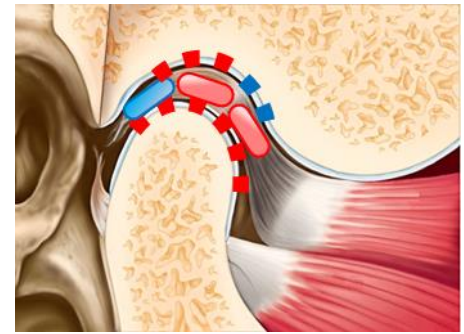


Fig. 4.2.2. The pattern of distribution of the Von Mises stresses (MPa) in the thickness category is illustrated comparing right (blue) and left (red) sides. Stresses were higher at the anterior and middle levels of the disk, the middle region of the temporal bone and all parts of the condyle (anterior, middle, posterior) on the left side. On the right side, higher stresses were found on the posterior disk, and anterior part of the temporal bone.
 Modified from image by: www.thenextdds.com

4.2.1.2. C. Dental displacement

Greater displacement was noted on the left side of the mandibular crowns (Appendix 1, Table 4.2.11). No statistically significant differences were found on both sides across all the crowns of the teeth (Table 4.2.12); both the right and the left sides apparently displaced similarly.

Table 4.2.10. Right vs with Left Von Mises stresses (MPa) on dental components under thickness variations in CI II/6s group

Modality:		CI II from 1st molars		
Region	Area	Mean		p
		R	L	
47 D vs 37 D	Coronal	0.0057	0.0036	0.277
	Middle	0.0054	0.0027	0.246
	Apical	0.0032	0.0030	0.861
47 M vs 37 M	Coronal	0.0039	0.0045	0.421
	Middle	0.0038	0.0036	0.884
	Apical	0.0050	0.0101	0.532
46 D vs 36 D	Coronal	0.0034	0.0046	0.023
	Middle	0.0026	0.0041	0.014
	Apical	0.0025	0.0040	0.005
46 M vs 36 M	Coronal	0.0046	0.0042	0.122
	Middle	0.0048	0.0041	0.100
	Apical	0.0045	0.0036	0.037
43 D vs 33 D	Coronal	0.0046	0.0041	0.158
	Middle	0.0043	0.0037	0.130
	Apical	0.0044	0.0037	0.051
43 M vs 33 M	Coronal	0.0047	0.0044	0.281
	Middle	0.0047	0.0041	0.082
	Apical	0.0045	0.0039	0.082
41 D vs 31 D	Coronal	0.0030	0.0033	0.029
	Middle	0.0025	0.0029	0.003
	Apical	0.0022	0.0028	0.013
41 M vs 31 M	Coronal	0.0035	0.0038	0.016
	Middle	0.0030	0.0029	0.756
	Apical	0.0026	0.0027	0.555

D: Distal; **M:** Mesial

R: Right; **L:** Left

Table 4.2.12. Right vs. left dental displacement (mm) of dental components under thickness variations in CI II/6s group

		Mean		p
		R	L	
Thickness	47 vs 37	-0.02838	-0.03042	0.269
	46 vs 36	-0.02752	-0.03092	0.311
	43 vs 33	-0.02698	-0.03115	0.290
	41 vs 31	-0.02841	-0.02812	0.650

D: Distal; **M:** Mesial

R: Right; **L:** Left

Values have a negative sign indicating mesial direction of displacement.

4.2.2. CI II/7s

4.2.2.1. Stiffness Variation

4.2.2.1. A. TMJ

Higher stresses were noted on the left side (Appendix 1, Table 4.2.13). Lowest stress values were recorded at the level of the articular disk on both sides compared with the condyle and the temporal fossa.

Right versus left differences were statistically significantly different for nearly all variables (Table 4.2.14). Of all the TMJ parts tested in the stiffness variation, the posterior section of the temporal bone was not statistically different between the right and the left sides (Fig. 4.3.1). The pattern of distribution of stresses within the condyle, disk, and temporal bone regions was similar to that observed in the CI II/6s group (Fig. 4.2.1, Fig. 4.2.3).

Table 4.2.14. Right compared with Left Von Mises stresses (MPa) on TMJ components under stiffness variations in CI II/7s group

Region	Area	Mean		p
		R	L	
Cond	Anterior	0.1478	0.1569	0.00001
	Middle	0.0877	0.0981	0.00001
	posterior	0.1061	0.1089	0.00005
Disk	Anterior	0.0315	0.0359	0.00001
	Middle	0.0227	0.0378	0.00001
	posterior	0.0351	0.0221	0.00001
Temp	Anterior	0.1302	0.1097	0.00001
	Middle	0.109	0.1046	0.00001
	posterior	0.0537	0.0689	0.00001

Cond: Condyle; Temp: Temporal Bone
R: Right; L: Left



Fig. 4.2.3. The pattern of distribution of the Von Mises stresses (MPa) in the stiffness category is illustrated comparing right (blue) and left (red) sides. Stresses were higher at the anterior and middle levels of the disk, the posterior region of the temporal bone and all parts of the condyle (anterior, middle, posterior) on the left side. On the right side, higher stresses were found on the posterior disk, and anterior and middle part of the temporal bone. Modified from image by: www.thenextdds.com

4.2.2.1. B. PDL

On average, statistically significant differences were found between the left and the right side across the dental regions of all the teeth (Appendix 1, Table 4.2.15). The right side showed the higher stress, except for the left central incisor (Table 4.2.16.).

Table 4.2.16. Right vs left Von Mises stresses (MPa) on the dental components under stiffness variations in CI II/7s group

Region	Area	Mean		p
		R	L	
47 D vs 37 D	Coronal	0.0063	0.0084	0.0001
	Middle	0.0059	0.0075	0.0001
	Apical	0.0053	0.0064	0.0001
47 M vs 37 M	Coronal	0.0037	0.0019	0.0001
	Middle	0.0041	0.0017	0.0001
	Apical	0.0039	0.0028	0.0001
46 D vs 36 D	Coronal	0.0032	0.0026	0.0001
	Middle	0.0028	0.0019	0.0001
	Apical	0.0027	0.0017	0.0001
46 M vs 36 M	Coronal	0.0045	0.0051	0.0001
	Middle	0.0046	0.0058	0.0001
	Apical	0.0042	0.0041	0.0001
43 D vs 33 D	Coronal	0.0043	0.0052	0.0001
	Middle	0.0039	0.0046	0.0001
	Apical	0.0035	0.0036	0.0001
43 M vs 33 M	Coronal	0.0045	0.0055	0.0001
	Middle	0.0042	0.0050	0.0001
	Apical	0.0044	0.0041	0.0001
41 D vs 31 D	Coronal	0.0031	0.0024	0.0001
	Middle	0.0024	0.0022	0.0001
	Apical	0.0021	0.0021	0.0001
41 M vs 31 M	Coronal	0.0024	0.0030	0.0001
	Middle	0.0023	0.0024	0.0001
	Apical	0.0024	0.0022	0.0001

D: Distal; **M:** Mesial
R: Right; **L:** Left

4.2.2.1. C. Dental displacement

In a parallel pattern to the PDL response, a greater displacement was demonstrated on the left side for most of the teeth except the lower central incisor (Appendix 1, Table 4.2.17. and Table 4.2.18).

Table 4.2.18. Right compared with left / dental displacement (mm) of the dental components under stiffness variations in CI II/7s group

		Mean		p VAL
		R	L	
Stiffness	47 vs 37	-0.01009	-0.01183	0.0001
	46 vs 36	-0.00885	-0.00995	0.0001
	43 vs 33	-0.01056	-0.01156	0.0001
	41 vs 31	-0.01231	-0.01178	0.0001

R: Right; **L:** Left

Values have a negative sign indicating mesial direction of displacement.

4.2.2.2. Thickness Variation

4.2.2.2. A. TMJ

The left side of the TMJ demonstrated higher degrees of stress with greater standard deviations than around the mean observed under stiffness variations (Appendix 1, Table 4.2.19). Nearly all differences were statistically significant except for the posterior section of the temporal bone (Table 4.2.20).

The left side of the TMJ demonstrated higher stress levels at all condylar regions, anterior and middle disk region, and middle region of the temporal bone. The regions of the posterior disk and all the anterior temporal bone parts showed higher stresses on the right side (Fig 4.2.4).

Table 4.2.20. Right compared with Left Von Mises stresses (MPa) on TMJ components under thickness variations in CI II/7s group

Region	Area	Mean		p
		R	L	
Cond	Anterior	0.101	0.1407	0.0001
	Middle	0.0725	0.0848	0.004
	posterior	0.0903	0.1071	0.031
Disk	Anterior	0.0227	0.0323	0.001
	Middle	0.0227	0.0321	0.003
	posterior	0.0378	0.0241	0.002
Temp	Anterior	0.1127	0.0978	0.002
	Middle	0.0832	0.1189	0.011
	posterior	0.0773	0.0778	0.939

Cond: Condyle; **Temp:** Temporal Bone
R: Right; **L:** Left

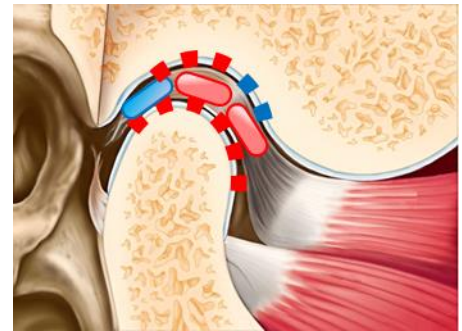


Fig. 4.2.4. The pattern of distribution of the Von Mises stresses (MPa) in the stiffness category is illustrated comparing right (blue) and left (red) sides. Stresses were higher at the anterior and middle levels of the disk, the middle region of the temporal bone and all parts of the condyle (anterior, middle, posterior) on the left side. On the right side, higher stresses were found on the posterior disk, and anterior part of the temporal bone.
 Modified from image by www.thenextdds.com

4.2.2.2. B. PDL

The right side demonstrated higher stress values (Appendix 1, Table 4.2.21).

The PDL mean tested under thickness variation demonstrated greater standard deviations when compared with the stiffness variation for the same units.

Statistically significant differences for the PDL regions of the first molars and canines were greater on the right side than the left side. Unlike the findings of the CI II/6s thickness variation, the recognizable pattern of difference is at the mesial side of the lower 1st molars across all its regions (Table 4.2.22).

4.2.2.2. C. Dental displacement

The right mandibular teeth displaced at a greater degree when compared with the left side (Appendix 1, Table 4.2.23). No significant differences were observed (Table 4.2.24), indicating similar displacement on both sides.

Table 4.2.22. Von Mises Stresses (MPa) of Right compared with left the dental components under thickness variations in the CI II/7s group

Region	Area	Mean		p
		R	L	
47 D vs 37 D	Coronal	0.00972	0.00805	0.324
	Middle	0.00917	0.00816	0.568
	Apical	0.00702	0.00737	0.706
47 M vs 37 M	Coronal	0.00456	0.00346	0.183
	Middle	0.00478	0.00325	0.210
	Apical	0.00671	0.00395	0.267
46 D vs 36 D	Coronal	0.00370	0.00334	0.568
	Middle	0.00310	0.00253	0.345
	Apical	0.00323	0.00215	0.107
46 M vs 36 M	Coronal	0.00467	0.00386	0.047
	Middle	0.00478	0.00341	0.012
	Apical	0.00454	0.00274	0.005
43 D vs 33 D	Coronal	0.00394	0.00330	0.070
	Middle	0.00357	0.00296	0.108
	Apical	0.00341	0.00269	0.042
43 M vs 33 M	Coronal	0.00389	0.00339	0.047
	Middle	0.00392	0.00325	0.028
	Apical	0.00360	0.00297	0.063
41 D vs 31 D	Coronal	0.00224	0.00231	0.542
	Middle	0.00175	0.00194	0.144
	Apical	0.00152	0.00177	0.176
41 M vs 31 M	Coronal	0.00248	0.00265	0.159
	Middle	0.00208	0.00200	0.663
	Apical	0.00161	0.00169	0.595

D: Distal; **M:** Mesial
R: Right; **L:** Left

Table 4.2.24. Right compared with left of Von Mises stresses (MPa) on TMJ complex under thickness variations in CI II/7s group

Thickness		Mean		P
		R	L	
Thickness	47 vs 37	-0.01547	-0.01407	0.035
	46 vs 36	-0.01352	-0.01239	0.011
	43 vs 33	-0.01427	-0.01401	0.580
	41 vs 31	-0.01612	-0.01595	0.114

R: Right; **L:** Left

4.2.3. CI III

4.2.3.1. Stiffness Variation

4.2.3.1. A. TMJ

The left side of the TMJ demonstrated on average higher Von Mises stresses (MPa) compared with the right side (Appendix 1, Table 4.2.25) with statistically significant differences nearly across all variables (Table 4.2.26).

Table 4.2.26. Right compared with left Von Mises stresses (MPa) on TMJ components under stiffness variations in CI III group

Region	Area	Mean		p
		R	L	
Cond	Anterior	0.1712	0.2026	0.005
	Middle	0.1033	0.1307	0.005
	posterior	0.1249	0.1457	0.005
Disk	Anterior	0.0362	0.0473	0.005
	Middle	0.0258	0.0517	0.005
	posterior	0.0408	0.0303	0.005
Temp	Anterior	0.1532	0.1212	0.005
	Middle	0.1268	0.1200	0.005
	posterior	0.0631	0.0699	0.007

Cond: Condyle; Temp: Temporal Bone
R: Right; L: Left



Fig. 4.2.5. The pattern of distribution of the Von Mises stresses (MPa) in the stiffness category is illustrated comparing right (blue) and left (red) sides. Stresses were higher at the anterior and middle levels of the disk, the posterior region of the temporal bone and all parts of the condyle (anterior, middle, posterior) on the left side. On the right side, higher stresses were found on the posterior disk, and anterior and middle part of the temporal bone. Modified from image by: www.thenextdds.com

The higher stress levels occurred on all left condylar regions, as well as on the anterior and middle sections of the disk, and the posterior section of the temporal fossa. The regions of the posterior disk and the anterior and middle parts of the temporal bone showed significantly higher stresses on the right side (Fig 4.2.5).

4.2.3.1. B. PDL

The right side showed greater Von Mises stress on almost all sides of the teeth at the exception of the mesial side of the central incisor, with statistically significant differences (Appendix 1, Table 4.2.27 and Table 4.2.28).

Table 4.2.28. Right compared with left of Von Mises stresses (MPa) on dental components under stiffness variations in CI III group

Region	Area	Mean		p
		R	L	
47 D vs 37 D	Coronal	0.00301	0.00287	0.00506
	Middle	0.00279	0.00196	0.00506
	Apical	0.00281	0.00138	0.00506
47 M vs 37 M	Coronal	0.00356	0.00348	0.00506
	Middle	0.00339	0.00303	0.00506
	Apical	0.00317	0.00172	0.00506
46 D vs 36 D	Coronal	0.00366	0.00337	0.00506
	Middle	0.00338	0.00241	0.00506
	Apical	0.00340	0.00195	0.00506
46 M vs 36 M	Coronal	0.00564	0.00513	0.00506
	Middle	0.00584	0.00467	0.00506
	Apical	0.00530	0.00372	0.00506
43 D vs 33 D	Coronal	0.00493	0.00324	0.00506
	Middle	0.00466	0.00171	0.00506
	Apical	0.00528	0.00167	0.00506
43 M vs 33 M	Coronal	0.00527	0.00327	0.00506
	Middle	0.00508	0.00225	0.00506
	Apical	0.00551	0.00210	0.00506
41 D vs 31 D	Coronal	0.00439	0.00345	0.00506
	Middle	0.00355	0.00299	0.00506
	Apical	0.00297	0.00275	0.00506
41 M vs 31 M	Coronal	0.00292	0.00446	0.00506
	Middle	0.00205	0.00349	0.00506
	Apical	0.00210	0.00311	0.00506

D: Distal; **M:** Mesial
R: Right; **L:** Left

4.2.3.1. C. Dental displacement

The teeth on the left side demonstrated a greater displacement generated by the CI III elastics (Appendix 1, Table 4.2.29), with statistically significant differences across all the crowns of the teeth except the mandibular central incisor (Table 4.2.30).

Table 4.2.30. Right (R) compared with left (L) Von Mises stresses (MPa) on TMJ complex under stiffness variations in CI III group

Stiffness		Mean		p Val
		R	L	
Stiffness	47 vs 37	0.01155	0.01274	0.005
	46 vs 36	0.01075	0.01226	0.005
	43 vs 33	0.01511	0.01593	0.005
	41 vs 31	0.01768	0.01667	0.005

R: Right; **L:** Left

4.2.3.2. Thickness Variation

4.2.3.2. A. TMJ

The Von Mises stresses (MPa) were higher on the left side of the joint space compared with the right side (Appendix 1, Table 4.2.31). Greater standard deviations were observed under thickness variation. Statistically significant differences were prevalent between the right and left sides nearly across all variables except for the posterior section of the temporal bone (Table 4.2.32).

The TMJ higher stress were observed levels at all the left condylar regions and the anterior and middle parts of the disk. The regions of the posterior disk and the anterior temporal fossa parts showed higher stresses on the right side. No statistically significant difference was recorded on the middle and the posterior temporal fossa between right and left sides (Fig 4.2.6).

Table 4.2.32. Right compared with left Von Mises stresses (MPa) on TMJ components under thickness variations in CI III group

Region	Area	Mean		p
		R	L	
Cond	Anterior	0.0961	0.1401	0.005
	Middle	0.0705	0.0851	0.009
	Posterior	0.0878	0.1078	0.013
Disk	Anterior	0.0207	0.0313	0.007
	Middle	0.0164	0.0320	0.005
	Posterior	0.0349	0.0233	0.005
Temp	Anterior	0.1098	0.0907	0.005
	Middle	0.0818	0.1083	0.093
	Posterior	0.0751	0.0652	0.074

Cond: Condyle; Temp: Temporal Bone
R: Right; L: Left



Fig. 4.2.6. The pattern of distribution of the Von Mises stresses (MPa) in the stiffness category is illustrated comparing right (blue) and left (red) sides. Stresses were higher at the anterior and middle levels of the disk and all parts of the condyle (anterior, middle, posterior) on the left side. On the right side, higher stresses were found on the posterior disk, and anterior and middle part of the temporal bone.

Modified from image by: www.thenextdds.com

4.2.3.2. B. PDL

Von Mises stresses (MPa) at the level of the PDL were higher on average on the right side compared to the left side (Appendix 1, Table 4.2.33). As with other parameters tested under thickness variation, standard deviations around the mean were higher for similar testing under stiffness variation. Significant differences in the Von Mises response were observed in some regions of both sides of the dental units (Table 4.2.34).

In most areas of the PDL regions, the right side showed a higher statistically significant stress, most notably in the posterior segments of the 2nd molar and the mesial side of the 1st molar.

Table 4.2.34. Right compared with left Von Mises stresses (MPa) on dental components under thickness variations in CI III group

Region	Area	Mean		p
		R	L	
47 D vs 37 D	Coronal	0.00446	0.002138	0.005
	Middle	0.00424	0.001685	0.007
	Apical	0.00298	0.001419	0.017
47 M vs 37 M	Coronal	0.00379	0.00225	0.007
	Middle	0.00405	0.002037	0.017
	Apical	0.00463	0.007739	0.114
46 D vs 36 D	Coronal	0.00310	0.002288	0.028
	Middle	0.00259	0.001865	0.093
	Apical	0.00263	0.001671	0.005
46 M vs 36 M	Coronal	0.00415	0.003141	0.007
	Middle	0.00429	0.002902	0.005
	Apical	0.00402	0.00239	0.005
43 D vs 33 D	Coronal	0.00372	0.003026	0.093
	Middle	0.00357	0.002479	0.005
	Apical	0.00392	0.002354	0.005
43 M vs 33 M	Coronal	0.00375	0.003231	0.333
	Middle	0.00365	0.002769	0.059
	Apical	0.00399	0.002482	0.005
41 D vs 31 D	Coronal	0.00278	0.002789	0.508
	Middle	0.00210	0.002363	0.074
	Apical	0.00171	0.002138	0.037
41 M vs 31 M	Coronal	0.00292	0.00337	0.037
	Middle	0.00228	0.002537	0.386
	Apical	0.00161	0.002109	0.017

D: Distal; **M:** Mesial

R: Right; **L:** Left

4.2.3.2. C. Dental displacement

On average, the right side demonstrated a greater movement (Appendix 1, Table 4.2.35). Wider standard deviations were also noticed around the displacement mean. Statistically significant differences in the response on both sides were observed across all the crowns of the teeth except for the central incisor (Table 4.2.36).

Table 4.2.36. Right side compared with left Von Mises stresses (MPa) on dental units under thickness variations in CI III group

		Mean		P
		R	L	
Thickness	47 vs 37	0.0131	0.0127	0.241
	46 vs 36	0.0124	0.0123	0.333
	43 vs 33	0.0151	0.0144	0.169
	41 vs 31	0.0172	0.0169	0.047

R: Right; L: Left

4.3. Stiffness compared with Thickness

In this section, the same sides (right or left) of treatment models are compared within the same modality of treatment. Such comparison allows to highlight the contributing role of stiffness and thickness to stress generation and dental crown displacement.

4.3.1. CI II/6s

4.3.1.1. TMJ

Few statistical differences appeared in the comparison. The only remarkable pattern was at the temporal bone region. On the left side, across all its segments whereby higher stresses were attributed to thickness variation (Table 4.3.1).

Table 4.3.1 Von Mises Stresses (MPa) of stiffness compared with thickness on TMJ components in the CI II/6s group

Right Side					Left Side				
Region	Area	Mean		p	Region	Area	Mean		p
		Stiffness	Thickness				Stiffness	Thickness	
Cond	Anterior	0.1373	0.1116	0.0069	Cond	Anterior	0.1434	0.1569	0.1937
	Middle	0.0812	0.0846	0.4619		Middle	0.0925	0.0994	0.1374
	Posterior	0.0993	0.0973	0.8379		Posterior	0.1032	0.1154	0.2595
Disk	Anterior	0.0293	0.0245	0.0158	Disk	Anterior	0.0336	0.0363	0.0625
	Middle	0.0204	0.0219	0.4071		Middle	0.0370	0.0349	0.2897
	Posterior	0.0324	0.0495	0.0693		Posterior	0.0216	0.0325	0.0696
Temp	Anterior	0.1216	0.1275	0.4874	Temp	Anterior	0.0825	0.1122	0.0022
	Middle	0.0978	0.0878	0.1033		Middle	0.0837	0.1330	0.0039
	Posterior	0.0510	0.0980	0.0001		Posterior	0.0471	0.0846	0.0051

Cond: Condyle; **Temp:** Temporal Bone; **SD:** Standard Deviation

Only stresses at the posterior temporal were significantly different on both sides.

Otherwise, only on the left side all components of the temporal bone showed a statistical difference between stiffness and thickness.

4.3.1.2. Dental Components

The only statistical significance in the comparison between stresses under stiffness versus thickness was found on the right side on the distal side of the 1st molar and both sides of the canine (Table 4.3.2).

Table 4.3.2. Von Mises stresses (MPa) of stiffness versus thickness variations on PDL in CI II/6s group

Right Side					Left Side				
Region	Area	Mean		p	Region	Area	Mean		p
		Stiffness	Thickness				Stiffness	Thickness	
47 D	Coronal	0.0035	0.0057	0.136	37 D	Coronal	0.002	0.0036	0.191
	Middle	0.0026	0.0054	0.171		Middle	0.0013	0.0027	0.175
	Apical	0.0021	0.0032	0.038		Apical	0.0009	0.003	0.267
47 M	Coronal	0.0029	0.0039	0.002	37 M	Coronal	0.0023	0.0045	0.071
	Middle	0.0028	0.0038	0.016		Middle	0.002	0.0036	0.384
	Apical	0.0023	0.005	0.243		Apical	0.0011	0.0101	0.253
46 D	Coronal	0.0031	0.0034	0.001	36 D	Coronal	0.0022	0.0046	0.056
	Middle	0.003	0.0026	0.001		Middle	0.0016	0.0041	0.103
	Apical	0.0027	0.0025	0.001		Apical	0.0014	0.004	0.51
46 M	Coronal	0.0047	0.0046	0.208	36 M	Coronal	0.0038	0.0042	0.777
	Middle	0.005	0.0048	0.08		Middle	0.0033	0.0041	0.437
	Apical	0.0044	0.0045	0.007		Apical	0.0025	0.0036	0.817
43 D	Coronal	0.0037	0.0046	0.005	33 D	Coronal	0.0023	0.0041	0.151
	Middle	0.0034	0.0043	0.002		Middle	0.0018	0.0037	0.144
	Apical	0.0035	0.0044	0.001		Apical	0.0014	0.0037	0.206
43 M	Coronal	0.0038	0.0047	0.013	33 M	Coronal	0.0024	0.0044	0.238
	Middle	0.0038	0.0047	0.004		Middle	0.002	0.0041	0.176
	Apical	0.0037	0.0045	0.004		Apical	0.0017	0.0039	0.271
41 D	Coronal	0.0025	0.003	0.08	31 D	Coronal	0.002	0.0033	0.459
	Middle	0.0021	0.0025	0.165		Middle	0.0019	0.0029	0.57
	Apical	0.0019	0.0022	0.206		Apical	0.0018	0.0028	0.609
41 M	Coronal	0.0019	0.0035	0.149	31 M	Coronal	0.0025	0.0038	0.081
	Middle	0.0019	0.003	0.246		Middle	0.0021	0.0029	0.149
	Apical	0.002	0.0026	0.266		Apical	0.0019	0.0028	0.558

4.3.1.3. Dental Displacement

Upon comparing the stiffness to thickness effects on the dental displacements of both sides of the CI II/6s, no statistical significant was observed, denoting a similar effect of both conditions (Table 4.3.3.).

Table 4.3.3. Von Mises stresses (MPa) comparing stiffness versus thickness variations on dental displacement (mm) in CI II/6s group

Measure	Mean		p
	Stiffness	Thickness	
Disp 47	-0.010	-0.028	0.250
Disp 46	-0.009	-0.028	0.245
Disp 43	-0.010	-0.028	0.268
Disp 41	-0.011	-0.031	0.245
Disp 37	-0.009	-0.031	0.225
Disp 36	-0.008	-0.03	0.244
Disp 33	-0.010	-0.03	0.270
Disp 31	-0.011	-0.031	0.233

4.3.2. CI II/7s

4.3.2.1. TMJ

Some of the TMJ components on the right side were statistically significantly different, but none on the left side, although the trend of difference between the mean was generally similar. The stiffness variation showed the higher stresses except at the posterior temporal fossa region (Table 4.3.4).

4.3.2.2. Dental Components

Statistically significant differences between variables under stiffness versus thickness conditions were found on both sides, unlike the CI II/6s group, particularly in the regions of the 2nd molars (Table 4.3.5).

Table 4.3.4. Von Mises stresses (MPa) compared under stiffness versus thickness on TMJ components in CI II/7s group

		Right Side			Left Side				
		Mean		p			Mean		p
Region	Area	Stiffness	Thickness		Region	Area	Stiffness	Thickness	
Cond	Anterior	0.148	0.101	0.0001	Cond	Anterior	0.157	0.141	0.233
	Middle	0.088	0.072	0.034		Middle	0.098	0.085	0.093
	Posterior	0.106	0.090	0.081		Posterior	0.109	0.107	0.862
Disk	Anterior	0.032	0.023	0.003	Disk	Anterior	0.036	0.032	0.294
	Middle	0.023	0.018	0.017		Middle	0.038	0.032	0.118
	Posterior	0.035	0.038	0.559		Posterior	0.022	0.024	0.503
Temp	Anterior	0.130	0.113	0.016	Temp	Anterior	0.110	0.098	0.165
	Middle	0.109	0.083	0.001		Middle	0.105	0.119	0.311
	Posterior	0.054	0.077	0.018		Posterior	0.069	0.078	0.305

Cond: Condyle; **Temp:** Temporal Bone; **SD:** Standard Deviation

More significance was observed on the right central incisor, compared to the left central incisor, whereby higher stresses were found with the thickness variation, unlike in the CI II/6s group.

4.3.2.3. Dental Displacement

Upon comparing the stiffness to thickness effects on dental displacements in the CI II/7s group, no statistical significance was noted except at the mandibular right 2nd molar, which displaced more under thickness than stiffness variation (Table 4.3.6).

Table 4.3.5. Von Mises stresses (MPa) compared under stiffness versus thickness on the PDL in CI II/7s group

Right side					Left side				
Region	Area	Mean		p	Region	Area	Mean		p
		Stiffness	Thickness				Stiffness	Thickness	
47 D	Coronal	0.0064	0.0097	0.062	37 D	Coronal	0.0084	0.0081	0.001
	Middle	0.0059	0.0092	0.001		Middle	0.0076	0.0082	0.001
	Apical	0.0054	0.007	0.049		Apical	0.0064	0.0074	0.001
47 M	Coronal	0.0038	0.0046	0.001	37 M	Coronal	0.002	0.0035	0.001
	Middle	0.0041	0.0048	0.003		Middle	0.0018	0.0033	0.001
	Apical	0.004	0.0067	0.001		Apical	0.002	0.004	0.005
46 D	Coronal	0.0033	0.0037	0.124	36 D	Coronal	0.0026	0.0033	0.081
	Middle	0.0028	0.0031	0.003		Middle	0.0019	0.0025	0.006
	Apical	0.0028	0.0032	0.116		Apical	0.0017	0.0022	0.002
46 M	Coronal	0.0046	0.0047	0.001	36 M	Coronal	0.0051	0.0039	0.026
	Middle	0.0046	0.0048	0.317		Middle	0.005	0.0034	0.83
	Apical	0.0042	0.0045	0.814		Apical	0.0042	0.0027	0.824
43 D	Coronal	0.0038	0.0039	0.878	33 D	Coronal	0.0031	0.0033	0.199
	Middle	0.0036	0.0036	0.058		Middle	0.0025	0.003	0.166
	Apical	0.0038	0.0034	0.227		Apical	0.0022	0.0027	0.128
43 M	Coronal	0.0041	0.0039	0.0001	33 M	Coronal	0.0033	0.0034	0.926
	Middle	0.004	0.0039	0.197		Middle	0.0028	0.0033	0.39
	Apical	0.004	0.0036	0.001		Apical	0.0025	0.003	0.593
41 D	Coronal	0.003	0.0022	0.001	31 D	Coronal	0.0025	0.0023	0.959
	Middle	0.0024	0.0018	0.001		Middle	0.0022	0.0019	0.007
	Apical	0.0021	0.0015	0.001		Apical	0.0021	0.0018	0.949
41 M	Coronal	0.0024	0.0025	0.044	31 M	Coronal	0.003	0.0027	0.001
	Middle	0.0023	0.0021	0.001		Middle	0.0024	0.002	0.001
	Apical	0.0025	0.0016	0.448		Apical	0.0022	0.0017	0.01

Table 4.3.6. Dental displacement (mm) under stiffness versus thickness in CI II/7s group

Modality: CI II from 2nd molars			
Measure	Mean		p
	Stiffness	Thickness	
Disp 47	-0.0101	-0.0283	0.03
Disp 46	-0.0086	-0.0275	0.0610
Disp 43	-0.0099	-0.0284	0.1676
Disp 41	-0.0112	-0.0309	0.1107
Disp 37	-0.008	-0.0311	0.3175
Disp 36	-0.0083	-0.0296	0.2678
Disp 33	-0.0101	-0.0296	0.3137
Disp 31	-0.0105	-0.031	0.0920

4.3.3. CI III's

4.3.3.1. TMJ

Both right and left sides exhibited nearly similar significance across all its variables. The stiffness variation showed the higher stresses (Table 4.3.7).

Table 4.3.7. Von Mises stresses (MPa) under stiffness versus thickness variations on TMJ components in CI III's group

Right side					Left side					
Region	Area	Mean		p	Region	Area	Mean		p	
		Stiffness	Thickness				Stiffness	Thickness		
Cond	Anterior	0.1712	0.0961	0.005	Cond	Anterior	0.2026	0.1401	0.007	
	Middle	0.1033	0.0705	0.005		Posterior	Middle	0.1307	0.0851	0.005
	Posterior	0.1249	0.0878	0.005			Posterior	0.1457	0.1078	0.009
Disk	Anterior	0.0362	0.0207	0.005	Disk	Anterior	0.0473	0.0313	0.005	
	Middle	0.0258	0.0164	0.005		Posterior	Middle	0.0517	0.0321	0.007
	Posterior	0.0408	0.0349	0.285			Posterior	0.0303	0.0233	0.007
Temp	Anterior	0.1532	0.1098	0.005	Temp	Anterior	0.1212	0.0907	0.022	
	Middle	0.1268	0.0818	0.005		Posterior	Middle	0.1201	0.1084	0.646
	Posterior	0.0631	0.0751	0.139			Posterior	0.0699	0.0652	0.646

Cond: Condyle; Temp: Temporal Bone; SD: Standard Deviation

4.3.3.2. Dental components

In the comparison of stiffness to thickness variations in the CI III group, the most remarkable significance was on the right canine and parts of the mesial side of the 1st molar and the distal side of the central incisor.

On the left side, significant differences were noted at the level of the mesial side of the 1st molar and all regions of the central as well as parts of the mesial side of the 2nd molar and the distal sides of the 1st molar (Table 4.3.8).

Table 4.3.8. Von Mises stresses (MPa) compared under stiffness versus thickness on the PDL in CI III group

Right Side					Left Side				
Region	Area	Mean		p	Region	Area	Mean		p
		Stiffness	Thickness				Stiffness	Thickness	
47 D	Coronal	0.0031	0.0044	0.575	37 D	Coronal	0.0028	0.0021	0.059
	Middle	0.0027	0.0042	0.878		Middle	0.0019	0.0016	0.093
	Apical	0.0028	0.0029	0.445		Apical	0.0013	0.0014	0.575
47 M	Coronal	0.0035	0.0037	0.445	37 M	Coronal	0.0034	0.0022	0.013
	Middle	0.0033	0.0040	0.445		Middle	0.0030	0.0020	0.013
	Apical	0.0031	0.0046	0.721		Apical	0.0017	0.0077	0.646
46 D	Coronal	0.0036	0.0031	0.093	36 D	Coronal	0.0033	0.0022	0.009
	Middle	0.0033	0.0026	0.093		Middle	0.0024	0.0018	0.013
	Apical	0.0034	0.0026	0.093		Apical	0.0019	0.0016	0.114
46 M	Coronal	0.0054	0.0041	0.059	36 M	Coronal	0.0051	0.0031	0.007
	Middle	0.0058	0.0042	0.017		Middle	0.0046	0.0029	0.007
	Apical	0.0053	0.0040	0.017		Apical	0.0037	0.0023	0.007
43 D	Coronal	0.0049	0.0037	0.017	33 D	Coronal	0.0032	0.0030	0.241
	Middle	0.0046	0.0035	0.022		Middle	0.0017	0.0024	0.037
	Apical	0.0052	0.0039	0.009		Apical	0.0016	0.0023	0.114
43 M	Coronal	0.0052	0.0037	0.013	33 M	Coronal	0.0032	0.0032	0.721
	Middle	0.0050	0.0036	0.009		Middle	0.0022	0.0027	0.114
	Apical	0.0055	0.0039	0.009		Apical	0.0021	0.0024	0.333
41 D	Coronal	0.0043	0.0027	0.005	31 D	Coronal	0.0034	0.0027	0.013
	Middle	0.0035	0.0021	0.007		Middle	0.0029	0.0023	0.037
	Apical	0.0029	0.0017	0.007		Apical	0.0027	0.0021	0.047
41 M	Coronal	0.0029	0.0029	0.799	31 M	Coronal	0.0044	0.0033	0.009
	Middle	0.0020	0.0022	0.386		Middle	0.0034	0.0025	0.017
	Apical	0.0021	0.0016	0.037		Apical	0.0031	0.0021	0.017

4.3.3.3. Dental Displacement

No statistically significant difference was observed between dental displacements. Upon comparing the stiffness to thickness effects on the dental displacements of both sides of the CI III group (Table 4.3.9).

Table 4.3.9. Dental displacement (mm) compared under stiffness versus thickness in CI III group

Measure	Mean		p
	Stiffness	Thickness	
Disp 47	0.0115	0.0131	0.959
Disp 46	0.0107	0.0124	0.646
Disp 43	0.0151	0.0150	0.285
Disp 41	0.0176	0.0172	0.285
Disp 37	0.0127	0.0127	0.241
Disp 36	0.0122	0.0123	0.241
Disp 33	0.0159	0.0144	0.139
Disp 31	0.0166	0.0169	0.508

4.4. Correlations between stresses and variations in stiffness and thickness

4.4.1. Stiffness Variations

4.4.1.1. CI II/6s

4.4.1.1. A. TMJ.

Statistically significant, positive and high correlations existed between Von Mises stresses and stiffness variations on the CI II models almost across all partitions of the TMJ and on both sides ($0.666 < r < 0.999$ $p < 0.005$) (Table 4.4.1).

All regions correlated significantly with the buccal mask of cortical bone. However, not all regions correlated with the lingual body, less correlations were noted on the left side.

Table 4.4.1. Correlations between Von Mises stresses on TMJ and stiffness variations in CI II/6 group

Right Side						Left Side					
Region	Area	Dark Buccal	p	Light Lingual	p	Region	Area	Dark Buccal	p	Light Lingual	p
Cond	Anterior	0.969**	4E-06	0.694*	0.025	Cond	Anterior	0.909**	0.001	0.811**	0.004
	Middle	0.789**	7E-03	0.925**	0.0001		Middle	0.909**	0.001	0.528	0.116
	Posterior	0.822**	4E-03	0.902**	0.0003		Posterior	0.909**	0.001	0.534	0.111
Disk	Anterior	0.919**	2E-04	0.796**	0.005	Disk	Anterior	0.909**	0.001	0.762*	0.010
	Middle	0.915**	2E-04	0.800**	0.005		Middle	0.909**	0.001	0.748*	0.013
	Posterior	0.9050**	3E-05	-0.338	0.338		Posterior	0.909**	0.001	0.781**	0.008
Temp	Anterior	0.983**	3E-07	0.630	0.05	Temp	Anterior	0.909**	0.001	0.690*	0.027
	Middle	0.893**	5E-04	0.830**	0.002		Middle	0.909**	0.001	0.732*	0.016
	Posterior	0.741*	1E-02	0.950**	0.0001		Posterior	0.909**	0.001	0.666*	0.035

** : very high correlations

* : high correlations

4.4.1.1. B. Dental Components

Almost across all elements of the dental units, a statistically significant high correlation existed between the variation of stiffness and the Von Mises stresses on the PDL levels (Table 4.4.2).

Strong correlations were observed between the buccal cortical plate ($-0.8 < r < -0.99$) and the various groups of models. Corresponding correlations were lower with the lingual cortical plate ($-0.674 < r < -0.897$). Similar findings were reported for dental displacements (Table 4.4.3).

The posterior units correlate negatively with the change of stiffness of all the modalities of elastics used ($-0.678 < r < -0.999$).

On dental displacements, unlike the correlations in the CI II group, in the CI III group, a negative correlation exists between the displacement of dental units and the stiffness changes (Table 4.4.3).

Table 4.4.2. Correlations between Von Mises stresses at the PDL and stiffness variations in CI II/6 group

Right side

Left side

Region	Area	Dark Buccal	p	Light Lingual	p
47 D	Coronal	-0.967**	4.824E-06	-0.689*	0.027
	Middle	-0.972**	2.622E-06	-0.674*	0.032
	Apical	-0.971**	3.090E-06	-0.678*	0.031
47 M	Coronal	-0.960**	1.057E-05	-0.708*	0.021
	Middle	-0.966**	5.599E-06	-0.694*	0.026
	Apical	-0.967**	5.233E-06	-0.692*	0.026
46 D	Coronal	-0.960**	1.117E-05	-0.708*	0.022
	Middle	-0.971**	2.81E-06	-0.676*	0.031
	Apical	-0.972**	2.644E-06	-0.675*	0.032
46 M	Coronal	-0.975**	1.6106E-06	-0.664*	0.036
	Middle	-0.966**	5.839E-06	-0.696*	0.025
	Apical	-0.951**	2.410E-05	-0.733*	0.0157
43 D	Coronal	0.915**	0.000201	0.799**	0.005
	Middle	-0.800**	0.005499	-0.879**	0.0007
	Apical	0.985**	1.971E-07	0.6032	0.064
43 M	Coronal	0.957**	1.439E-05	0.719*	0.019
	Middle	0.973**	2.202E-06	0.671*	0.033
	Apical	0.981**	5.893E-07	0.634*	0.048
41 D	Coronal	0.954**	1.797E-05	0.727*	0.017
	Middle	0.985**	2.304E-07	0.3817	0.276
	Apical	-0.910**	0.0002531	-0.791**	0.006
41 M	Coronal	0.953**	1.97E-05	0.728*	0.017
	Middle	0.961**	9.69E-06	0.710*	0.021
	Apical	0.960**	1.08E-05	0.712*	0.020

Region	Area	Dark Buccal	p	Light Lingual	p
37 D	Coronal	0.126	0.729	0.914**	0.0002
	Middle	-0.985**	2.4E-07	-0.550	0.098
	Apical	-0.961**	9.8E-06	-0.677*	0.031
37 M	Coronal	0.765**	0.009	0.938**	6.1E-05
	Middle	-0.952**	2.2E-05	-0.245	0.49
	Apical	-0.962**	8.7E-06	-0.694*	0.02
36 D	Coronal	0.872**	0.0011	0.857**	0.001
	Middle	-0.965**	6E-06	-0.687*	0.02
	Apical	-0.963**	8E-06	-0.698*	0.02
36 M	Coronal	-0.959**	1.1E-05	-0.705*	0.02
	Middle	-0.888**	0.0006	-0.830**	0.002
	Apical	0.284	0.4	-0.675*	0.032
33 D	Coronal	0.957**	1.4E-05	0.722*	0.018
	Middle	0.997**	4.3E-10	0.542	0.11
	Apical	0.971**	2.9E-06	0.688*	0.027
33 M	Coronal	0.961**	9.7E-06	0.710*	0.021
	Middle	0.994**	5.7E-09	0.585	0.075
	Apical	0.979**	8.8E-07	0.664*	0.036
31 D	Coronal	0.956**	1.5E-05	0.723*	0.018
	Middle	-0.270	0.45	-0.864**	0.001
	Apical	-0.889**	0.0005	-0.808**	0.004
31 M	Coronal	0.953**	1.9E-05	0.729*	0.0166
	Middle	0.997**	1.8E-10	0.547	0.101
	Apical	-0.905**	0.0003	-0.798**	0.0056

** : very high correlations

* : high correlations

Table 4.4.3. Correlations between dental displacements and stiffness variations in CI II/6s group

Measure	Dark Buccal	p	Light Lingual	p
Disp 47	0.944**	4.10E-05	0.749*	0.012
Disp 46	0.940**	5.31E-05	0.756*	0.011
Disp 43	0.938**	5.98E-05	0.760*	0.010
Disp 41	0.934**	7.45E-05	0.766**	0.009
Disp 37	0.927**	0.0011	0.780**	0.007
Disp 36	0.927**	0.0011	0.780**	0.007
Disp 33	0.928**	0.0001	0.778**	0.008
Disp 31	0.932**	8.7E-05	0.771**	0.009

** : very high correlations

* : high correlations

4.4.1.2. CI II/7s

4.4.1.2. A. TMJ

Similar to the CI II/6s, statistically significant, positive and high correlations existed between Von Mises stresses and stiffness variations on the CI II/7s models almost across all partitions of the TMJ and on both sides ($0.647 < r < 0.999$; $p < 0.005$) (Table 4.4.4).

Table 4.4.4. Correlations between Dental displacements and stiffness variation in CI II/7s group

Right Side						Left Side					
Region	Area	Dark Buccal	p	Light Lingual	p	Region	Area	Dark Buccal	p	Light Lingual	p
Cond	Anterior	0.952**	2.255E-05	0.738*	0.015	Cond	Anterior	0.965**	5.97758E-06	0.701*	0.024
	Middle	0.784**	0.007	0.928**	0.000		Middle	0.999**	3.15235E-12	0.501	0.141
	Posterior	0.819**	0.003	0.904**	0.000		Posterior	0.999**	2.77556E-12	0.492	0.148
Disk	Anterior	0.903**	0.0003	0.818**	0.004	Disk	Anterior	0.968**	4.54649E-06	0.689*	0.028
	Middle	0.903**	0.0003	0.818**	0.004		Middle	0.971**	3.05299E-06	0.677*	0.032
	Posterior	0.647*	0.043	0.982**	0.000		Posterior	0.772**	0.008857299	-0.166	0.646
Temp	Anterior	0.945**	3.731E-05	0.747*	0.013	Temp	Anterior	0.990**	4.30631E-08	0.403	0.247
	Middle	0.845**	0.0020623	0.881**	0.001		Middle	0.993**	8.44731E-09	0.556	0.095
	Posterior	0.623	0.0543298	0.988**	0.000		Posterior	0.556	0.095122143	0.441	0.201

** : very high correlations

* : high correlations

All regions correlated significantly with the buccal mask of cortical bone. Not all regions correlated with the lingual body: less correlations noted on the left side.

4.4.1.2. B. Dental Components

Almost across all elements of the dental units in the CI II/7s, a statistically significant high correlation was found between the variation of stiffness with the Von Mises stresses at the PDL (Table 4.4.5).

Similar to CI II/6 group, stronger correlations were found between the buccal cortical plate ($-0.89 < r < -0.99$) and the various groups of models compared with the corresponding correlations with the lingual cortical plate ($-0.616 < r < -0.825$). Similar patterns were observed for dental displacements (Table 4.4.6).

Also, similarly, the posterior units correlated negatively with the change of stiffness for all the modalities of elastics used ($-0.678 < r < -0.999$).

Table 4.4.5. Correlations between dental displacements and stiffness variation in CI II/7s group

Right side						Left side					
Region	Area	Dark Buccal	p	Light Lingual	p	Region	Area	Dark Buccal	p	Light Lingual	p
47 D	Coronal	-0.984**	2.61E-07	-0.616	0.05	37 D	Coronal	-0.957**	1.43E-05	-0.715*	0.154
	Middle	-0.987**	1.18E-07	-0.606	0.06		Middle	-0.958**	1.24E-05	-0.715*	0.020
	Apical	-0.989**	6.64E-08	-0.596	0.06		Apical	-0.956**	1.59E-05	-0.722*	0.018
47 M	Coronal	-0.990**	4.39E-08	-0.584	0.07	37 M	Coronal	-0.951**	2.45E-05	-0.731*	0.016
	Middle	-0.973**	2.22E-06	-0.671*	0.03		Middle	-0.951**	2.29E-05	-0.728*	0.017
	Apical	-0.978**	9.34E-07	-0.651*	0.04		Apical	-0.957**	1.41E-05	-0.717*	0.019
46 D	Coronal	-0.995**	2.1E-09	-0.516	0.12	36 D	Coronal	-0.953**	2.02E-05	-0.724*	0.017
	Middle	-0.981**	5.84E-07	-0.639*	0.046		Middle	-0.945**	3.62E-05	-0.743*	0.013
	Apical	-0.955**	1.68E-05	-0.719*	0.019		Apical	-0.932**	8.56E-05	-0.766**	0.009
46 M	Coronal	-0.859**	0.001449	0.003	0.99	36 M	Coronal	-0.936**	6.62E-05	-0.763*	0.010
	Middle	-0.953**	2E-05	-0.232	0.51		Middle	-0.928**	0.000106	-0.778**	0.008
	Apical	-0.992**	1.62E-08	-0.5189	0.12		Apical	-0.920**	0.000166	-0.791**	0.006
43 D	Coronal	0.899**	0.000405	0.825**	0.003	33 D	Coronal	0.954**	1.92E-05	0.727*	0.017
	Middle	0.926**	0.00012	0.786**	0.007		Middle	0.999**	2.35E-12	0.506	0.135
	Apical	0.960**	1.09E-05	0.713*	0.02		Apical	0.967**	4.75E-06	0.696*	0.025
43 M	Coronal	0.948**	3.02E-05	0.740*	0.014	33 M	Coronal	0.957**	1.45E-05	0.719*	0.019
	Middle	0.954**	1.86E-05	0.727*	0.017		Middle	0.995**	3.13E-09	0.566	0.087
	Apical	0.960**	1.02E-05	0.710*	0.021		Apical	0.979**	8.08E-07	0.658*	0.038
41 D	Coronal	0.950**	2.67E-05	0.737*	0.014	31 D	Coronal	0.949**	2.74E-05	0.738*	0.014
	Middle	0.973**	2.23E-06	0.680*	0.03		Middle	0.976**	1.44E-06	0.673*	0.032
	Apical	0.982**	4.55E-07	0.418	0.22		Apical	0.989**	7.48E-08	0.615	0.058
41 M	Coronal	0.949**	2.74E-05	0.737*	0.015	31 M	Coronal	0.949**	2.84E-05	0.739*	0.014
	Middle	0.955**	1.68E-05	0.723*	0.018		Middle	0.970**	3.36E-06	0.689*	0.027
	Apical	0.954**	1.8E-05	0.725*	0.017		Apical	0.993**	9.51E-09	0.4855	0.154

** : very high correlations

* : high correlations

Table 4.4.6. Correlations between Dental displacements and stiffness variations in CI II/7s group

Measure	Dark Buccal	p	Light Lingual	p
Disp 47	0.942**	4.461E-05	0.751*	0.012
Disp 46	0.935**	7.097E-05	0.765**	0.009
Disp 43	0.934**	7.566E-05	0.767**	0.009
Disp 41	0.935**	7.412E-05	0.766**	0.009
Disp 37	0.936**	6.923E-05	0.764*	0.011
Disp 36	0.935**	7.397E-05	0.766**	0.009
Disp 33	0.933**	8.364E-05	0.770**	0.009
Disp 31	0.934**	7.869E-05	0.768**	0.009

** : very high correlations

* : high correlations

4.4.1.3. CI IIIs

4.4.1.3. A. TMJ

Unlike both CI II groups, no statistically significant correlations were noted across the variables of the TMJ units, except on solitary regions with no specific pattern (Table 4.4.7).

4.4.1.3. B. Dental Components

Almost across all elements of the dental units in the CI III group, a statistically significant high correlation existed between the variation of stiffness with the Von Mises stresses on the PDL at the buccal cortical plate (Table 4.4.7). A lesser significant correlation was shown at the lingual cortical plate.

Table 4.4.7. Correlations between Von Mises (MPa) TMJ stresses and stiffness variations in CI III group

Right Side						Left Side					
Region	Area	Dark Buccal	p	Light Lingual	p	Region	Area	Dark Buccal	p	Light Lingual	p
Cond	Anterior	0.539	0.107	0.261	0.467	Cond	Anterior	0.527	0.117	0.297	0.405
	Middle	0.454	0.186	0.345	0.328		Middle	.661*	0.038	-0.030	0.934
	posterior	0.454	0.186	0.345	0.328		posterior	.661*	0.038	-0.030	0.934
Disk	Anterior	0.527	0.117	0.297	0.405	Disk	Anterior	0.539	0.108	0.261	0.467
	Middle	0.527	0.117	0.297	0.405		Middle	0.539	0.108	0.261	0.467
	posterior	0.357	0.311	0.394	0.260		posterior	0.067	0.855	-0.758*	0.011
Temp	Anterior	0.539	0.107	0.261	0.467	Temp	Anterior	0.624	0.054	0.067	0.855
	Middle	0.454	0.186	0.345	0.328		Middle	0.539	0.108	0.261	0.467
	posterior	0.357	0.310	0.394	0.260		posterior	0.624	0.054	0.067	0.855

*: high correlations

Table 4.4.8. Correlations between Von Mises stresses (MPa) at the PDL and stiffness variations in CI III group

Right side						Left side					
Region	Area	Dark Buccal	p	Light Lingual	p	Region	Area	Dark Buccal	p	Light Lingual	p
47 D	Coronal	-0.952**	0.001	-0.588	0.074	37 D	Coronal	-0.745*	0.013	0.055	0.881
	Middle	-0.903**	0.001	-0.709*	0.022		Middle	-0.988**	0.000	-0.491	0.150
	Apical	-0.903**	0.001	-0.709*	0.022		Apical	-0.903**	0.000	-0.709*	0.022
47 M	Coronal	-0.952**	0.001	-0.588	0.074	37 M	Coronal	0.152	0.676	0.927**	0.000
	Middle	-0.927**	0.001	-0.685*	0.029		Middle	-0.988**	0.000	-0.394	0.260
	Apical	-0.903**	0.001	-0.709*	0.022		Apical	-0.903**	0.000	-0.709*	0.022
46 D	Coronal	-0.952**	0.001	-0.588	0.074	36 D	Coronal	0.515	0.128	0.988**	0.000
	Middle	-0.903**	0.001	-0.709*	0.022		Middle	-0.952**	0.000	-0.588	0.074
	Apical	-0.903**	0.001	-0.709*	0.022		Apical	-0.903**	0.000	-0.709*	0.022
46 M	Coronal	-0.879**	0.001	-0.055	0.881	36 M	Coronal	-0.867**	0.001	-0.782**	0.008
	Middle	-1.000**		-0.430	0.214		Middle	-0.855**	0.002	-0.818**	0.004
	Apical	-0.867**	0.001	-0.782**	0.008		Apical	-0.782**	0.008	-0.867**	0.001
43 D	Coronal	-0.188	0.603	0.697*	0.025	33 D	Coronal	0.867**	0.001	0.782**	0.008
	Middle	-0.855**	0.002	-0.818**	0.004		Middle	0.867**	0.001	0.030	0.934
	Apical	0.988**	0.000	0.491	0.150		Apical	0.867**	0.001	0.782**	0.008
43 M	Coronal	0.867**	0.001	0.782**	0.008	33 M	Coronal	0.867**	0.001	0.782**	0.008
	Middle	0.903**	0.000	0.709*	0.022		Middle	0.903**	0.000	0.709*	0.022
	Apical	0.952**	0.000	0.588	0.074		Apical	0.867**	0.001	0.782**	0.008
41 D	Coronal	0.867**	0.001	0.782**	0.008	31 D	Coronal	0.867**	0.001	0.782**	0.008
	Middle	-0.855**	0.002	-0.818**	0.004		Middle	-0.855**	0.002	-0.818**	0.004
	Apical	-0.855**	0.002	-0.818**	0.004		Apical	-0.855**	0.002	-0.818**	0.004
41 M	Coronal	0.867**	0.001	0.782**	0.008	31 M	Coronal	0.867**	0.001	0.782**	0.008
	Middle	0.867**	0.001	0.782**	0.008		Middle	-0.855**	0.002	-0.818**	0.004
	Apical	0.867**	0.001	0.782**	0.008		Apical	-0.855**	0.002	-0.818**	0.004

** : very high correlations

* : high correlations

No statistically significant correlations were found between the dental displacement and stiffness variation in the CI III group. Solitary regions had high correlations, without a specific trend for the total model (Table 4.4.8).

Table 4.4.9. Correlations between dental displacements and stiffness variations in CI III group

Measure	buccal	p	lingual	p
Disp 47	-0.867**	0.001	-0.782**	0.007
Disp 46	-0.855**	0.001	-0.818**	0.003
Disp 43	-0.855**	0.001	-0.818**	0.003
Disp 41	-0.855**	0.001	-0.818**	0.003
Disp 37	-0.855**	0.001	-0.818**	0.003
Disp 36	-0.855**	0.001	-0.818**	0.003
Disp 33	-0.855**	0.001	-0.818**	0.003
Disp 31	-0.855**	0.001	-0.818**	0.003

** : very high correlations

* : high correlations

4.4.2. Thickness Variations

4.4.2.1. CI II/6s

4.4.2.1. A. TMJ

Unlike the stiffness variations, the CI II 6/s group showed no statistically significant correlations between the Von Mises stresses on the TMJ and the thickness variations across the different variables, except for solitary units (Tables 4.6.10, 4.6.11).

Table 4.4.10. Correlations between Von Mises stresses on TMJ and thickness variations in CI II/6s group (right side)

Region	Area	lingual	p	Combined	p	cortical	p
Cond	Anterior	0.571	0.084	-0.135	0.709	0.059	0.871
	Middle	0.863**	0.001	-0.244	0.496	-0.054	0.882
	Posterior	0.2596	0.469	-0.065	0.859	0.084	0.817
Disk	Anterior	0.2552	0.477	-0.235	0.513	-0.129	0.723
	Middle	0.2444	0.496	0.227	0.529	0.444	0.198
	Posterior	-0.0535	0.883	-0.066	0.856	-0.192	0.596
Temp	Anterior	0.6082	0.062	-0.099	0.785	0.358	0.309
	Middle	0.3153	0.375	-0.094	0.796	0.216	0.549
	Posterior	0.1373	0.705	-0.256	0.474	0.135	0.710

** : very high correlations

* : high correlations

Table 4.4.11. Correlations between Von Mises stresses on TMJ and thickness variations in CI II/6s group (left side)

Region	Area	lingual	p	Combined	p	Hard Cortical	p
Cond	Anterior	0.298	0.402	0.0649	0.858	0.223	0.536
	Middle	0.817**	0.004	0.1215	0.738	0.548	0.101
	Posterior	0.211	0.558	-0.2870	0.421	-0.153	0.674
Disk	Anterior	0.003	0.994	0.1382	0.703	-0.077	0.834
	Middle	0.102	0.780	-0.4020	0.249	-0.335	0.344
	Posterior	0.125	0.730	0.2282	0.526	0.054	0.883
Temp	Anterior	0.318	0.370	-0.0469	0.898	0.461	0.180
	Middle	0.061	0.868	0.1513	0.676	0.256	0.475
	Posterior	-0.139	0.703	-0.0038	0.992	0.133	0.713

** : very high correlations

* : high correlations

4.4.2.1. B. Dental Components

Similar to the TMJ units, a weak correlation existed between the Von Mises stresses gauged around the PDL of the dental units and the thickness variations (Tables 4.6.12, 4.6.13).

Solitary regions, mostly on the incisor, correlated highly with the thickness variation

All dental displacements the CI II/6s models, correlate significantly and highly in a negative pattern with the variation of the lingual cortical plate thickness ($-0.635 < r < -0.778$).

Table 4.4.12. Correlations between Von Mises stresses at the PDL and thickness variations in CI II/6s group (right side)

Region	Area	lingual	p	Combined	p	Hard Cortical	p
47 D	Coronal	-0.30	0.40	0.31	0.38	0.23	0.53
	Middle	-0.22	0.54	0.30	0.39	0.10	0.79
	Apical	0.636*	0.05	-0.24	0.50	-0.48	0.16
47 M	Coronal	-0.19	0.59	0.23	0.51	-0.02	0.97
	Middle	-0.29	0.41	0.33	0.36	0.03	0.93
	Apical	-0.18	0.61	0.33	0.35	0.10	0.78
46 D	Coronal	0.60	0.07	-0.31	0.39	0.28	0.44
	Middle	-0.687*	0.03	0.09	0.80	-0.13	0.73
	Apical	-0.12	0.74	0.21	0.55	0.20	0.58
46 M	Coronal	0.662*	0.04	-0.20	0.58	0.37	0.29
	Middle	0.44	0.21	-0.14	0.70	0.50	0.14
	Apical	0.26	0.46	-0.05	0.90	0.61	0.06
43 D	Coronal	0.56	0.09	-0.12	0.75	0.49	0.15
	Middle	0.49	0.15	-0.08	0.83	0.56	0.09
	Apical	0.55	0.10	-0.09	0.80	0.54	0.11
43 M	Coronal	0.60	0.07	-0.12	0.75	0.49	0.15
	Middle	0.53	0.11	-0.13	0.72	0.50	0.14
	Apical	0.55	0.10	-0.09	0.80	0.52	0.13
41 D	Coronal	0.61	0.06	-0.07	0.85	0.45	0.20
	Middle	0.655*	0.04	-0.10	0.79	0.42	0.22
	Apical	0.727*	0.02	-0.21	0.56	0.37	0.29
41 M	Coronal	0.56	0.09	-0.09	0.81	0.39	0.27
	Middle	0.691*	0.03	-0.25	0.49	0.37	0.29
	Apical	0.710*	0.03	-0.19	0.62	0.38	0.31

*: high correlations

Table 4.4.13. Correlations between Von Mises stresses at the PDL and thickness variations in CI II/6s group (left side)

Region	Area	lingual	p	Combined	p	Hard Cortical	p
37 D	Coronal	0.648*	0.042	-0.156	0.665	0.405	0.245
	Middle	0.674*	0.032	-0.166	0.644	0.345	0.327
	Apical	0.643*	0.045	-0.145	0.687	0.372	0.289
37 M	Coronal	0.282	0.429	-0.215	0.550	0.371	0.290
	Middle	0.482	0.157	-0.225	0.531	0.294	0.407
	Apical	0.250	0.484	-0.383	0.273	0.058	0.872
36 D	Coronal	0.062	0.868	-0.132	0.714	0.413	0.234
	Middle	-0.108	0.765	-0.081	0.826	0.426	0.218
	Apical	-0.027	0.939	-0.034	0.924	0.591	0.072
36 M	Coronal	0.232	0.518	-0.445	0.196	0.175	0.628
	Middle	-0.499	0.141	-0.321	0.364	-0.145	0.689
	Apical	-0.477	0.162	-0.342	0.332	-0.086	0.813
33 D	Coronal	0.286	0.421	-0.044	0.894	0.341	0.334
	Middle	0.169	0.639	0.001	0.998	0.339	0.337
	Apical	0.329	0.353	-0.037	0.917	0.382	0.275
33 M	Coronal	0.468	0.172	-0.102	0.777	0.351	0.319
	Middle	0.354	0.315	-0.035	0.921	0.356	0.311
	Apical	0.367	0.296	-0.093	0.796	0.331	0.351
31 D	Coronal	0.594	0.069	-0.059	0.876	0.416	0.231
	Middle	0.623	0.053	-0.024	0.945	0.454	0.187
	Apical	0.667*	0.035	-0.026	0.942	0.455	0.186
31 M	Coronal	0.577	0.081	-0.013	0.971	0.473	0.166
	Middle	0.587	0.074	-0.114	0.752	0.406	0.243
	Apical	0.635*	0.048	-0.131	0.716	0.361	0.306

** : very high correlations

* : high correlations

Table 4.4.14. Correlations between dental displacements and thickness variations in CI II/6s group

Measure	lingual	p	Combined	p	Hard Cortical	p
Disp 47	-0.670*	0.034	0.072	0.843	-0.458	0.182
Disp 46	-0.673*	0.032	0.074	0.837	-0.455	0.186
Disp 43	-0.684*	0.029	0.083	0.817	-0.447	0.195
Disp 41	-0.668*	0.034	0.066	0.854	-0.465	0.175
Disp 37	-0.664*	0.036	0.074	0.838	-0.466	0.174
Disp 36	-0.668*	0.034	0.069	0.849	-0.465	0.174
Disp 33	-0.678*	0.031	0.074	0.837	-0.458	0.182
Disp 31	-0.666*	0.035	0.069	0.847	-0.461	0.178

* : high correlations

4.4.2.2. CI II/7s

4.4.2.2. A. TMJ

Similar to the CI II/6s group, weak correlations were noted in the CI II/7s group. Solitary units on the TMJ were found to highly correlate with the thickness variations (Table 4.4.15, 4.6.16).

Table 4.4.15. Correlations between Von Mises stresses on TMJ and thickness variations in CI II/7s group (right side)

Region	Area	lingual	p	Combined	p	Hard Cortical	p
Cond	Anterior	-0.345	0.329	-0.063	0.864	-0.620	0.056
	Middle	-0.135	0.711	-0.178	0.623	-0.644*	0.045
	Posterior	-0.357	0.312	-0.001	0.997	-0.451	0.191
Disk	Anterior	-0.264	0.461	-0.150	0.680	-0.489	0.152
	Middle	-0.420	0.227	0.129	0.722	-0.131	0.718
	Posterior	-0.362	0.305	-0.320	0.367	-0.663*	0.037
Temp	Anterior	-0.493	0.148	-0.102	0.779	-0.579	0.080
	Middle	-0.431	0.214	-0.017	0.963	-0.404	0.247
	Posterior	-0.604	0.064	-0.272	0.448	-0.500	0.141

*: high correlations

Table 4.4.16. Correlations between Von Mises stresses on TMJ and thickness variations in CI II/7s group (left side)

Region	Area	Light Lingual	p	Combined	p	Hard Cortical	p
Cond	Anterior	-0.446	0.195	0.003	0.99	-0.62	0.051
	Middle	-0.398	0.253	0.027	0.94	-0.59	0.07
	Posterior	-0.362	0.302	-0.22	0.53	-0.781**	0.007
Disk	Anterior	-0.405	0.245	-0.04	0.89	-0.62	0.055
	Middle	-0.439	0.203	-0.25	0.47	-0.786**	0.006
	Posterior	-0.170	0.638	0.12	0.72	-0.48	0.15
Temp	Anterior	-0.511	0.130	0.02	0.93	-0.48	0.15
	Middle	-0.373	0.287	0.021	0.95	-0.51	0.12
	Posterior	-0.565	0.088	-0.022	0.95	-0.57	0.08

** : very high correlations

4.4.2.2. B. Dental Components

Also, similar to the CI II/6s group, Von Mises stresses at the PDL were found to correlate weakly with the thickness variations (Table 4.4.17).

Table 4.4.17. Correlations between Von Mises stresses at the PDL and thickness variations in CI II/7s group (right side)

Region	Area	lingual	p	Combined	p	Hard Cortical	p
47 D	Coronal	-0.133	0.714	0.280	0.433	0.316	0.374
	Middle	-0.079	0.828	0.281	0.431	0.207	0.567
	Apical	0.775**	0.008	-0.161	0.658	0.049	0.894
47 M	Coronal	0.536	0.110	0.160	0.660	0.473	0.167
	Middle	0.247	0.492	0.294	0.409	0.413	0.235
	Apical	-0.035	0.924	0.328	0.355	0.326	0.358
46 D	Coronal	0.761*	0.011	-0.088	0.808	0.410	0.239
	Middle	0.659*	0.038	-0.029	0.936	0.518	0.125
	Apical	0.609	0.062	-0.011	0.976	0.560	0.093
46 M	Coronal	0.770**	0.009	-0.171	0.636	0.380	0.279
	Middle	0.693*	0.026	-0.141	0.697	0.457	0.185
	Apical	0.412	0.237	-0.057	0.875	0.594	0.070
43 D	Coronal	0.550	0.100	-0.067	0.854	0.533	0.113
	Middle	0.240	0.505	0.021	0.954	0.626	0.053
	Apical	-0.124	0.733	0.002	0.996	0.331	0.350
43 M	Coronal	0.618	0.057	-0.099	0.787	0.492	0.149
	Middle	0.316	0.374	-0.137	0.706	0.491	0.150
	Apical	0.076	0.835	0.045	0.902	0.439	0.205
41 D	Coronal	0.449	0.193	0.051	0.889	0.157	0.665
	Middle	0.380	0.279	-0.042	0.909	-0.167	0.644
	Apical	0.545	0.103	-0.481	0.159	-0.380	0.279
41 M	Coronal	0.143	0.693	-0.049	0.894	-0.189	0.601
	Middle	0.299	0.401	-0.596	0.069	-0.419	0.228
	Apical	0.415	0.233	-0.567	0.087	-0.494	0.146

** : very high correlations

* : high correlations

Solitary regions were found to correlate highly only with the lingual thickness variation on the right side, and on the hard-cortical region on the left side.

For dental displacements, the lingual cortical thickness variation was found to correlate negatively and highly with displacement of mandibular teeth ($-0.693 < r < -0.778$). No other correlations were noted between other thickness variations and other displacements (Table 4.4.19).

Table 4.4.18. Correlations between Von Mises stresses at the PDL and thickness variations in CI II/7s group (left side)

Left side							
Region	Area	Light Lingual	p	Combined	p	Hard Cortical	p
37 D	Coronal	-0.616	0.058	0.073	0.842	0.263	0.463
	Middle	-0.608	0.062	0.069	0.850	0.266	0.458
	Apical	-0.545	0.104	0.079	0.829	0.392	0.262
37 M	Coronal	0.203	0.574	-0.246	0.493	-0.139	0.702
	Middle	0.463	0.178	-0.398	0.254	-0.193	0.594
	Apical	0.423	0.223	-0.419	0.229	0.107	0.768
36 D	Coronal	0.599	0.067	-0.199	0.582	0.319	0.369
	Middle	-0.204	0.572	-0.229	0.524	-0.033	0.928
	Apical	-0.638*	0.047	-0.051	0.889	-0.244	0.497
36 M	Coronal	0.587	0.075	-0.114	0.755	0.274	0.443
	Middle	0.085	0.815	-0.078	0.831	-0.046	0.899
	Apical	-0.317	0.372	-0.012	0.975	-0.255	0.477
33 D	Coronal	-0.476	0.165	0.227	0.528	-0.255	0.477
	Middle	-0.680*	0.030	0.257	0.473	-0.310	0.384
	Apical	-0.651*	0.041	0.169	0.641	-0.418	0.229
33 M	Coronal	0.104	0.774	0.035	0.923	-0.239	0.506
	Middle	-0.350	0.322	0.254	0.479	-0.250	0.486
	Apical	-0.567	0.087	0.136	0.709	-0.437	0.206
31 D	Coronal	0.224	0.533	0.089	0.808	-0.253	0.481
	Middle	-0.170	0.639	0.269	0.452	-0.370	0.292
	Apical	-0.172	0.634	0.215	0.551	-0.447	0.196
31 M	Coronal	-0.057	0.876	0.381	0.277	-0.067	0.853
	Middle	-0.425	0.221	-0.105	0.773	-0.676*	0.032
	Apical	-0.258	0.472	-0.285	0.425	-0.801**	0.005

** : very high correlations

* : high correlations

Table 4.4.19. Correlations between dental displacements on dental units and thickness variations in CI II/7s group

Measure	lingual	p	Combined	p	Hard Cortical	p
Disp 47	-0.693*	0.026	0.191	0.597	-0.338	0.340
Disp 46	-0.722*	0.018	0.154	0.670	-0.366	0.298
Disp 43	-0.778**	0.008	0.197	0.586	-0.316	0.373
Disp 41	-0.719*	0.019	0.093	0.798	-0.425	0.221
Disp 37	-0.739*	0.015	0.086	0.813	-0.410	0.239
Disp 36	-0.756*	0.011	0.103	0.776	-0.386	0.270
Disp 33	-0.777**	0.008	0.123	0.735	-0.376	0.284
Disp 31	-0.711*	0.021	0.103	0.777	-0.405	0.245

** : very high correlations

* : high correlations

4.4.2.3. CI III's

4.4.2.3. A. TMJ

Weak and non-statistically significant correlations were found between the Von Mises stresses on the TMJ and the thickness variations in the CI III. All values demonstrated a negative pattern of correlation, underscoring an inversely proportional correlation.

Table 4.4.20. Correlations between Von Mises stresses on TMJ and thickness variations in CI III group (right side)

Region	Area	lingual	p	Combined	p	Hard Cortical	p
Cond	Anterior	-0.413	0.235	-0.055	0.881	-0.479	0.162
	Middle	-0.073	0.841	-0.285	0.425	-0.527	0.117
	Posterior	-0.498	0.143	0.042	0.907	-0.152	0.676
Disk	Anterior	-0.116	0.751	-0.430	0.214	-0.515	0.128
	Middle	-0.365	0.300	0.176	0.627	0.139	0.701
	Posterior	-0.407	0.243	-0.539	0.108	-0.600	0.067
Temp	Anterior	-0.553	0.097	0.067	0.855	-0.188	0.603
	Middle	-0.432	0.213	-0.152	0.676	-0.370	0.293
	Posterior	-0.663*	0.037	-0.430	0.214	-0.406	0.244

** : very high correlations

* : high correlations

Table 4.4.21. Correlations between Von Mises stresses on TMJ and thickness variations in CI III's group (left side)

Region	Area	lingual	p	Combined	p	Hard Cortical	p
Cond	Anterior	-0.255	0.476	-0.200	0.580	-0.248	0.489
	Middle	-0.152	0.675	-0.030	0.934	-0.103	0.777
	Posterior	-0.249	0.487	-0.345	0.328	-0.442	0.200
Disk	Anterior	-0.207	0.567	-0.139	0.701	-0.248	0.489
	Middle	-0.334	0.345	-0.418	0.229	-0.564	0.090
	Posterior	0.030	0.934	0.018	0.960	-0.042	0.907
Temp	Anterior	-0.261	0.466	-0.006	0.987	-0.103	0.777
	Middle	-0.128	0.725	-0.176	0.627	-0.224	0.533
	Posterior	-0.225	0.532	-0.200	0.580	-0.152	0.676

4.4.2.3. B. Dental Components

Correlations between Von Mises stresses at the PDL and thickness variations were weak and not statistically significant (Table 4.4.22, 4.6.23).

Similarly, no correlations were found between any of the represented variables for dental displacements (Table 4.4.24).

Table 4.4.22. Correlations between Von Mises stresses on PDL and thickness variations in CI III group (right side)

Region	Area	lingual	p	Combined	p	Hard Cortical	p
47 D	Coronal	-0.255	0.476	0.067	0.855	0.152	0.676
	Middle	0.128	0.725	0.188	0.603	0.152	0.676
	Apical	0.717*	0.020	-0.224	0.533	-0.091	0.803
47 M	Coronal	-0.018	0.960	0.115	0.751	0.236	0.511
	Middle	-0.085	0.815	0.261	0.467	0.321	0.365
	Apical	0.207	0.567	0.152	0.676	0.164	0.651
46 D	Coronal	0.438	0.206	-0.285	0.425	-0.103	0.777
	Middle	0.334	0.345	-0.394	0.260	-0.055	0.881
	Apical	0.456	0.185	-0.467	0.174	-0.152	0.676
46 M	Coronal	0.182	0.614	-0.297	0.405	-0.079	0.829
	Middle	0.195	0.590	-0.406	0.244	-0.200	0.580
	Apical	0.280	0.434	-0.406	0.244	-0.139	0.701
43 D	Coronal	-0.036	0.920	-0.042	0.907	-0.152	0.676
	Middle	-0.061	0.868	-0.055	0.881	-0.103	0.777
	Apical	-0.243	0.498	-0.370	0.293	-0.430	0.214
43 M	Coronal	0.061	0.868	-0.115	0.751	-0.188	0.603
	Middle	-0.012	0.973	0.006	0.987	-0.103	0.777
	Apical	-0.097	0.789	-0.176	0.627	-0.152	0.676
41 D	Coronal	-0.182	0.614	-0.212	0.556	-0.345	0.328
	Middle	-0.371	0.291	0.067	0.855	-0.176	0.627
	Apical	-0.286	0.424	-0.176	0.627	-0.285	0.425
41 M	Coronal	-0.395	0.258	-0.394	0.260	-0.552	0.098
	Middle	-0.401	0.250	-0.661*	0.038	-0.709*	0.022
	Apical	-0.468	0.172	-0.418	0.229	-0.624	0.054

** : very high correlations

* : high correlations

Table 4.4.23. Correlations between Von Mises stresses on PDL and thickness variations in CI III's group (left side)

Region	Area	Light Lingual	p	Combined	p	Hard Cortical	p
37 D	Coronal	0.043	0.907	-0.285	0.425	-0.127	0.726
	Middle	0.134	0.713	-0.382	0.276	-0.273	0.446
	Apical	0.000	1.000	-0.321	0.365	-0.224	0.533
37 M	Coronal	0.055	0.881	-0.297	0.405	-0.236	0.511
	Middle	0.006	0.987	-0.285	0.425	-0.273	0.446
	Apical	0.340	0.336	-.709*	0.022	-0.297	0.405
36 D	Coronal	0.219	0.544	-0.382	0.276	-0.261	0.467
	Middle	0.103	0.776	-0.382	0.276	-0.321	0.365
	Apical	0.152	0.675	-0.394	0.260	-0.285	0.425
36 M	Coronal	0.134	0.713	-0.358	0.310	-0.224	0.533
	Middle	-0.316	0.374	-0.442	0.200	-0.661*	0.038
	Apical	-0.456	0.185	-0.358	0.310	-0.661*	0.038
33 D	Coronal	-0.535	0.111	-0.297	0.405	-0.661*	0.038
	Middle	-0.614	0.059	-0.273	0.446	-0.624	0.054
	Apical	-0.650*	0.042	-0.248	0.489	-0.564	0.090
33 M	Coronal	-0.432	0.213	-0.285	0.425	-0.588	0.074
	Middle	-0.590	0.073	-0.224	0.533	-0.576	0.082
	Apical	-0.663*	0.037	-0.212	0.556	-0.552	0.098
31 D	Coronal	-0.456	0.185	-0.079	0.829	-0.309	0.385
	Middle	-0.602	0.066	0.152	0.676	-0.139	0.701
	Apical	-0.626	0.053	0.103	0.777	-0.188	0.603
31 M	Coronal	-0.498	0.143	0.067	0.855	-0.224	0.533
	Middle	-0.766**	0.010	0.018	0.960	-0.321	0.365
	Apical	-0.717*	0.020	-0.127	0.726	-0.394	0.260

** : very high correlations

* : high correlations

Table 4.4.24. Correlations between dental displacements on dental units and thickness variations in CI III group

Measure	Light Lingual	p	Combined	p	Hard Cortical	p
Disp 47	0.219	0.544	-0.370	0.293	-0.103	0.777
Disp 46	0.219	0.544	-0.370	0.293	-0.103	0.777
Disp 43	0.152	0.675	-0.370	0.293	-0.176	0.627
Disp 41	0.109	0.763	-0.358	0.310	-0.164	0.651
Disp 37	0.158	0.663	-0.345	0.328	-0.127	0.726
Disp 36	0.158	0.663	-0.345	0.328	-0.127	0.726
Disp 33	0.286	0.424	-0.382	0.276	-0.091	0.803
Disp 31	0.134	0.713	-0.382	0.276	-0.224	0.533

4.5. Correlations between model components

4.5.1. CI III/6s

Weak correlations existed between the anterior section of the condyle and the dental components, with a single high correlation noted for the mandibular left 2nd molar (#37) at the coronal and middle at the mesial side, and another at the level of the canine (all sections except the apical portion at the distal side) ($r > 0.713$; Table 4.4.1).

Strong correlations were observed between the middle condylar region and the dental components, particularly with the mandibular left 2nd molar (#37) (except the apical mesial section), with the canine (except with the middle section of the distal side), and the central incisor at all levels.

At the posterior level of the condyle correlations with the dental components were weak, the highest found at the level of the mandibular left 1st molar, coronal section, at the distal side. No high correlation was observed between any region of the disk and the Von Mises stresses at the PDL

Strong correlations occurred between the anterior temporal bone with the dental components, notably with the mandibular left 2nd molar (#37) at the coronal levels on both sides and at the middle section of the mesial side, and with the canine at all levels except the apical section of the distal side. While weak correlations marked the association between the central incisor at the coronal levels and at the middle section of the distal side, no other significant correlations were detected with the middle and posterior temporal bones.

The stress levels at all the regions of the mandibular left 2nd molar (#37), except for the apical section at the mesial side, correlated well with the displacements of all the investigated mandibular left teeth (Table 4.5.1).

Table 4.5.1. Correlations between Von Mises stress on PDL and dental displacement under thickness variations in CI II/6s group (left side)

		Disp 37	Disp 36	Disp 33	Disp 31			Disp 37	Disp 36	Disp 33	Disp 31
37 Cor	<i>r</i>	-0.987**	-0.986**	-0.985**	-0.986**	33 Cor	<i>r</i>	-0.796**	-0.792**	-0.784**	-0.795**
	<i>P</i>	0.001	0.001	0.001	0.001		<i>P</i>	0.006	0.006	0.007	0.006
37 Mid	<i>r</i>	-0.986**	-0.986**	-0.986**	-0.986**	33 Mid	<i>r</i>	-0.725*	-0.721*	-0.711*	-0.724*
	<i>P</i>	0.001	0.001	0.001	0.001		<i>P</i>	0.018	0.019	0.021	0.018
37 Api	<i>r</i>	-0.983**	-0.983**	-0.983**	-0.984**	33 Api	<i>r</i>	-0.864**	-0.862**	-0.855**	-0.864**
	<i>P</i>	0.001	0.001	0.001	0.001		<i>P</i>	0.001	0.001	0.002	0.001
37 Cor	<i>r</i>	-0.805**	-0.798**	-0.790**	-0.798**	33 Cor	<i>r</i>	-0.908**	-0.906**	-0.901**	-0.908**
	<i>P</i>	0.005	0.006	0.007	0.006		<i>P</i>	0.001	0.001	0.001	0.001
37 Mid	<i>r</i>	-0.901**	-0.897**	-0.893**	-0.898**	33 Mid	<i>r</i>	-0.834**	-0.831**	-0.824**	-0.834**
	<i>P</i>	0.001	0.001	0.001	0.001		<i>P</i>	0.003	0.003	0.003	0.003
37 Api	<i>r</i>	-0.01	-0.004	-0.007	0.003	33 Api	<i>r</i>	-0.854**	-0.851**	-0.844**	-0.853**
	<i>P</i>	0.978	0.992	0.985	0.993		<i>P</i>	0.002	0.002	0.002	0.002
36 Cor	<i>r</i>	-0.584	-0.575	-0.563	-0.574	31 Cor	<i>r</i>	-0.973**	-0.973**	-0.971**	-0.975**
	<i>P</i>	0.076	0.082	0.09	0.083		<i>P</i>	0.001	0.001	0.001	0.001
36 Mid	<i>r</i>	-0.402	-0.392	-0.378	-0.39	31 Mid	<i>r</i>	-0.982**	-0.983**	-0.981**	-0.984**
	<i>P</i>	0.25	0.263	0.281	0.265		<i>P</i>	0.001	0.001	0.001	0.001
36 Api	<i>r</i>	-0.481	-0.474	-0.464	-0.471	31 Api	<i>r</i>	-0.986**	-0.987**	-0.987**	-0.988**
	<i>P</i>	0.16	0.167	0.176	0.169		<i>P</i>	0.001	0.001	0.001	0.001
36 Cor	<i>r</i>	-0.453	-0.445	-0.44	-0.443	31 Cor	<i>r</i>	-0.975**	-0.974**	-0.972**	-0.976**
	<i>P</i>	0.189	0.198	0.203	0.2		<i>P</i>	0.001	0.001	0.001	0.001
36 Mid	<i>r</i>	0.32	0.331	0.34	0.331	31 Mid	<i>r</i>	-0.989**	-0.989**	-0.988**	-0.990**
	<i>P</i>	0.368	0.351	0.336	0.35		<i>P</i>	0.001	0.001	0.001	0.001
36 Api	<i>r</i>	0.262	0.27	0.276	0.27	31 Api	<i>r</i>	-0.948**	-0.950**	-0.953**	-0.951**
	<i>P</i>	0.464	0.451	0.441	0.451		<i>P</i>	0.001	0.001	0.001	0.001

Regarding the left 1st molar, the stress levels at all the regions did not correlate with the displacements of the investigated mandibular left teeth. However, the canine correlated highly ($r > 0.711$) with displacements of all the examined mandibular left teeth.

At the level of the central incisor, the stress measurements correlated highly ($r > 0.948$) with displacements of all the examined mandibular left teeth. Both sides behaved similarly with almost identical patterns of correlation.

Also, high correlations exist between the TMJ components and the dental displacements at almost all regions except at the posterior temporal region with the displacement of the left 2nd molar ($r < 0.645$) (Table 4.5.2).

Table 4.5.2. Correlation between TMJ components and dental displacements under thickness variations in CI II/6s group (left side)

		Disp 37	Disp 36	Disp 33	Disp 31
Cond Ant	<i>r</i>	0.839**	0.835**	0.783**	0.851**
	<i>P</i>	0.002	0.003	0.007	0.002
Cond Mid	<i>r</i>	0.702*	0.703*	0.645*	0.737*
	<i>P</i>	0.024	0.023	0.044	0.015
Cond Post	<i>r</i>	0.802**	0.784**	0.761*	0.795**
	<i>P</i>	0.005	0.007	0.011	0.006
Disk Ant	<i>r</i>	0.740*	0.740*	0.684*	0.759*
	<i>P</i>	0.014	0.014	0.029	0.011
Disk Mid	<i>r</i>	0.710*	0.737*	0.769**	0.760*
	<i>P</i>	0.022	0.015	0.009	0.011
Disk Post	<i>r</i>	0.688*	0.712*	0.689*	0.761*
	<i>P</i>	0.028	0.021	0.028	0.011
Temp Ant	<i>r</i>	0.868**	0.885**	0.869**	0.909**
	<i>P</i>	0.001	0.001	0.001	0.000
Temp Mid	<i>r</i>	0.802**	0.824**	0.809**	0.835**
	<i>P</i>	0.005	0.003	0.005	0.003
Temp Post	<i>r</i>	0.602	0.664*	0.704*	0.729*
	<i>P</i>	0.065	0.036	0.023	0.017

4.5.2. CI II/7s

Weak correlations were observed between the Von Mises stresses at the PDL and the dental displacement produced in this group. With solitary units showing high

correlations, no specific pattern of associations can be generalized on the whole model (Table 4.5.3).

Table 4.5.3. Correlations between Von Mises stress on PDL and dental displacement under thickness variations in CI II/7s group (left side)

		Disp 37	Disp 36	Disp 33	Disp 31			Disp 37	Disp 36	Disp 33	Disp 31
37	<i>r</i>	0.318	0.358	0.364	0.344	33	<i>r</i>	0.445	0.441	0.463	0.385
Cor D	<i>P</i>	0.37	0.31	0.301	0.331	Cor D	<i>P</i>	0.198	0.202	0.178	0.272
37	<i>r</i>	0.367	0.399	0.405	0.369	33	<i>r</i>	0.728*	0.725*	0.744*	.675*
Mid D	<i>P</i>	0.297	0.253	0.245	0.295	Mid D	<i>P</i>	0.017	0.018	0.014	0.032
37	<i>r</i>	0.198	0.214	0.225	0.161	33 Api	<i>r</i>	0.786**	0.781**	0.794**	0.740*
Api D	<i>P</i>	0.584	0.553	0.532	0.656	D	<i>P</i>	0.007	0.008	0.006	0.014
37	<i>r</i>	-0.259	-0.276	-0.268	-0.322	33	<i>r</i>	-0.149	-0.16	-0.144	-0.199
Cor M	<i>P</i>	0.47	0.44	0.455	0.364	Cor M	<i>P</i>	0.682	0.658	0.692	0.582
37	<i>r</i>	-0.478	-0.498	-0.498	-0.537	33	<i>r</i>	0.395	0.385	0.405	0.333
Mid M	<i>P</i>	0.163	0.143	0.143	0.11	Mid M	<i>P</i>	0.259	0.272	0.245	0.347
37	<i>r</i>	-0.234	-0.229	-0.259	-0.215	33 Api	<i>r</i>	0.719*	0.712*	0.725*	0.673*
Api M	<i>P</i>	0.515	0.524	0.47	0.55	M	<i>P</i>	0.019	0.021	0.018	0.033
36	<i>r</i>	-0.745*	-0.746*	-0.749*	-0.759*	31	<i>r</i>	-0.121	-0.121	-0.111	-0.138
Cor D	<i>P</i>	0.013	0.013	0.013	0.011	Cor D	<i>P</i>	0.739	0.74	0.76	0.704
36	<i>r</i>	-0.006	0.023	0.031	-0.014	31	<i>r</i>	0.512	0.52	0.522	0.535
Mid D	<i>P</i>	0.987	0.949	0.932	0.969	Mid D	<i>P</i>	0.13	0.123	0.122	0.111
36	<i>r</i>	0.384	0.416	0.436	0.372	31 Api	<i>r</i>	0.615	0.614	0.609	.644*
Api D	<i>P</i>	0.274	0.232	0.207	0.29	D	<i>P</i>	0.058	0.059	0.061	0.044
36	<i>r</i>	-0.521	-0.506	-0.529	-0.444	31	<i>r</i>	0.178	0.185	0.198	0.156
Cor M	<i>P</i>	0.123	0.136	0.116	0.199	Cor M	<i>P</i>	0.622	0.608	0.583	0.666
36	<i>r</i>	0.14	0.165	0.141	0.231	31	<i>r</i>	.646*	.638*	.637*	.653*
Mid M	<i>P</i>	0.7	0.649	0.698	0.52	Mid M	<i>P</i>	0.043	0.047	0.048	0.041
36	<i>r</i>	0.554	0.581	0.566	0.626	31 Api	<i>r</i>	0.557	0.533	0.524	0.575
Api M	<i>P</i>	0.096	0.078	0.088	0.053	M	<i>P</i>	0.095	0.113	0.12	0.082

In a pattern similar to the CI II/6s group, high correlations existed between the TMJ units and the dental displacements ($r < 0.645$), except between the posterior region of the temporal space and the displacement at the 2nd molar ($p = 0.065$) (Table 4.5.4).

Table 4.5.4. Correlations between TMJ components and dental displacements under thickness variations in CI II/7s group (left side)

		Disp 37	Disp 36	Disp 33	Disp 31
Cond Ant	<i>r</i>	0.839	0.835	0.783	0.851
	<i>P</i>	0.002	0.003	0.007	0.002
Cond Mid	<i>r</i>	0.702*	0.703	0.645*	0.737
	<i>P</i>	0.024*	0.023	0.044	0.015
Cond Post	<i>r</i>	0.802	0.784	0.761*	0.795
	<i>P</i>	0.005	0.007	0.011	0.006
Disk Ant	<i>r</i>	0.740	0.740*	0.684*	0.759
	<i>P</i>	0.014	0.014	0.029	0.011
Disk Mid	<i>r</i>	0.710	0.737*	0.769**	0.760
	<i>P</i>	0.022	0.015	0.009	0.011
Disk Post	<i>r</i>	0.688	0.712*	0.689*	0.761
	<i>P</i>	0.028	0.021	0.028	0.011
Temp Ant	<i>r</i>	0.868**	0.885**	0.869**	0.909**
	<i>P</i>	0.001	0.001	0.001	0.000
Temp Mid	<i>r</i>	0.802	0.824	0.809	0.835
	<i>P</i>	0.005	0.003	0.005	0.003
Temp Post	<i>r</i>	0.602	0.664*	0.704*	0.729*
	<i>P</i>	0.065	0.036	0.023	0.017

4.5.3. CI III

Only the stresses at the molars (at most regions) correlated with the crown displacements in the CI III group. The anterior dentition had weak correlations with the displacements produced (Table 4.5.5).

Table 4.5.5. Correlations between Von Mises stresses on PDL and dental displacement under thickness variations in CI III group (left side)

		Disp 37	Disp 36	Disp 33	Disp 31			Disp 37	Disp 36	Disp 33	Disp 31
37	<i>r</i>	0.806**	0.806**	0.806**	0.842**	33	<i>r</i>	0.188	0.188	0.03	0.333
Cor D	<i>P</i>	0.005	0.005	0.005	0.002	Cor D	<i>P</i>	0.603	0.603	0.934	0.347
37	<i>r</i>	0.770**	0.770**	0.782**	0.879**	33	<i>r</i>	-0.079	-0.079	-0.261	0.042
Mid D	<i>P</i>	0.009	0.009	0.008	0.001	Mid D	<i>P</i>	0.829	0.829	0.467	0.907
37	<i>r</i>	0.624	0.624	0.612	0.758*	33 Api	<i>r</i>	-0.139	-0.139	-0.285	0.006
Api D	<i>P</i>	0.054	0.054	0.06	0.011	D	<i>P</i>	0.701	0.701	0.425	0.987
37	<i>r</i>	0.721*	0.721*	0.721*	0.855**	33	<i>r</i>	0.139	0.139	-0.042	0.285
Cor M	<i>P</i>	0.019	0.019	0.019	0.002	Cor M	<i>P</i>	0.701	0.701	0.907	0.425
37	<i>r</i>	0.697*	0.697*	0.709*	0.830**	33	<i>r</i>	-0.03	-0.03	-0.224	0.115
Mid M	<i>P</i>	0.025	0.025	0.022	0.003	Mid M	<i>P</i>	0.934	0.934	0.533	0.751
37	<i>r</i>	0.685*	0.685*	0.782**	0.612	33 Api	<i>r</i>	-0.115	-0.115	-0.297	-0.006
Api M	<i>P</i>	0.029	0.029	0.008	0.06	M	<i>P</i>	0.751	0.751	0.405	0.987
36	<i>r</i>	0.758*	0.758*	0.758*	0.855**	31	<i>r</i>	0.309	0.309	0.261	0.491
Cor D	<i>P</i>	0.011	0.011	0.011	0.002	Cor D	<i>P</i>	0.385	0.385	0.467	0.15
36	<i>r</i>	0.721*	0.721*	0.733*	0.818**	31	<i>r</i>	0.152	0.152	0.127	0.309
Mid D	<i>P</i>	0.019	0.019	0.016	0.004	Mid D	<i>P</i>	0.676	0.676	0.726	0.385
36	<i>r</i>	0.745*	0.745*	0.745*	0.842**	31 Api	<i>r</i>	0.103	0.103	0.091	0.236
Api D	<i>P</i>	0.013	0.013	0.013	0.002	D	<i>P</i>	0.777	0.777	0.803	0.511
36	<i>r</i>	0.915**	0.915**	0.903**	0.903**	31	<i>r</i>	0.188	0.188	0.139	0.333
Cor M	<i>P</i>	0.001	0.001	0.001	0.001	Cor M	<i>P</i>	0.603	0.603	0.701	0.347
36	<i>r</i>	0.479	0.479	0.43	0.527	31	<i>r</i>	0.139	0.139	0.091	0.285
Mid M	<i>P</i>	0.162	0.162	0.214	0.117	Mid M	<i>P</i>	0.701	0.701	0.803	0.425
36	<i>r</i>	0.297	0.297	0.248	0.345	31 Api	<i>r</i>	0.139	0.139	0.139	0.248
Api M	<i>P</i>	0.405	0.405	0.489	0.328	M	<i>P</i>	0.701	0.701	0.701	0.489

The TMJ units did not correlate significantly with the dental displacements in the CI III group (Table 4.5.6).

Table 4.5.6. Correlations between TMJ components and dental displacements under thickness variations in CI III group (left side)

		Disp 37	Disp 36	Disp 33	Disp 32	Disp 31
Cond Ant	<i>r</i>	0.333	0.333	0.370	0.309	0.273
	<i>P</i>	0.347	0.347	0.293	0.385	0.446
Cond Mid	<i>r</i>	0.127	0.127	0.200	0.091	0.067
	<i>P</i>	0.726	0.726	0.580	0.803	0.855
Cond Post	<i>r</i>	0.176	0.176	0.273	0.188	0.224
	<i>P</i>	0.627	0.627	0.446	0.603	0.533
Disk Ant	<i>r</i>	0.345	0.345	0.333	0.297	0.236
	<i>P</i>	0.328	0.328	0.347	0.405	0.511
Disk Mid	<i>r</i>	0.418	0.418	0.394	0.382	0.333
	<i>P</i>	0.229	0.229	0.260	0.276	0.347
Disk Post	<i>r</i>	0.067	0.067	0.188	0.006	-0.018
	<i>P</i>	0.855	0.855	0.603	0.987	0.960
Temp Ant	<i>r</i>	0.164	0.164	0.176	0.115	0.042
	<i>P</i>	0.651	0.651	0.627	0.751	0.907
Temp Mid	<i>r</i>	0.248	0.248	0.224	0.188	0.115
	<i>P</i>	0.489	0.489	0.533	0.603	0.751
Temp Post	<i>r</i>	0.091	0.091	0.139	0.067	0.030
	<i>P</i>	0.803	0.803	0.701	0.855	0.934

CHAPTER 5

DISCUSSION

5.1. Strengths

We have investigated modalities heretofore not studied or documented in a global morphological context, while at the same time accounting for individual variation, thus inching the FE analysis closer to clinical interpretation.

The primary aim of the study was to numerically investigate the stresses distributed on the teeth and on the TMJ complex. In this process, the following panels emerged simultaneously, overcoming the fractioning of testing and responses thus far prevalent in the literature, and providing more encompassing information:

1. A comparison of the effects of Class II versus Class III elastics on the condyle.

Both had an impact on the various regions of the condylar components, Class III providing more stress levels at all TMJ levels in the stiffness variations. The effect of the elastics on dental units reflected the expectations from clinical practice: CI III impacted the mandibular canines and incisors, CI II targeted the molars and incisors.

2. A comparison of the effects of stiffness versus thickness on the mandibular response.

Stiffness induced higher stresses and more variability on condylar and dental response.

3. An assessment of symmetrical response.

Differences were observed between right and left sides at all levels. Whether or not of clinical significance, the findings were important in disclosing this potential. In the present model, the asymmetry may be related to the different alignment of right

and left incisors (left lateral incisor was more lingually placed) and/or inherent minor asymmetries in the mandibular structure of the patient whose CBCT was used. Nevertheless, this model was not manipulated to mirror perfect symmetry; it was left in natural alignment reflecting the reality of human morphology.

5.1.1. Individual Variation

To date, most FE studies have been used in scenarios where engineering parameters like stresses, energy storage, and displacements are investigated. A simplified model was often employed to model a fractioned clinical scenario. However, in medical studies, patient variations can widely change the parameters of clinical settings. Such variables include tissue thickness, density, stiffness and other properties inherent to every component of a structure.

In the clinical settings that we investigated, bone-related material was tested to examine the possible effect of bone properties on other elements of the orofacial complex such as TMJ and teeth. Because of individual variations in bone quantity and stiffness, it was imperative to account for patient-specific responses to determine a central tendency of response, with the knowledge that outliers may exist outside the average response.

Accordingly, not only did we set-up the experiment on changing mechanical loads as in most previous FE studies, but injecting patient-related variations in the anatomical model and the associated statistical explorations to test hypotheses and determine variances of outcome measures. Given the difficulty of computing differences in material properties on living persons at this point, we were able to vary the model on data from human cadavers.

5.1.2. Overcoming the difficulty of direct clinical investigation

To date, comparisons of different bone material and bone thickness on the TMJ structure have never been explored. FEA is a non-invasive method amenable to such an exploration because of its long-standing proven abilities in engineering for answering questions of mechanical underpinning. Such a comparison falls outside the realm of investigation in a clinical setting because:

- Optimizing research conditions is difficult, such as finding a group of individuals with the same bone properties, or even if available, recruiting enough of them to eliminate individual insignificant differences, notwithstanding the difficulty to find patients in similar-to identical conditions of healthy TMJ with minimal to no effect of occlusal trauma, asymmetry or any deformation on this structure.
- Individual biologic conditions may translate in different responses given the patient-specific remodeling when the TMD is subjected to stresses and loads (Carlton & Nanda, 2002)
- Obtaining the approval for invasive methods of inquiry may not materialize given the ethical undertones of ‘testing’ altered mechanical loading in the clinical setting, or validating the use of CI II elastics and later a CI III elastic on the same individual, when only one of these may be indicated for treatment.
- Increased ability for the examiner to interpret the difference of stresses applied on the teeth while the model is loaded under a given scenario. Other measurements, such as the initial real-time representation of the initial stresses and displacements, are not attainable clinically.

5.1.3. Qualified research in the TMJ structure

The TMJ is a delicately balanced system that included various biological structures involved in highly specialized functions such as mastication and speech. The disk is a fibrous connective tissue made of cartilage and mostly collagenous material (Tanaka, 2001). Based on clinical data, patients have been reported to complain of symptoms of pain upon usage of interarch elastics because of the generated pressure exerted on the disk, often compressed or displaced from its normal position between the mandibular condyle and the glenoid fossa of the temporal bone.

Compared to other orofacial structures, the TMJ is reported to possess weak physical material properties, with an average stiffness of 44.1 MPa compared to that of the cortical bone in contact with the disk, which enlists a stiffness of 13700 MPa (Schwartz-Dabney & Dechow, 2003). With such a discrepancy in material properties, the disk particularly lends itself to investigation with FE analysis. In the present study, the aim was to investigate the correlations of stresses at the TMJ with those at the level of the teeth, not only to measure the stresses around the TMJ complex. Such measures have already been provided in the literature (Gupta, Kohli, Hazarey, Kharbanda, & Gunjal, 2009), but only in the context of simulating mandibular advancement of 5 mm, with an opening of 4 mm (through a functional appliance) without associating the findings with stresses at the level of the dentition. In this study, we also accounted for patient variation, and the change of treatment modality.

5.1.4. Effect of bone characteristics on tooth movement

None of the prior studies had examined to date the behavior of the total mandibular structures in a FE model that included variations of the bone properties,

loading conditions, and individual human characteristics. Our model combined all these variables.

Tooth movement has been widely investigated in all directions, including distalization and mandibular protraction of molars (Iwasaki, Haack, Nickel, & Morton, 2000; Nihara et al., 2015). Different factors must be considered when comparing findings in clinical studies and in FE experiments. Bone thickness and stiffness affect the rate of displacement, but other biologic responses like bone turn-over, PDL vascularization, human metabolism also widely impact dental movement (Proffit W. R., 2013). Other parameters contribute to the process, such as tooth size, proximity of teeth to cortical bone, abundance of trabecular bone, and difficulty of implementing the planned force system because of morphological constraints, such as achieving bodily movement in comparison to tipping. These features have been examined in the biological model as well as in the numerical model.

The major added value in FE studies is the possibility to examine stress areas and pressure points that are otherwise not amenable to study in the biological model because of various barriers, the most significant of which is the difficulty of probing the stresses in a clinical setting with a non-invasive method.

5.1.5. Model construction

Finite element analysis is most accurate when it replicates the clinical features and more accurately and predictably approaches the clinical conditions (Hohmann et al., 2011). Precise FE model construction requires significant effort and time. Prior studies, on the other hand, have only modeled parts of the jaws, limiting the investigation to a narrowed field with theoretical outcomes that may not find clinical applications (Nihara

et al., 2015). Other studies examined either jaws alone with assumptions of the behavior of the modeled sections on the other jaw (Shrivastava, Hazarey, Kharbanda, & Gupta, 2015). Some studies encompassed the totality of the head but with a reduced number of “elements” or meshes representing lesser details of the models, hence a lower resolution model with restrained clinical relevance.

In the present study, all bony parts of the mandible (in particular) and the maxilla, including the temporal bone and joints and both the mandibular trabecular and cortical bones were modeled. Later, the mandibular bone was sectioned in areas where segments behaving similar to each other were grouped together. Our model incorporated the area from the chin to the zygomatic process, including the glenoid fossa and the maxilla to account for patient specific variation within the entire mandible.

Bone: The bony representation was not restricted to segment cortical from trabecular bone. The cortical bone itself was segmented into different regions that represented the human variation provided for by the original human cadavers samples investigated for bone material properties by Schwartz-Dabney & Dechow (2003). In the stiffness variation, the parts of the bone stiffness were adjusted to the values that were reported in the cadaver study by averaging the different variations of the grouped parts. In the thickness variation, the grouped parts of the stiffness were kept constant while the thickness was modified.

In this process of modeling, the values of the modeled material properties (Young’s Modulus of Elasticity and Poisson’s ratios) of cortical and trabecular bone, teeth, articular disk and PDL ligament were defined from available data in the literature (Table 3.2.3). The chosen material properties applied in the study were in line to those used by many authors who attempted to study material properties of the mandible and

the TMJ complex. (Carter & Spengler, 1978; Chen, Akyuz, Xu, & Pidaparti, 1998; Gupta et al., 2009; Kayumi, Takayama, Yokoyama, & Ueda, 2015; Tanaka et al., 2004; Tanaka et al., 2000; Tanaka et al., 2001; Tanne, Tanaka, & Sakuda, 1996).

Other authors have reported differing values for the cortical bone and trabecular bone, with wide variation. For example, trabecular bone was modeled at 1370 whereas the compact bone was kept at 13700 (Nihara et al., 2015).

However, such a big difference between the trabecular and cortical stiffness (10 folds) did not seem clinically valid.

Periodontal ligament: Prior studies have diverged in modeling the PDL, despite using isotropic homogenous material. The range of the Young's elastic moduli is wide in the literature from 0.07 to 1750 MPa (Rees & Jacobsen, 1997). Within the range of the loads applied in our study 1.5N, it was proposed that the Young's modulus of the PDL would be around 0.69 MPa (Yoshida, Koga, Peng, Tanaka, & Kobayashi, 2001).

Accordingly, based on other studies conducted in the mandible (Carter & Spengler, 1978; Chen et al., 1998; Gupta et al., 2009; Kayumi et al., 2015; Tanaka et al., 2004; Tanaka et al., 2000; Tanaka et al., 2001; Tanne et al., 1996), the chosen young's modulus was applied in an isotropic, hyper-elastic property.

5.2. Contributions of the study

5.2.1. Information at various levels of a multifaceted and multifactorial system

The stresses distributed on the teeth and on the TMJ complex were tested following the simulation of three different elastic configurations in variations of stiffness and thickness representing patient variations as reported from the cadaver studies. In the process, information was gathered at various levels:

- Comparison of CI II elastics delivered from the 1st molars vs. CI II elastics delivered from the 2nd molars. Such comparisons were not made earlier. Moreover, this comparison would be best interpreted in FE analysis, because of accurate computation of stresses and representation of dental displacements.
- Comparisons of thickness vs. stiffness. The assessment of stiffness variation yielded a clear comparison of the behavior of interarch elastics on an unaltered model geometry. Under thickness variation, the geometry was modified to determine its effect on the pattern of stress generation and the dental displacements produced.
- Comparisons of right vs. left side within the same models. This comparison was valuable not only because it was not previously investigated, but mainly because it raises the awareness of an omnipresent factor that often is not considered in studies of the mechanics of tooth movement.
- Simultaneous assessment of the units engaged during tooth movement: teeth, bone, joint.

5.2.2. Comparison of treatment modalities

From a clinical perspective, the comparison of the two types of elastics, CI III vs. CI II, and the comparison of CI II elastics applied from different molars, allows for a treatment-oriented interpretation of the findings.

5.2.2.1. Stiffness variation

- i. On the TMJ area

Compared to the different configurations of interarch elastics, the CI III elastic demonstrated the highest stress levels generated at all levels of the TMJ area (statistically higher compared with the CI II elastics when delivered from the 1st molar). This finding may be related to the geometric encapsulation of the condyle within the

glenoid fossa, the condyle having a posterior boundary that limits its backward positioning.

Although not statistically significant ($p=0.076$), the CI II elastics delivered from the 1st molars demonstrated lower stresses on all components of the TMJ complex compared to the group where the CI II was applied on the 2nd molars. The lower stresses may be explained by the more vertical line of action of the elastics, whereby the horizontal component of the 150 grams force is reduced compared to the more horizontally inclined force applied from the 2nd molars.

ii. On the dental units

The CI II elastic from the 2nd molars generated a significantly higher stress compared to the CI II/1st molar or CI III elastics. However, the highest stresses on dental units were recorded with CI III elastics on almost all the teeth. The effect followed a nearly similar pattern on left and right sides. Differences between both sides remain the same as in the comparison of left vs. right (section 5.6.2).

- Degree and direction of displacement: A greater displacement was observed when applying the CI III elastics with statistically significant differences when compared with the other elastics. Given that the force magnitude was identical in all instances, this increased displacement may also be related to the fact that the condyle resists a necessarily limited posterior positioning in the CI III mechanism, hence the residual pressure of the elastics is transmitted to the teeth.

- Amount of displacement (*in absolute value*): When the direction of the displacement was factored out, a high statistical significance differentiated the CI III group, which exhibited the greatest potential of displacement, from the CI II/1st molars

group. Although not all comparisons were statistically significant, the gradation of displacement was in favor of Cl III > Cl II/2nd molars > Cl II/1st molars.

5.2.2.2.Thickness variation

i. On the TMJ area

Within the comparisons in the thickness variations, less conclusive findings can be extracted because of the reduced significant differences, probably because mandibular geometry with increased thickness did not change the materials properties of the other elements at play, particularly stiffness. Statistically significant differences were observed between the Cl III group and the Cl II/6's group, whereby the latter showed more stresses than under stiffness variations. Since the pattern of significance involved mostly the disk (at all areas) and the mandibular canines (see next section), an environment similar to that generated by the Cl III elastics under stiffness variation might have existed.

ii. On the dental units

Findings were similar to those on the TMJ components, indicating that altered thickness induced similar changes at the condyle and the PDL levels. Whenever significant differences were present, Cl III elastics showed the least amount of stresses generated on the dental units, statistically significantly different from the Cl II/1st molars group. However, findings are less conclusive under thickness variations than the more solid patterns demonstrated under stiffness variation. A higher prevalence of significance was noted on the left side.

- Degree and direction of displacement: The greatest displacement was produced by the Cl II elastic delivered from the 1st molars, followed by Cl II delivered from the

2nd molars, then Cl III elastics. This finding possibly indicates that under thickness variation, Cl II forces are more potent than Class III because of less resistance to movement (see section on correlations below).

- Amount of displacement (*in absolute value*): The pattern of significance was similar to that of the degree of displacement along with similar interpretations. The Cl II elastic from the 1st molars had the greatest potential in producing displacement.

5.2.3. *Stiffness vs. thickness comparisons*

Keeping the same configuration of elastics constant, the models were tested independently under thickness and stiffness variation to examine which factor determined the creation of additional stresses on the TMJ complex and on the teeth. Two major findings emerged along with associated theories to explain them:

1. *Effect on the TMJ area; increase in stiffness was associated with an increase in stress level; increase in thickness did not change the stress levels.*

Theory 1: Modifications in thickness do not affect the outer surface of the condyle

This phenomenon relates directly to the geometry of the model. Whenever the thickness is changed, the modifications are applied towards the inside of the condyle rather than on the outside surface. Accordingly, whenever the cortical bone is thickened, it is at the expense of the inner trabecular bone. Since the disk and the glenoid fossa are in contact with the outer surface of the condyle, which is not modified, no increase of stress level is felt at the counterparts of the TMJ complex.

Theory 2: Modifications in thickness increase the stresses at the level of the teeth

The increase of cortical thickness increases cortical anchorage of the lower teeth. The mandibular teeth would then withstand greater stresses from the force transmitted by the elastics. Therefore, lesser effects and less stresses are transmitted on the TMJ.

1. Effect on the dental units: increase in stiffness was associated with increase in stress level; increase in thickness did not change the stress levels significantly.

The generated stress varies across the teeth depending on the initial inclination of the dental roots. When the cortical plate is in contact with the roots, stiffness variation of the cortical plate greatly influences the amount of stress when the loads of the elastics are applied. However, when the cortical plate is away from the roots of teeth, thickness changes do not necessarily translate into bringing the cortical plate into contact with the teeth, and hence the stresses are not varied.

This morphology may be related to the fact that the model was constructed on a CBCT from a single patient. It is plausible that variable topographies would yield different results when the variation in thickness (and stiffness) is drawn from multiple CBCT images representing living subjects. More advanced research is needed to elucidate this premise.

Clinically, the mandible is restrained by soft tissue, which includes muscles, ligaments and teguments. However, in Abaqus, the mandible is modeled as a free body, and connected solely at the level of the TMJ. Hence, as a result of the application of the elastics, the mandible as a whole was brought sagittally, therefore possibly contributing to an elevated total displacement of the crowns of the teeth. Thus, the displacements recorded on the mandibular crowns might correspond partly to jaw advancement, not only dental response to the elastics applied.

In this context, the response to Class III elastics might have reflected a closer representation of clinical reality, as the soft tissue restraints against the mandible are not as significant when the mandible is displaced posteriorly as anteriorly.

The comparison between the effects of stiffness and thickness was made to compute which variation has a larger effect on stress generation. While thickness of the cortical plate is easily measurable with a 3D scan, the stiffness may be determined from the density (and associated bone type) of the cortical plate. Hence, the practitioner may rate the bone type of a certain individual, most valuably in patients who present certain temporomandibular dysfunctions, yet in whom Cl II elastics are needed. In these patients, Cl II from the 1st molars might be preferable to Cl II from the 2nd molars. Also, temporary anchorage mechanics may be applied to enhance the anteroposterior dental relationship to decrease reliance on and the side effects (e.g. proclination of incisors) of Class II elastics.

5.2.4. Correlations

Correlations between stiffness and thickness variations and the facial components (condyle and dental units) were revealing. Stiffness and thickness correlated with condylar and dental components in both Cl II/6s and Cl II/7s groups. However, stiffness correlated only with the dental units of the Class III combination. These findings would suggest that condylar response to Class III is not affected by stiffness and thickness, and more likely by the topographical anatomy, just the mechanical effect of the elastics that have more direct bearing on the dental units and displacement under stiffness variation. On the contrary, Class II elastics, whether from first or second molars, appear to have a direct impact on the TMJ components. These results may reflect 1- the more sensitive response to the 1N force in Class II rather than Class III, which may require a heavier load for a similar response; or 2- simply the existing geometric relations, such as the posterior mandibular constraints, regardless of

stiffness or thickness. However, stiffness and thickness play a role in Class II elastics, possibly because with their configuration in a postero-anterior direction, more geometric leeway exists for the mandible to come forward than to move back (as is the case with Class III elastics).

Another important insight emerged from the correlations. In all elastics groups, the statistically significant correlations between stiffness and dental units were negative for the posterior teeth (molars), with less stress under greater stiffness. The same follows for displacement. In Class II groups where high correlations were found between the Von Mises stresses and stiffness on the TMJ components, these findings might suggest that the change of stress due to the variation of stiffness is mostly felt on the TMJ, whereas the opposite is applied on the PDL of the teeth.

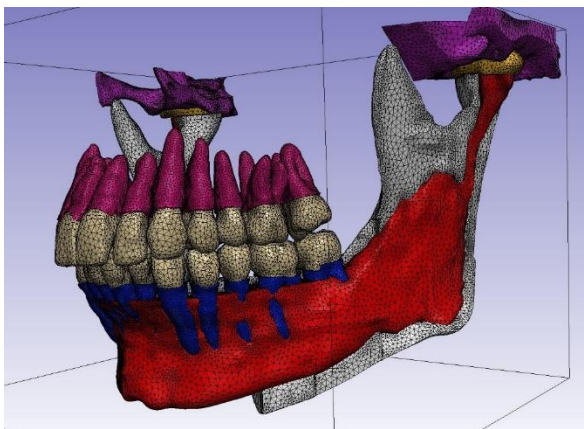


Fig 3.2.10. Legend in Material and Methods of this figure is summarized for the purpose of the pertinent discussion FE model showing the lingual cortical (white) and trabecular (red) layers. The buccal cortical plate was resected to illustrate the positions of mandibular teeth relative to the buccal cortical bone. Not all the mandibular teeth are well positioned in the trabecular bone. Note that some teeth (e.g. canine, premolar) have a cortical contact (cortical anchorage).

On the canine, however, a positive correlation exists with the change of stiffness, probably because initially the buccal surface of the canine is totally in contact with the buccal cortical plate (Fig. 5.3). A negative correlation in the apical portion of the central incisor, as in the molar regions, suggests that initial contact with the cortical plate responds different than the other areas of the tooth with the change of stiffness.

The same pattern of correlations was observed in all groups of elastics at the level of the molars, canines and incisors, while the directions of elastics and displacement were opposite. This finding indicates that tooth position within the alveolus is a determining factor in the response to force, dictated by the trabecular track and limited by the closeness of the teeth to the cortical bone.

Remarkably, higher correlations were noted with the buccal cortical plate, again reflecting the closer contact of the buccal cortical with the mandibular crowns compared with the lingual cortical. The finding also reflects the more buccal vector of force in response to elastics drawn from the buccal side of the teeth.

The general lack of correlation of the studied condylar and dental components with thickness variation may simply indicate that thickness has no additional bearing on the initial “shell” of cortical bone. It would be plausible that every time thickness varies, the new ‘geometry ‘of the model is not predictive of the level of Von Mises stresses generated by the intermaxillary forces. Under thickness variation, high negative correlations were observed for the displacement of the dental crowns in the CI II groups, again recalling the more sensitive response in Class II to the force of 1N, while Class III may require a greater load.

5.2.5. Applications of the different treatment modalities under stiffness and thickness variations

Within this comparison, the extracted results of the TMJ complex and the stresses and displacements reported at the dental units were compared between right and left sides, a comparison heretofore not conducted in FEA studies. The following implications emerged:

- ❖ Differences in crowding between right and left sides: *the greater the crowding, the less uniform is the transmission of the force between the different teeth.*
- ❖ Initial tooth position, inclination and torque relative to the underlying bony structures: *if the tooth is initially in contact with the cortical plate, any force to move the tooth would generate high resistance compared to a tooth well aligned in the alveolar bone.*
- ❖ Cortical and trabecular bone thickness in certain areas providing a greater cortical anchorage relative to other sites: *the alveolar width provides a greater path for better tooth movement; the narrower the alveolus, the narrower the trabecular thickness, thus a greater cortical thickness is present.*
- ❖ Differences in root size and shape: *the greater the root dimensions (width, height and thickness), the greater the resistance to displace the root; accordingly, a greater force may be needed to for tooth movement*
- ❖ Direction of the applied elastics: *in instances where the maxillary canine is misaligned, a less uniform line of force action is created. Any deviation of the direction of the elastics away from the antero-posterior horizontal line of action provides for a greater friction in the applied system, and lower displacement will be generated. For example, when the Cl II elastics were applied from the 2nd molars, the elastic had a greater horizontal line of action.*

The teeth respond differently to forces when comparing right and sides. Such a difference affected the responses at the TMJ components. For instance, when the teeth took most of the stress, less stress was transmitted on the TMJ components of the same side. This theory is further elaborated in other sections (below) of this chapter.

5.3. Comparison with other FEA studies evaluating condylar response to intermaxillary elastics

Several articles evaluated stresses around the TMJ area. Comisso et al (2015) examined the TMJ space was examined during the mastication cycle and their work could not be compared to the present study. Gupta et al., (2009), investigated the effect of functional appliance on the condyle by simulating advancement (5 mm) and opening (4mm) of the jaw.

The only study investigating interarch elastics during orthodontic therapy was conducted by Chinese authors and is available in their native language (Hu, Xiang, Li, Guo, & Wang, 2010). The authors simulated one side of the face comprising the TMJ, maxilla and mandible with the teeth in occlusion. They tested four types of interarch elastics (100 grams each): CI II and CI III elastics, both long (from the mandibular 1st molar to the maxillary canines) and short (from the mandibular 1st premolar to the maxillary canine). The long and short CI III configuration extended from the mandibular canine to the maxillary 1st molar and 1st premolar, respectively. Stresses and displacements were recorded only on the TMJ condyle and disk. Both configurations of CI II elastics behaved similarly with minor differences, the short CI II elastic producing lower stresses on the condyle and on the disk than the long elastic. The same pattern of results was reported with the CI III elastics, with lower stresses from the short than the long CI III elastic. This investigation deserves recognition within the FEA literature, but the present study extended the envelope of inquiry and understanding farther.

1. In the current study, the jaw anatomy is represented bilaterally and with the interarch elastics were applied accordingly, thus the findings reflected bilateral responses.

2. A more complete examination of the TMJ region is provided, included the glenoid fossa of the temporal bone, and all the parts of the TMJ complex are segmented into three parts for a closer probing (condyle – disk – glenoid fossa of temporal bone)
3. The mandibular teeth are studied in the present investigation, encompassing both the stresses at the teeth and displacement. Accordingly, practical clinical implications may be drawn from the results.
4. In the study by Hu et al, the short interarch elastics are rarely used and conclusions about the responses they generate not necessarily consistent with clinical applicability. Also, no comparison was carried out in the stress patterns if the CI II vs. the CI III elastics. In this comparison, practitioners may better interpret which type of elastic produces the highest stress on the TMJ when applied.
5. On a strictly methodological ground, Hu et al's study lacks explanation of the modeling performed, such as not reporting relevant information about bone properties, i.e. stiffness, or information of the boundary conditions applied during the modeling process, or other settings related to the engineering considerations of the model.

Yet, as the only FEA study available on interarch elastics, it reflects how demanding this field of investigation is, particularly when the entire anatomy was reproduced as in our undertaking. Literally dozens of hours are invested in creating the model. As such, our study stands out for its unique model and expanded analyses.

5.4. Clinical implications

5.4.1. From the comparisons between right and left findings

Upon the application of any load (elastics), components of the model would respond differently, depending on several factors, such as dimensions of roots of teeth

and other geometrical differences inherent to each site. In a setting where stress produces displacement: the greater the stresses on the teeth, the greater the corresponding displacement (within the conditions of the present research). Moreover, it appears that the more the pressure on the condyle and disk, the less the pressure on the teeth, and therefore the less the displacement.

Such conclusions can be best explained in a scenario where the mandibular molars are in contact with buccal cortical plate. Upon the application of CI II elastics, the mandibular molars would hardly displace because of the “cortical anchorage.” As a result, the force is transmitted on the condyle and the disk generating a high level of stress. To reduce this effect on the condyle, the roots of the mandibular molars should be oriented in the trabecular bone of the mandible before applying the mesialising force of the elastic- if the goal is to move the dentition rather than using it for anchorage to move the maxillary teeth.

A hypothetical example to reduce the stress on the TMJ complex would involve corticotomies to reduce the resistance of the molars. Hence, pressure generated by elastics in this scenario is better oriented to produce tooth movement rather than generating pressure on the condyle. On the other hand, to reduce TMJ stresses when the mandibular arch is used as anchorage, light forces should be used, or temporary anchorage devices (mini-implants in the maxilla) considered.

All such implications are advanced with the knowledge that clinical research in conjunction with FE analysis should establish the threshold at which condylar pressure translates to clinical dysfunction (pain, clicking) in the individual patient. In the stiffness variation group, differences between groups were more statistically significant, showing a more accurate difference in the TMJ responses to elastic forces (Fig 5.1).

Regarding the thickness variations, minor differences were present in the distribution of stresses on the temporal bone compared with the stress distribution under stiffness variation (Fig. 5.3). However, the same interpretation of stress distribution applies as elaborated in the stiffness variation group.



Fig 5.1. The highest stresses in the stiffness variation group on the TMJ (comparison of both sides together) are illustrated graphically. **Red:** Left side – **Blue:** Right side. Interpretation of the results is displayed in arrow graphics below.

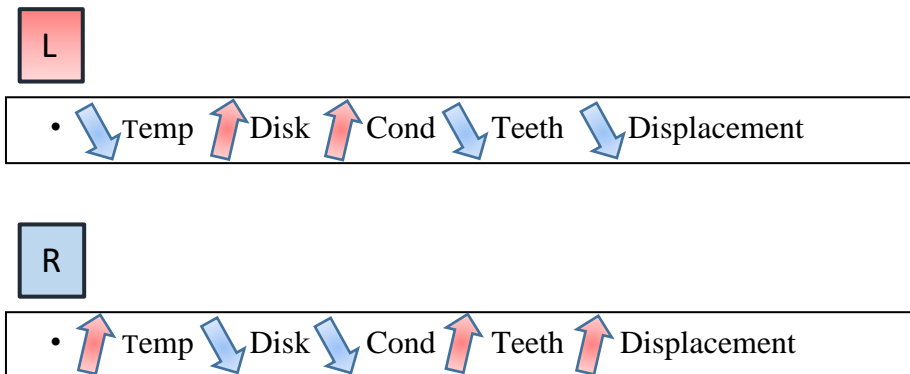


Fig 5.2. The highest stresses in the thickness variation group on the TMJ (comparison of both sides together) are illustrated graphically. **Red:** Left side – **Blue:** Right side

5.4.2. From the comparisons between stiffness and thickness

As mentioned earlier, changes in thickness did not alter significantly the stresses at the TMJ level; however, change in stiffness created on average a greater stress at the level of TMJ components. Less conclusive findings can be made at the dental level. The key element in determining whether stiffness or thickness produces more stress might be the contact between the teeth and the cortical plate. If the teeth are already away from the cortical bone, stiffness variation of the cortical plate would not vary the stresses around those teeth (e.g. the mandibular 2nd molars, as shown in Fig. 5.1). However, on teeth with PDL already in contact with the cortical, such as the mandibular canines, the stiffness changes produced, on average, greater stress augmentation as compared with thickness changes, especially when the CI III elastic was applied.

5.4.3. From the comparisons between the applied elastics

As detailed in section 5.4.1., CI II elastics act differently on the dental units and on the TMJ complex, the most consistent pattern of significance drawn from the comparisons in the stiffness groups. The CI II elastics delivered from the mandibular 1st molars produced a lower stress on the teeth and on the TMJ components in general, hence less dental displacements. The elastics delivered from the 2nd molar produced greater dental and TMJ stress possibly because of a more effective anteroposterior component of action. In a clinical situation where a patient has a history of TM dysfunction, it may be advisable to move teeth with mini-implants rather than interarch elastics.

Among all elastics, those with the highest potential of stress on the teeth produced the highest displacement. CI III elastics generated the highest initial

displacement in our study possibly because of the posterior binding of the condyle across the posterior wall of the glenoid fossa.

5.4.4. From the analysis of correlations of the various parts of the model

The highest correlations were found between models run under stiffness variations. Since the variations do not change the geometry of the model, the different simulations of the cadavers resemble highly making the comparisons very similar. Therefore, a high correlation exists among all the units of the models. Thus, whenever the models are compared together, patterns where stresses are increased or decreased behave similarly almost with the same pattern of change.

When comparing the different models run under the thickness variation, less highly-significant correlations were found. The advantage of having the thickness variation was that the true evident patterns were maintained highly significant. On the other hand, the stiffness variation revealed all units of the model correlating highly with each other.

Under thickness variation, the highest significant stresses were between the 2nd molars, the canines, and the condyle when comparing the teeth with the TMJ. As the elastics is applied, all teeth responded with a moderate to high correlation when compared to each other. Likewise, displacements of the teeth were moderately to highly correlated together, suggesting a positive transmission of the force antero-posteriorly.

5.5. Limitations and research considerations

5.5.1. FE modeling

Accuracy in FEA requires the precise replication of the clinical scenario as much as possible. The most realistic findings are computed in settings considering all the

elements found in a clinical setting. In the present study, one of the major limitations is the lack of modeling of the soft tissues. Muscular attachments on the mandibular ramus, as well as capsular surrounding of the glenoid fossa, and ligaments connecting the mandible, are among others, factors that contribute to the outcome in the clinical scenario upon application of interarch elastics.

Another limitation of FEA is that it provides a real-time exploration of the initial occurrences of stresses only. In all biologic systems, in particular orthodontics, tissues respond differently to initial stresses. Bone remodeling and functional adaptation occur, that are hard to simulate, thus reducing the tenets of the clinical scenario. Thus, the results may indicate general trends rather than detailed outcome.

To overcome some of these limitations, time-dependent FEA would better illustrate clinical scenarios, considering the rate of changes taking place in the biologic model such as bone remodeling. Time-dependent FEA offers a closer look at the changes of stresses from a dynamic perspective, allowing to elucidate how the pattern of stresses alters with displacement of a member under a certain force.

Within the variations of thickness, no major pattern of differences was noticeable. Hence a greater, it may seem valid that a greater number of individual variation in the thickness group might better disclose underlying responses.

5.5.2. Data collection

Two different variables were collected in this study: Von Mises stresses and displacements in the antero-posterior direction. Von Mises stresses were gathered in the TMJ complex and at the level of the periodontal ligament at 6 zones facing the roots of all mandibular teeth. The displacements were measured at the centers of the crowns of all the mandibular teeth at the occlusal level.

Other FEA studies included different sites of stress assessment and displacements of the model investigated. In a study evaluating mandibular molar protraction, the displacement was measured at three nodes—the tip of the mesiolingual cusp, the tip of the mesiobuccal cusp, and the apex of the distal root (Nihara et al., 2015).

Other studies investigating the mandibular condyle (Shrivastava et al., 2015) not only divided the condyle into 3 areas antero-posteriorly, but also mesio-distally (in the inside-outside direction). Since their investigation was carried out only on one model, no statistical computation was available to determine if the stresses differed significantly between the zones. In our study, as the movements were only in the antero-posterior direction, the areas of interest were divided in the antero-posterior direction only, and the inclusion of individual variation allowed for the description of central tendencies and standard deviations.

Upon force application, Von Mises stresses were recorded as a result of the applied forces at both the anterior and posterior portions of all members of the models. It may be surprising to detect pressure at the posterior side of the disk once the CI II elastics for instance were applied. However, tensile stresses may have been at play to elongate the parts in question.

Regarding dental displacements at the level of the crowns, one degree of freedom was permitted in the antero-posterior direction. However, the orientation of all our models in the stress solver program was such, that the displacement in the mesialising direction was negative, and positive in the distalizing direction. Therefore, the CI III elastics produced displacements displayed in positive value, whereas the CI II elastics produced displacements with a negative value.

In comparison with other studies that have used intermaxillary elastics, no studies had collected and computed results as extensively as in the present study. In one study, the investigators had used one type of CI II elastics delivered from the mandibular 2nd molars (Chang, Shin, & Baek, 2004) to simulate the MEAW (multi-loop edgewise appliance) system, limiting their results to a comparison of the MEAW archwire vs. the ideal archwire and the respective displacements. They highlighted the increased control of the dental units with the MEAW. Compared to the displacements they reported, our average displacements were higher, possibly because of the applied (simulated) archwire system.

The investigation of interarch elastics and their effects on condylar stress found in the literature (Hu et al., 2010) were in Chinese and difficult to interpret, however short of the extensive recordings we report, an without examination of the dental units. In a study investigating the activator (Ulusoy & Darendeliler, 2008), stresses reported at the coronoid process and at the TMJ were similar to stresses reported in our study in the condylar region in response to CI II elastics. Similarly, higher degrees of stresses were found at the neck of the condyle and the surrounding regions (i.e. neck of the coronoid).

5.5.3. Static versus dynamic loading

The findings in this study have been generated under specific research-related circumstances: 1. tests were under static conditions; 2- the mouth was in a closed position, at the same time reflecting the CBCT initial record and assuming that the patient held the jaws together while wearing the elastics. While this set up reflects a certain amount of the time of elastic wear when the mouth is close (usually in a small portion of the day, and likely with heavier forces), the experimental set-up did not

include assumptions of open mouth conditions while the elastics are worn (e.g. during verbal communication or even “rest” position).

In a dynamic state, the mandible displaces, changing the stretch of the elastics, and a different force system would be produced with less horizontal and more vertical components of the force. Consequently, different stress and displacement would be generated on all components of the model including the TMJ. Therefore, the results in a static position cannot be generalizable to a dynamic condition of the mouth.

5.5.4. *Considerations within model construction*

Given the already wide scope of data generation related to studying the effects of inter-arch elastics on the TMJ and mandibular teeth, we did not explore the response of the maxillary teeth and the interaction between them and the mandibular findings. Moreover, because the patient’s CBCT reflected an asymmetric occlusion, whereby the left side was in a full Cl II molar occlusion and the right side was in a Cl I molar occlusion, the occlusion with the maxillary arch was not considered in Abaqus. Therefore, in regard to occlusion, both right and left sides were studied regardless of their intercuspation with the antagonist dentition.

In addition, the groups of elastics compared were attached to different maxillary and/or mandibular teeth. During the planning of the application of the Cl III elastics, the set of nodes bearing the distalising load was oriented towards the maxillary 1st molars. Unlike the maxillary 2nd molars, the maxillary 1st molars are more widely used to anchor Cl III elastics. While the difference in “stretch” is considered from a clinical perspective, as programmed in Abaqus, the value of the force of the elastic was set constant at 150 grams, equivalent to 1.5 Newtons, regardless of the antero-posterior

location of the anchoring teeth. The reported differences would relate to the angulation of the Class II elastics.

We only considered a CI III elastic from mandibular canine to maxillary 1st molars. Given the significant difference in some comparisons of the CI II elastics, it is conceivable that a CI III elastic anchored on the maxillary 2nd molars would yield a difference with that stretched to the first molars. Such a comparison between CI III elastics warrants additional research.

5.6. Future research

- Time-dependent FEA is needed to develop a new perspective to the adaptation process after load application. Such analysis shall provide a dynamic assessment of actual changes in dental position that would allow for more precise projection of tooth movement, thus more practical treatment planning and pursuant reduction of side effects. For instance, time-dependent FE analysis may show that with longer periods of elastics application, the mandibular dentition surpasses its alveolar perimeter possibly leading to “cortical anchorage” and variable stresses on the condyle and its counter parts.

- Within the same context of the present study, the inclusion of the maxillary dentition would disclose reactions on the maxillary dentition in parallel with the mandibular dentition. including changes in the occlusal plane, bite depth, and occlusal “prematurities.”

- The current study related the effects of elastics in a healthy individual, with normodivergence and a skeletal CI I jaw-relationship. Ideally, the used elastics should be applied in subjects with corresponding Class II and Class III malocclusions.

CHAPTER 6

CONCLUSIONS

I. Contribution of the study

1. This study was the first investigation of interarch elastics on mandibular teeth, applied on the entire mandibular arch and employing loading scenarios simulating the clinical settings of Class II and Class III malocclusions. This study also introduced a comparison between Class II elastics delivered from the mandibular 1st molars, 2nd molars, and Class III elastics from the mandibular canines.
2. As a finite element study, it is the first to have evaluated simultaneously Von Mises stress on TMJ and teeth as well as displacements on teeth, all in a unique investigation of individual variation drawn from the material properties of human cadavers.

II. Key conclusions on the impact of anatomic factors

1. Contact of teeth with cortical bone

A key determining factor in affecting initial stress and displacement was the original contact of teeth with cortical bone. Additional alterations in bone stiffness did not differ across initial movements and Von Mises stresses as much as the variations of thickness. Therefore, a determining factor of the response to force is the presence of the compact bone in the immediate vicinity of the teeth withstanding the orthodontic force. This result was further demonstrated by the

negative correlations between stiffness and stresses on mandibular molars under all interarch elastics (Class II/6s, Class II/7s and Class III).

2. Asymmetry

Differences were observed between right and left sides at all levels in the present model. The asymmetry may be related to the different alignment of right and left incisors and/or inherent minor asymmetries in the mandibular structure of the patient whose CBCT was used.

III. Key conclusions on the effect of material properties

1. High impact of stiffness

Stiffness induced higher stresses and more variability on condylar and dental response. Under stiffness variation, CI III elastics demonstrated the highest stresses on the TMJ and mandibular teeth, while CI II/6s resulted in the weakest stresses on these components. The CI II/7s demonstrated higher displacements compared to the CI II/6s, although not statistically significant ($p=0.076$). Under thickness variations, CI II/7s showed higher stresses, with a greater potential of tooth displacement compared to CI II/6s. The difference was statistically significant, likely due to the more horizontal line of action and reduced vertical component of the force.

a. High correlations in the stiffness variations in the CI II mechanics reflected a proportional relationship with the TMJ component but inversely related on the dental components posteriorly. This finding suggests that the teeth in contact with the cortical bone behave in an opposite direction to stiffness changes as compared with the TMJ.

b. Minor significant correlations were found between stiffness and Von Mises stresses and displacements than between these components and thickness variation.

2. Role of mandibular geometry

The correlations between stiffness and TMJ were high in the Class II groups, and not in the Class III group, unlike the high correlations between stiffness and dental units that were significant across elastics groups. These findings suggest that geometry of the model, more than stiffness or thickness apparently determines condylar response.

IV. Clinical inferences

1. Determinant factors in affecting tooth movement were mostly related to the anatomy of the models. Tooth dimension and orientation, alveolar width, and contact with the cortical bone are essential elements in determining the stress system in a model. Hence, it may be required to align the teeth and adjust their root torque in the alveolar bone. Thereafter, elastics can be applied to favor dental movement.

2. Both Class II and Class III elastics had an impact on the various regions of the condylar components, Class III providing more stress levels at all TMJ levels in the stiffness variations. The effect of the elastics on dental units reflected the expectations from clinical practice: Cl III impacted the mandibular canines and incisors, Cl II targeted the molars and incisors.

V. Future research

Future prospects would include gathering clinical data in conjunction with FE analysis results and force dissipation in a time-dependent model. The results should allow the clinician to accurately plan stress generation on various regions during orthodontic therapy, actually controlling the rate of orthodontic tooth movement under a forecasted course of treatment.

REFERENCES

- ACKERMAN, J. L. & PROFFIT, W. R. 1969. The characteristics of malocclusion: a modern approach to classification and diagnosis. *Am J Orthod*, 56, 443-54.
- AL-SALEH, M. A., ALSUFYANI, N., FLORES-MIR, C., NEBBE, B. & MAJOR, P. W. 2015. Changes in temporomandibular joint morphology in class II patients treated with fixed mandibular repositioning and evaluated through 3D imaging: a systematic review. *Orthod Craniofac Res*, 18, 185-201.
- AMERICAN ASSOCIATION OF ORTHODONTISTS 2013. Your Child's First Orthodontic Check-Up.
- ANGLE, E. H. 1899. Classification of malocclusion. *Dental Cosmos*, 245-264, 350-357.
- ANTUNES ORTEGA, A. P., DH. ROCHA RODRIQUES, LL. GUIMARÃES, AS. 2016. Relationship Between Orthodontics and Temporomandibular Disorders: A Prospective Study. *Journal of Oral & Facial Pain and Headache*, 134-8.
- ASBELL, M. B. 1990. A brief history of orthodontics. *Am J Orthod Dentofacial Orthop*, 98, 206-13.
- ASHMAN, R. B., COWIN, S. C., VAN BUSKIRK, W. C., & RICE, J. C. (1984). A continuous wave technique for the measurement of the elastic properties of cortical bone. *J Biomech*, 17(5), 349-361.
- ASHMAN, R. B., & VAN BUSKIRK, W. C. (1987). The elastic properties of a human mandible. *Adv Dent Res*, 1(1), 64-67. doi:10.1177/08959374870010011401
- ASMUSSEN, E. & PEUTZFELDT, A. 2008. Class I and Class II restorations of resin composite: an FE analysis of the influence of modulus of elasticity on stresses generated by occlusal loading. *Dent Mater*, 24, 600-5.
- BEEK, M., KOOLSTRA, J. H., VAN RUIJVEN, L. J. & VAN EIJDEN, T. M. 2000. Three-dimensional finite element analysis of the human temporomandibular joint disC. *J Biomech*, 33, 307-16.
- BEEK, M. K., J. H. VAN RUIJVEN, L. J. VAN EIJDEN, T. M. 2001. Three-dimensional finite element analysis of the cartilaginous structures in the human temporomandibular joint. *J Dent Res*, 80, 1913-8.
- BOWERS, G. M. (1963). A study of the width of the attached gingiva. *Journal of Periodontology*(34), 201-209.
- CARLTON, K. L., & NANDA, R. S. (2002). Prospective study of posttreatment changes in the temporomandibular joint. *Am J Orthod Dentofacial Orthop*, 122(5), 486-490. doi:10.1067/mod.2002.128863
- CARTER, D. R., & SPENGLER, D. M. (1978). Mechanical properties and composition of cortical bone. *Clin Orthop Relat Res*(135), 192-217.
- CATTANEO, P. M. D., M. MELSEN, B. 2005. The finite element method: a tool to study orthodontic tooth movement. *J Dent Res*, 84, 428-33.
- CHANG, Y. I., SHIN, S. J., & BAEK, S. H. (2004). Three-dimensional finite element analysis in distal en masse movement of the maxillary dentition with the multiloop edgewise archwire. *Eur J Orthod*, 26(3), 339-345.
- CHAVAN, S. J., BHAD, W. A. & DOSHI, U. H. 2014. Comparison of temporomandibular joint changes in Twin Block and Bionator appliance therapy: a magnetic resonance imaging study. *Prog Orthod*, 15, 57.
- CHEN, J., AKYUZ, U., XU, L., & PIDAPARTI, R. M. (1998). Stress analysis of the human temporomandibular joint. *Med Eng Phys*, 20(8), 565-572.

- CHINTAKANON, K., SAMPSON, W., WILKINSON, T. & TOWNSEND, G. 2000. A prospective study of Twin-block appliance therapy assessed by magnetic resonance imaging. *Am J Orthod Dentofacial Orthop*, 118, 494-504.
- COMMISSO, M. S., MARTINEZ-REINA, J., OJEDA, J. & MAYO, J. 2015. Finite element analysis of the human mastication cycle. *J Mech Behav Biomed Mater*, 41, 23-35.
- DAHAN, J. 1964. [Treatment of Angle's Class II, Division I with the Andresen-Hauepl Activator Modified by Eschler]. *Orthod Fr*, 35, 265-73.
- DECHOW, P. C., NAIL, G. A., SCHWARTZ-DABNEY, C. L., & ASHMAN, R. B. (1993). Elastic properties of human supraorbital and mandibular bone. *Am J Phys Anthropol*, 90(3), 291-306. doi:10.1002/ajpa.1330900304
- DE CLERCK, H. N., T. DE PAULA, L. K. CEVIDANES, L. 2012. Three-dimensional assessment of mandibular and glenoid fossa changes after bone-anchored Class III intermaxillary traction. *Am J Orthod Dentofacial Orthop*, 142, 25-31.
- DOS SANTOS, M. B., DA SILVA NETO, J. P., CONSANI, R. L. & MESQUITA, M. F. 2011. Three-dimensional finite element analysis of stress distribution in peri-implant bone with relined dentures and different heights of healing caps. *J Oral Rehabil*, 38, 691-6.
- EL-ZAWAHRY, M. M., EL-RAGI, A. A., EL-ANWAR, M. I. & IBRAHEEM, E. M. 2015. The Biomechanical Effect of Different Denture Base Materials on the Articular Disc in Complete Denture Wearers: A Finite Element Analysis. *Open Access Maced J Med Sci*, 3, 455-61.
- FRANCO, A. A., YAMASHITA, H. K., LEDERMAN, H. M., CEVIDANES, L. H., PROFFIT, W. R. & VIGORITO, J. W. 2002. Frankel appliance therapy and the temporomandibular disc: a prospective magnetic resonance imaging study. *Am J Orthod Dentofacial Orthop*, 121, 447-57.
- FRICTON, J., LOOK, J. O., WRIGHT, E., ALENCAR, F. G., JR., CHEN, H., LANG, M., OUYANG, W. & VELLY, A. M. 2010. Systematic review and meta-analysis of randomized controlled trials evaluating intraoral orthopedic appliances for temporomandibular disorders. *J Orofac Pain*, 24, 237-54.
- GONZÁLEZ, F. P., TK. DALSTRA, M. HERLIN, T. VERNA, C. 2015. 3D Evaluation of mandibular skeletal changes in juvenile Arthritis patients treated with a distraction splint - a retrospective follow-up study. *American Journal of Orthodontics and Dentofacial Orthopedics*.
- GREEN, J. 2014. The origins and evolution of fixed orthodontic appliances. *Dental Nursing*, 10.
- GUNER, D. D., OZTURK, Y. & SAYMAN, H. B. 2003. Evaluation of the effects of functional orthopaedic treatment on temporomandibular joints with single-photon emission computerized tomography. *Eur J Orthod*, 25, 9-12.
- GUPTA, A., KOHLI, V. S., HAZAREY, P. V., KHARBANDA, O. P. & GUNJAL, A. 2009. Stress distribution in the temporomandibular joint after mandibular protraction: a 3-dimensional finite element method study. Part 1. *Am J Orthod Dentofacial Orthop*, 135, 737-48.
- HARVOLD, E. P., TOMER, B. S., VARGERVIK, K. & CHIERICI, G. 1981. Primate experiments on oral respiration. *Am J Orthod*, 79, 359-72.
- HOHMANN, A., KOBER, C., YOUNG, P., DOROW, C., GEIGER, M., BORYOR, A., ... SANDER, F. G. (2011). Influence of different modeling strategies for the

- periodontal ligament on finite element simulation results. *Am J Orthod Dentofacial Orthop*, 139(6), 775-783. doi:10.1016/j.ajodo.2009.11.014
- HU, L., ZHAO, Z., SONG, J., FAN, Y., JIANG, W. & CHEN, J. 2001. [The influences of the stress distribution on the condylar cartilage surface by Herbst appliance under various bite reconstruction--a three dimensional finite element analysis]. *Hua Xi Kou Qiang Yi Xue Za Zhi*, 19, 46-8.
- HU, M., XIANG, Y. N., LI, H., GUO, K. F., & WANG, F. (2010). [The stress distribution of the temporomandibular joint under four types of inter-arch elastics--a three dimensional finite element model analysis]. *Hua Xi Kou Qiang Yi Xue Za Zhi*, 28(2), 145-148.
- ICHIM, I., SCHMIDLIN, P. R., KIESER, J. A. & SWAIN, M. V. 2007A. Mechanical evaluation of cervical glass-ionomer restorations: 3D finite element study. *J Dent*, 35, 28-35.
- ICHIM, I. P., SCHMIDLIN, P. R., LI, Q., KIESER, J. A. & SWAIN, M. V. 2007B. Restoration of non-carious cervical lesions Part II. Restorative material selection to minimise fracture. *Dent Mater*, 23, 1562-9.
- IVORRA-CARBONELL, L., MONTIEL-COMPANY, J. M., ALMERICH-SILLA, J. M., PAREDES-GALLARDO, V. & BELLOT-ARCIS, C. 2016. Impact of functional mandibular advancement appliances on the temporomandibular joint - a systematic review. *Med Oral Patol Oral Cir Bucal*, 21, e565-72.
- IWASAKI, L. R., HAACK, J. E., NICKEL, J. C., & MORTON, J. (2000). Human tooth movement in response to continuous stress of low magnitude. *Am J Orthod Dentofacial Orthop*, 117(2), 175-183.
- KATADA, H., ARAKAWA, T., ICHIMURA, K., SUEISHI, K. & SAMESHIMA, G. T. 2009. Stress distribution in mandible and temporomandibular joint by mandibular distraction: a 3-dimensional finite-element analysis. *Bull Tokyo Dent Coll*, 50, 161-8.
- KAYUMI, S., TAKAYAMA, Y., YOKOYAMA, A. & UEDA, N. 2015. Effect of bite force in occlusal adjustment of dental implants on the distribution of occlusal pressure: comparison among three bite forces in occlusal adjustment. *Int J Implant Dent*, 1, 14.
- KINZINGER, G., FRYE, L. & DIEDRICH, P. 2009. Class II treatment in adults: comparing camouflage orthodontics, dentofacial orthopedics and orthognathic surgery--a cephalometric study to evaluate various therapeutic effects. *J Orofac Orthop*, 70, 63-91.
- LECORNU, M., CEVIDANES, L. H., ZHU, H., WU, C. D., LARSON, B. & NGUYEN, T. 2013. Three-dimensional treatment outcomes in Class II patients treated with the Herbst appliance: a pilot study. *Am J Orthod Dentofacial Orthop*, 144, 818-30.
- LUTHER, F. 1998. Orthodontics and the temporomandibular joint: where are we now? Part 1. Orthodontic treatment and temporomandibular disorders. *Angle Orthod*, 68, 295-304.
- LUTHER, F., LAYTON, S. & MCDONALD, F. 2010. Orthodontics for treating temporomandibular joint (TMJ) disorders. *Cochrane Database Syst Rev*, CD006541.
- MARUO, I. T., MARUO, H., SAGA, A. Y., DE OLIVEIRA, D. D., ARGENTA, M. A. & TANAKA, O. M. 2016. Tridimensional finite element analysis of teeth movement induced by different headgear forces. *Prog Orthod*, 17, 18.

- MCNAMARA, J. A., JR. 1973. Neuromuscular and skeletal adaptations to altered function in the orofacial region. *Am J Orthod*, 64, 578-606.
- MCNAMARA, J. A., JR., SELIGMAN, D. A. & OKESON, J. P. 1995. Occlusion, Orthodontic treatment, and temporomandibular disorders: a review. *J Orofac Pain*, 9, 73-90.
- MEYER, R. A. 1990. The Temporomandibular Joint Examination. In: WALKER, H. K., HALL, W. D. & HURST, J. W. (eds.) *Clinical Methods: The History, Physical, and Laboratory Examinations*. 3rd ed. Boston.
- MIDDLETON, J., JONES, M., & WILSON, A. (1996). The role of the periodontal ligament in bone modeling: the initial development of a time-dependent finite element model. *Am J Orthod Dentofacial Orthop*, 109(2), 155-162.
- MOSS, M. L. & SALENTIJN, L. 1969. The primary role of functional matrices in facial growth. *Am J Orthod*, 55, 566-77.
- NARRA, N., VALASEK, J., HANNULA, M., MARCIAN, P., SANDOR, G. K., HYTTINEN, J. & WOLFF, J. 2014. Finite element analysis of customized reconstruction plates for mandibular continuity defect therapy. *J Biomech*, 47, 264-8.
- NIHARA, J., GIELO-PERCZAK, K., CARDINAL, L., SAITO, I., NANDA, R. & URIBE, F. 2015. Finite element analysis of mandibular molar protraction mechanics using miniscrews. *Eur J Orthod*, 37, 95-100.
- NIMERI, G., KAU, C. H., ABOU-KHEIR, N. S. & CORONA, R. 2013. Acceleration of tooth movement during orthodontic treatment--a frontier in orthodontics. *Prog Orthod*, 14, 42.
- O'REILLY, M. T., RINCHUSE, D. J. & CLOSE, J. 1993. Class II elastics and extractions and temporomandibular disorders: a longitudinal prospective study. *Am J Orthod Dentofacial Orthop*, 103, 459-63.
- OLIVEIRA, P. G., TAVARES, R. R. & FREITAS, J. C. 2013. Assessment of motivation, expectations and satisfaction of adult patients submitted to orthodontic treatment. *Dental Press J Orthod*, 18, 81-7.
- OP HEIJ, D. G., OPDEBEECK, H., VAN STEENBERGHE, D. & QUIRYNEN, M. 2003. Age as compromising factor for implant insertion. *Periodontol 2000*, 33, 172-84.
- PANCHERZ, H. & MICHAILEDIOU, C. 2004. Temporomandibular joint growth changes in hyperdivergent and hypodivergent Herbst subjects. A long-term roentgenographic cephalometric study. *Am J Orthod Dentofacial Orthop*, 126, 153-61; quiz 254-5.
- PROFFIT W. R, S. D. M., FIELDS H. W., 2013. *Contemporary Orthodontics*, Missouri USA, Elsevier Mosby.
- REES, J. S., & JACOBSEN, P. H. (1997). Elastic modulus of the periodontal ligament. *Biomaterials*, 18(14), 995-999.
- RUDOLPH, D. J., WILLES, P. M. G. & SAMESHIMA, G. T. 2001. A finite element model of apical force distribution from orthodontic tooth movement. *Angle Orthod*, 71, 127-31.
- SANTOS, L. S., ROSSI, A. C., FREIRE, A. R., MATOSO, R. I., CARIA, P. H. & PRADO, F. B. 2015. Finite-element analysis of 3 situations of trauma in the human edentulous mandible. *J Oral Maxillofac Surg*, 73, 683-91.

- SCHWARTZ-DABNEY, C. L., & DECHOW, P. C. (2003). Variations in cortical material properties throughout the human dentate mandible. *Am J Phys Anthropol*, 120(3), 252-277. doi:10.1002/ajpa.10121
- SHRIVASTAVA, A., HAZAREY, P. V., KHARBANDA, O. P. & GUPTA, A. 2015. Stress distribution in the temporomandibular joint after mandibular protraction: a three-dimensional finite element study. *Angle Orthod*, 85, 196-205.
- STAHL, F., BACCETTI, T., FRANCHI, L. & MCNAMARA, J. A., JR. 2008. Longitudinal growth changes in untreated subjects with Class II Division 1 malocclusion. *Am J Orthod Dentofacial Orthop*, 134, 125-37.
- STRAIT, D. S., WANG, Q., DECHOW, P. C., ROSS, C. F., RICHMOND, B. G., SPENCER, M. A., & PATEL, B. A. (2005). Modeling elastic properties in finite-element analysis: how much precision is needed to produce an accurate model? *Anat Rec A Discov Mol Cell Evol Biol*, 283(2), 275-287. doi:10.1002/ar.A.20172
- TANAKA, E., DEL POZO, R., TANAKA, M., ASAI, D., HIROSE, M., IWABE, T., & TANNE, K. (2004). Three-dimensional finite element analysis of human temporomandibular joint with and without disc displacement during jaw opening. *Med Eng Phys*, 26(6), 503-511. doi:10.1016/j.medengphy.2004.03.001
- TANAKA, E., RODRIGO, D. P., MIYAWAKI, Y., LEE, K., YAMAGUCHI, K., & TANNE, K. (2000). Stress distribution in the temporomandibular joint affected by anterior disc displacement: a three-dimensional analytic approach with the finite-element method. *J Oral Rehabil*, 27(9), 754-759.
- TANAKA, E., SASAKI, A., TAHMINA, K., YAMAGUCHI, K., MORI, Y., & TANNE, K. (2001). Mechanical properties of human articular disk and its influence on TMJ loading studied with the finite element method. *J Oral Rehabil*, 28(3), 273-279.
- TANNE, K., LU, Y. C., TANAKA, E. & SAKUDA, M. 1993. Biomechanical changes of the mandible from orthopaedic chin cup force studied in a three-dimensional finite element model. *Eur J Orthod*, 15, 527-33.
- TANNE, K., TANAKA, E. & SAKUDA, M. 1996. Stress distribution in the temporomandibular joint produced by orthopedic chincup forces applied in varying directions: a three-dimensional analytic approach with the finite element method. *Am J Orthod Dentofacial Orthop*, 110, 502-7.
- THOMAS M. GRABER, R. L. V., JR. 2000. *Orthodontics - Current Principles and Techniques*, St. Louis, Missouri Mosby InC.
- TWEED, C. H. 1932. Reports of Cases Treated with the Edgewise Arch Mechanism. *The Angle Orthodontist*.
- ULUSOY, C., & DARENDELILER, N. (2008). Effects of Class II activator and Class II activator high-pull headgear combination on the mandible: a 3-dimensional finite element stress analysis study. *Am J Orthod Dentofacial Orthop*, 133(4), 490 e499-415. doi:10.1016/j.ajodo.2007.10.032
- VINOD KRISHNAN, Z. E. D. 2012. *Integrated Clinical Orthodontics*, United Kingdom, Blackwell Publishing Ltd.
- WAHL, N. 2005. Orthodontics in 3 millennia. Chapter 1: Antiquity to the mid-19th century. *Am J Orthod Dentofacial Orthop*, 127, 255-9.
- WANG, W., ZENG, X. L., ZHANG, C. F. & YANG, Y. Q. 2012. Malocclusions in Xia Dynasty in China. *Chin Med J (Engl)*, 125, 119-22.

- XIE, F., YANG, L., GUO, L., WANG, Z. J. & DAI, G. 2009. A study on construction three-dimensional nonlinear finite element model and stress distribution analysis of anterior cruciate ligament. *J Biomech Eng*, 131, 121007.
- YANG, C., WANG, C., DENG, F. & FAN, Y. 2015. Biomechanical effects of corticotomy approaches on dentoalveolar structures during canine retraction: A 3-dimensional finite element analysis. *Am J Orthod Dentofacial Orthop*, 148, 457-65.
- YOSHIDA, N., KOGA, Y., PENG, C. L., TANAKA, E., & KOBAYASHI, K. (2001). In vivo measurement of the elastic modulus of the human periodontal ligament. *Med Eng Phys*, 23(8), 567-572.
- ZHANG, M. O., T. CHEN, Y. LV, X. WU, S. SONG, H. ZHAO, R. WANG, Y. 2009. Effects of condylar elastic properties to temporomandibular joint stress. *J Biomed Biotechnol*, 2009, 509848.
- ZURFLUH, M. A., KLOUKOS, D., PATCAS, R. & ELIADES, T. 2015. Effect of chin-cup treatment on the temporomandibular joint: a systematic review. *Eur J Orthod*, 37, 314-24.

APPENDIX 1

Results

Table 4.2.1. Von Mises stresses (MPa) on the TMJ complex under stiffness variations in CI II/7s group

Right Side						Left Side					
Region	Area	Mean	SD	Min	Max	Region	Area	Mean	SD	Min	Max
Cond	Anterior	0.1478	0.0043	0.1403	0.1556	Cond	Anterior	0.1569	0.0019	0.1534	0.1604
	Middle	0.0877	0.0019	0.0848	0.0905		Middle	0.0981	0.0016	0.0953	0.1012
	Posterior	0.1061	0.002	0.1029	0.1094		Posterior	0.1089	0.0013	0.1067	0.1114
Disk	Anterior	0.0315	0.0005	0.0306	0.0324	Disk	Anterior	0.0359	0.0003	0.0352	0.0365
	Middle	0.0227	0.0005	0.0219	0.0235		Middle	0.0378	0.0005	0.0369	0.0387
	Posterior	0.0351	0.0001	0.035	0.0352		Posterior	0.0221	0.0005	0.0221	0.0222
Temp	Anterior	0.1302	0.0007	0.1289	0.1315	Temp	Anterior	0.1097	0.0004	0.1089	0.1104
	Middle	0.109	0.0007	0.1079	0.1101		Middle	0.1046	0.0006	0.1036	0.1057
	Posterior	0.0537	0.0002	0.0534	0.0541		Posterior	0.0689	0.0001	0.0687	0.0691

Cond: Condyle; **Temp:** Temporal Bone; **SD:** Standard Deviation

**Table 4.2.3. Von Mises stresses (MPa) on the PDL of dental units
under stiffness variations in C1 II/7s group**

Right Side						Left Side					
Region	Area	Mean	SD	Min.	Max.	Region	Area	Mean	SD	Min.	Max.
47 D	Coronal	0.0063	0.00001	0.0063	0.0063	37 D	Coronal	0.0084	0.00001	0.0083	0.0084
	Middle	0.0059	0.00001	0.0059	0.0059		Middle	0.0075	0.00002	0.0075	0.0075
	Apical	0.0053	0.00002	0.0053	0.0054		Apical	0.0064	0.00002	0.0063	0.0064
47 M	Coronal	0.0037	0.00001	0.0037	0.0038	37 M	Coronal	0.0019	0.00001	0.0019	0.0020
	Middle	0.0041	0.00002	0.0040	0.0041		Middle	0.0017	0.00001	0.0017	0.0017
	Apical	0.0039	0.00002	0.0039	0.0039		Apical	0.002	0.00001	0.0019	0.0020
46 D	Coronal	0.0032	0.00001	0.0032	0.0032	36 D	Coronal	0.0026	0.00001	0.0026	0.0026
	Middle	0.0028	0.00001	0.0027	0.0028		Middle	0.0019	0.00001	0.0019	0.0019
	Apical	0.0027	0.00001	0.0027	0.0027		Apical	0.0017	0.00001	0.0017	0.0017
46 M	Coronal	0.0045	0.00001	0.0045	0.0045	36 M	Coronal	0.0051	0.00003	0.0050	0.0051
	Middle	0.0046	0.00001	0.0046	0.004		Middle	0.005	0.00003	0.0049	0.0050
	Apical	0.0042	0.00001	0.0041	0.0042		Apical	0.0041	0.00002	0.0041	0.0042
45 D	Coronal	0.0043	0.00001	0.0043	0.0043	35 D	Coronal	0.0052	0.00003	0.0052	0.0053
	Middle	0.0039	0.00001	0.0039	0.0039		Middle	0.0046	0.00003	0.0045	0.0046
	Apical	0.0035	0.00001	0.0035	0.0035		Apical	0.0036	0.00001	0.0036	0.0036
45 M	Coronal	0.0045	0.00001	0.0045	0.0045	35 M	Coronal	0.0055	0.00003	0.0054	0.0055
	Middle	0.0040	0.00001	0.0040	0.0040		Middle	0.0050	0.00002	0.0050	0.0051
	Apical	0.004	0.00001	0.0039	0.0040		Apical	0.0041	0.00001	0.0040	0.0041
44 D	Coronal	0.0038	0.00001	0.0038	0.0038	34 D	Coronal	0.0050	0.00002	0.0049	0.0050
	Middle	0.0037	0.00001	0.0037	0.0037		Middle	0.0048	0.00002	0.0047	0.0048
	Apical	0.0034	0.00001	0.0034	0.0034		Apical	0.0045	0.00002	0.0045	0.0046
44 M	Coronal	0.0041	0.00002	0.0041	0.0042	34 M	Coronal	0.0043	0.00002	0.0043	0.0043
	Middle	0.0038	0.00002	0.0038	0.0039		Middle	0.0047	0.00002	0.0047	0.0047
	Apical	0.0037	0.00001	0.0037	0.0037		Apical	0.0046	0.00001	0.0045	0.0046
43 D	Coronal	0.0038	0.00001	0.0037	0.0038	33 D	Coronal	0.0031	0.00002	0.0030	0.0031
	Middle	0.0036	0.00001	0.0036	0.0036		Middle	0.0025	0.00002	0.0025	0.0025
	Apical	0.0038	0.00002	0.0038	0.0038		Apical	0.0022	0.00002	0.0021	0.0022
43 M	Coronal	0.0040	0.00003	0.0040	0.0041	33 M	Coronal	0.0032	0.00003	0.0032	0.0033
	Middle	0.0039	0.00002	0.0039	0.0040		Middle	0.0028	0.00001	0.0028	0.0028
	Apical	0.0040	0.00003	0.0039	0.0040		Apical	0.0025	0.00002	0.0025	0.0025
42 D	Coronal	0.0035	0.00003	0.0034	0.0035	32 D	Coronal	0.0023	0.00004	0.0022	0.0023
	Middle	0.0036	0.00001	0.0035	0.0036		Middle	0.0015	0.00003	0.0015	0.0016
	Apical	0.0038	0.00002	0.0038	0.0039		Apical	0.0016	0.00005	0.0015	0.0017
42 M	Coronal	0.0038	0.00003	0.0038	0.0039	32 M	Coronal	0.0022	0.00004	0.0022	0.0023
	Middle	0.0034	0.00002	0.0033	0.0034		Middle	0.0017	0.00003	0.0016	0.0018
	Apical	0.0034	0.00003	0.0033	0.0035		Apical	0.0017	0.00005	0.0016	0.0018
41 D	Coronal	0.0030	0.00004	0.0029	0.0030	31 D	Coronal	0.0024	0.00004	0.0024	0.0025
	Middle	0.0024	0.00001	0.0024	0.0024		Middle	0.0022	0.00001	0.0022	0.0022
	Apical	0.0021	0.00001	0.0021	0.0021		Apical	0.0021	0.00001	0.0020	0.0021
41 M	Coronal	0.0024	0.00005	0.0023	0.0025	31 M	Coronal	0.0030	0.00004	0.0029	0.0031
	Middle	0.0023	0.00004	0.0022	0.0024		Middle	0.0024	0.00002	0.0024	0.0024
	Apical	0.0024	0.00004	0.0024	0.0025		Apical	0.0021	0	0.0021	0.0021

Table 4.2.5. Dental displacement (mm) of dental units under stiffness variations for models in the CI II/7s group

Right Side					Left Side				
Measure	Mean	SD	Min.	Max.	Measure	Mean	SD	Min.	Max.
Disp 47	-0.01009	0.00011	-0.01029	-0.00991	Disp 37	-0.01183	0.00013	-0.01207	-0.01161
Disp 46	-0.00885	0.00011	-0.00904	-0.00867	Disp 36	-0.00995	0.00012	-0.01017	-0.00975
Disp 45	-0.00854	0.00011	-0.00873	-0.00836	Disp 35	-0.00909	0.00011	-0.0093	-0.0089
Disp 44	-0.00886	0.00011	-0.00905	-0.00867	Disp 34	-0.01058	0.00013	-0.01081	-0.01037
Disp 43	-0.01056	0.00012	-0.01079	-0.01035	Disp 33	-0.01156	0.00014	-0.01181	-0.01133
Disp 42	-0.01224	0.00015	-0.01251	-0.01199	Disp 32	-0.01198	0.00014	-0.01223	-0.01173
Disp 41	-0.01231	0.00016	-0.0126	-0.01204	Disp 31	-0.01178	0.00015	-0.01205	-0.01152

SD: Standard Deviation

Table 4.2.7. Von Mises stresses (MPa) on the TMJ complex under thickness variations in CI II/7s group

Right Side						Left Side					
Region	Area	Mean	SD	Min	Max	Region	Area	Mean	SD	Min	Max
Cond	Anterior	0.101	0.0277	0.0305	0.1345	Cond	Anterior	0.1407	0.0413	0.0324	0.1955
	Middle	0.0725	0.0206	0.0257	0.1049		Middle	0.0848	0.0232	0.0245	0.1159
	Posterior	0.0903	0.0267	0.0261	0.119		Posterior	0.1071	0.0331	0.0265	0.1594
Disk	Anterior	0.0227	0.0071	0.0063	0.0294	Disk	Anterior	0.0323	0.0104	0.005	0.0451
	Middle	0.0227	0.0071	0.0062	0.0248		Middle	0.0321	0.0108	0.0062	0.0474
	Posterior	0.0378	0.0142	0.005	0.0546		Posterior	0.0241	0.0091	0.0039	0.0396
Temp	Anterior	0.1127	0.019	0.062	0.1262	Temp	Anterior	0.0978	0.025	0.0297	0.1146
	Middle	0.0832	0.0175	0.0415	0.1037		Middle	0.1189	0.0423	0.0168	0.1663
	Posterior	0.0773	0.0261	0.022	0.115		Posterior	0.0778	0.0259	0.0101	0.1018

Cond: Condyle; Temp: Temporal Bone; SD: Standard Deviation

**Table 4.2.9. Von Mises stresses (MPa) on the PDL of dental units
under thickness variations in CI II/7s group**

Right Side						Left Side					
Region	Area	Mean	SD	Min.	Max.	Region	Area	Mean	SD	Min.	Max.
47 D	Coronal	0.0097	0.00497	0.00645	0.02284	37 D	Coronal	0.0081	0.00132	0.00536	0.00947
	Middle	0.0091	0.00528	0.00606	0.02324		Middle	0.0081	0.00109	0.00604	0.00967
	Apical	0.0070	0.0023	0.00528	0.01226		Apical	0.0073	0.00091	0.00541	0.00856
47 M	Coronal	0.0045	0.00243	0.00276	0.01036	37 M	Coronal	0.0034	0.00051	0.00212	0.00388
	Middle	0.0047	0.00368	0.00189	0.01253		Middle	0.0032	0.00066	0.00187	0.00413
	Apical	0.0067	0.00631	0.00321	0.02315		Apical	0.0039	0.00321	0.00197	0.01255
46 D	Coronal	0.0037	0.00217	0.00254	0.0098	36 D	Coronal	0.0033	0.00039	0.00272	0.00415
	Middle	0.0031	0.00179	0.00203	0.00809		Middle	0.0025	0.00026	0.00206	0.003
	Apical	0.0032	0.00173	0.00203	0.0079		Apical	0.0021	0.00034	0.00176	0.00298
46 M	Coronal	0.0046	0.00135	0.00344	0.00837	36 M	Coronal	0.0038	0.0008	0.00289	0.00539
	Middle	0.0047	0.00109	0.00374	0.00774		Middle	0.0034	0.00078	0.00255	0.00522
	Apical	0.0045	0.00098	0.00314	0.00676		Apical	0.0027	0.00083	0.00121	0.00432
45 D	Coronal	0.0068	0.00673	0.00395	0.02573	35 D	Coronal	0.0041	0.00134	0.0028	0.00723
	Middle	0.0044	0.00117	0.00348	0.00715		Middle	0.0056	0.00798	0.00237	0.02833
	Apical	0.0083	0.01052	0.00307	0.03571		Apical	0.0046	0.00635	0.00153	0.02268
45 M	Coronal	0.0091	0.01264	0.00412	0.04481	35 M	Coronal	0.0049	0.00306	0.00289	0.01338
	Middle	0.0080	0.01179	0.00353	0.04154		Middle	0.0053	0.00579	0.00259	0.02166
	Apical	0.0081	0.01033	0.00325	0.0368		Apical	0.0048	0.0062	0.00157	0.0224
44 D	Coronal	0.00446	0.00194	0.00309	0.00984	34 D	Coronal	0.0068	0.00963	0.00222	0.03414
	Middle	0.00488	0.00245	0.00278	0.01064		Middle	0.0036	0.00113	0.00182	0.00605
	Apical	0.00413	0.00275	0.00249	0.01166		Apical	0.0038	0.00249	0.00156	0.01039
44 M	Coronal	0.00572	0.00309	0.00358	0.01338	34 M	Coronal	0.0038	0.0007	0.00244	0.00516
	Middle	0.00505	0.00304	0.00293	0.0129		Middle	0.0056	0.00647	0.00214	0.02392
	Apical	0.00944	0.01331	0.00261	0.04571		Apical	0.0042	0.00337	0.00168	0.01348
43 D	Coronal	0.00394	0.00062	0.00321	0.00549	33 D	Coronal	0.0033	0.00058	0.0024	0.00412
	Middle	0.00358	0.00054	0.00255	0.00452		Middle	0.0029	0.00075	0.00148	0.00382
	Apical	0.00341	0.00041	0.00264	0.00389		Apical	0.0027	0.00088	0.00076	0.00366
43 M	Coronal	0.0039	0.00056	0.0032	0.00524	33 M	Coronal	0.0034	0.00049	0.00257	0.004
	Middle	0.00393	0.0005	0.00313	0.00482		Middle	0.0032	0.00057	0.00238	0.00401
	Apical	0.0036	0.00042	0.00287	0.00404		Apical	0.0029	0.00082	0.0013	0.00396
42 D	Coronal	0.00496	0.00377	0.0028	0.01367	32 D	Coronal	0.0028	0.00083	0.0019	0.00481
	Middle	0.0031	0.00104	0.00186	0.00572		Middle	0.0029	0.00261	0.00133	0.01017
	Apical	0.00457	0.00615	0.002	0.02202		Apical	0.0037	0.00628	0.00073	0.02148
42 M	Coronal	0.00446	0.00308	0.00293	0.01319	32 M	Coronal	0.0028	0.00064	0.00167	0.00354
	Middle	0.00431	0.00392	0.0021	0.01539		Middle	0.0032	0.00209	0.00148	0.00875
	Apical	0.004	0.00406	0.00208	0.0155		Apical	0.0032	0.00403	0.00084	0.01455
41 D	Coronal	0.00224	0.00036	0.00164	0.00282	31 D	Coronal	0.0023	0.00039	0.00166	0.00282
	Middle	0.00175	0.00031	0.00135	0.00235		Middle	0.0019	0.00041	0.00128	0.0025
	Apical	0.00152	0.00043	0.00099	0.00215		Apical	0.0017	0.00047	0.00088	0.00243
41 M	Coronal	0.00249	0.0005	0.00157	0.00308	31 M	Coronal	0.0026	0.00038	0.00196	0.00323
	Middle	0.00209	0.00053	0.00156	0.0032		Middle	0.0022	0.0003	0.00143	0.00235
	Apical	0.00161	0.00043	0.00107	0.00215		Apical	0.0017	0.00047	0.00089	0.00246

Table 4.2.11. Dental displacement (mm) of dental units under thickness variations in CI II/7s group

Right Side					Left Side				
Measure	Mean	SD	Min.	Max.	Measure	Mean	SD	Min.	Max.
Disp 47	-0.01547	0.00666	-0.03393	-0.01101	Disp 37	-0.01407	0.00676	-0.03297	-0.01028
Disp 46	-0.01352	0.00696	-0.03302	-0.00955	Disp 36	-0.01239	0.00661	-0.03092	-0.009
Disp 45	-0.01298	0.007	-0.03257	-0.00897	Disp 35	-0.0119	0.00656	-0.03026	-0.00867
Disp 44	-0.01356	0.00811	-0.03621	-0.00894	Disp 34	-0.01244	0.00707	-0.03203	-0.00867
Disp 43	-0.01427	0.00788	-0.036	-0.00759	Disp 33	-0.01401	0.00732	-0.03444	-0.01024
Disp 42	-0.01588	0.00719	-0.03615	-0.01198	Disp 32	-0.01552	0.00717	-0.03572	-0.01177
Disp 41	-0.01612	0.0069	-0.03564	-0.0127	Disp 31	-0.01595	0.00709	-0.03597	-0.01249

SD: Standard Deviation

Table 4.2.13. Von Mises stresses (MPa) on the TMJ complex under stiffness variations in CI III group

Right Side						Left Side					
Region	Area	Mean	SD	Min	Max	Region	Area	Mean	SD	Min	Max
Cond	Anterior	0.1712	0.0124	0.1392	0.185	Cond	Anterior	0.2027	0.0206	0.1447	0.2144
	Middle	0.1033	0.0077	0.0824	0.1097		Middle	0.1307	0.0134	0.093	0.1396
	posterior	0.1249	0.009	0.1005	0.1324		posterior	0.1457	0.0149	0.1036	0.1542
Disk	Anterior	0.0362	0.0024	0.0295	0.0381	Disk	Anterior	0.0473	0.0048	0.0338	0.0498
	Middle	0.0259	0.0019	0.0206	0.0275		Middle	0.0517	0.0051	0.0372	0.0545
	posterior	0.0409	0.003	0.0324	0.042		posterior	0.0304	0.0031	0.0216	0.0314
Temp	Anterior	0.1532	0.011	0.1219	0.1584	Temp	Anterior	0.1213	0.0135	0.0828	0.1271
	Middle	0.1268	0.0101	0.0981	0.1313		Middle	0.1201	0.0127	0.0842	0.1264
	posterior	0.0632	0.0042	0.0512	0.065		posterior	0.07	0.008	0.0473	0.0738

Cond: Condyle; Temp: Temporal Bone; SD: Standard Deviation

Table 4.2.15. Von Mises stresses (MPa) on the PDL of dental units under stiffness variations in CI III group

Right Side						Left Side					
Region	Area	Mean	SD	Min.	Max.	Region	Area	Mean	SD	Min.	Max.
47 D	Coronal	0.0031	0.00003	0.0029	0.0030	37 D	Coronal	0.0028	0.00001	0.00286	0.00288
	Middle	0.0027	0.00004	0.0027	0.0028		Middle	0.0019	0.00001	0.00194	0.00199
	Apical	0.0028	0.00005	0.0027	0.0029		Apical	0.0013	0.00002	0.00135	0.00141
47 M	Coronal	0.0035	0.00002	0.0035	0.0036	37 M	Coronal	0.0034	0.00001	0.00347	0.00349
	Middle	0.0033	0.00003	0.0033	0.0034		Middle	0.0030	0.00001	0.00301	0.00305
	Apical	0.0031	0.00004	0.0031	0.0032		Apical	0.0017	0.00002	0.00168	0.00175
46 D	Coronal	0.0036	0.00002	0.0036	0.0036	36 D	Coronal	0.0033	0.00001	0.00336	0.00337
	Middle	0.0033	0.00002	0.0033	0.0034		Middle	0.0024	0.00001	0.00239	0.00243
	Apical	0.0034	0.00003	0.0033	0.0034		Apical	0.0019	0.00001	0.00192	0.00197
46 M	Coronal	0.0056	0.00001	0.0056	0.0056	36 M	Coronal	0.0051	0.00001	0.00511	0.00515
	Middle	0.0058	0.00001	0.0058	0.0058		Middle	0.0046	0.00001	0.00464	0.00469
	Apical	0.0053	0.00001	0.0052	0.0053		Apical	0.0037	0.00001	0.00371	0.00374
45 D	Coronal	0.0055	0.00001	0.0055	0.0055	35 D	Coronal	0.0055	0.00001	0.00555	0.00559
	Middle	0.0050	0.00001	0.005	0.0050		Middle	0.0047	0.00001	0.00475	0.00479
	Apical	0.0044	0.00001	0.0044	0.0044		Apical	0.0034	0.00001	0.00339	0.00341
45 M	Coronal	0.0058	0.00001	0.0058	0.0058	35 M	Coronal	0.0060	0.00002	0.00601	0.00607
	Middle	0.0051	0.00001	0.0051	0.0051		Middle	0.0053	0.00001	0.00531	0.00535
	Apical	0.0050	0.00001	0.0050	0.0050		Apical	0.0040	0.00001	0.00402	0.00403
44 D	Coronal	0.0051	0.00001	0.0050	0.0051	34 D	Coronal	0.0062	0.00002	0.00621	0.00628
	Middle	0.0048	0.00001	0.0048	0.0048		Middle	0.0061	0.00002	0.00612	0.00619
	Apical	0.0042	0.00001	0.0042	0.0042		Apical	0.0059	0.00002	0.00595	0.006
44 M	Coronal	0.0053	0.00002	0.0053	0.0054	34 M	Coronal	0.0055	0.00002	0.00547	0.00556
	Middle	0.0049	0.00001	0.0049	0.0049		Middle	0.0059	0.00001	0.00592	0.00593
	Apical	0.0045	0.00001	0.0045	0.0045		Apical	0.0057	0.00001	0.00578	0.00581
43 D	Coronal	0.0049	0.00001	0.0049	0.0049	33 D	Coronal	0.0032	0.00002	0.0032	0.00328
	Middle	0.0046	0.00001	0.0046	0.0046		Middle	0.0017	0.00001	0.00171	0.00171
	Apical	0.0052	0.00001	0.0052	0.0053		Apical	0.0016	0.00004	0.00159	0.00175
43 M	Coronal	0.0052	0.00003	0.0052	0.0053	33 M	Coronal	0.0032	0.00003	0.00321	0.00333
	Middle	0.0050	0.00001	0.0050	0.0051		Middle	0.0022	0.00002	0.00221	0.00229
	Apical	0.0055	0.00002	0.0054	0.0055		Apical	0.0021	0.00005	0.00201	0.00219
42 D	Coronal	0.0049	0.00003	0.0049	0.0050	32 D	Coronal	0.0032	0.00003	0.00322	0.00333
	Middle	0.0046	0.00001	0.0046	0.0046		Middle	0.0018	0.00002	0.00185	0.00191
	Apical	0.0053	0.00001	0.0052	0.0053		Apical	0.0015	0.00006	0.00146	0.00168
42 M	Coronal	0.0056	0.00003	0.0056	0.0057	32 M	Coronal	0.0032	0.00004	0.00318	0.00332
	Middle	0.0047	0.00001	0.0047	0.0048		Middle	0.0021	0.00002	0.00208	0.00216
	Apical	0.0043	0.00002	0.0043	0.0044		Apical	0.0017	0.00006	0.00162	0.00185
41 D	Coronal	0.0043	0.00003	0.0043	0.0044	31 D	Coronal	0.0034	0.00003	0.0034	0.00351
	Middle	0.0035	0.00001	0.0035	0.0035		Middle	0.0029	0.00002	0.00295	0.00303
	Apical	0.0029	0.00004	0.0029	0.0030		Apical	0.0027	0.00004	0.00269	0.00283
41 M	Coronal	0.0029	0.00006	0.0028	0.0030	31 M	Coronal	0.0044	0.00004	0.0044	0.00452
	Middle	0.0020	0.00003	0.002	0.0021		Middle	0.0034	0.00001	0.00348	0.00351
	Apical	0.0021	0.00003	0.0020	0.0021		Apical	0.0031	0.00004	0.00305	0.00317

Table 4.2.17. Dental displacement (mm) of dental units under stiffness variations in the CI III group

Right Side					Left Side				
Measure	Mean	SD	Min.	Max.	Measure	Mean	SD	Min.	Max.
Disp 47	0.01155	0.00013	0.01133	0.01178	Disp 37	0.01274	0.00015	0.01248	0.01301
Disp 46	0.01075	0.00013	0.01053	0.01098	Disp 36	0.01226	0.00015	0.01201	0.01252
Disp 45	0.01077	0.00013	0.01055	0.01101	Disp 35	0.01168	0.00014	0.01144	0.01194
Disp 44	0.01184	0.00013	0.01161	0.01208	Disp 34	0.01485	0.00015	0.01459	0.01513
Disp 43	0.01511	0.00015	0.01485	0.01539	Disp 33	0.01593	0.00017	0.01565	0.01623
Disp 42	0.01745	0.00018	0.01714	0.01779	Disp 32	0.01658	0.00018	0.01628	0.0169
Disp 41	0.01768	0.0002	0.01734	0.01805	Disp 31	0.01667	0.00019	0.01635	0.01701

SD: Standard Deviation

Table 4.2.19. Von Mises stresses (MPa) on the TMJ complex under thickness variations in the CI III's group

Right Side						Left Side					
Region	Area	Mean	SD	Min	Max	Region	Area	Mean	SD	Min	Max
Cond	Anterior	0.0961	0.0294	0.0268	0.1406	Cond	Anterior	0.1401	0.049	0.0313	0.2165
	Middle	0.0705	0.0196	0.0214	0.0918		Middle	0.0851	0.0302	0.0218	0.1338
	posterior	0.0878	0.0283	0.0226	0.1251		posterior	0.1078	0.0364	0.0238	0.1624
Disk	Anterior	0.0207	0.007	0.0052	0.0328	Disk	Anterior	0.0313	0.0128	0.0048	0.0474
	Middle	0.0165	0.0058	0.0052	0.0239		Middle	0.0321	0.0145	0.0059	0.0549
	posterior	0.0349	0.0135	0.0043	0.0477		posterior	0.0233	0.0083	0.0036	0.0315
Temp	Anterior	0.1098	0.0278	0.05	0.1493	Temp	Anterior	0.0907	0.0302	0.0243	0.1352
	Middle	0.0819	0.0246	0.0322	0.1238		Middle	0.1084	0.0464	0.0181	0.1748
	posterior	0.0752	0.0241	0.0198	0.1031		posterior	0.0652	0.0241	0.0106	0.1021

Cond: Condyle; Temp: Temporal Bone; SD: Standard Deviation

Table 4.2.21. Von Mises stresses (MPa) on the PDL of dental units under thickness variations in the CI III's group

Right Side						Left Side					
Region	Area	Mean	SD	Min.	Max.	Region	Area	Mean	SD	Min.	Max.
47 D	Coronal	0.0044	0.00411	0.0020	0.0137	37 D	Coronal	0.0021	0.00087	0.0013	0.0042
	Middle	0.0042	0.00415	0.0016	0.0142		Middle	0.0016	0.00088	0.0008	0.0039
	Apical	0.0029	0.00266	0.0006	0.0085		Apical	0.0014	0.00094	0.0005	0.0038
47 M	Coronal	0.0037	0.00231	0.0022	0.0091	37 M	Coronal	0.0022	0.00078	0.0013	0.0035
	Middle	0.0040	0.00323	0.0020	0.0115		Middle	0.0020	0.00074	0.0010	0.0031
	Apical	0.0046	0.00519	0.0017	0.0183		Apical	0.0077	0.01914	0.0006	0.0621
46 D	Coronal	0.0031	0.0021	0.0012	0.0088	36 D	Coronal	0.0022	0.00066	0.0015	0.0033
	Middle	0.0026	0.00169	0.0010	0.0070		Middle	0.0018	0.00046	0.0012	0.0025
	Apical	0.0026	0.0016	0.0011	0.0068		Apical	0.0016	0.00048	0.0008	0.0023
46 M	Coronal	0.0041	0.00173	0.0019	0.0080	36 M	Coronal	0.0031	0.00091	0.0021	0.0052
	Middle	0.0042	0.0015	0.0023	0.0074		Middle	0.0029	0.00089	0.0020	0.0048
	Apical	0.0040	0.00118	0.0023	0.0063		Apical	0.0023	0.00082	0.0013	0.0038
45 D	Coronal	0.0060	0.00465	0.0032	0.0186	35 D	Coronal	0.0036	0.00114	0.0025	0.0057
	Middle	0.0044	0.00144	0.0029	0.0072		Middle	0.0045	0.00589	0.0018	0.0211
	Apical	0.0074	0.00877	0.0027	0.0309		Apical	0.0038	0.00567	0.0012	0.0198
45 M	Coronal	0.0078	0.00948	0.0035	0.0344	35 M	Coronal	0.0044	0.00244	0.0028	0.0108
	Middle	0.0073	0.0097	0.0031	0.0348		Middle	0.0045	0.00475	0.0017	0.0176
	Apical	0.0072	0.00753	0.0029	0.0274		Apical	0.0039	0.00504	0.0009	0.0180
44 D	Coronal	0.0042	0.00216	0.0024	0.0097	34 D	Coronal	0.0062	0.00837	0.0027	0.0298
	Middle	0.0046	0.00275	0.0020	0.0107		Middle	0.0032	0.00134	0.0021	0.0063
	Apical	0.0034	0.00311	0.0013	0.0120		Apical	0.0030	0.00186	0.0015	0.0067
44 M	Coronal	0.0051	0.0025	0.0031	0.0112	34 M	Coronal	0.0036	0.00068	0.0030	0.0053
	Middle	0.0047	0.00326	0.0026	0.0130		Middle	0.0052	0.00621	0.0022	0.0226
	Apical	0.0084	0.01053	0.0021	0.0342		Apical	0.0034	0.00253	0.0015	0.0097
43 D	Coronal	0.0037	0.00116	0.0024	0.0060	33 D	Coronal	0.0030	0.00071	0.0017	0.0043
	Middle	0.0035	0.001	0.0025	0.0057		Middle	0.0024	0.00102	0.0010	0.0042
	Apical	0.0039	0.00089	0.0028	0.0057		Apical	0.0023	0.00116	0.0004	0.0042
43 M	Coronal	0.0037	0.00114	0.0023	0.0057	33 M	Coronal	0.0032	0.0007	0.0019	0.004
	Middle	0.0036	0.00107	0.0022	0.0058		Middle	0.0027	0.00092	0.0012	0.0044
	Apical	0.0039	0.00092	0.0028	0.0058		Apical	0.0024	0.00113	0.0001	0.0042
42 D	Coronal	0.0047	0.00231	0.0028	0.0089	32 D	Coronal	0.0034	0.0008	0.0021	0.0049
	Middle	0.0036	0.0016	0.0018	0.0071		Middle	0.0029	0.00157	0.0014	0.0067
	Apical	0.0046	0.00612	0.0018	0.0218		Apical	0.0032	0.00508	0.0007	0.0175
42 M	Coronal	0.0047	0.00239	0.0030	0.0109	32 M	Coronal	0.0034	0.00086	0.0019	0.005
	Middle	0.0044	0.0031	0.0018	0.0128		Middle	0.0037	0.00213	0.0017	0.0090
	Apical	0.0037	0.00322	0.0018	0.0122		Apical	0.0027	0.00293	0.0008	0.0108
41 D	Coronal	0.0027	0.00081	0.0014	0.0041	31 D	Coronal	0.0027	0.00063	0.0017	0.0039
	Middle	0.0021	0.00086	0.0007	0.0036		Middle	0.0023	0.00073	0.0014	0.0036
	Apical	0.0017	0.00073	0.0010	0.0033		Apical	0.0021	0.00078	0.0011	0.0034
41 M	Coronal	0.0029	0.00085	0.0011	0.0043	31 M	Coronal	0.0033	0.00077	0.0021	0.0049
	Middle	0.0022	0.00065	0.0013	0.0032		Middle	0.0025	0.00083	0.0017	0.0042
	Apical	0.0016	0.00055	0.0009	0.0025		Apical	0.0021	0.00091	0.0012	0.0038

**Table 4.2.23. Dental displacement (mm) of dental units
under thickness variations in C1 III group**

Right Side					Left Side				
Measure	Mean	SD	Min.	Max.	Measure	Mean	SD	Min.	Max.
Disp 47	0.013	0.00595	0.00866	0.02914	Disp 37	0.01275	0.0061	0.00868	0.02897
Disp 46	0.01248	0.00605	0.00812	0.02901	Disp 36	0.01234	0.00617	0.0083	0.02892
Disp 45	0.01223	0.00621	0.0078	0.02927	Disp 35	0.01183	0.0063	0.00777	0.02891
Disp 44	0.01318	0.00738	0.00821	0.03354	Disp 34	0.01284	0.0067	0.00822	0.03041
Disp 43	0.01507	0.00753	0.00714	0.03471	Disp 33	0.01443	0.00676	0.00974	0.03207
Disp 42	0.01683	0.00698	0.01155	0.03503	Disp 32	0.01615	0.00661	0.0115	0.03346
Disp 41	0.01721	0.00671	0.01212	0.03439	Disp 31	0.01691	0.00665	0.01214	0.03416

SD: Standard Deviation

Table 4.2.25. Von Mises stresses (MPa) on the TMJ complex under stiffness variations in C1 II/6s group

Right Side						Left Side					
Region	Area	Mean	SD	Min	Max	Region	Area	Mean	SD	Min	Max
Cond	Anterior	0.1373	0.0039	0.1304	0.1445	Cond	Anterior	0.1434	0.0021	0.1398	0.1469
	Middle	0.0812	0.0016	0.0786	0.0837		Middle	0.0925	0.0016	0.0897	0.0957
	posterior	0.0993	0.0017	0.0966	0.1021		posterior	0.1032	0.0014	0.1008	0.1058
Disk	Anterior	0.0293	0.0004	0.0285	0.03	Disk	Anterior	0.0336	0.0004	0.0329	0.0342
	Middle	0.0204	0.0004	0.0196	0.0211		Middle	0.0370	0.0004	0.0362	0.0377
	posterior	0.0324	0.0004	0.0324	0.0325		posterior	0.0216	0.0004	0.0216	0.0216
Temp	Anterior	0.1216	0.0006	0.1206	0.1226	Temp	Anterior	0.0825	0.0006	0.0814	0.0836
	Middle	0.0978	0.0004	0.0971	0.0985		Middle	0.0837	0.001	0.0819	0.0854
	posterior	0.051	0.0002	0.0508	0.0513		posterior	0.0471	0.0006	0.046	0.0481

Cond: Condyle; Temp: Temporal Bone; SD: Standard Deviation

**Table 4.2.27. Von Mises stresses (MPa) on PDL of dental units
under stiffness variations in the CI II/6s group**

Right Side						Left Side					
Region	Area	Mean	SD	Min.	Max.	Region	Area	Mean	SD	Min.	Max.
47 D	Coronal	0.0034	2.30E-05	0.0034	0.0035	37 D	Coronal	0.0015	3.16E-06	0.0019	0.0019
	Middle	0.0025	2.82E-05	0.0025	0.0026		Middle	0.0012	7.03E-06	0.0012	0.001
	Apical	0.0021	3.29E-05	0.0020	0.0022		Apical	0.0008	9.89E-06	0.0008	0.0008
47 M	Coronal	0.0028	1.74E-05	0.0028	0.0029	37 M	Coronal	0.0022	6.64E-06	0.0022	0.002
	Middle	0.0027	2.93E-05	0.0027	0.0028		Middle	0.0019	3.28E-06	0.0019	0.0019
	Apical	0.0023	3.58E-05	0.0022	0.0023		Apical	0.0010	1.15E-05	0.0010	0.0011
46 D	Coronal	0.0031	1.06E-05	0.0031	0.0031	36 D	Coronal	0.0021	6.10E-06	0.0021	0.0021
	Middle	0.0029	1.61E-05	0.0029	0.0030		Middle	0.0015	7.05E-06	0.0015	0.0015
	Apical	0.0027	2.29E-05	0.0026	0.0027		Apical	0.0013	1.26E-05	0.0013	0.0014
46 M	Coronal	0.0046	1.76E-05	0.0046	0.0047	36 M	Coronal	0.0037	1.01E-05	0.0037	0.0038
	Middle	0.0050	2.03E-05	0.0049	0.0050		Middle	0.0033	6.51E-06	0.0033	0.0033
	Apical	0.0044	2.41E-05	0.0043	0.0044		Apical	0.0025	1.31E-06	0.0025	0.0025
45 D	Coronal	0.0043	1.60E-05	0.0043	0.0044	35 D	Coronal	0.0039	1.19E-05	0.0039	0.004
	Middle	0.0039	1.57E-05	0.0039	0.0039		Middle	0.0034	7.39E-06	0.0033	0.0034
	Apical	0.0035	1.55E-05	0.0035	0.0035		Apical	0.0024	3.85E-06	0.0024	0.0025
45 M	Coronal	0.0045	7.66E-06	0.0045	0.0045	35 M	Coronal	0.0041	1.41E-05	0.0041	0.0042
	Middle	0.0040	8.82E-06	0.0040	0.0040		Middle	0.0037	5.96E-06	0.0037	0.0037
	Apical	0.0039	1.13E-05	0.0039	0.0039		Apical	0.0028	3.32E-06	0.0028	0.0029
44 D	Coronal	0.0038	9.31E-06	0.0038	0.0038	34 D	Coronal	0.0037	1.31E-05	0.0037	0.0037
	Middle	0.0036	1.08E-05	0.0036	0.0037		Middle	0.0035	1.09E-05	0.0035	0.0035
	Apical	0.0034	1.00E-05	0.0034	0.0034		Apical	0.0033	7.91E-06	0.0032	0.0033
44 M	Coronal	0.0040	1.17E-05	0.0039	0.0040	34 M	Coronal	0.0032	2.15E-05	0.0032	0.0033
	Middle	0.0037	4.18E-06	0.0037	0.0037		Middle	0.0035	4.33E-06	0.0035	0.0035
	Apical	0.0036	4.71E-06	0.0036	0.0036		Apical	0.0033	3.84E-06	0.0033	0.0033
43 D	Coronal	0.0036	7.82E-06	0.0036	0.0036	33 D	Coronal	0.0022	1.95E-05	0.0022	0.0023
	Middle	0.0033	1.69E-06	0.0033	0.0034		Middle	0.0017	3.91E-06	0.00175	0.0017
	Apical	0.0034	7.59E-06	0.0034	0.0035		Apical	0.0014	1.71E-05	0.0013	0.0014
43 M	Coronal	0.0038	2.71E-05	0.0037	0.0038	33 M	Coronal	0.0024	2.80E-05	0.0023	0.0024
	Middle	0.0037	1.40E-05	0.0037	0.0037		Middle	0.0020	7.78E-06	0.0020	0.0020
	Apical	0.0036	1.13E-05	0.0036	0.0037		Apical	0.0016	1.51E-05	0.00164	0.0016
42 D	Coronal	0.0031	2.90E-05	0.0031	0.0032	32 D	Coronal	0.0016	3.52E-05	0.001	0.0017
	Middle	0.0033	9.21E-07	0.0033	0.0033		Middle	0.0009	2.70E-05	0.0009	0.0010
	Apical	0.0035	7.92E-06	0.0034	0.0035		Apical	0.0009	4.89E-05	0.0008	0.0010
42 M	Coronal	0.0034	2.64E-05	0.0033	0.0034	32 M	Coronal	0.0016	3.66E-05	0.0015	0.0017
	Middle	0.0030	1.64E-05	0.0030	0.0030		Middle	0.0011	2.69E-05	0.0010	0.0011
	Apical	0.0030	2.25E-05	0.0029	0.0030		Apical	0.0010	4.89E-05	0.0009	0.0011
41 D	Coronal	0.0025	3.32E-05	0.0024	0.0025	31 D	Coronal	0.0019	3.16E-05	0.0019	0.0020
	Middle	0.0021	2.52E-06	0.0021	0.0021		Middle	0.0018	1.76E-06	0.0019	0.0019
	Apical	0.0018	1.39E-05	0.0018	0.0018		Apical	0.0018	9.77E-06	0.0017	0.0018
41 M	Coronal	0.0019	4.78E-05	0.0018	0.002	31 M	Coronal	0.0025	3.37E-05	0.0024	0.0025
	Middle	0.0018	3.00E-05	0.0018	0.0019		Middle	0.0020	4.37E-06	0.0020	0.0021
	Apical	0.0020	2.70E-05	0.0019	0.0020		Apical	0.00191	1.17E-05	0.0018	0.0019

D: Distal; M: Mesial

Table 4.2.29. Dental displacement (mm) of dental units under stiffness variations in CI II/6s group

Right Side					Left Side				
Measure	Mean	SD	Min.	Max.	Measure	Mean	SD	Min.	Max.
Disp 47	-0.0101	0.00013	-0.01033	-0.00987	Disp 37	-0.00878	0.00009	-0.00894	-0.00862
Disp 46	-0.00867	0.00012	-0.00889	-0.00846	Disp 36	-0.00832	0.00009	-0.00848	-0.00817
Disp 45	-0.00837	0.00012	-0.00859	-0.00816	Disp 35	-0.00783	0.00009	-0.00798	-0.00768
Disp 44	-0.00866	0.00013	-0.00889	-0.00844	Disp 34	-0.00909	0.0001	-0.00927	-0.00893
Disp 43	-0.00992	0.00014	-0.01017	-0.00969	Disp 33	-0.01003	0.00011	-0.01023	-0.00984
Disp 42	-0.01134	0.00015	-0.01161	-0.01109	Disp 32	-0.01055	0.00012	-0.01077	-0.01035
Disp 41	-0.01127	0.00015	-0.01154	-0.01101	Disp 31	-0.01052	0.00013	-0.01076	-0.0103

Table 4.2.31. Von Mises stresses (MPa) at the TMJ complex under thickness variations in CI II/6s group

Right Side						Left Side					
Region	Area	Mean	SD	Min	Max	Region	Area	Mean	SD	Min	Max
Cond	Anterior	0.1116	0.022	0.0715	0.1477	Cond	Anterior	0.1569	0.0301	0.0825	0.1939
	Middle	0.0846	0.0142	0.0601	0.1042		Middle	0.0994	0.0124	0.0891	0.1314
	posterior	0.0973	0.0303	0.0263	0.1241		posterior	0.1154	0.0319	0.0305	0.1401
Disk	Anterior	0.0245	0.0052	0.0156	0.0307	Disk	Anterior	0.0363	0.0043	0.031	0.0434
	Middle	0.0219	0.0056	0.0123	0.0328		Middle	0.0349	0.0059	0.0216	0.043
	posterior	0.0495	0.0261	0.0226	0.1171		posterior	0.0325	0.0168	0.0185	0.0779
Temp	Anterior	0.1275	0.0254	0.0944	0.1908	Temp	Anterior	0.1122	0.0221	0.0758	0.1501
	Middle	0.0878	0.0174	0.0499	0.113		Middle	0.133	0.0408	0.0427	0.1986
	posterior	0.098	0.0197	0.0706	0.1282		posterior	0.0846	0.0323	0.002	0.1195

Cond: Condyle; Temp: Temporal Bone; SD: Standard Deviation

Table 4.2.33. Von Mises stresses (MPa) at the PDL of dental units under thickness variations in CI II/6s group

Right Side						Left Side					
Region	Area	Mean	SD	Min.	Max.	Region	Area	Mean	SD	Min.	Max.
47 D	Coronal	0.0056	0.00491	0.00283	0.01938	37 D	Coronal	0.0035	0.00316	0.00136	0.01241
	Middle	0.0053	0.00596	0.00237	0.02182		Middle	0.0027	0.00309	0.00097	0.01138
	Apical	0.0031	0.00271	0.0013	0.01037		Apical	0.0029	0.00275	0.00129	0.01063
47 M	Coronal	0.0039	0.0016	0.00274	0.00818	37 M	Coronal	0.0045	0.00161	0.00199	0.00813
	Middle	0.0037	0.00332	0.0018	0.01284		Middle	0.0035	0.00173	0.00119	0.00792
	Apical	0.0050	0.00695	0.00109	0.02404		Apical	0.0101	0.02294	0.00104	0.0751
46 D	Coronal	0.0034	0.00044	0.0029	0.00445	36 D	Coronal	0.0046	0.00164	0.00163	0.00721
	Middle	0.0025	0.00069	0.00091	0.00317		Middle	0.0041	0.00142	0.00149	0.0056
	Apical	0.0025	0.00092	0.00163	0.00483		Apical	0.0039	0.00097	0.00171	0.00524
46 M	Coronal	0.0046	0.00083	0.00348	0.00651	36 M	Coronal	0.0041	0.00087	0.00313	0.00556
	Middle	0.0048	0.00077	0.00384	0.00654		Middle	0.0040	0.00117	0.00254	0.00578
	Apical	0.0041	0.00103	0.00263	0.00669		Apical	0.0036	0.00097	0.00194	0.00505
45 D	Coronal	0.0069	0.00689	0.00404	0.02642	35 D	Coronal	0.0043	0.00143	0.00312	0.00793
	Middle	0.0045	0.00125	0.00351	0.00712		Middle	0.0060	0.00922	0.00242	0.03221
	Apical	0.0089	0.01116	0.00307	0.03894		Apical	0.0053	0.00706	0.00178	0.02526
45 M	Coronal	0.0099	0.01459	0.00409	0.05121	35 M	Coronal	0.0054	0.00365	0.00324	0.01566
	Middle	0.0087	0.0125	0.00365	0.04407		Middle	0.0056	0.0066	0.00258	0.02438
	Apical	0.0091	0.01164	0.00328	0.04118		Apical	0.0054	0.007	0.00208	0.02527
44 D	Coronal	0.0045	0.00165	0.00347	0.00912	34 D	Coronal	0.0072	0.00981	0.0025	0.03506
	Middle	0.0048	0.0019	0.00298	0.00822		Middle	0.0041	0.00146	0.00195	0.00729
	Apical	0.0041	0.00204	0.00259	0.0097		Apical	0.0044	0.00301	0.00168	0.01236
44 M	Coronal	0.0065	0.00405	0.00371	0.01552	34 M	Coronal	0.0047	0.00152	0.00277	0.00812
	Middle	0.0054	0.0033	0.003	0.0128		Middle	0.0064	0.00715	0.00237	0.02652
	Apical	0.0109	0.01509	0.00267	0.04948		Apical	0.0048	0.00386	0.00179	0.01517
43 D	Coronal	0.0046	0.00188	0.00313	0.00975	33 D	Coronal	0.0041	0.00157	0.00176	0.00761
	Middle	0.0042	0.00176	0.00231	0.00896		Middle	0.0037	0.00141	0.00134	0.00656
	Apical	0.0043	0.00207	0.0024	0.01		Apical	0.0036	0.00147	0.00222	0.00725
43 M	Coronal	0.0047	0.00224	0.00315	0.01093	33 M	Coronal	0.0044	0.002	0.00199	0.0095
	Middle	0.0047	0.00209	0.00284	0.01036		Middle	0.0041	0.00172	0.0016	0.00812
	Apical	0.0045	0.00226	0.00264	0.01064		Apical	0.0039	0.00186	0.00138	0.00835
42 D	Coronal	0.0059	0.00436	0.00306	0.01617	32 D	Coronal	0.0038	0.0022	0.00081	0.00894
	Middle	0.0038	0.00188	0.0021	0.00843		Middle	0.0040	0.00361	0.00059	0.01261
	Apical	0.0056	0.00659	0.00229	0.0231		Apical	0.0051	0.00777	0.00136	0.0263
42 M	Coronal	0.0054	0.00365	0.00293	0.01424	32 M	Coronal	0.0038	0.00237	0.00095	0.00989
	Middle	0.0053	0.0047	0.00212	0.01778		Middle	0.0042	0.00294	0.00071	0.00981
	Apical	0.0048	0.00438	0.00185	0.0151		Apical	0.0045	0.00492	0.00164	0.01692
41 D	Coronal	0.0030	0.00221	0.00189	0.00926	31 D	Coronal	0.0033	0.00213	0.00195	0.00917
	Middle	0.0024	0.00198	0.00155	0.00807		Middle	0.0028	0.00204	0.00168	0.00857
	Apical	0.0022	0.0021	0.00109	0.00807		Apical	0.0027	0.00228	0.00153	0.00921
41 M	Coronal	0.0034	0.00254	0.00166	0.01046	31 M	Coronal	0.0037	0.0025	0.00208	0.01068
	Middle	0.0011	0.00222	0.00173	0.00906		Middle	0.0029	0.00216	0.00184	0.00901
	Apical	0.0025	0.00271	0.00115	0.0097		Apical	0.0028	0.00237	0.00112	0.00926

**Table 4.2.35. Dental displacement (mm) of dental units
under thickness variations for models in the CI II/6s group**

Right Side

Measure	Mean	SD	Min.	Max.
Disp 47	-0.02838	0.0471	-0.16235	-0.01118
Disp 46	-0.02752	0.04802	-0.16412	-0.00969
Disp 45	-0.02698	0.0487	-0.16551	-0.0094
Disp 44	-0.02751	0.0494	-0.16802	-0.00965
Disp 43	-0.02841	0.04962	-0.16951	-0.00855
Disp 42	-0.03042	0.04973	-0.17189	-0.01259
Disp 41	-0.03092	0.05001	-0.1732	-0.01254

Left Side

Measure	Mean	SD	Min.	Max.
Disp 37	-0.03115	0.0544	-0.18583	-0.00957
Disp 36	-0.02965	0.05421	-0.18386	-0.00908
Disp 35	-0.02812	0.05414	-0.18216	-0.00856
Disp 34	-0.02841	0.0539	-0.18174	-0.00971
Disp 33	-0.02964	0.05278	-0.17978	-0.01098
Disp 32	-0.03085	0.05147	-0.17726	-0.01159
Disp 31	-0.03105	0.05083	-0.17563	-0.01166

SD: Standard Deviation